Investigations into novel signalling pathways in the response to viral and bacterial infections.

Enda J. Shevlin BA (Mod.)

Department of Biology

NUI MAYNOOTH

Ollscoil na hÉireann Má Nuad

Thesis submitted for the degree of Doctor of Philosophy

National University of Ireland, Maynooth

October 2013

Head of Department: Prof. Paul Moynagh

Supervisor: Dr. Sinead Miggin

Contents

Declaration

I hereby declare that the contents of this thesis are entirely my own work and that it has not been previously submitted as an exercise for a degree to this or any other university. The work and information of others have been acknowledged and cited in the text.

Signed: Date:

Publications

Shevlin, Enda and Miggin, Sinéad M. 'Toll-like receptor adaptor proteins'. *Encyclopedia of Signaling Molecules* Sangdun Choi (Ed.) Springer (2011)

Ahmed S, Maratha A, Butt AQ, **Shevlin E**, Miggin SM. 'TRIF-mediated TLR3 and TLR4 signaling is negatively regulated by ADAM15' *The Journal of Immunology* 190 pp 2217-2228 (2013)

Poster Presentations

Shevlin, E. and Miggin SM. 'Broad functional characterisation of the roles of TRIF and TRAM in TLR signalling'. Toll 2011 Meeting - Decoding Innate Immunity, 2011, Riva del Garda, Italy.

Shevlin, E. and Miggin SM. 'TLR7 signalling in macrophages activates IRF3 and is dependent on the adaptor TRAM'. 15th International Congress of Immunology 2013, Milan, Italy.

Acknowledgements

I would like to thank Sinead for allowing me to work in her lab for the past three years. Her ability to explain complex procedures in a simple language is a rare talent as is her ability to describe as "beeeeautiful", results which one might have thought were disheartening. Thanks to Edel, Suaad, Ashwini and Aisha from the lab for protocols and essential advice whenever I asked for it. I owe a debt of gratitude to the friends I've made here: Ruaidhri, Ronan, Marc, Eoin, Dave and Anthony. I would also like to thank my parents, Sean and Mary for their ying and yang presence throughout my time here. My sister Karen too deserves a mention for stoically putting up with my 'PhD blues'. Finally, a special thanks to Pamela who has been there through the darkest days. We made it!

This work was funded by the Health Research Board in Ireland under Grant No. PhD/20007/9

Abstract

Our current understanding of the host response to pathogenic insult is in constant flux. The long term goal is to better understand the host response so as to design better therapeutics with higher efficacies and less side effects. Thus, the current work sought to increase our understanding the immune response to viral and bacterial perturbation of host signalling pathways. The TIR-domain containing adaptor TRAM is a relatively understudied protein with regard to TLR signalling, particularly with respect to type-I inferferon production. A re-evaluation of the role of TRAM in TLR7 signalling showed that TRAM is required for maximal levels of TLR7 mediated RANTES, CXCL10 and IFNβ cytokine secretion but not TNFα production. TLR7 signalling was shown to activate IRF3 and NFκB in murine bone marrow derived macrophages. However, while TLR7 mediated IRF3 activation was TRAM dependent, NFκB activation was not. TRAM was also shown to mediate signalling via a physiological activator of TLR7, human rhinovirus 16 (HRV16). TRAM's role in TLR7 is hypothesised to be dependent on its ability to membrane localise as overexpression of a TRAM myriostoylation mutant which is incapable of membrane localisation dose dependently inhibited TLR7 mediated activation of RANTES, IFNβ, IFNα but not NFκB reporter genes. Furthermore, TRAM was shown to co-immunoprecipitate with the TLR7 adaptor molecule MyD88 upon TLR7 activation. This is first time that either IRF3 or TRAM has been shown to play role in TLR7 signalling. The second part of this project focused on the characterisation of the proteomic response to two respiratory pathogens, HRV16 and *Bordetella pertussis* (*B. pertussis*) in a lung epithelial cell line using mass spectrometry. Significant alternations were observed in the host proteome in response to both pathogens with proteins involved in the immune response, redox signalling, cancer related pathways, metabolism and DNA binding being particularly well represented. There was also a significant overlap between proteins identified in response to both infections with immune

response proteins being responsible for a third of the overlap. Supression of endogenous levels of a number of protein hits prior to infection with either HRV16 or *B. pertussis* did not affect levels of cytokine secretion. However, suppression of two proteins, the microtubule regulator stathmin 1 and the protein phosphatase PPP1Cα led to a significant decrease in TLR4 mediated IL-6 production. Thus the current work has indicated novel roles for a number of proteins in the host response to pathogen challenge. TRAM is required for maximal TLR7 mediated anti-viral cytokine secretion and both stathmin 1 and PPP1Cα are required for maximal TLR4 mediated IL-6 production.

List of Abbreviations

2D-PAGE	Two-dimensional Polyacrylamide gel electrophoresis
2D-DIGE	Two-dimensional difference gel electrophoresis
aa	Amino acid
AIM2	Absent in melanoma 2
Ambic	Ammonium bicarbonate
Amp	Ampicillin
ANOVA	Analysis of variance
APC	Antigen presenting cell
ARM	Armadillo repeat motif
APS	Ammonium persulfate
ASC	Apoptosis-associated speck-like protein containing a CARD
ASCC1	Activating signal cointegrator 1 complex subunit 1
ATF-2	Activating transcription factor-2
B	*Bordetella*
bp	Base pair
BSA	Bovine serum albumin
BMDM	Bone marrow derived macrophages
BTK	Bruton's tyrosine kinase
C	Control
C-terminal	-COOH terminal
cAMP	Cyclic adenosine 3', 5'-monophosphate
CARD	Caspase recruiting domain
CBP	CREB-binding protein
CCL5	C-C motif ligand 5
CD	Cluster of differentiation
cDC	Conventional dendritic cell
cDNA	Complementary DNA

CFU	Colony forming unit
CHAPS	3-[(3-cholamidopropyl)dimethylammonio]-1-propanesulfonate
CNS	Central nervous system
CpG	2’-deoxyribo cytidine-phosphate-guanosine
CREB	cAMP-responsive element binding protein
CRID	Cytokine release inhibitory drugs
Da	Dalton
DAMP	Danger associated molecular pattern
DC	Dendritic cell
DD	Death domain
DDX	DEAD box helicase
DHX	DEAH box helicase
DIGE	Differneital in gel electrophoresis
DMEM	Dulbecco’s Modified Eagle’s medium
DMSO	Dimethyl sulfoxide
DNA	Deoxyribonucleic acid
dNTPs	Deoxyribonucleid triphosphates
dsRNA	Double-stranded RNA
DTT	Dithiothreitol
E. coli	*Escherichia coli*
ECL	Electrochemiluminescence
EDTA	Ethylenediaminetetraacetic acid
eGFP	esiRNA against green fluorescent protein
ER	Endoplasmic reticulum
ERK	Extracellular signal regulated kinase
Esi-RNA	endonuclease-prepared small interfering RNA
EST	Express sequence tag
EV	Empty vector
FA	Formic acid

FADD	Fas-associated death domain
FASTA	Fast-All
FBS	Foetal bovine serum
FHA	Filamentous hemagglutinin
GE	General Electric
GFP	Green fluorescent protein
GOLD	Golgi dynamics
GSTO1	Glutathione S-transferase
GTP	Guanosine triphosphate
hr	Hour(s)
HEAT motif	Huntingitin, elongation factor 3, protein phosphatase 2A, TOR1
HEK cell	Human embryonic kidney cell
HCD	Higher-energy collisional dissociation
HCV	Hepatitis C virus
HRP	Horseradish peroxidase
HRV	Human rhinovirus
HSP	Heat shock proteinIAP Inhibitor of apoptosis protein
IAA	Iodoacetamide
IB	Immunoblot
iBMDM	Immortalised bone marrow derive macrophage
ICAM	Intercellular adhesion molecule 1
IEC	Intestinal epithelial cell
IEF	Isoelectric focusing
IFN	Interferon
Ig	Immunoglobulin
IκB	Inhibitor of κB
IKK	IκB kinase
IL	Interleukin
IL-1R	IL-1 Receptor

IL-18R	IL-18 Receptor
iNOS	Inducible nitric oxide synthase
IP	Immunoprecipitation
IPG	Immobilised pH gradient
IPI	International protein index
IRAK	IL-1 receptor associated kinase
IRF	Interferon regulatory factor
ISRE	Interferon stimulated response element
JNK	c-Jun N-terminal kinase
kb	Kilo base
kD	Kilo Dalton
L	Litre
LAL	Limulous amoebocyte lysate
LB	Lysogeny broth
LC/MS	Liquid chromatography mass spectrometry
LFQ	Label free quantitation
LPS	Lipopolysaccharide
LRR	Leucine-rich repeat
MAL	MyD88-adaptor like
MALDI	Matrix assisted laser desorption/ionisation
MAPK	Mitogen acticated protein kinase
MAVS	Mitochondria anti-viral signalling protein
MDA5	Melanoma differentiation-associated gene 5
MEF	Mouse embryonic fibroblast
MHC	Major histocompatibility complex
min	minute
ml	millilitre
mm	milimetre
mM	milli molar

MMLV RT	Moloney murine leukemia virus reverse transcriptase
mRNA	Messenger RNA
MS	Mass Spectrometry/er
MyD88	Myeloid differentiation factor 88
m/z	mass/charge
N-terminal	$-NH_2$ terminal
NLRP	NACHT, LRR and PYD domains-containing protein
NaN	Not a number
NAP1	NF-κB-activating kinase (NAK)-associated protein1
NDK	Nucleoside diphosphate kinase
NEMO	NF-κB essential modulator
NF-κB	Nuclear Factor-κB
ng	nanogram
NK	Natural killer
NLR	Nod-like receptor
nM	nanomolar
NOD	Nucleotide-binding oligomerisation domain
NTP	Nucleotide triphosphate
OD	Optical Density
P	phosphorylated
PAGE	Polyacrylamide gel electrophoresis
PAMP	Pathogen associated molecular pattern
PBS	Phosphate buffered saline
PCR	Polymerase chain reaction
pDC	Plasmacytoid dendritic cell
PEST	Proline, glutamic acid, serine, threonine
PIP_2	Phosphatidylinositol 4-5, bisphosphate
PKC	Protein kinase C
PMA	Phorbol 12-myristate 13-acetate

PMSF	Phenylmethylsulfonyl Fluoride
PMT	Photomultiplier
Poly(I:C)	Polyinosinic:polycytidylic acid
PP/PPP	Protein phosphotase
PRN	Pertactin
PRR	Pattern recognition receptor
PTx	Pertussis toxin
PVDF	Polyvinylidene difluoride
RANTES	Regulated upon activation, normal T cell expressed and secreted
RBP	RNA binding protein
RHIM	RIP homotypic interaction motif
RIG-I	Retinoic acid-inducible gene I
RIP	Receptor interacting protein
RISC	RNA-induced silencing protein
RNA	Ribonucleic acid
ROS	Reactive oxygen species
RP105	Radioprotective 105
RPM	Revolutions per minute
RPMI	Roswell Park Memorial Institute
RT	Room temperature
RT-PCR	Reverse transcriptase PCR
sec	second(s)
S. typhimurium	*Salmonella typhimurium*
SARM	Sterile α and HEAT-Armadillo motifs
Sec	second
SD	Standard deviation
SDS	Sodium dodecyl sulphate
SEAP	Secreted embryonic alkaline phosphatase
SILAC	Stable isotope labelling by/with amino acids in cell culture

siRNA	Small interfering RNA
SOCS	Suppressor of cytokine signalling
SOS	Superoxide dismutase
S&S	Stainer-Scholte
ssRNA	Single stranded RNA
STAT	Signal transducer and activator of transcription
TAB	TAK1-binding protein
TAE	Tris-acetate-EDTA
TAG	TRAM adaptor with GOLD domain
TAK	TGF-β-activated protein kinase
TANK	TRAF-family-member associated NF-κB activator
Taq	Thermophilus aquaticus
TBK1	TANK-binding protein 1
TBS	Tris-buffered saline
TBST	Tris-buffered saline containing Tween 20
TE	Tris-EDTA
TEMED	N, N, N', N' – Tetramethylethylene-diamine
TFA	Trifluroacetic acid
TGF-β	Transforming growth factor-β
$T_H1/2$	Helper type 1/2 T cell
TICAM	Toll-IL-1 receptor (TIR)-containing adaptor molecule
TIR	Toll/IL-1 receptor
TIRAP	TIR domain-containing adaptor protein
TLR	Toll-like receptor
TMED7	Transmembrane emp24 domain-containing protein 7
TNFα	Tumour necrosis factor α
TPI	Triose phosphate isomerase
TRADD	TNFR1 associated death domain protein
TRAF	TNF receptor associated factor

TRAM	TRIF-related adaptor molecule
TRIF	TIR domain-containing adaptor inducing IFN-β
Ubc	Ubiquitin conjugating enzyme
Uev1A	Ubiquitin-conjugating enzyme E2 variant isoform
UTR	Untranslated region
UV	Ultraviolet
VACV	Vaccinia virus
VIPER	Viral inhibitory peptide of TLR4
VP	Viral protein
VRTI	Viral respiratory tract infection
VSV	Vesicular stomatitis virus
v/v	volume per volume
WCL	Whole cell lysate
WT	Wild Type
w/v	weight per volume
µg	micro grams
µl	micro litre
µM	micro molar

Chapter 1

Introduction

1.1 Innate Immunity and Toll-like receptors

The innate immune system encompasses an array of systemic defences whose principle role is to clear an infection or, failing that, to keep it in check until the pathogen can be recognised and cleared by the adaptive immune response. These defences range from relatively simple yet effective physical barriers such as the body's epithelia or the respiratory tract's cilia to those at the molecular level such as the production of nitric oxide by macrophages to degrade phagocytosed pathogens [1]. It is at this molecular level of innate immunity where an explosion of research has occurred over the past fifteen years allowing for the discovery and characterisation of several intrinsic classes of proteins and their associated signalling pathways in exquisite detail [2]. Toll-like receptors (TLRs) are one such class. Belonging to an evolutionary ancient molecular recognition and signalling system, these type 1 transmembrane glycoproteins represent a link between the innate and adaptive immune responses [3].

1.1.1 TLRs

The transmembrane Toll protein was first discovered in the fruit fly *Drosophila melanogaster* and was originally known only for its function in embryogenesis [4]. It took over a decade for proof of its role in defence against fungal and bacterial infections in the fruit fly to become apparent [5, 6]. A similar role in the mouse was also discovered where defects in the bacterial cell wall component lipopolysaccharide (LPS), mediated immune responses were attributed to mutations in the *tlr4* gene [7]. TLRs have since been described in insects and vertebrates including humans and the chicken [8-10]. Structurally similar proteins which include the functionally crucial toll/interleukin-1 receptor (TIR) domain and leucine-rich repeats (LRR) (Figure 1.1A) have also been reported in plants [11], emphasising their broad conservation throughout evolution and thus their fundamental importance in defence against pathogens.

TLRs function by recognizing conserved structural motifs, or pathogen associated molecular patterns (PAMPs) which are inherent to infectious organisms and rarely found in the host. These are unique to pathogens and allow the host immune system to distinguish non-self from self and thus initiate an intracellular signalling cascade which can bring about the appropriate innate and adaptive immune response (Figure 1.1B).

There are 10 functional human TLRs, each with their own particular ligand(s) specificity and effector function. For example, TLR2 can heterodimerise with either TLR1 or TLR6 to recognise triacylated or diacylated lipopeptides respectively [12]. TLR4 recognises the gram-negative bacterial cell wall component LPS, whereas TLR3 and TLR9 recognise signature double stranded RNA (dsRNA) and unmethylated -cytosine-phosphate-guanine- (CpG) motifs respectively [13]. TLR5 senses flagellin, a component of bacterial flagella [14] and TLR 7 and TLR8 sense viral single stranded RNA (ssRNA) [15]. Mysteries remain however, as the ligand for TLR10 has yet to be discovered [16]. TLRs are also activated by host derived, sterile inflammatory mediators known as danger-associated molecular pattern (DAMPs), for example hyaluronan - an extracellular matrix fragment [17]. Thus each member of the TLR family senses different PAMPs and DAMPs, leading to the activation of TLR signalling.

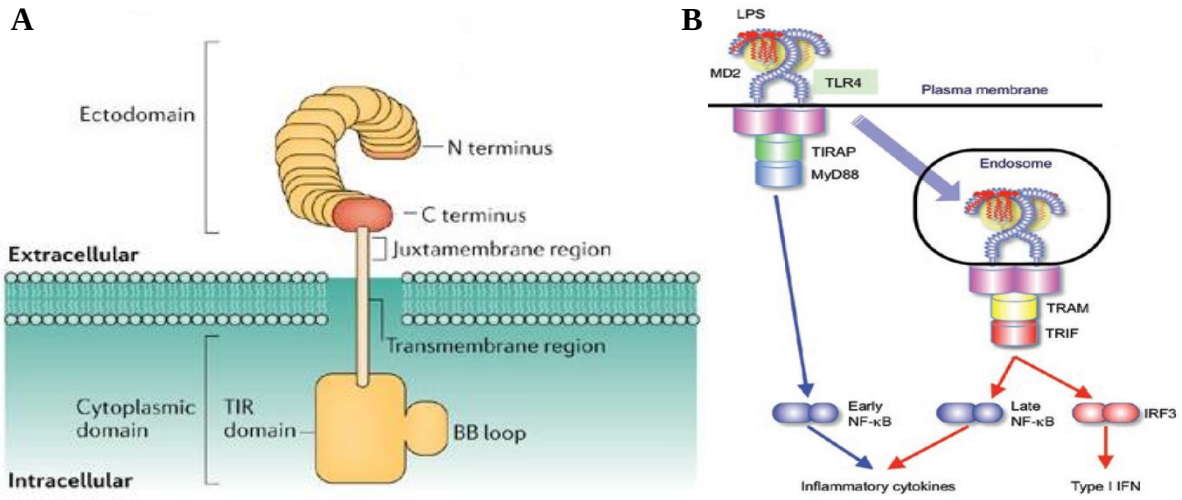

Figure 1.1: Basic TLR structure and signalling. (A) The divergent ligand binding ectodomain of all TLRs consists of multiple leucne rich repeats (LRRs) interspersed with cysteine-rich regions. There is a short transmembrane domain linking the ectodomain to the highly conserved intracellular TIR domain which bears close resemblance to the IL-1R intracellular domain. (B) Recognition of a conserved pathogen associated molecular pattern (PAMP) by TLR4 causes TLR activation, typically by dimerisation and subsequent TIR-TIR domain interactions and autophosphorylation. This induces a downstream signalling process involving a MyD88 dependent or MyD88 independent pathway which culminates in the transcription of inflammatory and anti-viral cytokines. Adapted from [15, 18].

1.1.2 TLR adaptor proteins

The downstream dissemination of TLR signalling involves the recruitment of appropriate adapter proteins which bind to the cytoplasmic TIR-domain of the TLRs via their own intrinsic TIR-domains. There are four activating TLR adaptor proteins: myeloid differentiation factor 88 (MyD88), MyD88 adaptor-like (MAL); also known as Toll-IL-1 adaptor protein (TIRAP), TIR-domain-containing adaptor inducing IFN-β (TRIF; also known as TICAM-1) and TRIF related adaptor molecule (TRAM; also known as TICAM-2 and TIRP) [12]. These adapter proteins couple to downstream protein kinases that ultimately lead to the activation of transcription factors such as nuclear factor-κB (NF-κB) and members of the interferon (IFN)-regulatory factor (IRF) family. The critical domain common to all five of the TLR adaptors as well as to the TLRs themselves is the TIR domain. This is located on the cytoplasmic portion of all TLRs and allows binding to the reciprocal TIR-domain on the

exposed surface of the adaptor molecule. The IL-1 receptor (IL-1R) also contains a TIR-domain hence the existence of the TLR/IL-1R superfamily [13]. Despite the TLRs having somewhat similar signal transduction pathways, there is specificity with regard to their adaptor usage (Figure 1.6) [19]. MyD88 is the common downstream adaptor that is recruited by all TLRs, except TLR3 [20]. MAL is required for TLR4, and to a lesser extent, TLR2 signalling [21, 22]. TRIF mediates TLR3 and TLR4 signalling [23]. Finally, TRAM mediates TLR4 signalling exclusively, acting as a bridging adaptor to recruit TRIF to the TLR4 complex [23, 24]. In addition, an inhibitory TLR adaptor protein called sterile alpha and TIR motif-containing protein (SARM) has also been identified which negatively regulates TRIF mediated signalling (Figure 1.6) [25].

TLR4 is the only TLR whose activation utilises all five TLR adaptor proteins and as a result, its signalling is split into two broad categories according to its use of the MyD88 adaptor. The 'MyD88 dependent' pathway is used by all TLRs except TLR3. TLR3 utilises TRIF only (Figure 1.6) [12]. However, loss of MyD88 does not completely abolish TLR4 signalling as is the case with other TLRs. The 'MyD88 independent' pathway uses the adapters TRAM and TRIF in the case of TLR4 signalling to activate anti-viral and late-stage inflammatory responses. Thus, the function of the adaptor proteins is to provide specificity to TLR signalling in order to tailor the resulting cytokine profile to best defend against the infectious agent. To summarise, TLR engagement in response to a PAMP or DAMP instigates the recruitment of the relevant TLR adaptor protein(s) which provides a docking platform for downstream effector signalling molecules. This culminates in the production of proinflammatory cytokines, chemokines, and antimicrobial type I IFNs (IFN-β and IFN-α) which serve to trigger an inflammatory and/or antimicrobial immune response to limit the infectious agent. The remainder of this section will provide a more detailed discussion of the functionality of each of the TLR adaptors.

1.1.3 MyD88

Figure 1.2: Schematic illustrating domain segmentation of MyD88. MyD88 is 296 amino acids (aa) in length and contains two domains. At the C terminus (aa 1–110) is the death domain (DD) and at the N terminus (aa 155–296) is the TIR domain. Adapted from [26].

Human myeloid differentiation factor 88 (MyD88) was first identified in 1990 as the 88 th gene that was induced during the terminal differentiation of myeloid precursor cells in response to IL-6 [27]. It is 296 amino acids (aa) in length and contains three domains: an N-terminal death domain (DD) which enables interactions with downstream DD containing proteins, an interdomain, and a C-terminal TIR domain which facilitates homotypic interaction with other TIR-containing proteins (Figure 1.2) [28]. Early studies indicated that its 5' upstream sequences contained an interferon regulatory factor 1 (IRF-1) binding site and in 1997, it was identified as an adaptor in the IL-1R complex that was required for IL-1 and IL-18 signalling [29-32]. Almost immediately after these discoveries, the fundamental importance of MyD88 in an immunological setting was becoming evident as mice deficient in the protein were shown to be unresponsive to the bacterial cell wall component endotoxin, a critical mediator of septic shock [33, 34]. It was eventually shown to be the master adaptor molecule in mediating TLR2 signalling and subsequently also in TLR4, TLR5, TLR7/8, TLR9, TLR13 but not TLR3 [35-42].

1.1.3.1 MyD88 mediated signalling

MyD88 exists primarily in the cytoplasm of resting cells wherein it is thought to exist in a weak and reversible oligomerised form [43, 44]. Upon TLR activation and consequent TIR-dimerisation, MyD88 binds to the TLR complex via its TIR-domain, thus stabilising its oligomeric form to provide a platform for downstream molecules to bind via DD-DD interactions. Interleukin-1 receptor-associated kinase 4 (IRAK4), is the critical molecule downstream of MyD88, being absolutely required for MyD88 dependent signalling and for the recruitment of further downstream molecules, IRAK1 and IRAK2 (Figure 1.3) [45]. A crystal structure has been generated of the MyD88, IRAK4, IRAK2 DD complex which has shown that a left-handed helical oligomer is formed consisting of 6 MyD88, 4 IRAK4 and 4 IRAK2 molecules [43]. Complex formation is hierarchical whereby MyD88 first recruits IRAK4. This complex, but not its individual parts, is required to recruit IRAK2 or the related IRAK1. The resulting structure has been termed the Myddosome and serves to bring the kinase domains of the IRAK molecules into close proximity to drive their autophosphorylation [43, 44]. Phosphorylation of the IRAKs recruits the E3 ubiquitin ligase, TNFR-associated factor -6 (TRAF6) which ubquitinates itself [46]. TRAF6 utilises its E3 ubiquitin ligase activity to ubiquitinate a scaffolding protein, NFκB essential modulator ((NEMO) [47] (Figure 1.3). The combination of TRAF6 mediated ubiquitin chain formation and NEMO functions to recruit TGF-β activated kinase 1 (TAK1) which itself recruits the TAK-1 binding proteins 1 (TAB1) and TAB2. TAK1 phosphorylates IKKβ as well as initiating a MAP kinase cascade leading to activation of the transcription factor CREB. IKKβ phosphorylates the inhibitors of κB (IκB) α and IκBβ leading to NFκB release and nuclear translocation to bind the promoter regions of pro-inflammatory cytokines such as TNFα and IL-12 (Figure 1.3).

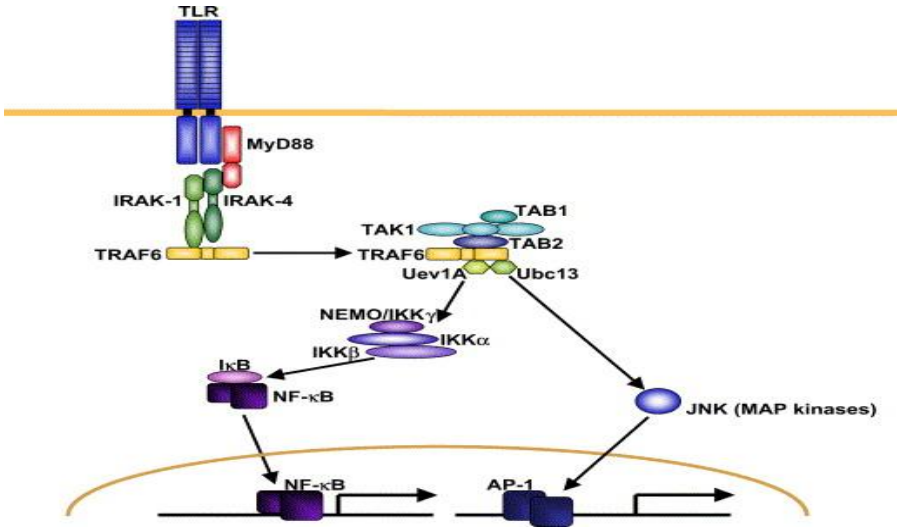

Figure 1.3: MyD88 dependent TLR signalling pathway. MyD88 binds to the intracellular protion of a TLR via TIR-TIR domain interactions. Upon TLR activation, IRAK-1, IRAK-4 and TRAF-6 are recruited to the receptor causing MyD88-IRAK-1 interactions via death domain (DD) interactions. IRAK-4 phosphorylates IRAK-1 which phosphorylates TRAF-6. TRAF-6 then dissociates and interacts with TAK1, TAB1, and TAB2 which in turn recruits Ubc13 and Uev1A. This induced TAK1 activation which in turn activates the IKK complex consisting of IKKα, IKKβ and IKKγ/NEMO. The MAP kinase JNK is also activated. These then activate the transcription factors NFκB and AP-1 respectively which induce pro-inflammatory gene expression. Adapted from [48].

1.1.4 MAL

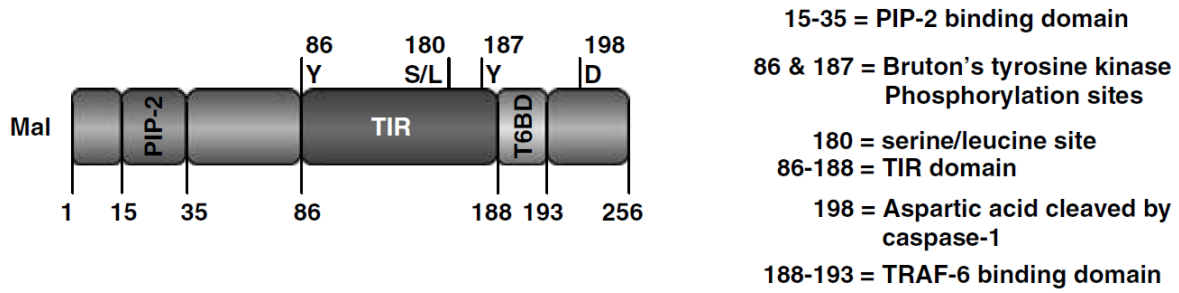

Figure 1.4: Schematic illustrating domain structure of MAL. Mal is 256 aa long. At the N terminus, there is a PIP_2-binding domain (aa 15–35). This is followed by the TIR domain (aa 86–188) and a TRAF6 domain (aa 188–196). There are two phosphorylation sites at positions 86 and 187. Located at position 180 is the serine/leucine site linked to the genetic susceptibility to several diseases including TB and malaria. At position 198 is the aspartic acid indicating the presence of the caspase-1 cleavage site. Adapted from [26].

MAL, or TIRAP, the second TLR adaptor to be identified, was simultaneously discovered by two independent labs in 2001 [22, 49]. Having observed late stage NF-κB and Jun N-terminal kinase (JNK) activation in MyD88 deficient mice, Fitzgerald and colleagues [22], speculated that another, as yet unidentified TIR domain-containing adaptor protein was mediating this effect. High-throughput sequencing of a human DC expressed sequence tag cDNA library identified MAL – a TIR domain-containing protein, 235 aa in length (Figure 1.4), that was capable of activating NF-κB (via IRAK2) and JNK as well as extracellular signal-regulated kinase (ERK) -1 and -2. MAL was shown to homodimerise and heterodimerize with MyD88. It was also shown that a dominant-negative form of Mal inhibited TLR4 (but not IL-1R or IL-18R) mediated NF-κB activation [22, 49]. It is generally accepted that MAL acts a bridging adaptor between MyD88 and TLR4 and TLR2 [15].

1.1.4.1 MAL Localization

MAL is localised primarily to the plasma membrane, although MAL-positive, actin-negative vesicles can be found throughout the cell [50]. MAL is concentrated at the leading edge of murine embryonic fibroblasts (MEFs) and in macrophages, MAL is localised to discrete regions of the plasma membrane called membrane ruffles which are biochemically similar to the leading edge of fibroblasts [50]. MAL interacts with the TIR domain of TLR2 and TLR4. This association is facilitated by the phosphatidylinositol 4,5-bisphosphate (PIP_2)-binding domain contained within the N-terminal region of MAL. This allows MAL to target to PIP_2-rich regions of the plasma membrane which contain high levels of TLR2 and TLR4, thus facilitating their association with MAL [12, 50]. Notably, MAL is not involved in the recruitment of MyD88 to other compartments, including endosomal compartments devoid of PIP_2. Further, in MAL/MyD88 double-deficient cells, transfection of a mutant construct which incorporates a PIP_2 binding site to the C-terminus of MyD88 directs MyD88 to the plasma membrane and restores lipopolysaccharide (LPS) signalling via TLR4 [50]. Surface charge distribution models of MAL, MyD88, and TLR4 have shown that the TIR domains of TLR4 and MyD88 are electropositive – and would thus be expected to repel each other under normal circumstances. However, the TIR domain of MAL is electronegative which would facilitate binding of TLR4 to MyD88 in order to transduce TLR4 signalling [12, 51]. Moreover, molecular docking experiments have suggested that MAL binds to a homodimer of TLR4 and that MAL binds to the same region of the TLR4 dimer interface [52].

1.1.4.2 Mal and TLR4 Signalling

Ligand engagement of TLR4, for example, binding of LPS via MD-2 and cluster of differentiation 14 (CD14), causes TLR4 dimerisation and nonexclusive interaction with MAL. Docking experiments have predicted that the MAL (and TRAM) interaction surfaces on the TLR4 dimer interface are at either side of the structure rather than at the top, a region that

would be sterically hindered by the membrane [52]. The TLR4 dimer:MAL complex provides a platform allowing MyD88 to bind which then facilitates the recruitment of IRAK1 and IRAK4. Tumour necrosis factor (TNF)-receptor-associated factor 6 (TRAF6) is subsequently recruited and activated via an oligomerisation/auto-ubiquitination event. Activated TRAF6 then recruits transforming growth factor activated kinase 1 (TAK1) and TAK1 binding protein 2 (TAB2). This complex interacts with the inhibitor of NF-κB kinase (IKK) complex, which consists of IKKα, IKKβ, and IKKγ (also known as NEMO), leading to the activation of NF-κB and subsequent activation of NF-κB-dependent genes, including the proinflammatory cytokines IL-1β, IL-6 and TNFα (Figure 1.6) [53].

1.1.4.3 MAL and TLR2 Signalling

The role of MAL in TLR2 signalling is complicated by the fact that TLR2 can heterodimerise with both TLR1 and TLR6 to recognize tri- and diacylated lipopeptides, respectively. Overexpression studies have shown that MAL interacts with TLR1 and TLR2, but not TLR6 [21]. Although MAL was originally suspected to be essential for TLR2 signalling, more recent studies have shown that MAL plays a lesser role here when compared to TLR4 [21, 49]. Specifically, whilst MAL is required for TLR2 signalling when exposed to low levels of *Salmonella typhimurium (S. typhimurium),* MAL is redundant at high concentrations of ligand or in response to high levels of *S. typhimurium* [21]. This suggests that the physiological role of MAL in the context of TLR2 signalling is to prime or amplify low strength bacterial signals.

1.1.4.4 Modulators of MAL Functionality

Additional levels of specificity and control are added to TLR signalling by virtue of the fact that the TLR adaptors themselves are subject to a myriad of regulatory mechanisms. MAL contains a proline, glutamic acid, serine, and threonine (PEST) domain, located at amino acids 32–72 in human MAL [54]. PEST domains are found in short-lived proteins which undergo phosphorylation, polyubiquitination of lysine residues, and subsequent degradation via the 26S proteasome. The presence of a PEST domain in MAL would therefore suggest that it may be a target for degradation. Interestingly, suppressor of cytokine signalling 1 (SOCS-1), has been shown to inhibit LPS signalling by ubiquitinating MAL and thus targeting it for proteosomal degradation [55] . The ubiquitination of MAL is facilitated by Bruton's tyrosine kinase (Btk) – a protein which is the case of MAL, performs two important functions. Specifically, Btk induces tyrosine phosphorylation of MAL, thus potentiating TLR2/4-driven NF-κB signalling [56]. However, the same phosphorylation event provides a platform for the aforementioned SOCS-1 mediated ubiquitination/degradation of MAL – thus serving to limit the over-activation of the inflammatory immune response [12]. IRAK1 and IRAK4 have also been shown to phosphorylate MAL, thereby facilitating its TLR4-ligand-mediated ubiquitination and degradation; IRAK1 and IRAK4 inhibitors blocked this effect [57]. MAL has also been shown to interact with caspase-1, with cleavage of MAL by caspase-1 being required to modulate MAL functionality [58]. A number of studies have been carried out on a variant of MAL that contains a leucine at position 180 instead of a serine [59-61]. It has been reported that MAL Ser180Leu does not associate with TLR2 and confers a protective phenotype in malaria and tuberculosis by inhibiting the inflammatory response. Other groups dispute this claim [28]. Overall, the studies to date indicate an association between heterozygosity at MAL Ser180Leu and protection against multiple infections.

1.1.5 TRIF

Initially, MAL was thought to mediate the MyD88-independent pathway following TLR4 engagement, leading to IRF3 activation and delayed activation of NF-κB [12]. However, given that MAL was instead shown to act as a bridging adaptor in the MyD88-dependent pathway which was activated following TLR4/TLR2 engagement, it remained unclear how TLR4 might mediate the MyD88 independent production of IFN-β [12]. In 2003, a third TLR adaptor, TRIF, also known as TICAM-1, was identified by two separate groups. One employed a database screen to identify novel TIR-domain containing proteins with the other employing a yeast two-hybrid screen using TLR3 as bait [41, 62]. It was found that overexpression of TRIF, 712 aa in length (Figure 1.5), leads to the induction of the IFN-β promoter. In TRIF-deficient mice, whilst impaired TLR3 and TLR4 mediated IRF3 activation and concomitant IFN-β induction was observed, TLR2, TLR7 and TLR9 signalling were unaffected [63]. Notably, TLR4 mediated NF-κB activation is completely abolished in cells deficient in both MyD88 and TRIF and a germline TRIF mutation in mice termed Lps2 confirmed TRIF's essential role in mediating 'MyD88-independent' pathway [28, 63, 64].

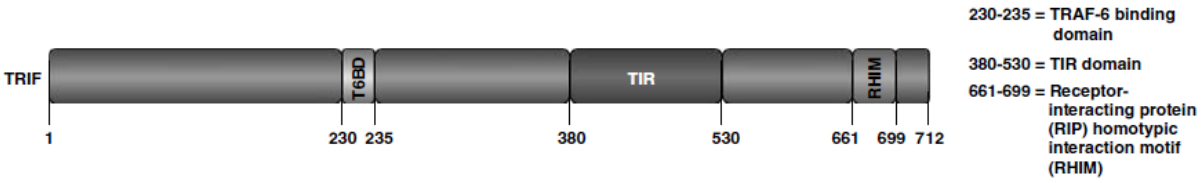

Figure 1.5: Schematic illustrating domain segmentation of TRIF. TRIF is 712 aa in length. It consists of a TRAF6-binding domain (aa 230–235), the TIR domain (aa 380–530) and a receptor-interacting protein (RIP) homotypic interaction motif (RHIM) (aa 661–699). Adapted from [26].

1.1.5.1 TRIF Localisation

TRIF is expressed at low levels in most tissues and cells and is diffusely localised in the cytoplasm of resting cells [65]. When endosomal TLR3 is activated by dsRNA, TRIF transiently colocalises with TLR3 and then dissociates from the receptor forming speckled structures that localise with downstream signalling molecules. Upon stimulation of TLR4 with LPS, TRIF is activated by endosomal TRAM, which associates with the internalised TLR4 complex [65]. Thus, TRIF is indirectly recruited to TLR4 via TRAM (Figure 1.6). Also, overexpression of TRIF leads to homo-oligomerisation through the TIR-domain and the C-terminus, forming a complex called the TRIF signalosome [28, 65].

1.1.5.2 TRIF and TLR3/4 Signalling

TRIF has consensus TRAF-6 and TRAF-2 binding motifs in the N-terminal region as well as a C-terminal receptor-interacting protein (RIP) homotypic interaction motif (RHIM) domain [12, 65]. The TIR domain of TRIF is essential for binding to the TIR domain of TLR3 [62]. These domains serve to facilitate TRIF-mediated signalling, with each domain playing a distinct role. The N-terminal region of TRIF participates in IRF3/7 activation by recruiting the IRF3-activating kinases, TANK-binding kinase 1 (TBK1), and inhibitor of NF-κB kinase ε (IKKε, also known as IKKi) [12]. NAK-associated protein 1 (NAP-1) forms part a kinase complex activating IRF3 and also serving to facilitate the association of TRIF with TBK1 and IKKε (Figure 1.6) [66]. Upon TBK1/IKKε-mediated phosphorylation of the IRF3/7 complex, the IRFs homo and heterodimerise followed by their translocation to the nucleus. Here, they bind to both the IFN-β enhanceosome and the IFN-stimulated response elements (ISREs) to induce the transcription of responsive genes including the type-I IFN and RANTES, otherwise known as CCL5, genes [67]. TRAF3 plays a crucial role in TLR3 signalling as various independent studies show that TRAF3 forms a complex with NAP-1 and TRIF (Figure 1.6) [68, 69]. Two separate NF-κB activation pathways bifurcate from TRIF, and

these map to distinct sites at the N- and C-termini. The binding motifs in the N-terminal region of TRIF serve to recruit TRAF6, although its role in TRIF signalling remains controversial [12]. Studies suggest that the participation of TRAF6 in TRIF-mediated NF-κB induction is cell type specific as TRAF6 is essential for NF-κB activation in mouse embryonic fibroblasts (MEFs), whereas TLR3 induced NF-κB activation is not impaired in TRAF6-deficient macrophages [70, 71]. There is a separate route to NFκB activation involving the RHIM domain of TRIF which facilitates the recruitment of both RIP1 and RIP3 through this domain (Figure 1.6) [72]. Adding credence to the importance of RIP1 and RIP3 in TRIF signalling is the fact that poly(I:C)-induced NF-κB activation is completely blocked in RIP-1-deficient MEFs [73]. In contrast, RIP3 has been shown to negatively regulate the TRIF–RIP1–NF-κB pathway [72]. TRIF also mediates the induction of apoptosis through TLR3 and TLR4. This is facilitated by direct recruitment of RIP1 to the C-terminal RHIM domain of TRIF, and involves activation of a complex containing TNFR1 associated death domain protein (TRADD), Fas-associated protein with death domain (FADD), and caspase-8 (Figure 1.6) [74]. This apoptotic pathway is believed to be responsible for bacterial-induced apoptosis of infected DCs [12].

1.1.5.3 TRIF and TLR5 Signalling

Although it was thought that TRIF mediated TLR3 and TLR4 signalling only, a number of recent studies have shown that TRIF also plays an important role in TLR5 signalling (Figure 1.6) [75, 76]. Stimulation of human colonic epithelial cells with the TLR5 ligand flagellin, allows TLR5 and TRIF, but not TRAM, to interact and mediate TLR5-induced NF-κB and mitogen-activated protein kinase (MAPK) activation in intestinal epithelial cells (IEC). TRIF-deficient IECs stimulated with flagellin exhibit decreased inflammatory cytokine expression compared to their wildtype counterparts. Furthermore, TRIF deficient mice are resistant to flagellin-mediated exacerbation of colonic inflammation and dextran sulphate

sodium–induced experimental colitis [75]. In contrast, studies by the same group have shown that TRIF-induced caspase activity causes the degradation of TLR5 indicating that TRIF can participate in the proteolytic modification of TLR functionality at the posttranslational level [76]. These recent findings therefore suggest that TRIF plays an important role in regulating host-microbial communication via TLR5 in the gut epithelium.

1.1.5.4 TRIF and Cytosolic dsRNA Detection

A further role for TRIF in innate immune signalling, independent of the TLRs, has recently been identified whereby TRIF appears to be an essential component of a novel dsRNA sensing pathway in DCs [77]. Specifically, the RNA helicases DEAD box helicase 1 (DDX1), DDX21, and DEAH box helicase 36 (DHX36) form a complex which enables the sequestration of cytosolic dsRNA. This complex then binds to TRIF to initiate the production of type I IFN and inflammatory cytokines. It has been shown that DDX1 binds dsRNA via its helicase A domain, with DHX36 and DDX21 binding to TRIF via their HA2-DUF and PRK domains respectively. The resulting complex triggers the innate antimicrobial response [77].

1.1.5.5 Negative Regulation of TRIF

Numerous strategies exist to curtail TRIF signalling, either directly, or via inhibition of downstream signalling molecules. A number of molecules have been identified that directly inhibit TRIF. For example, the inhibitory TLR adaptor protein SARM contains a TIR domain and serves to inhibit TRIF mediated signalling. SARM has been shown to interact with TRIF and both the TIR and SAM domains of SARM are vital for SARM's functionality in this regard. While the exact mechanism of inhibition has not been elucidated, it is suspected that SARM and TRIF interact via their TIR domains, thus preventing the binding of downstream effector molecules such as RIP1 (Figure 1.6) [25]. Alternatively, the SAM domain of SARM may facilitate recruitment of an as yet unidentified inhibitory molecule. Consistent with a role

for TRIF in restricting viral replication through type I IFN induction, at least two viruses have been shown to contain proteins that antagonize TRIF. Vaccinia virus (VACV) encoded proteins, A46R and A52R, differentially affect TRIF signalling. A46R interacts directly with TRIF and inhibits TRIF mediated TLR3 signalling. Notably, A46R also interacts with the other TLR adaptors and also inhibits TLR4 signalling [78]. In contrast, A52R acts downstream of the adaptors by targeting TRAF6 and IRAK2-containing complexes to inhibit TLR4, TLR2 and TLR5 signalling [79]. Hepatitis C virus (HCV) contains a serine protease NS3-4A that causes the proteolysis of TRIF. The cleavage of TRIF by NS3-4A inhibits both NF-κB and IRF3 activation by TLR3, thus disabling the innate immune response to the virus [80]. These examples illustrate the importance of TRIF in mediating the anti-viral signalling pathway such that specific inhibition by VACV and HCV confers an advantage to the viruses in vivo.

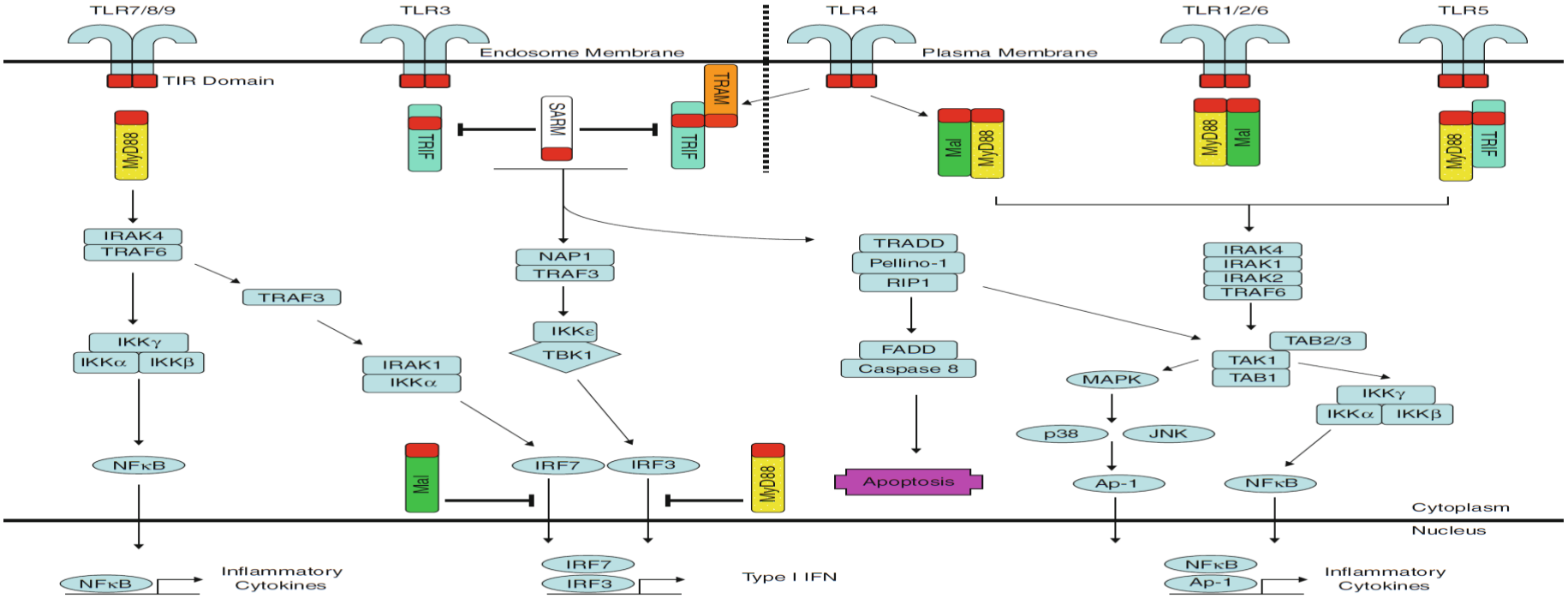

Figure 1.6: Overview of TLR signalling the role of the TIR-domain containing adaptors. MyD88 is the central adaptor in TLR signalling, capable of transducing signals mediated by all TLRs except TLR3. MyD88 does however negatively regulate TLR3-induced IRF3 activation. Regarding TLR1/2, TLR2/6, TLR4, and TLR5 signalling, MyD88 interacts with the each TLR though their TIR domains (red). IRAK4 is then recruited to the complex which in turn recruits IRAK1 and/or IRAK2 via death domain (DD) interactions. TRAF6 is then recruited to activate TAK1, leading to subsequent activation of MAPK and NF-κB. In the case of TLR7/8/9 signalling, the MyD88 complex can also recruit TRAF3 which activates IRF7. TRIF is the sole adaptor involved in TLR3 signalling and recruits NAP1 and TRAF3 to activate the noncanonical IKKs, TBK1, and IKKε. These in turn phosphorylate IRF3 and IRF7 causing their translocation into the nucleus where they bind to the type I IFN (IFNα and IFNβ) gene promoters. TRIF is also required to mediate maximal TLR5-induced NF-κB and MAPK activation by binding directly to TLR5. As part of a suspected negative feedback loop, TRIF can also mediate caspase-dependent TLR5 degradation. MAL acts as a bridge to allow TLR4 and to a lesser extent TLR2, to signal via the MyD88 pathway. MAL also negatively regulates TLR3-mediated IRF7 activation. TRAM, like MAL, is another bridging adaptor and links TLR4 to the TRIF pathway. The Mal-MyD88 and TRAM-TRIF complexes facilitate bifurcation of the TLR4 pathway to allow for the synthesis of both inflammatory cytokines and type I IFN, respectively. The fifth adaptor SARM interacts with TRIF and impairs TRIF signalling

1.1.6 TRAM

In 2003, the fourth TIR-domain-containing adaptor, TRAM, 235 aa in length, was identified following a bioinformatic search of the human genome database [23, 81]. It was initially thought that TRAM was involved in both TLR and IL-1R mediated NF-κB activation, but not IFN-β induction [81]. Subsequently, a more definitive description of TRAM showed that it interacts with TLR4 and TRIF to regulate TLR4-mediated IRF3 and IRF7 activation [23]. TRAM deficient cells have impaired TLR4-mediated cytokine production and B cell activation, as was observed with TRIF [24]. It is now accepted that TRAM acts as bridging adaptor between TLR4 and TRIF in the 'MyD88-independent' pathway [12].

1.1.6.1 TRAM localisation and involvement in TLR4 signalling

TRAM exclusively mediates TLR4 signalling. It activates the 'MyD88-independent' pathway by facilitating the association of TRIF with TLR4 - similar to the way in which MAL links TLR4 and MyD88 (Figure 1.6). To date, it serves no other known role in TLR signalling [15]. Regarding localisation, the N-terminal region of TRAM is constitutively myristoylated on its glycine at position two, which facilitates its association with the plasma membrane. Indeed, mutation of TRAM's myristoylation motif abolishes its ability to signal [82]. A distinct requirement for TRAM signalling to occur is its phosphorylation on serine 16 by protein kinase C epsilon (PKCε) [83]. TRAM has also been shown to contain a bipartite sorting signal that modulates its trafficking between the plasma membrane and the endosomes. In fact, TRAM must be delivered to the endosomes in a complex with TLR4 to facilitate the activation of IRF3 [84]. Thus, activation of TLR4 sequentially induces two signalling pathways from two different cellular locations. The 'MyD88-dependent' pathway is induced from the plasma membrane, whereas the 'MyD88-independent' pathway is induced from endosomes (Figure 1.6).

1.1.6.2 Negative Regulation of TRAM

VACV is capable of modulating TRAM functionality. An 11-aa-long peptide derived from the VACV protein A46R, termed viral inhibitor peptide of TLR4 (VIPER), has been shown to interact with TRAM (and MAL), towards inhibiting TLR4 signalling. Mechanistically, it has been postulated that masking of the critical binding sites on MAL and TRAM by VIPER specifically inhibits their ability to interact with the cytoplasmic TIR-domain of TLR4 - thus inhibiting its signalling [85]. A splice variant of TRAM, termed TRAM adaptor with Golgi dynamics (GOLD) domain (TAG), has been shown to competitively bind TRAM and displace TRIF during LPS signalling, leading to decreases in RANTES cytokine production without affecting NF-κB activation [86]. A second related protein, transmembrane emp24 domain-containing protein 7 (TMED7), which sits next to TRAM and TAG on chromosome five, is also a TRAM inhibitor and thus a negative regulator of TLR4 signalling. Is it is believed that TMED7 interacts with both TAG and TRAM and is required for TAG's ability to displace TRIF from TRAM [87].

1.1.7 SARM

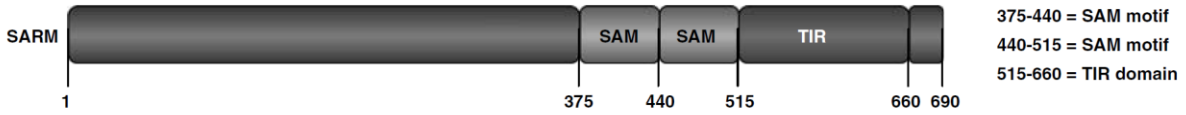

Figure 1.7: Schematic illustrating domain segmentation of SARM. SARM is 690 aa in length and is made up of several domains. There are two SAM motifs between amino acid 375 and 515 followed by the TIR domain between 515 and 660. Adapted from [26].

SARM was initially identified in 2001 as a human gene conserved across multiple taxa [88]. Structurally, SARM is 690 aa in length and contains two sterile alpha motifs (SAM) domains as well as a HEAT/Armadillo repeat motif (ARM) domain. Both the SAM and ARM domains are known to be involved in the formation of protein complexes [88]. It was initially shown that the *Caenorhabditis elegans* SARM homologue, TIR1, was important in the efficient immune response against fungal and bacterial infection [89]. However, in human cells, it was shown that unlike the other TIR-domain adaptors, overexpression of SARM failed to induce NF-κB or activate IRF3-dependent reporter genes and in fact inhibited their activation and expression [25]. In contrast, a later study showed that macrophages from SARM knockout mice responded normally to TLR3, TLR4, and TLR9 ligands, suggesting that mouse SARM has a redundant role in regulating macrophage responses to these TLR ligands [28]. Further research must be undertaken to definitively assign a role for SARM in TLR signalling.

1.1.7.1 SARM and TLR3/4 Signalling

Although disputed, it appears that in humans, SARM inhibits TRIF-mediated TLR3 and TLR4 signalling by selectively targeting TRIF. In unstimulated cells, SARM and TRIF are weak interactors, but stimulation with LPS or poly(I:C) induces SARM protein expression and enhances the interaction between SARM and TRIF [25]. SARM overexpression serves to inhibit TRIF-dependent, but not MyD88- or MAL dependent NF-κB activation. SARM also

inhibits poly(I:C)-mediated RANTES and IFN-β promoter activity (Figure 1.6). The exact mechanism utilized by SARM to impair TRIF functionality requires further investigation, however it is speculated that SARM may use its TIR domain to bind TRIF and use its SAM domains to recruit an as-yet-unidentified inhibitor. Alternatively, SARM may competitively block the ability of TRIF to directly interact with downstream signal transducers such as TBK1, RIP1, and TRAF6 [25].

1.1.7.2 SARM in the central nervous system

A study conducted in SARM deficient mice has indicated a role for SARM in protection from death after central nervous system (CNS) infection with vesicular stomatitis virus (VSV) [90]. This was associated with reduced CNS injury and significantly reduced inflammatory cytokine production which would suggest that at least in the murine CNS, SARM is in fact a positive regulator of the innate immune response. Moreover, a seperate study conducted in SARM -/- mice also indicated its requirement for inflammatory cytokine production in the reponse to infection with West Nile virus (WNV) [91]. WNV replication was increased specifically within the brain stem of SRAM deficient mice compared to WT and this was associated with decreased levels of TNFα, decreaeed microglia activation and increased neuronal death [91].

1.1.8 Negative Regulation of TLR Signalling by TLR Adaptors

A number of recent studies have highlighted the role of the TLR adaptors themselves in the curtailment of TLR signalling. For example, MyD88 has been shown to negatively regulate TLR3-TRIF-induced corneal inflammation through a mechanism involving JNK phosphorylation, but not p38, IRF3, or NF-κB and to inhibit TLR3-dependent IL-6 induction [21, 92]. MyD88 has also been shown to inhibit TLR3-dependent phosphorylation of IRF3 and thus curtail TLR3-mediated IFN-β and RANTES production [93]. Furthermore, MAL

has been shown to inhibit TLR3 dependent IFN-β production through a mechanism that is distinct from MyD88, instead inhibiting TLR3 mediated IRF7 activation [94]. As already stated, SARM has been shown to inhibit TRIF-dependent TLR3 and TLR4 signalling (Figure 1.6) [25].

1.2 Proteomics and its applications in immunology

The ability to compare the different functional states of a biological system has led to many major biological discoveries, a prime example being ubiquitination, having resulted from comparisons between stressed and normal cells [95]. Comparative genomics has fulfilled this need for the past decade and indeed led to many seminal discoveries particularly in genomic medicine [96]. However, proteins are typically the effector entities in biological systems and transcript analysis often poorly predicts the level of mature, activated protein [97]. A typical example is the inflammatory protein IL-1β whose function is dependent upon a bi-phasic regulatory process. An initial signal, termed signal 1, induces initial IL-1β mRNA transcription and subsequent translation to produce a zymogenic form called pro-IL-1β. A second signal is required to cleave pro-IL-1β into its active, secreted form [98]. Reliably defining the levels of this secreted, bioactive form of IL-1β would be impossible to detect by monitoring transcription levels alone. Therefore, proteomics can provide insights into key biological processes from a different and ultimately more functional perspective.

By definition, proteomics is the global study of organismal proteins and can include their structure, isoforms, modifications, interactions, ordering and in essence, anything relating to proteins that is post-genomic. Genomics is however, of central importance in proteomics as it provides the blueprint of possible gene products from which we can readily identify and comprehend the proteome [99].

1.2.1 Technique and Evolution

Mass spectrometry is an analytical technique that measures ionised molecules in a gas phase in order to qualitatively and quantitatively study proteins and their modifications. At its core, a mass spectrometer (MS) consists firstly of an inlet system, for example, liquid or gas chromatography which performs an initial separation of complex protein mixtures prior to injection into the MS. Immediately prior to their entry into the MS, the samples are ionised

by what is known as an ion source. Sample ionisation is critical for analysis as MS mediated protein identification essentially occurs by measuring the mass:charge ratio (m/z) of incoming molecules and these sample molecules must therefore be charged or ionised for this to occur. Biological samples such as proteins and peptides are thermolabile and are thus best suited to soft ionisation techniques such as electrospray ionisation (ESI) and matrix-assisted laser desorption/ionisation (MALDI). Non thermolabile samples can be ionised using electron impact or chemical ionisation. ESI ionises the proteins from solution and is therefore easily combined with liquid chromatography for complex sample analysis. MALDI uses laser pulses to first sublimate and then ionise samples from a dry crystalline matrix and is more suited to analysis of less complex sample mixtures. The contribution of sample ionisation techniques such ESI and MALDI to mass spectrometry is illustrated by the awarding of the 2002 Nobel Prize in Chemistry for their development. ESI was used exclusively in the current project.

There are many different types of mass analyser with the most used being ion trap, time-of-flight, quadrupole and Fourier transform ion cyclotron and orbitrap. Ion-trap and orbitrap were used in the current study.

1.2.1.1 2D PAGE and 2D DIGE

The study of proteomics was originally based upon two-dimensional polyacrylamide gel electrophoresis whereby protein lysates, solubilised from a cell population, tissue or biological fluid, are separated first according to their isoelectric point (first dimension) and secondly according to their molecular mass by SDS-PAGE (second dimension). Resolved proteins are then visualised by silver staining and the protein spot size between different gels (representing different biological conditions) could be visually, or as the technology matured, electronically compared. Protein spots with significant variations in expression between

biological conditions are then excised, destained, fragmented into peptides and analysed by mass spectrometry (MS) to identify the parent proteins based on peptide-protein databases (Figure 1.8). Problems with this technique included the large volumes of protein required (a particular drawback when analysing clinical samples), inter-gel variability which plagued reliability and most pressingly, the relatively limited cross-section of proteins visualised – typically consisting of only highly abundant proteins. Resolution was increased by fractionating the proteins over a narrower pH range in the first dimension thereby increasing resolution, albeit at the expense of proteins outside the pH. This advance was aided by the introduction of precast immobilised pH gradient (IPG) strips for the first dimension seperation in which the pH gradient is fixed within the acrylamide matrix. A further innovation was the development of a technique termed differential in-gel electrophoresis (DIGE) which utilised highly sensitive, fluorescent labelling of protein samples with up to three independent dyes to enable multiple biological samples to be subjected to electrophoresis on a single gel (Figure 1.9). This effectively eliminated the problem of inter-gel variability and greatly reduced the amount of sample required. 2D-DIGE was used extensively in the current work.

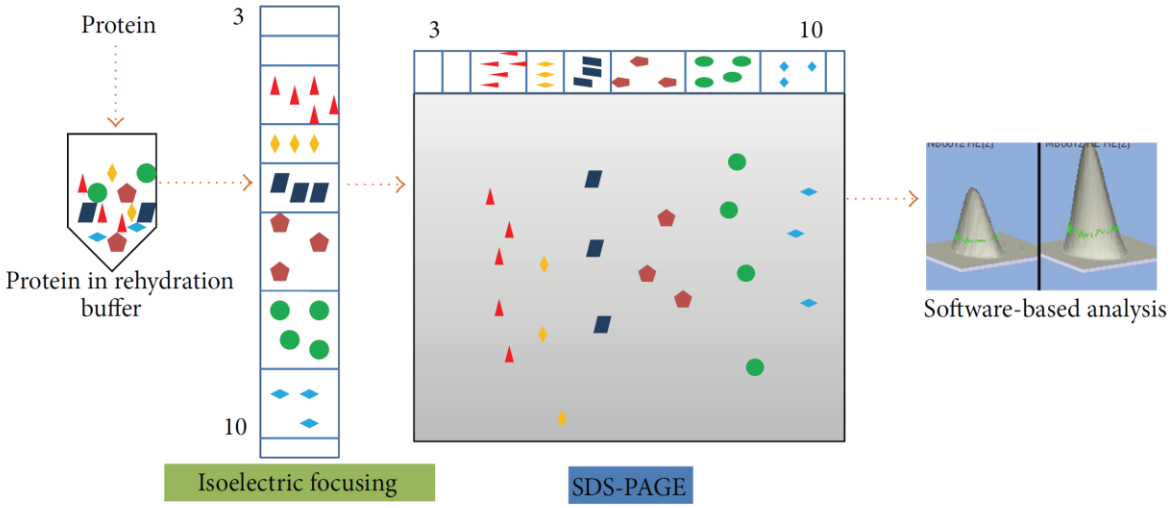

Figure 1.8: Schematic outlining 2-dimensional gel electrophoresis (2-DE). Protein is solubilized in rehydration buffer. The proteins are then immobilized on IPG strips of different pH ranges depending on the requirement of the experiment. In the first-dimension, the proteins are separated on the basis of their isoelectric points (pI) and are further resolved according to their molecular weight in the second-dimension. Finally, protein spots of interest are excised and subjected to tryptic digestion followed by MS. Adapted from [100].

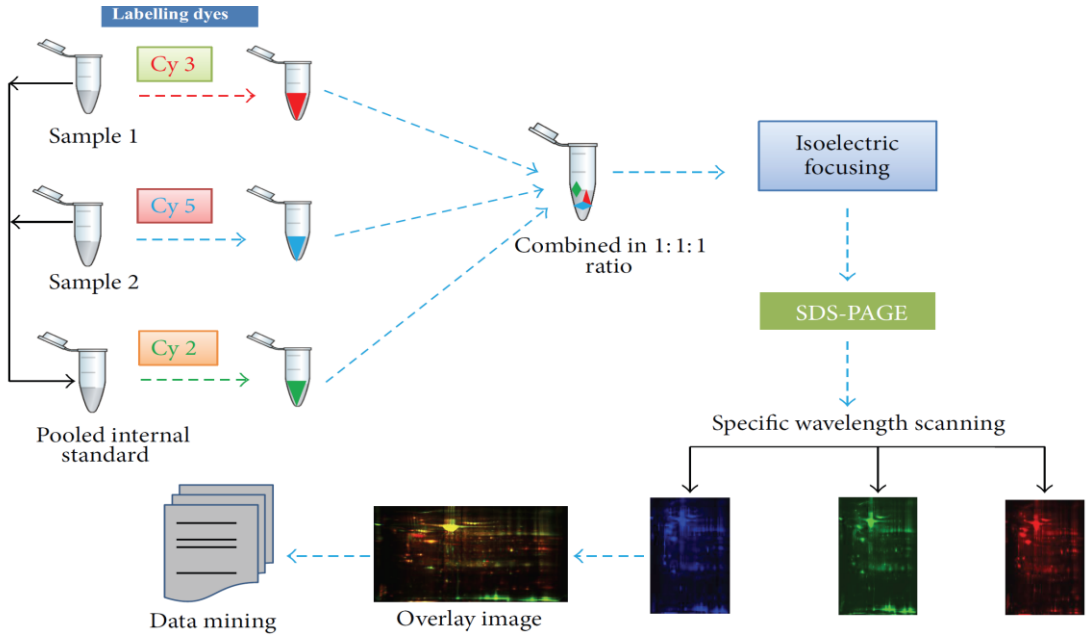

Figure 1.9: Schematic outlining 2D-DIGE experimental procedure. Whole cell lysates are from unstimulated and stimulated samples are labelled with different fluorophores (Cy 3 for sample 1, Cy 5 for sample 2, and Cy 2 for the pooled internal standard). All samples are resolved on the same 2D gel (this eliminating gel-to-gel variation) followed by protein spot pattern detection by scanning the gel at the wavelength corresponding to each Cy dye. The images are analyzed for significantly up or down regulated proteins which are then excised from the gel, trypsin digested and identified by MS. Adapted from [100].

1.2.1.2 SILAC and label-free quantitation

In the past 10-20 years, major advances have occurred in mass spectrometer instrumentation, sample preparation and computational analysis that have rapidly enabled proteomics to realise at least part of its potential and put it on a more equal footing with genomics in terms of scientific impact. Novel protocols have emerged enabling the use of much smaller amounts of biological samples whilst extracting more information and this, combined with the entwining of MS fragmentation spectra and sequence databases has greatly accelerated protein identification [97]. Quantitatively speaking, both labelled and label-free protein quantitation have allowed for the measurement and thus comparison of protein levels between samples [100]. Label-based, gel-free protein quantitation involves the differential labelling of separate biological conditions with stable isotopes. The most widely used method incorporating this strategy is termed stable isotope labelling by amino acids in cell culture (SILAC) [101]. Proliferating cells in culture, representing different biological states, are metabolically labelled with either light or heavy isotope versions of essential, stable amino acids. Labelled cells are then lysed, combined in a 1:1 stoichiometric ratio and trypsin digested followed by MS analysis. Assuming that isotopes are incorporated with equal efficiency across the different biological states, differences in isotopic incorpororation into particular proteins, again measured by the m/z ratios, must be due to differnces in abundance of these proteins between different biological states (Figure 1.10). *In vivo* labelling is also possible by feeding mouse populations with either natural or light isotope-lysine labelled food over four generations. Benefits of quantitative labelling such as SILAC include high accuracy and low error rate. However, it cannot be applied to human tissue and reagents are expensive [100]

Label-free quantitation (LFQ) is based on the assumption that the area of a peptide peak on a MS chromatogram is proportional to its concentration [102]. LFQ MS can be applied in

different forms: spectral counting and signal intensity. Spectral counting logs the number of spectra obtained between biological samples for a given peptide and integrates these into the total numbers of peptides detected for a given protein in each sample. Signal intensity determines the relative intensities of the extracted ion chromatograms to generate correlating protein intensities which can then be statistically compared between biological samples. The advantages of LFQ are many. It is considerably less cumbersome than label-based techniques and can provide robust and highly sensitive protein quantitation at a very low cost. Limitations include redundancy in detection as some peptides are shared between proteins. Moreover, this approach is not as accurate and therefore measurements of protein fold changes in lower with lower values are not as reliable and thus require repeat analysis. LFQ MS was used in the current study.

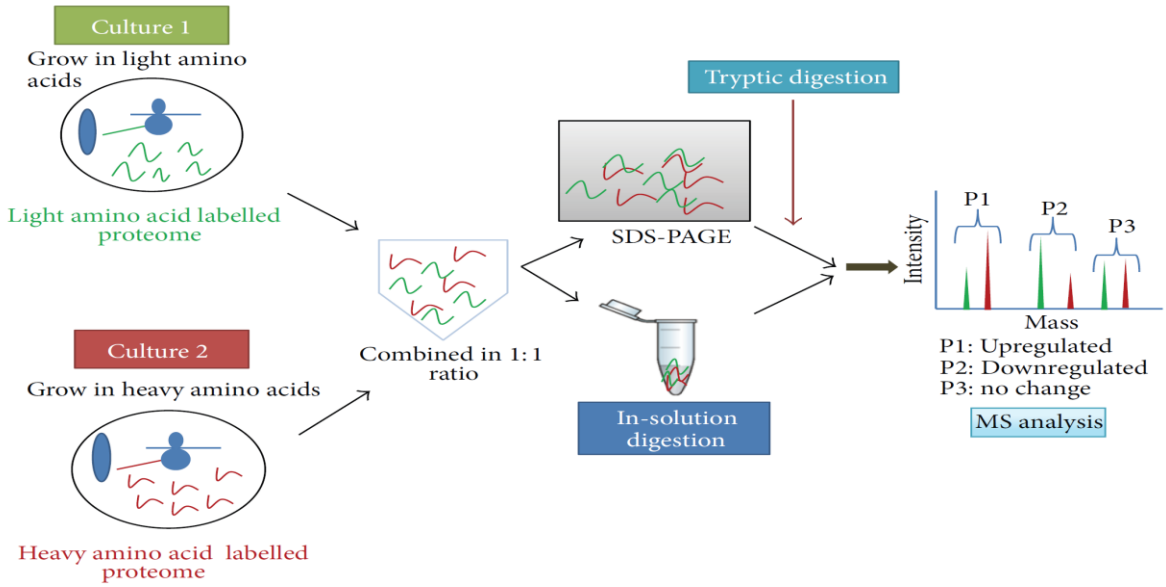

Figure 1.10: Schematic overview of SILAC. Cells are grown in medium containing light and heavy versions of essential amino acids for 6 generations to achieve maximal incorporation. Protein is extracted from both populations of cells and mixed in equal proportion and subjected to either in-gel or in-solution digestion. Relative abundance of the digested peptides is determined from the ratio of heavy to- light peptide signals as obtained by MS. Adapted from [100].

1.2.2 Applications to immunology and disease

Historically, the application of proteomics has been directed more frequently towards the identification of disease biomarkers rather than pure immunology. This approach primarily relied on the combination of 2D-PAGE with MS and later, on 2D-DIGE with MS. Despite the aforementioned limitations of these technologies, some successes were achieved, for example, in the classification of leukaemia subsets [103]. Online data troves of myocardial proteins associated with human heart failure similarly allowed researchers to establish standards to classify the myriad of pathological conditions associated with heart disease, particularly regarding onset [104-106]. 2D-DIGE has identified potential biomarkers of oesophageal carcinoma [107]. Proteomics has also been applied to the study of infectious pathogens. The arrival of increasing numbers of antibiotic resistant strains of bacteria has hastening research into prophylactic and remedial therapy [108]. Again, the genome sequencing of a particular pathogen is key to providing the blueprint for subsequent proteomic analysis, an example being the malaria parasite, *Plasmodium falciparum*. Comparative proteomic studies on both the parasite's innate proteome and life-cycle proteome have produced a number of novel drug and vaccine targets [109-111]. Indeed, the applications of proteomics to pathogen study are varied, as summarised in table 1.1.

Table 1.1: Proteomic approaches to the study of pathogenic organisms. Adapted from [104].

Targeted proteomic approaches to microbial pathogens
• Characterization of submicrobial proteomes (for example, secreted proteins, surface proteins and immunogenic proteins)
• Comparative analysis of different strains
• Comparative analysis of different physiological states
• Identification of proteins related to pathogenicity
• Identification of proteins involved in host–pathogen interactions
• Evaluation of mechanisms of action of antimicrobials

Despite these successes, proteomics has, until very recently, consistently remained in a distant second place when compared to the state-of-the-art advances and measurable

achievements associated with genomics [112-115]. Only in the past 5-6 years have radical new technologies encompassing both labelled and label free quantitation combined with MS become available to push immunologically-based proteomics into the top-tier scientific journals [97, 116, 117]. Notably, a recent study analysed the protein secretome of LPS stimulated, primary wild-type (WT), MyD88 deficient ($^{-/-}$) and TRIF $^{-/-}$ macrophages using LFQ on an Orbitrap MS [117]. The time-resolved release of 775 proteins was detected with low picogram sensitivity from only $1.5x10^5$ cells per condition. Fold changes in protein abundance upon stimulation ranged up to 10,000. A separate study utilised a similar approach to characterise differences in the proteome between different subsets of conventional dendritic cells (cDCs). Newly developed, quantitative algorithms permitted proteomic sequencing across subsets to an average depth of 5000 proteins with 99 % certainty in identification. Identification was also reliable across biological replicates with correlations between normalised protein intensities between 0.84 and 0.96 [116]. This study assigned key viral recognition abilities to $CD4^+$ and CD4, CD8 double negative cDC subsets but not to $CD8\alpha^+$ cells. Moreover, relatively few cells were required to achieve accurate reliable results (approximately $1.5x10^6$/condition), equivalent to a 1-5 micrograms of protein. Studies such as these foretell the potential application of proteomics towards the expansion of our knowledge base in areas such as immunology, disease pathologies, drug development and many other fields.

1.3.1 Bordetella genus

B. pertussis is a gram negative coccobacillus from the *Bordetella* genus of proteobacteria. It is the best known member of the *Bordetella* genus which consists of eight other members: *B. ansorpii*, *B. avium*, *B. bronchiseptica*, *B. hinzii*, *B. holmesii*, *B. parapertussis*, *B. petrii* and *B. trematum* [118].

B. parapertussis, *B. bronchiesptica* and *B. pertussis* are known as the 'classical' Bordetella species as they were the first to be successfully isolated and were therefore the defining members of the *Bordetella* family. They are also closely related morphologically, physiologically and antigenically and as such are referred to as a subspecies or as a strain of one species, known as the *B. bronchiesptica* cluster [118]. There are several similarities between the three. Infection occurs in the respiratory tract of humans, the resulting disease is whooping cough, or a variation of, with pathology resulting from infection and killing of ciliated tracheal epithelial cells [119]. Their genome contains a GC content of approximately 67 % with optimal growth for each occurring at a temperature between 35 °C and 37 °C (Table 1.2) [118].

1.3.2 *B. pertussis*: initial isolation and description

B. pertussis is aerobic, non-motile and is the cause of pertussis or whooping cough in humans. It is not known to infect any other species and as a result, humans are its sole reservoir [120]. It was first isolated in 1900 by Jules Bordet and Octave Gengou from a child upon which it was described it as a "small ovoid gram negative bacterium" [121]. Their first publication on the method of isolation was published six years later in 1906 [122]. Indeed the genus name *Bordetella* is derived from its cofounder, Jules Bordet [123]. The bacterium, whilst difficult to isolate from patients, (possible only within a very short timeframe during the initial period of infection called the catarrhal phase) was found to grow well on a medium consisting of blood, potato extract and glycerol, created by Bordet and Gengou and since

termed Bordet Gengou (BG) medium [121]. Transfer and subculture of the bacterium causes it to change both morphologically and physiologically turning from a bright yellow colour (Figure 1.11A) to white (Figure 1.11B) whilst also causing it to lose its haemolytic ability [121, 124].

Feature	*B. pertussis*	*B. parapertussis*	*B. bronchiseptica*	*B. holmesii*	*B. hinzii*	*B. avium*	*B. trematum*
Host	humans	humans, sheep	mammals	humans?	birds, humans	birds, reptiles	humans?
Disease	whooping cough	mild whooping cough	various respiratory diseases; atrophic rhinitis in piglets, kennel cough in dogs etc.	septicaemia, respiratory illness	septicaemia in patients with underlying disease; asymptomatic	turkey coryza	unknown
Site of isolation in humans	respiratory tract	respiratory tract	respiratory tract, blood	respiratory tract, blood	respiratory tract, blood	–	wounds, ear infections
G+C content (mol%)	66–68	66–68	66–68	61.5–62.3	65–67	62	64–65
Genome size (kbp)[a]	3 880–4 060	> 4 400	> 4 400	ND	ND	ND	ND
Growth on MacConkey agar	–	+	+	–/+	+	+	+
Catalase	+	+	+	+	+	+	+
Oxidase	+	–	+	–	+	+	–
Citrate assimilation	+	+	+	+	+	+	+

[a] Reference [70], The Sanger Centre; ND: not determined.

Table 1.2: Individual characteristics of members of the Bordetella family. Adapted from [118].

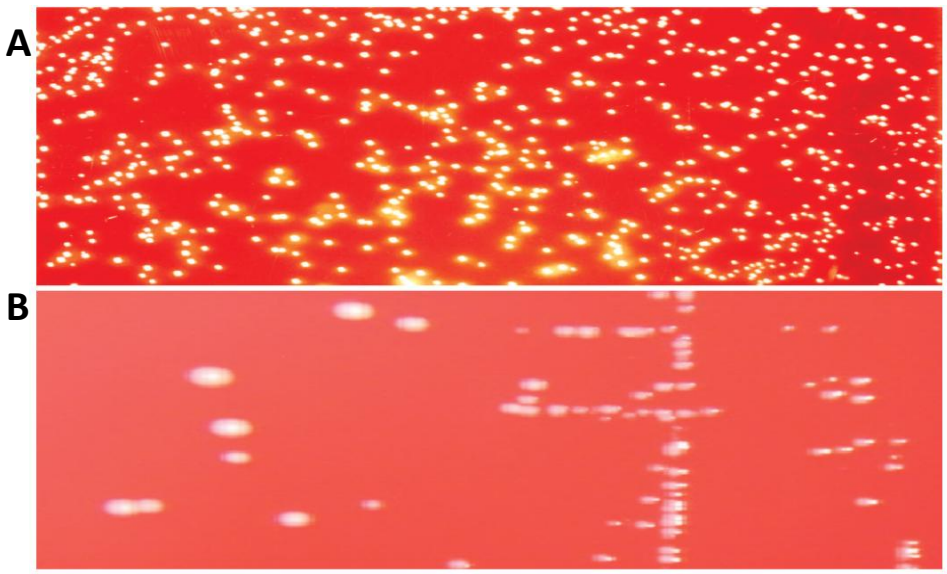

Figure 1.11: *Bordetella pertussis* on Bordet-Gengou medium. (A) Freshly isolated *B. pertussis* isolate. (B) Subcultured isolate. Adapted from [121].

1.3.3 Pathogenesis of *B. pertussis*

Initially, *B. pertussis* was considered an exclusively extracellular pathogen whose pathogenesis was derived from its secretion of several potent toxins. Local cytotoxic effects helped derive systemic metabolic disturbances which combine to generate characteristic symptoms [125, 126]. However, following several hints that *B. pertuss*is could reside intracellularly [127-129] it was definitively shown that it could infect HeLa cells and that this was dependent to varying degrees on the presence of virulence factors such as filamentous hemagglutinin (FHA) and cell bound pertussis toxin (PTx) in the bacterium as well as host microfilament mediated phagocytosis [130]. It is generally accepted that there are four main factors pertaining to *B. pertussis* infection and disease which are: attachment, host defence evasion, local damage and systemic damage [131]. *B. pertussis* bacteria attach to cilia of the upper respiratory tract via adherence factors such as FHA, fimbriae, PTx and pertactin (PRN) [132-135]. FHA is the major adhesin expressed on the cell surface and its role in mediating *B. pertussis* binding is believed to involve host upregulation of intracellular adhesion molecule-1 (ICAM-1) [136]. It initiates host phagocytosis by binding to and activating leukocyte integrin complement receptor 3 on multiple cell types [137]. Once inside the cell, the majority of bacteria are destroyed by the cells defence mechanisms, particularly by endosomal acidification [138]. However, approximately 25 % of bacteria taken up into the cell survive by residing in non-acidic compartments and begin to replicate. It is believed that this process occurs by inhibiting endosomal maturation and thus acidification [138]. The ability of *B. pertussis* to exist within the host's cells is believed to play a key role in its ability to evade the host's immune response for extended periods [139].

1.3.4 Immune Response to *B. pertussis*

Respiratory infection of mice with *B. pertussis* drives a large inflammatory cell infiltration into the lungs and particularly to the alveolar spaces with large numbers of macrophage, neutrophils and lymphocytes taking up residence (Figure 1.12) [140]. Resident macrophages

and DCs are first to arrive, followed by neutrophils, natural killer cells and T cells (Figure 1.12) [139]. Lymphocyte populations are composed primarily of CD4+ T cells with a smaller number of CD8+ cells [141]. Infiltration of small populations of gamma delta (γδ) T cells has also been noted in both animal models and in the very early stages of infection in children (Figure 1.12) [141].

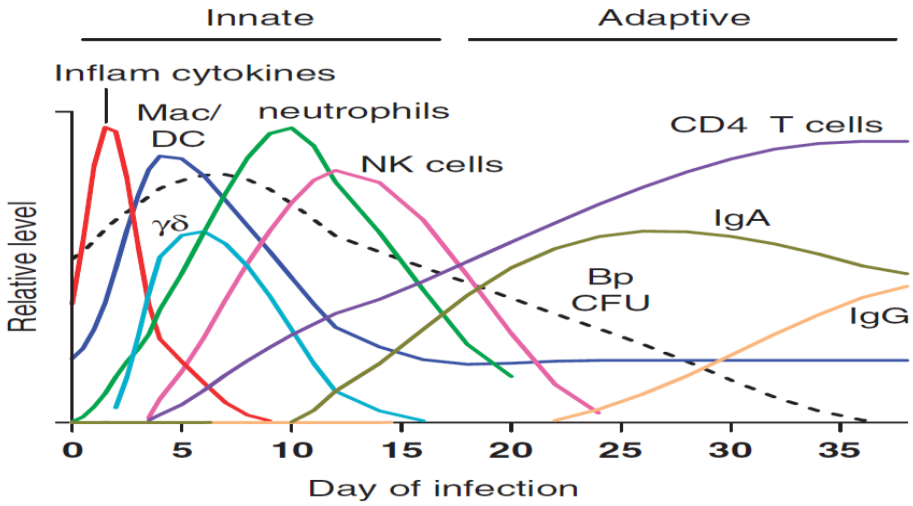

Figure 1.12: Time dependent kinetics of innate and adaptive immune cell recruitment to lungs following *B. pertussis* infection. Relative cell numbers are indicated by hypothetical curves. CD4 T cell: recruitment of $CD4^+$ T cells to lungs and response to *B. pertussis* antigens. IgG: anti-*B. pertussis* immunoglobulin G in serum. IgA: anti-*B. pertussis* immunoglobulin A in in lungs. Bp CFU: *B. pertussis* burden in lungs. DC: dendritic cells. Mac: macrophage. NK: natural killer cell. γδ: gamma-delta T cells. Adapted from [139].

Macrophages, whilst internally harbouring populations of bacteria, are also required for protection as depletion of resident airway macrophages enhances *B. pertussis* infection. They can be induced to kill intracellular bacteria by T-cell derived cytokines such as IFN-γ and IL-17 [142, 143]. Neutrophils reach the lungs of infected mice approximately five days post infection (Figure 1.12). Like macrophages, neutrophils are capable of phagocytosing and killing of intracellular bacteria but are considered unlikely reservoirs due to their relatively

short half-life [139]. NK cells are the early providers of the crucial cytokine IFN-γ which ensures macrophage mediated bacteria killing and promotes T_H1 responses. Depletion of NK cells results in bacterial escape from the lungs to the liver [144]. Specific antibody responses take much longer to develop in mice after *B. pertussis* challenge, only appearing in significant amounts when most bacteria have been cleared approximately five weeks post-infection. This would indicate that they are not of major importance the clearance of a primary infection however antibodies are important in vaccine-induced adaptive immunity to *B. pertussis* [139].

1.3.5 Vaccination

Vaccines using inactivated whole *B. pertussis* organisms followed by acellular pertussis vaccines have been in use since the 1940s and have led to a marked decline in resulting disease [145]. Being an exclusively human pathogen, the introduction of wide-spread vaccination programs have been twinned with the expectation of disease eradication, at least in industrialised countries. However, despite significant investment and high uptake, many first world countries have experienced a striking resurgence in the past decade, particularly amongst older children and adults [146, 147]. In Europe, a surveillance programme termed EUVAC-NET recorded a 115% increase in incidence rates in children over 14 between 1998 and 2002 [148]. An approximate doubling in incidence has also been reported in the US between 2001 and 2003 [145]. Possible explanations for the current epidemiology of *B. pertussis* infection include:

1. Waning immunity and shorter protection following vaccination: Duration of protection resulting from whole cell pertussis (wP) vaccination ranges from 4-14 years and between 5-6 years for acellular *B. pertussis* (aP) vaccination.
2. Strain polymorphism: Studies have indicated that certain strains of *B. pertussis* have adapted to express PT and PRN different from that contained within current vaccine

preparations with suspected links to observed reductions in vaccine effectiveness in The Netherlands and Finland [145, 149].

3. Increased diagnosis and reporting: It is generally accepted that improved awareness and diagnostic methodology are responsible for some, but not all of the increases in incidences. For example, a significant increase in observed disease Canada in 2006 was associated with a similarly significant increase in the number of tests carried out [145].

1.3.6 Application of proteomics to the study of *B. pertussis*

Several proteomic studies have been carried out on the *B. pertussis* bacterium in order to monitor its response to various infection relevant scenarios as well as to characterise potential novel antigens for future vaccine design. For example, one study utilised 2D gel electrophoresis combined with MALDI-TOF MS to profile protein expression in both whole cell lysates and outer membrane fractions of bacteria grown in either iron starvation or iron excess conditions [150]. Iron starvation is a common obstacle to overcome by many bacteria including *B. pertussis* during an infection and protein signatures linked to its ability to scavenge host iron are believed to be critical to its survival and therefore a source of potential therapeutic targets. The study identified multiple iron dependent proteins, four of which reacted strongly with sera from infected individuals and one which was highly immunogenic in vivo thus providing a potential vaccine target [150]. A further 2D gel electrophoresis study examined the protein signature of *B. pertussis* bacteria upon biofilm formation [151]. Biofilms allow pathogens to exhibit phenotypic traits that allow for increased resistance to host defences and antibiotics. It is also believed that adults carrying *B. pertussis* biofilms act as infection reservoirs by periodically shedding active bacteria [131]. The study identified significant alternations in proteins involved in cell attachment and bacterial virulence

indicating the impact biofilm formation likely has on *B. pertussis* pathogenesis [151]. Clinical isolates have also been examined using similar proteomic techniques [152]. To date however, despite a slew of proteomic studies having been conducted on the *B. pertussis* bacterium itself, a proteomic study as yet to be conducted which examines the response of host cells to *B. pertussis* infection. Evaluation of this host proteomic response to infection is important for a number of reasons. One is that studying the proteome itself, as opposed to the genome is a more reliable method of detecting crucial host effector mechanisms engaged to fight the infection as proteins, not genes, are responsible for this. Another is that novel host proteins subverted by the bacterium to acquire resources, for example transferrin for iron scavenging [150], could be identified and whose expression again, may not be detected by genetic studies. Identification of host protein signatures specific to certain functions or even cellular compartments could shed new light on *B. pertussis* infection and resilience strategies and in turn uncover multiple new targets for perturbation of the host immune response when the need to treat pathogenesis resulting from an acute inflammatory response arises.

To this end, it was decided to conduct a comparison of the proteomes of *B. pertussis* infected and uninfected lung-epithelial cells (BEAS-2B cells). 2D-DIGE combined with LC/MS as well as LFQ MS were used to identify and quantify dynamic regulation of proteins resulting from whole cell lysates from different cell treatments. Protein hits of interest were selected, verified by western blot and subjected to further analysis of their role in the host immune response to *B. pertussis* infection.

1.4.1 Human rhinovirus

Human rhinoviruses (HRVs) were first discovered in 1956 and were immediately associated with clinical disease in humans with symptoms almost identical to that of the common cold [153]. They are a member of the genus *enterovirus* within the *picornavirus* family and as such, exhibit characteristics synonymous with picronaviruses such as being non-enveloped, positive-sensed and single-stranded RNA viruses. To date, 102 serotypes have been documented and they are believed to be the major cause of common cold symptoms in adult humans [154, 155]. The serotypes can be organised into three 'receptor groups' based on the cellular receptor they bind to. These are classified as the major group, which bind to intracellular adhesion molecule-1 (ICAM-1) and account for 91 of the serotypes; the minor group, which bind to members of the low density lipoprotein receptor (LDLR) family and account for 10 serotypes; and finally, the remaining serotype, HRV87, which does not attach to receptors of the major or minor group and attaches to an unknown glycoprotein that unlike any other serotype, requires the presence of sialic acid [156].

1.4.2 Structure of HRV

Rhinoviruses are composed of sixty copies of each of four viral capsid proteins (VPs) which are arranged such that they form an icosahedral shell surrounding a single stranded RNA at the centre (Figure 1.13). VP1-3 are external whilst VP4 lines the internal surface and is therefore thought to contact the packaged RNA (Figure 1.13) [157]. Amino acid differences across these capsid proteins confer the antigenic differences between the HRV serotypes with VP1 exhibiting the greatest sequence variability and VP4 responsible for the least [158]. VP1 contains a hydrophobic pocket, often referred to as a canyon which serves as the binding site for ICAM-1 in the case of the major group of HRVs (Figure 1.13) [159]. Whilst still not completely understood, it is believed that during the initial stages of viral infection, HRV binds ICAM-1 followed by a loss of the viral capsid with VP4 first being externalised and

VP1 being lost next. This process ultimately leads to viral RNA internalisation via endocytosis or macropinocytosis through the host cell's plasma membrane [160-162].

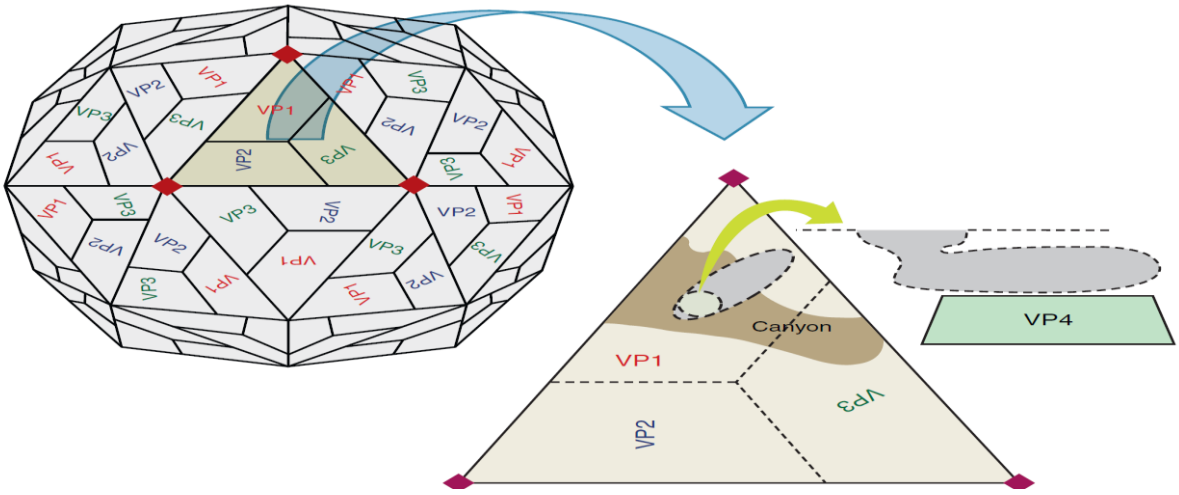

Figure 1.13: HRV structure. RV is a non-enveloped virus consisting of a protein shell surrounding the naked RNA genome. The protein capsid is composed of four polypeptides, viral capsid protein 1 (VP1), VP2, VP3 and VP4 in an icosahedral structure. A hydrophobic canyon exists within VP1 which is believed to contain the ICAM-1 binding site. VP4, unlike the other VPs, is contained within the viral internal surface. Adapted from [163].

1.4.3 HRV Replication

The picnoravirus genome is comprised of a single stranded RNA which itself consists of 3 distinct regions. At the 5' end is a single untranslated region (UTR), followed by an open reading frame (ORF) encoding the structural VPs 1-4 and non-structural proteins such as proteases and finally a short 3'UTR and poly(A) tail (Figure 1.14) [164]. Upon entry into the cell, HRVs follow a similar replication strategy to other picornaviruses. The previously packaged RNA functions as an mRNA and is translated by the host's translation machinery into a large polypeptide which is cleaved to yield mature viral proteins (Figure 1.15). The viral RNA is then transcribed into a negative sense complementary RNA which in turn serves as a template to transcribe complementary positive sense RNA and thus complete one cycle of replication (Figure 1.15).

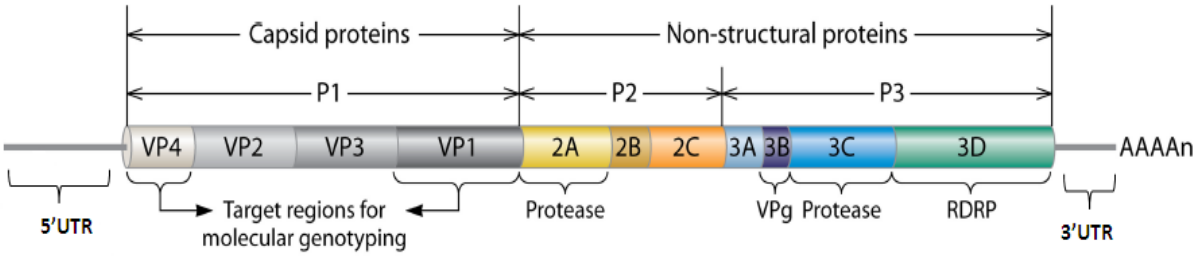

Figure 1.14: HRV genomic structure. HRV is 7.2 kb in length with a single open reading frame linkned to a 5' untranslated region (5'UTR). Protein P1 is translated into the HRV capsid. P2 and P3 are translated into VPg, protease and RNA-dependent RNA polymerase (RDRP). Adapted from [162].

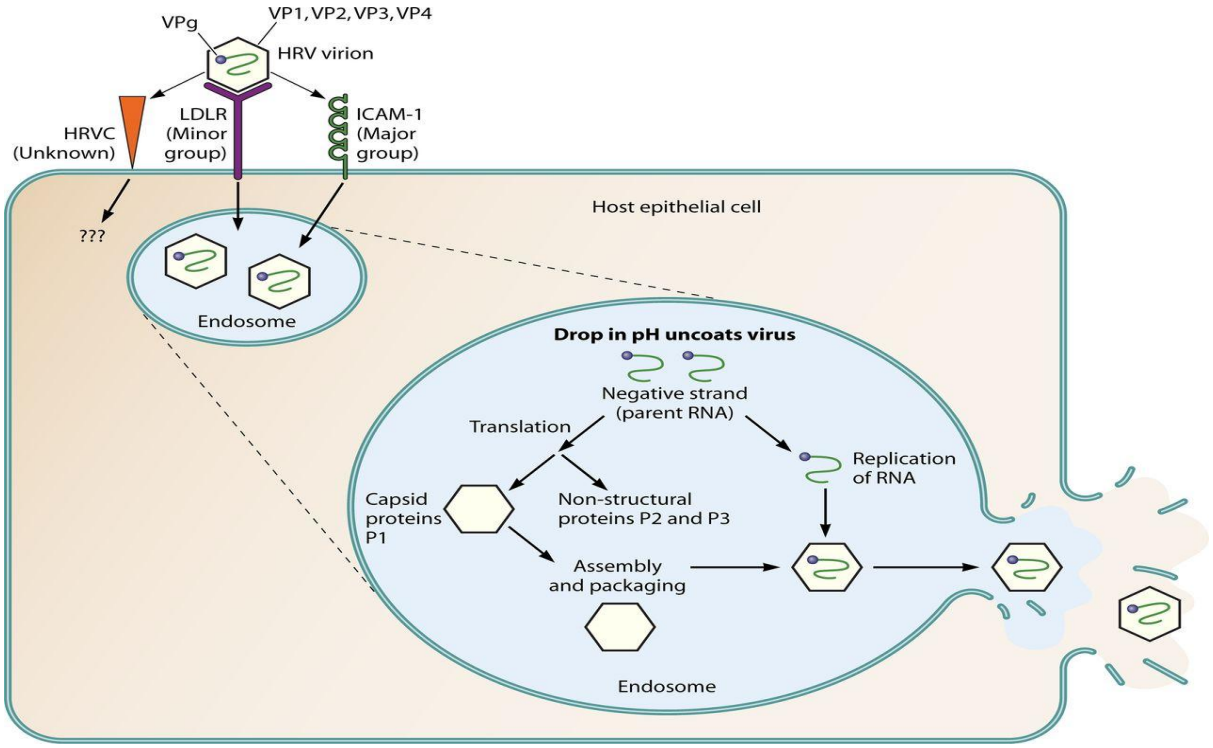

Figure 1.15: HRV replication in tracheal epithelial cells. Virus uptake can occur via clathrin-dependent endocytosis or macropinocytosis. Lowering of pH leads to viral uncoating. Negative strand RNA is replicated and translated into structural and non-structural proteins. Virions are packaged prior to export via cell lysis. LDLR, low density lipoprotein receptor; ICAM1, intracellular adhesion molecule 1. Adapted from [162].

1.4.4 HRV Pathogenesis

HRV is believed to preferentially infect and replicate in the upper respiratory tract of non-asthmatic individuals [163]. Although other respiratory viruses such as influenza and respiratory synthetical virus are associated with the destruction of airway epithelial cells, HRV is not, with nasal biopsies from patients both naturally and experimentally infected showing intact epithelial cell linings [165, 166]. However, HRV has been shown to disrupt epithelial cell tight-junctions thus reducing barrier function and allowing transmigration of bacteria [167]. Lower respiratory infections typically occur in those with pre-existing asthma or chronic lung disease [163] and are known to exacerbate asthma symptoms [168]. Rhinorrea (nasal filling with mucous) and consequent nasal obstruction are common symptoms of upper respiratory tract infections and are associated with a neutrophilic inflammatory response causing increased vascular permeability and mucus secretion [163].

1.4.5 Immune Response to HRV

HRV ssRNA , once internalised is known to be endosomally recognised by TLR7 and TLR8 [162]. During its replication cycle, dsRNA is generated which can then be recognised by cytosolic RIG-I and MDA5 (Figure 1.16) [169, 170]. The engagement of these PRRs leads to secretion of IFN-β, IFN-γ, RANTES, IL-6, TNF-α and IL-8 (Figure 1.16) [162]. Levels of IL-8 have been shown to correlate with HRV induced rhinorrea and nasal obstruction in experimentally inoculated individuals [171]. The vasodilators bradykinin and lysylbradykinin are also released in significant quantities upon HRV infection however histamines are not, which would suggest that basophils and mast cells play no role in HRV pathogenesis [172]. The humoral response is also important as evidenced by the observation that those with hypogammaglobulinemia, a condition in which levels of immunoglobulins are abnormally low, suffer from increased recurrence and severity of HRV infections [173]. Infection of patients with HRV is followed by generation of serotype specific neutralising IgG and IgA

antibodies with 1-2 weeks [174]. T cell infiltration of the airway epithelium and submucosa has also been observed [175].

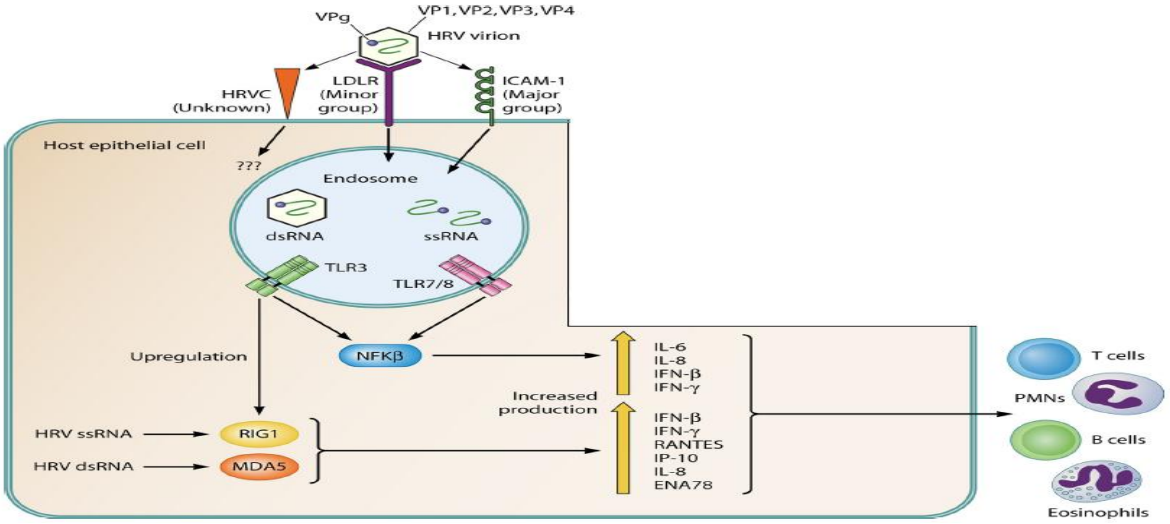

Figure 1.16: HRV recognition by various PRRs and signal transduction. HRV dsRNA and ssRNA in the endosome are recognised by TLR3 and TLR7/8 respectively to drive NFκB and IRF activation. This increased production of pro-inflammatory and anti-viral cytokines. TLR3 activation also upregulates expression of cytosolic PRRs RIG-I and MDA5 which sense cytosolic HRV ssRNA and dsRNA respectively. These PRRs also drive pro-inflammatory and anti-viral cytokine production. These cytokines can further act on T and B cells to activate the adaptive immune response. Adapted from [162].

1.4.6 Application of proteomics to HRV infection studies

Similar to *B. pertussis*, there has been no previous attempt to characterise the changes in a cell's proteome upon infection with any serotype of HRV. This therefore leaves a considerable gap in our knowledge about how HRV's modulate the host's intracellular environment and also how the host itself responds to infection. It was therefore decided to conduct a proteomic study examining the changes induced in the host cellular proteome in response to HRV infection. To achieve this aim, HRV serotype 16 (HRV16) was used as it is a member of the major group of ICAM-1 sensing HRVs and thus a good indicator of how the majority of known HRV serotypes modulate the cell. Also, as HRV16, like *B. pertussis* is primarily a respiratory pathogen, the same cell line, BEAS-2B, was used for the infection.

These cells have been used previously as an in vitro model for studying HRV infection in respiratory cells [93, 176, 177] but also carry the additional advantage in this case of allowing a comparison between the proteomes of a virally infected cell (HRV16) and a bacterially infected cell (*B. pertussis*). As in our opinion, the 2D-DIGE – *B. pertussis* study produced more hits that were of interest to an immunological setting compared to the LFQ MS, it was decided to also analyse the HRV16 infection proteome by 2D-DIGE also.

1.3 Project Aims

1.3.1 Project Aim 1

The current state of our knowledge of TLR signalling is in constant flux with systems that seemed impressively simple less than a decade ago, becoming increasingly complex. Taking the TIR-domain containing adaptors as an example, the current accepted dogma is that MyD88 is involved in signalling from all TLRs except TLR3, that TRIF is required for only TLR3 and TLR4 signalling or that MAL mediated only TLR2 and TLR3 signalling [15]. These claims, whilst once true, have been shown to be in need of updating. MAL and MyD88 negatively regulate TLR3 mediated type-I IFN production, whilst TRIF is required for TLR5 signalling [21, 75, 76, 93, 94]. TRAM, whose only known cellular function was to mediate TLR4 signalling, has been shown to also mediate IL-18R signalling and is believed to play a role in TLR2 signalling [178, 179]. With this is mind, we questioned whether there were additional unknown roles for the adaptor molecules in TLR signalling, with a focus on TRAM. A factor in the dissemination of the initial characterisation data from knockout mice specific to TRAM is a lack of strenuous controls that eliminate the role of TRAM in alternative TLR pathways. For example, whilst cells from TRAM deficient mice have had NFκB dependent pathways from multiple TLRs examined, not once have IRF mediated cytokines been examined apart from those mediated by TLR3 and TLR4 [23, 24]. A major aim of the current work was therefore to:

Characterise the role of the adaptor TRAM in both NFκB and IRF mediated pathways derived from multiple TLRs.

1.3.2 Project Aim 2

The advances in proteomics technology discussed herewith have made the direct study of the proteome pre and post infection faster and cheaper as well as bringing increased protein identification accuracy, reliability and depth [97]. Characterisation of the proteome following infection with human-relevant pathogens remains an understudied field of study. Whilst there have been reports of the application of transcriptomics to the field [180, 181], the application of proteomics is still lacking. Two pathogens of relevance to human health, both currently and historically, are the human rhinoviruses and the gram negative bacterium, *Bordetella pertussis* (*B. pertussis*). Proteomic profiling of the cellular response to infection with these two respiratory pathogens has never been completed and therefore represents a missing link in our knowledge of what proteins are involved in tailoring and modulating the immune response to these significant human health pathogens.

Therefore, the second major aim of the project is to define the proteome of lung epithelial cells following infection with two pathogens of significance to human health, namely human rhinovirus 16 and *B. pertussis*.

Chapter 2

Materials and Methods

2.1 General methods:

2.1.1 Mamalian cell culture techniques

All mammalian cells were maintained in a humidified atmosphere, with 5 % CO_2 at 37 °C. Wild-type (WT), TRAM $^{-/-}$ and MAL $^{-/-}$ immortalised bone marrow derived macrophage (iBMDM) cell lines, human embryonic kidney 293 (HEK293) cells stably transfected with human TLR3 (HEK293-TLR3), HEK293-TLR4, HEK293-TLR7, HEK-Blue™ TLR4 and bronchial epithelial cells, strain AS-2B (BEAS-2B) were grown in Dulbecco's Modified Eagle's Medium (DMEM) supplemented with 10% (v/v) fetal bovine serum (FBS), 1 % (v/v) penicillin/streptomycin solution and 1% (v/v) sodium pyruvate. Difficulties were experienced using the iBMDM cell lines with differing growth rates and unreliable phenotypes often observed. Efforts were made to source primary cells direct from WT and TRAM $^{-/-}$ mice however the cells did not survive the international shipping process. HEK293-TLR3 and HEK-Blue™ TLR4 cells were additionally supplemented with blasticidin (25 μg/ml). HEK293-TLR4 and HEK293-TLR7 cells were additionally supplemented with G418 (250 μg/ml). HEK-Blue™ IFN-α/β cells and the human leukemic monocyte cell line, THP-1 were grown in Roswell Park Memorial Institute 1640 (RPMI 1640) medium supplemented with 10 % (v/v) FBS, 1% (v/v) penicillin/streptomycin solution and 1% (v/v) sodium pyruvate. HEK-Blue™ IFN-α/β cells were additionally supplemented with Normocin™ (100 μg/ml) and Zeocin™ (50 μg/ml). Adherent cell monolayers were detached from tissue culture flasks using trypsin/ ethylenediaminetetraacetic acid (EDTA) upon 90% confluency and re-cultured at a 1:5 or 1:10 dilution depending upon growth rate. Non-adherent cells were similarly re-cultured upon 90% confluency at a 1:5 or 1:10 dilution.

2.1.2 Cell stock freezing and resuscitation

Adherent cells were trypsinised, re-suspended in complete growth medium, and centrifuged at 306 g-force (g) for 5 min. Pelleted cells were re-suspended in freezing medium (90 % (v/v)

growth medium, 10 % (v/v) DMSO) and aliquoted into cryovials. Typically, a confluent T175 flask would be split into 3 cyrovials with 1ml per vial. Cryovials were stored at -80 °C in a NALGENE™ Cryo 1 °C Freezing Container to achieve a -1 °C/min rate of cooling for a minimum of 4 hours before long-term storage in liquid nitrogen.

To resuscitate cells, cryovials were removed from liquid nitrogen storage and rapidly thawed in a water bath heated to 37 °C. Cells were immediately re-suspended in complete growth medium before centrifugation at 306 g for 5 min. Medium containing DMSO was removed and the cell pellet was re-suspended in complete growth medium and transferred to a T75 culture flask in the appropriate incubation conditions (see section 2.2.1).

2.1.3 Transformation of competent cells

Plasmid DNA (1-2 µl corresponding to 100-800 ng) was added directly to 20 µl of thawed *E. coli* DH5α competent cells (Invitrogen) and incubated on ice for 30 min. Thereafter, cells were heat shocked for 20 sec at 37 °C before being immediately returned to ice for a further 2 min. Cells were re-suspended in 0.5 ml lysogeny broth (LB) and agitated in a shaker at 10 g and at 37 °C for 1 hour. Approximately 100 µl of the transformed bacteria were plated out onto LB-agar plates supplemented with antibiotic to select for plasmid containing bacteria. Plates were inverted and incubated at 37 °C overnight.

2.1.4 Preparation of plasmid DNA

Note: All centrifugations carried out chilled at 4,503 g. Single colonies were inoculated into 100 ml of LB (preheated to 37 °C) supplemented with appropriate antibiotic and incubated at 37 °C with gentle shaking for approximately 16 hr. Bacterial cells were subsequently pelleted by centrifugation for 30 min. DNA was extracted from the cells using a QIAGEN Plasmid Midi Kit as described by the manufacturer. Briefly, the bacterial pellet was resuspended in 4

ml Buffer P1, followed immediately by 4 ml Buffer P2, inversion 5 times and incubation for 5 min at RT. Chilled buffer P3 was added, the bacteria inverted 5 times and incubated on ice for 15 min followed by centrifugation for 30 min. Supernatant containing plasmid was removed, transferred to a fresh tube and re-centrifuged, chilled for 15 min. The supernatant was then applied to an equilibrated QIAGEN-tip 100 and allowed to empty by gravity flow. The tip was washed twice with 10mls of Buffer QC before elution into a fresh falcon with 5mls Buffer QF. DNA was precipitated using 3.5 ml 100% isopropanol, mixed and centrifuged for 30 min. The supernatant was discarded and the DNA pellet washed with 2 ml 70 % ethanol, before centrifugation for 10 min.

The DNA concentration determined in ng/µl using the NanoDrop 2000 spectrophotometer (Thermo Scientific). Note that centrifugations were carried out at 4,503 g at 4 °C.

2.1.5 Plasmid glycerol stock preparation

A 500 µl aliquot of transformed cells was mixed with 500 µl of 50 % glycerol and stored at -80 °C. A 'stab' of this secondary culture was used to inoculate 100 ml liquid cultures as necessary.

2.1.6 Transfection of cells with plasmid DNA:

On day 1, confluent cells were plated in complete growth medium in a 6-well plate at a density of $0.4x10^6$ cells/ml (3 ml/well) and incubated for 24 hr at 37 °C. On day 2, a solution of plasmid DNA was prepared containing DNA in a maximum of 250 µl Opti-MEM® Reduced Serum Medium (hereafter referred to as Opti-MEM®). Separately, a solution containing 1 µl lipofectamine/µg DNA was prepared in a total volume of 250 µl Opti-MEM®. Solutions were the incubated for 5 min at RT before combining, mixing and incubating for a further 20 min at RT. At this point, 1 ml of medium was removed from each well in the cells

plated previously. After 20 min, the DNA-lipofectamine-Opti-MEM® solution was added drop-wise to the cells and the tissue culture plate was incubated for 24 hr at 37 °C.

2.1.7 Transfection of cells with siRNA:

On day 1, confluent THP1 monocytes were plated in complete growth medium in a 12-well plate at a density of $0.7x10^6$ cells/ml (2 ml/well) containing 40 nM Phorbol 12-myristate 13-acetate (PMA)/well and incubated for 48 hr at 37 °C. On day 3, separate solutions of human TRAM (200 nM) or scrambled siRNA (200 nM) were prepared in total volume of 125 µl of Opti-Mem®. In a fresh eppendorf, a solution containing 4 µl lipofectamine/sample was prepared to a total volume of 125 µl Opti-MEM®. Solutions were incubated for 5 min at RT before adding 125 µl lipofectamine solution to each individual siRNA mix followed by incubation for 20 min at RT. At this point, 250 µl of medium was removed from each well in the cells plated previously. After 20 min, the individual siRNA-lipofectamine-Opti-MEM® solutions were added drop-wise to the cells and the tissue culture plate was incubated for 48 hr at 37 °C.

2.1.8 Transfection of cells with esiRNA:

On day 1, confluent BEAS-2B cells were plated in complete growth medium in a 6-well plate at a density of $0.4x10^6$ cells/ml (1 ml/well) and incubated for 24 hr at 37 °C. On day 2, separate solutions of target specific esiRNA (200 ng) or negative control GFP esiRNA (200 ng) were prepared in a total volume of 250 µl Opti-Mem®. In a fresh eppendorf, a solution containing 3.5 µl lipofectamine/sample was prepared in a total volume of 250 µl with Opti-MEM®. Solutions were incubated for 5 min at RT before adding 250 µl lipofectamine solution to each individual esiRNA mix followed by incubation for 20 min at RT. After 20

min, the individual esiRNA-lipofectamine-Opti-MEM® solutions were added drop-wise to the cells and the tissue culture plate was incubated for 24 hr at 37 °C.

2.1.9 *B. pertussis* culture and infection

Pre-warmed, Bordet-Gengou (BG) agar plates (3 % (w/v) BG agar base, 1 % (v/v) glycerol, 17 % (v/v) defibrinated horse blood), containing 100 μg/ml streptomycin, were inoculated with a streptomycin resistant, *B. pertussis* Tohama I derivative strain (BPSM) using a sterile spreader and incubated inverted at 37 °C for 72 hr. Using a sterile inoculation loop, colonies were harvested and transferred to a sterile, 200 ml conical flask containing 100 ml of pre-warmed Stainer and Scholte (S&S) medium (per 500 ml: 10.72 g L-Glutamic acid, 0.24 g L-Proline, 2.5 g NaCl, 0.5 g KH_2PO_4, 0.2 g KCl, 0.1 g $MgCl_2.6H_2O$, $CaCl_2.2H_2O$) and 1 ml supplement medium (per 90 ml: 0.1 g iron sulphate, 0.2 g ascorbic acid, 0.04 g nicotinic acid, 1 g glutathione and 0.4 g L-Cysteine). The flask was then placed in a 37 °C shaker for a 36 hr at 9 g. 100 μl of the liquid culture was removed, placed in a quartz cuvette and the number of colony forming units (CFU)/ml was estimated by spectrophotometry at 595 nm. Typically, an OD of 1 equalled approximately $2x10^{10}$ CFU/ml. BEAS-2B cells were infected by directly pipetting the required volume of bacterial liquid culture into the mammalian cell culture media to achieve an MOI of 200. Cells were incubated for 12 hr before harvesting.

2.1.10 HRV16 infection

Human rhinovirus 16 (HRV16) containing stock solution was removed from -80 °C storage and rapidly thawed in a 37 °C incubator. Mammalian cells were infected by pipetting the HRV16 containing solution directly into the mammalian cell culture medium (MOI of 3). Cells were incubated at 33 °C for 72 hr to permit infection and viral replication to occur.

2.1.11 Sodium dodecyl sulphate polyacrylamide gel electrophoresis (SDS-PAGE)

SDS-PAGE was performed based on the Laemmli method [182] and carried out using the mini-gel system (Bio-Rad). Polyacrylamide gels were cast in two layers with a lower, resolving layer containing 10 % acrylamide and an upper, stacking layer containing 5 % acrylamide. After solidification, gel plates were transferred from the casting rig to the electrophoresis chamber (Bio-Rad) which was filled with 1x SDS running buffer (25 mM Tris-Base, 192 mM Glycine, 0.1 % SDS (w/v)). Samples to be analysed were mixed with 5x Laemmli sample buffer (300 mM Tris-HCl, 50 % (v/v) Glycerol, 10 % (w/v) SDS, 0.02 % (w/v) Bromophenol Blue, 10 % (v/v) β-Mercaptoethanol, 20 %), followed by boiling at 100 °C for 5 min. Samples and standard protein marker (Bio-Rad) were loaded into individual wells and electrophoresis was performed at 90 V for the first 30 min followed by 100 V for approximately 1 hr.

2.1.12 Western blot

Proteins were transferred to polyvinylidene difluoride membrane (PVDF; Santa Cruz), using a wet transfer apparatus (Owl VEP-2, Thermo Scientific). Briefly, PVDF membranes were cut to the required size and activated by soaking in 100 % methanol for 1 min followed by washing in 1x transfer buffer (25 mM Tris-HCl (pH 7.6), 192 mM glycine, 20% methanol) for a further 1 min. A transfer sandwich was assembled as follows: one sponge, two pieces of Whatman™ chromatography paper, gel containing electrophoresed samples, PVDF membrane, a further two pieces of Whatman™ chromatography paper and a final sponge. The transfer sandwiches were then clamped, placed in the transfer chamber containing 1x transfer buffer and transferred at 100 V for 70 min at 4 °C. At this point, the PVDF membrane was blocked in either 5 % (w/v) fat free dry milk or 5% (w/v) bovine serum albumin (BSA) in 1x TBST for a minimum of 50 min at RT. Primary antibodies against the target protein were appropriately diluted in 5 % (w/v) fat free dry milk in 1x TBST or 5 %

(w/v) BSA in 1xTBST and incubated on the membrane overnight at 4 °C with gentle agitation. Following this, membranes were washed three times with 1x TBST, before addition with a horseradish peroxidase (HRP)-conjugated secondary antibody raised against the appropriate species, diluted 1:2500 in 5 % (w/v) fat free dry milk in 1x TBST for 1 hr. Unbound antibody was removed by washing the membrane three further times with TBST before visualisation of immunoreactive bands protein bands by electrochemiluminescence (ECL). Visualised bands were recorded using autoradiography film (Santa Cruz) which was exposed in developer solution (Devalex M™, Champion Photochemistry), washed in H_2O, fixed (Fixaplus™, Champion Photochemistry) and washed again prior to electronic image scanning.

2.1.13 RNA isolation

The medium was removed from experimental cells followed by washing in ice-cold phosphate buffered saline (PBS) and centrifugation at 161 g for 5 min. Supernatant free pellets were lysed in 0.5 ml of TRI Reagent (Sigma) and left for 5 min at RT. Next, 100 µl of 100 % chloroform was added, followed by mixing and incubation for 3 min at RT. Samples were centrifuged at 16,464 g for 15 min at 4 °C to separate the lysates into three phases: an upper, aqueous phase containing the RNA, a DNA containing interphase and a lower organic phase containing proteins. The upper aqueous phase was pipetted into a fresh eppendorf, to which 250 µl of 100 % isopropyl alcohol was added and incubated for 10 min at RT to precipitate the RNA. Samples were centrifuged at 16,464 g for 10 min at 4 °C at which point the supernatant was removed and 500 µl of 70 % ethanol added to the RNA pellet. The samples were subjected to centrifugation at 16,464 g for 5 min at 4 °C, after which, the ethanol was removed and the pellet air dried for 10 min at RT. The RNA pellet was resuspended in 25-50 µl RNAase free water (Fisher), depending upon the original number of cells. Samples were heated at 59 °C for 10 min to aid RNA resuspension and immediately

placed on ice. The RNA concentration was determined using a NanoDrop ND-1000 spectrophotometer (Thermo Scientific). Samples were stored at -80 °C until required for first strand cDNA synthesis.

2.1.14 First-strand cDNA synthesis

Total cellular RNA was used as a template for first stand cDNA synthesis. Additional reagents and volumes used are summarised in Table 2.1. All samples and reagents were kept on ice unless otherwise indicated. Final reaction volume was 25 µl in 0.2 ml PCR grade eppendorfs (Corning). Upon preparation, the samples were placed in a thermocycler (Eppendorf) and cDNA synthesis was performed according to the cycling conditions in Table 2.2.

Table 2.1: Reagents and volumes required for first-strand cDNA synthesis

Component	Volume (µl)
RNA	X µl equivalent to 1 µg
Random hexamer primers (500 ng/µl)	3
H_2O	Make to 17
70 °C for 5 min followed by pulse centrifuge	
5x Buffer	5
dNTP (10 mM)	1.3
Reverse Transcriptase (200 units/µl)	0.5
RNase Inhibitor (40 units/µl)	0.5
Gentle mix and centrifuge	

Table 2.2: Thermal cycler conditions for first-strand cDNA synthesis

Temperature (°C)	Time (min)
85°C – Lid	
37	40
42	40
80	10
4	∞

2.1.15 Polymerase chain reaction (PCR)

Template cDNA was diluted 1:5 in nuclease-free H_2O (Fisher). To 0.2ml PCR grade eppendorfs (Corning), additional reagents were added as per Table 2.3. Samples were gently mixed, pulse centrifuged and loading into a thermal cycler (Eppendorf) and ran according to the conditions in Table 2.4.

Table 2.3: Reagents for PCR

Component	Volume (µl)
cDNA	1
Forward primer (4pM)	1
Reverse primer (4pM)	1
dNTP (10nM)	2
Taq DNA Polymerase (5 units/µl)	0.2
10x Buffer A	5
Nuclease free H_2O	15.8

Table 2.4: Thermal cycler conditions for PCR

Step	Temperature (°C)	Time (min)
Lid 100		
1	95	3
2	94	1
3	60	0.5
4	72	1
Repeat steps 2-4 for 35 cycles		
5	72	7
6	80	10
7	4	∞

2.1.16 Quantitative real time-PCR (qRT-PCR)

Template cDNA was thawed, diluted 1:25 in nuclease free H_2O (Fisher) and set aside. Additional reagents were aliquotted into eppendorfs to make master-mix solutions as per the required target gene, according to Table 2.5.

Table 2.5: qRT-PCR reagents and volumes.

Component	Volume per sample (µl)
Nuclease free H_2O	1.25
Forward primer (4pM)	1.25
Reverse primer (4pM)	1.25
SYBR® Green JumpStart™ *Taq* ReadyMix™	5
Template cDNA (1:25)	1.25

Samples were loaded in duplicate into a FrameStar™ LC half-skirted, 96 well plate and sealed with an optically clear adhesive cover (Rainin Instrument, LLC). Plates were pulse centrifuged to ensure complete sample collection within wells. QRT-PCR was performed using a Roche Lightcycler® 480 system according to parameters specified in Table 2.6.

Table 2.6: Cycler conditions for qRT-PCR

Step	Temperature (°C)	Time (min)
1	94	2
2	94	0.25
3	60	1
Repeat steps 2-3 for 40 cycles		
4	65-95	10

Table 2.7: Primer sequences for qRT-PCR

Primer	Sequence
Murine TNF-α Forward	5’-CATCTTCTCAAAATTCGAGTGACAA-3’
Murine TNF-α Reverse	5’-TGGGAGTAGACAAGGTACAACCC-3’
Murine RANTES Forward	5’-GGAGATGAGCTAGGATAGAGGG-3’
Murine RANTES Reverse	5’-TGCCCATTTTCCCAGGACCG-3’
Murine GAPDH Forward	5’-GCACAGTCAAGGCCGAGAAT-3’
Murine GAPDH Reverse	5’-GCCTTCTCCATGGTGGTGAA-3’
Human IFN-β Forward	5’-AACTGCAACCTTTCGAAGCC-3’
Human IFN-β Reverse	5’-TGTCGCCTACTACCTGTTGTGC-3’
Human TNF-α Forward	5’-CACCACTTCGAAACCTGGGA-3’
Human TNF-α Reverse	5’-CACTTCACTGTGCAGGCCAC-3’
Human RANTES Forward	5’-TGCCTGTTTCTGCTTGCTCTTGTC-3’
Human RANTES Reverse	5’-TGTGGTAGAATCTGGGCCCTTCAA-3’
Human TPI Forward	5’-TGGTTTGTGCTCCCCCTACT-3’
Human TPI Reverse	5’-CACAGCAATCTTGGGATCTAGCT-3’
Human SOD1 Forward	5’-GGTGTGGCCGATGTGTCTAT-3’
Human SOD1 Reverse	5’-CCTTTGCCCAAGTCATCTGC-3’
Human NME2 Forward	5’-CCATGGCCAACCTGGAG-3’
Human NME2 Reverse	5’-CTTCAGGTGTTCTTCAGAGGC-3’
Human TRAM Forward	5’-AAGGAAGACAGAAAAGCCGC-3’
Human TRAM Reverse	5’-ATCCAAGGCAGAAGAGGAAAACT-3’
Human Ferritin HC Forward	5’-GCCAGAACTACCACCAGGACT-3’
Human Ferritin HC Reverse	5’-GCCACATCATCGCGGTCAAA-3’
Human Ferritin LC Forward	5’-CAACCTCCGGGACCATCTTC-3’
Human Ferritin LC Reverse	5’-TGGGAGCTCATGGTTGGTTG-3’
Human IL-6 Forward	5’-AGCCACTCACCTCTTCAGAACGAA-3’
Human IL-6 Reverse	5’-CAGTGCCTCTTTGCTGCTTTCACA-3’
Human IFNα Forward	5’-GAAATACTTCCAAAGAATCACTCT-3’
Human IFNα Reverse	5’-GATCTCATGATTTCTGCTCTGACA-3’
Human CXCL10 Forward	5’-ATTATTCCTGCAAGCCAATTTTG-3’
Human CXCL10 Reverse	5’-TCACCCTTCTTTTTCATTGTAGCA-3’
Human NLRP12 Forward	5’-TGTTGGTGCAGCTCAGACCAG-3’
Human NLRP12 Reverse	5’-ATCAGTGTGAGAATCCAGCA-3’
Human DJ-1 Forward	5’-CTGTTGGCTATGAAATAGG-3’
Human DJ-1 Reverse	5’-GTGTAATGACCTCCATTCATC-3’
Human STMN1 Forward	5’-AGATGTACTTCTGGACTCAC-3’
Human STMN1 Reverse	5’-GATCAGACCAGGTAATCAATG-3’
Human GSTO1 Forward	5’-GGTGGCAATTCTATCTCTATG-3’
Human GSTO1 Reverse	5’-GTGGTCTACACACTCATTTACA-3’
Human PPP1Cα Forward	5’-TGCTGGCCATAAGATCAAG-3’
Human PPP1Cα Reverse	5’-CTTGCACTCATCGTAGAAAC-3’

2.1.17 Reporter assays

HEK293-TLR7 cells were seeded into 96 well plates ($2x10^5$ cells/ml – 200 µl/well). After 48 hr, cells were transfected with vectors encoding a reporter gene for either the IFNα promoter (p125), IFNβ, NF-κB, or RANTES promoters (60 ng/well) and co-transfected with either empty vector (EV) or increasing amounts of an expression vector encoding mutated versions of the human TLR adaptors TRAM (TRAM G2A), TRIF (TRIF ΔCΔN), or MAL (MAL P126H) using Lipofectamine 2000 (Invitrogen), according to the manufacturer's instructions. A total of 20 ng/well Renilla-luciferase reporter gene was transfected simultaneously to noramlise transfection efficiency. After 24 hr, cells were stimulated with 5 µg/ml of CLO97 for an additional 24 hr. Thereafter, cell lysates were prepared and reporter gene activity was measured using the Dual-Luciferase Assay system (Promega). Data were expressed as the mean fold induction relative to the control.

2.1.18 Enzyme-Linked Immunosorbent Assay (ELISA)

Appropriate capture antibody was plated onto Maxisorp 96-well plates (NUNC) (1 µg/ml for TNFα and RANTES, 2 µg/ml for IL-6) overnight at RT. The following day, plates were washed four times with wash buffer (sterile 1x PBS containing 0.05 % (v/v) Tween-20) followed by blocking with blocking buffer (PBS containing 1 % (w/v) BSA) for minimum 2 hr. The plates were then washed four times with wash buffer. Next, serial dilutions of the standards (ranging from 0 to 4000 pg/ml; 100 µl/well) and samples were added (100 µl/well) followed by incubation at 4 °C overnight. Plates were washed again four times with wash buffer followed by the addition of the appropriate biotinylated detection antibody (0.2 µg/ml for IL-6, 0.25 µg/ml for RANTES and 0.5 µg/ml for TNFα) for 2 hr at RT. Plates were washed four times with wash buffer followed by the addition of Avidin-HRP conjugate (1:2000 for RANTES, TNFα and IL-6) for 30 min. Thereafter, plates were washed five times with wash buffer followed by addition of citric acid substrate buffer (100 µl/well) supplemented with o-Phenylenediamine (Sigma) and 30 % hydrogen peroxide (Sigma).

Plates were incubated in the dark with gentle shaking with the absorbance measured at various intervals at 490 nm using a spectrophotometer (BioTek).

2.1.19 Nuclear Extraction

Cellular nuclear extracts were prepared according to the manufacturer's instructions (Nuclear Extraction Kit, Cayman Chemical). Briefly, experimental cells were washed in ice-cold PBS, harvested and pelleted by chilled centrifugation in PBS. Cell pellets were resuspended in PBS/Phosphatase Inhibitor Solution and re-centrifuged. This was repeated once, after which, 250 µl Hypotonic Buffer solution was added to the pellets, mixed gently by pipetting, transferred to a fresh, chilled eppendorf and incubated for on ice for 15 min. Next, 50 µl Nonidet P-40 Assay Reagent was added to lyse the plasma membrane and the samples were pulse centrifuged at 16,464 g for 30 sec. The supernatant was discarded and the nuclear pellet was resuspended in Complete Nuclear Extraction Buffer, vortexed for 15 sec and incubated on ice with gentle shaking for 15 min. Samples were vortexed again for 30 sec and incubated on ice with gentle shaking for an additional 15 min. Samples were centrifuged at 16,464 g for a final 10 min and the nuclear fraction-containing supernatant was removed to a fresh eppendorf and stored at -80 °C.

2.2 Methods in Proteomics: 2D-DIGE and LC/MS

2.2.1 Sample lysis

Experimental cell culture samples were washed in 10 ml ice-cold PBS, harvested and subjected to centrifugation at 4°C for 5 min at 161 g. Pelleted samples were then lysed in 2D lysis buffer (7 M Urea, 2 M Thiourea, 100 mM DTT, 4% (w/v) CHAPS, 1% (v/v) Triton X-100, 0.06 % (v/v) ampholytes pH4-7, 0.06 % (v/v) bromophenol blue) with repeated pipetting until all cell clumps were solubilised. Samples were incubated on ice for a further 30 min with frequent pipetting to aid lysis before chilled centrifugation at 16,464 g for 10 min. Whole cell lysate-containing supernatants were removed to fresh, chilled eppendorfs and frozen at -80 °C prior to a 'clean-up' step to remove impurities.

2.2.2 Sample Clean-up

Sample clean-up was undertaken using a 2D Clean-Up Kit according to the manufacturer's instructions (General Electric (GE) Healthcare). Briefly, to each sample, 300 µl precipitant was added, followed by vortexing and incubation on ice for 15 min. A further 300 µl of co-precipitant was then added, followed by mixing. Samples were centrifuged at 16,464 g for 8 min followed by removal of the supernatant (Note: all centrifugation steps were carried out at 4 °C.) Next, 40 µl of co-precipitant was added to the sample followed by incubation on ice for 5 min and centrifugation at 16,464 g for 5 min. Supernatants were removed and 25 µl distilled H_2O was added followed by sample vortexing to disperse the pellet. Next, 1 ml ice-cold wash buffer, containing 5 µl wash buffer additive, was added followed by vortexing for 30 sec every 10 min for a total of 40 min. Samples were then centrifuged at 16,464 g for 5 min after which, the supernatant was removed. The samples were allowed to air dry for 5 min on ice. Approximately 100 µl 2x DIGE labelling buffer (8 M urea, 30 mM Tris, 4% CHAPS, pH 9) was then added followed by pipetting and water bath sonication to aid resuspension.

2.2.3 Protein Quantification

Proteins were quantified using a Bradford assay [183]. Protein standards ranging from 0 – 2 mg/ml were prepared by diluting a BSA stock (5 mg/ml) in 0.1 M HCl, 2D lysis buffer and dH_2O in 4 ml polystyrene cuvettes (Sarstedt). In separate cuvettes, samples were prepared by mixing 10 µl whole cell lysate with 10 µl 0.1 M HCl plus 80 µl dH_2O. To both samples and standards, 3.5 ml of Protein Assay solution (Bio-Rad) (diluted 1:4 with dH_2O) was added and incubated at room temperature for 5 min. The protein content of both standards and samples was measured by spectrophotometric analysis at 595 nm. A standard curve was plotted according to the known standards and the line equation calculated. Sample protein concentrations were calculated by inputting their spectrophotometric readings into the line equation.

2.2.4 DIGE Labelling

Quantified protein samples were labelled with CyDye DIGE Fluor minimal dyes according to the manufacturer's instructions (GE Healthcare). Briefly, Cy2, Cy3 and Cy5 DIGE dyes were reconstituted to a concentration of 1 mM in fresh dimethylformamide (DMF) (Sigma) and stored at -20 °C when not in use. Stock dye solutions were then further diluted to a working concentration of 400 µM using DMF immediately prior to labelling. Next, 50 µg of protein from each unstimulated and stiulated biological replicate was quantified and minimally labelled with 400 pmol of Cy3 and Cy5 working solution respectively. A further 25 µg of protein from unstimulated and stimulated samples corresponding to each biological replicate were pooled and minimally labelled with 400 pmol Cy2 as the internal standard. Samples were immediately mixed, pulse centrifuged and incubated on ice in the dark for 30 min. Labelling was quenched by adding 1 µl of 10 mM lysine with mixing and incubation for 10 min in the dark on ice. At this point, labelled samples corresponding to each biological replicate were pooled in single eppendorfs. For example, Cy2, Cy3 and Cy5 labelled labelled

samples from biological replicate one were pooled into one eppendorf followed by gentle mixing and centrifugation. To this mix, an equal volume of 2x lysis buffer (7 M urea, 2 M thiourea, 4 % CHAPS, 0.04 % bromophenol blue) was added and made to 450 µl with rehydration buffer (8 M urea, 2 % CHAPS, 0.5 % IPG 4-7 buffer, 0.002% bromophenol blue).

2.2.5 IPG strip rehydration

Each sample was pipetted into a re-swelling tray (Amersham Bioscience) and overlaid with individual, 24 cm linear pH 4-7 IPG strips (GE Healthcare). The IPG strips were overlaid with 3 ml of mineral oil (Sigma) per strip. The re-swelling tray was then placed in darkness at RT for a minimum of 14 hr to allow passive strip rehydration to occur.

2.2.6 1st Dimension isoelectric focusing (IEF)

Rehydrated IPG strips were loaded gel-side up on an Amersham Ettan IPG-phor manifold and overlaid in mineral oil in order to keep the IPG gel matrix moist and aid conduction. 1st dimension IEF was performed in darkness using the Amersham IPG-phor IEF system according to table 2.8.

Table 2.8: 1st dimension IEF running conditions.

	Step	Voltage (V)	Time
1	Hold	250	3 hr
2	Gradient	8,000	4 hr
3	Hold	8,000	80,000 Vhr
4	Hold	500	24 hr

2.2.7 Gel Casting

Acrylamide gels (250 x 200 x 1 milimetre (mm), 10 % acrylamide) for 2nd dimension SDS-Page were prepared 24 hr prior to running to allow time for complete gel polymerisation. Gel composition was as follows: 10% Acrylamide, 0.38 M Tris-HCl pH 8.8, 0.1 % SDS (v/v), APS 0.05 % (v/v) and TEMED 0.04 % (v/v). Gels were poured to 98 % capacity, overlaid

with 30 % isopropanol and allowed to set at RT overnight. Immediately prior to IPG strip loading, the 30% isopropanol was removed.

2.2.8 2nd Dimension Gel Electrophoresis

Following 1st dimension IEF, proteins within the IPG strips were reduced by overlaying with DTT equilibration solution (6 M urea, 30 % (w/v) glycerol, 2 % (w/v) SDS, 100 mM DTT) for 15 min at RT with gentle agitation. This solution was removed and the proteins were alkylated by overlaying with iodoacetamide equilibration solution (6M urea, 30 % (w/v) glycerol, 2 % (w/v) SDS, 100 mM DTT, 0.25 M iodoacetamide) for a further 15 min, again with gentle agitation. The IPG strips were briefly washed in 1x SDS running buffer and applied, gel-side out, to the resolving gels. The interface between the IPG strip and the resolving gel was sealed with melted 0.5 % agarose sealing solution (25 mM Tris base, 192 mM glycine, 0.1 % SDS, 0.5 % agarose, 0.002 % bromophenol blue) and allowed to solidify at RT for 5 min. Sealed glass plates were then loaded into an electrophoresis tank (Ettan DALT*twelve* Separation Unit, GE Healthcare) and filled to 75 % capacity with 7 L of 1x SDS running buffer. Remaining slots were filled with artificial plates and the tank was topped off with 2 L of 2x SDS running buffer. For 2nd dimension separation, electrophoresis was performed in darkness at 0.5 watt/gel for 1 hr followed by 1 watt/gel until the tracking dye reached the bottom of the plate.

2.2.9 Image Acquisition

Gel images were scanned using the Typhoon Trio Variable Mode Imager (Amersham Biosciences/GE Healthcare). The photomultiplier tube (PMT) voltage values for gels analysed were between 500 V and 700 V and the maximum pixel volume was between 85,000 and 95,000. Scanning was performed at 50 mm resolution and saved in the .gel file format.

2.2.10 Image Analysis

Gel images were analysed using Progenesis Same Spots software version 3.2.3 (NonLinear Dynamics). Images were categorised according to their label: Cy3 (unstimulated), Cy5 (stimulated) and Cy2 (internal standard) for later protein abundance comparisons and normalisation. To ensure correct protein spot alignment between replicate gels, all images in an experiment were virtually overlaid through a combination of manual and automatic alignments against a manually determined 'reference gel' that displayed optimal spot separation across all dimensions. Spots were automatically detected and filtered to eliminate false detections (typically by size exclusion). Next, the images were separated into control and stimulated groups and individual spots were analysed to detect changes in abundance between the two sets and across their biological replicates. A spot list was generated displaying those with significant protein abundance fold changes between biological conditions. Only spots with a fold change <1.3 and a P value less than 0.05 were taken into consideration. Further manual analysis was carried out to eliminate false detections. Spots that met these criteria were subsequently visualised, excised and prepared for LC/MS.

2.2.11 Protein Visualisation

As DIGE labelled spot patterns are invisible to the human eye, the proteins must be visualised to facilitate manual excision. Therefore, the reference gel was subjected to silver staining in order to visual the proteins within the gel. Briefly, the reference gel was removed from its plate and gently placed in 500 ml fixing solution (30 % ethanol, 10 % glacial acetic acid) and gently rocked for 60 min. This step was repeated once with fresh fixing solution. The fixing solution was removed and the gels were sensitised using 250 ml sensitising solution (30 % ethanol, 0.2 % (w/v) sodium thiosulphate and 6.8 % (w/v) sodium acetate for 2 hr. Sensitising solution was removed and gels were washed 5 x 8 min in Milli-Q water. Gels were impregnated with silver by addition of 250 ml silver solution (0.25 % silver nitrate) for 1 hr.

Silver solution was removed and gels were washed 4 x 1 min in Milli-Q water. Developing solution (2.5 % sodium carbonate, 0.08 % (v/v) of 37 % (w/v) formaldehyde) was then added for approximately 5-10 min until protein spots became visible. Before high background development, the developing solution was removed and replaced with fixing solution (4 % Tris, 2 % acetic acid) for 10 min. Finally, gels were washed for 2 x 30 min in Milli-Q water and stored in plastic film at 4 °C in 5 % acetic acid solution prior to spot excision.

2.2.12 Spot Excision

Protein spots selected for mass spectrometry analysis were manually excised from the silver stained gel using a cut pipette tip and transferred to a 1.5 ml eppendorf tube.

2.2.13 Gel Destaining

Silver stained gel pieces were destained using a standard lab protocol. Briefly, 10 ml each of 30 mM potassium ferricyanide and 100 mM sodium thiosulphate were freshly prepared and mixed. Next, 50 µl of this solution was added to each excised gel piece and incubated at RT with gentle shaking until the brown, silver nitrate residue disappeared from the gel. The gel pieces were washed with Milli-Q water until the yellow potassium ferricyanide residue was removed. Gel pieces were incubated in 100 µl of 200 mM ammonium bicarbonate (Ambic) for 20 min with gentle shaking. The solution was then removed and 100 µl of a 2:3 ratio of 200 mM Ambic/100 % acetonitrile was added and placed at 37 °C for 10 min. The solution was removed and 100 µl of 50 mM Ambic added to each tube and placed at 37 °C for 10 min. This solution was removed and 100 µl of 100 % acetonitrile was added and placed at 37 °C for 10 min. This final solution was removed. The gel piece was now ready for trypsin digestion.

2.2.14 In-gel Trypsin Digestion

Following de-staining of the individual gel plugs, protein digestion was performed as per Mann et al., [184]. Briefly, the trypsin digestion solution was prepared by resuspending 20 µg sequencing grade trypsin (Promega) in 1.5 mL 10mM Ammonium Bicarbonate containing 10 % (v/v) acetonitrile. Next, 50 µl of trypsin solution was incubated with each gel piece on ice for 2 hr followed by the layering of 10 µl of a 10 mM AmBic, 10 % Acetonitrile solution on top of the gel pieces to prevent drying out. At this point, gel pieces were incubated at 37 ^{o}C overnight. Peptides were extracted from the gel plugs using 100 µl extraction buffer (1:2 (v/v) 5% formic acid (FA)/acetonitrile) followed by incubation at 37 ^{o}C for 15 min with shaking. The solution containing the extracted peptides was then removed from each sample and placed in a fresh eppendorf. Samples were vacuum dried using a concentrator (Eppendorf) and stored at -20 °C prior to MS analysis.

2.2.15 LC/MS/MS

All peptide identifications were carried out using the Ion Trap 6340 LC/MS/MS system supplied by Agilent. Digested samples were resuspended in 20 µl 0.1 % (v/v) trifluroacetic acid (TFA) in Milli-Q water. Samples were then filtered in 0.22 µm spin filters (Corning) and 5 µl of the trypsin digested sample was loaded onto a C18 chip (G4240-62006) (Agilent) at a rate of 0.6 µl/min in 0.1 % FA. The mobile phases were aqueous solutions of 0.1 % (v/v) FA and an acetonitrile solution of 0.1 % (v/v) FA. A 10 min gradient was carried out to increase the acetonitrile concentration to 100 % linearly. Charged ions were generated using an electrospray ionisation source. Spray voltage was set to 2000 V.

2.3.16 Protein Identification

All peptides were submitted to the Mascot search engine (Matrix Science) to identify proteins. All peptides were searched in both the NCBinr and Swiss-Prot databases. The enzyme used was selected as trypsin and up to 2 missed cleavages were allowed. Peptide mass tolerance was set at ±2 for precursor ions and a tolerance of ±1 for fragment ions. Variable modifications allowed for were carboxymethyl (C) and oxidation (M). Taxonomy was selected as mammalian. When using the NCBinr database individual ion scores >54 indicate protein identity or extensive homology. Only peptides matched with an ion score above 54 were accepted as significant. When using the Swiss-Prot database individual ion scores >40 indicate protein identity or extensive homology. Only peptides matched with a score >40 were accepted as significant.

2.3 Methods in Proteomics: Label Free Quantitative Mass Spectrometry (LFQ MS)

2.3.1 Sample Clean-up

Protein samples were cleaned and desalted using a 2D clean-up kit (GE Healthcare, UK) according to the manufacturer's instructions. Protocol was carried out as per section 2.2.2 with one modification: the final protein pellet was resuspended in 300 µl of resuspension solution (50 mM Ambic, 1 mM calcium chloride ($CaCl_2$)).

2.3.2 Sample Quantification

Cleaned protein samples were quantified for protein concentration using the Qubit® Quant-IT™ Protein Assay Kit (Invitrogen, UK) on a Qubit® flourometer v.2.0 according to the manufacturer's instructions. Briefly, three protein standards equivalent to 0 ng/µl, 200 ng/µl and 400 ng/µl were prepared by diluting the supplied protein reagent (10 µl) in Qubit® Protein Buffer (190 µl). Equivalent volumes of Protein Buffer were also mixed with the samples to be analysed followed by incubation of both samples and standards at RT for 15 min. Finally, the fluorometer was calibrated using the prepared standards before measuring of the samples.

2.3.3 Sample Acetlyation and Trypsin Digestion

Following sample quantification, 50µg from each was pipetted into a fresh 1.5 ml microcentrifuge tube. Next, 10 µl of 200 mM dithiothreitol (DTT) suspended in 100 mM Ambic solution was added to each sample followed by incubation at 95 °C for 15 min. Protein acetylation was performed by adding 4 µl of 1 M iodoacetamide (IAA) suspended in 100 mM Ambic to each sample followed by incubation at 25 °C for 45 min. The acetylation reaction was stopped by adding 20 µl of 200 mM DTT with incubation at 25 °C for 45 min. Samples were quantified again for protein concentration and 10 µg was removed from each sample and transferred into a fresh 1.5 ml microcentrifuge tube. To these, 0.5 µl of 0.5 µg/µl

trypsin was added. To ensure maximal tryspin digestion, samples were incubated at 37 °C overnight followed by speed vacuuming to concentrate the peptide preparation.

2.3.4 Peptide Purification

Lyophilised, trypsin digested protein peptides were further purified for MS using the ZipTip procedure (Millipore) according to the manufacturer's instructions. Briefly, trypsin digested peptides were resuspended in 20 µl Resuspension Buffer (0.5 % TFA in LC/MS grade H_2O). The protein samples were sonicated for 2 min to aid resuspension followed by a pulse centrifugation. The ZipTips were wetted by aspirating and dispensing 10 µl of Wetting Solution (0.1 % TFA in 80 % acetonitrile) five times. Tip equilibration was carried out by aspirating and dispensing 10 µl Equilibration Solution (0.1 % TFA in LC/MS grade H_2O) five times. To bind the peptides, 10 µl of each sample was aspirated and dispensed into the ZipTips. This was repeated a further 9 times, each time aspirating and dispensing into the same eppendorf. The sample containing tips were then washed by aspirating and dispensing 10 µl of Washing Solution (0.1 % TFA in 80 % acetonitrile) from the tip to waste five times in total. Elution of the peptide samples was achieved by aspirating and dispensing 10 µl of Elution Solution (0.1 % TFA, 60% acetonitrile) from the tip into a 1.5 ml eppendorf tube five times. The resulting peptide solution was speed vacuumed and resuspended in 12 µl of loading buffer (0.05 % TFA, 98 % LC/MS grade H_2O, 2 % LC/MS grade acetonitrile). Finally, samples were transferred to MS compatible vials ensuring no bubbles were present in the solution.

2.3.5 Label-Free Mass Spectrometry

Peptide samples were run on a Thermo Scientific Q Exactive mass spectrometer connected to a Dionex Ultimate 3000 (RSLCnano) chromatography system in the University College Dublin, Conway Institute of Biomolecular and Biomedical Research, Mass Spectrometry Resource unit. Each sample was loaded onto Biobasic Picotip Emitter (120 mm length, 75

μm ID) packed with Reprocil Pur C18 (1.9 μm) reverse phase media and was separated by an increasing acetonitrile gradient over 43 minutes at a flow rate of 250 nL/min. The mass spectrometer was operated in positive ion mode with a capillary temperature of 220 °C and with a potential of 2000 V applied to the frit. All data were acquired with the mass spectrometer operating in automatic data dependent switching mode. A high resolution (70,000) MS scan (300-2000 Dalton) was performed using the Q Exactive to select the 15 most intense ions prior to MS/MS analysis using higher-energy collisional dissociation (HCD).

2.3.6 LFQ analysis

Protein identification and LFQ analysis was conducted using MaxQuant (version 1.3.0.5; http://maxquant.org/). The Andromeda database search engine was used to correlate MS/MS data against the IPI Human FASTA protein database provided by MaxQuant version 1.3.0.5. Protein identification was performed according to the search parameters specified in Table 2.9.

Table 2.9: Search parameters for protein identification on Andromeda protein database.

Search Parameter	**Parameter used**
Precursor-ion mass tolerance	1.5 Da
Fragment ion mass tolerance	6 parts per million
Fixed modification	Cysteine carbamidomethylation
Variable modifications	Protein N-acetylation Methionine Oxidation
Missed Cleavage Sites	Max 2 missed cleavage sites
False Discovery Rates	0.01 (peptides and proteins)
Min. peptide length considered for identification	6 aa
Min. peptides for protein identification	2 peptides

Differentially expressed proteins among experimental groups were determined by LFQ using MaxQuant and Perseus (version 1.2.0.17). Peptides were matched across samples based on mass to charge ratio, elution time (within a 2 min boundary) and spectral features. Protein intensities were determined using unique and razor (those most likely to have originated from a protein based on the principle of parsimony) peptides. Protein intensities were normalised across runs to account for variation in sample loading and pair-wise ratios of all peptides of a particular protein group were calculated across all samples and the protein intensities were corrected in order to reflect the median peptide ratios. The final data matrix was generated containing the normalised intensities (presented as LFQ intensities) for each individual sample where imported into Perseus for quantitative analysis. LFQ intensities measured for individual runs were grouped based on their experimental treatment, log2 transformed and an analysis of variance (ANOVA) (p<0.05) was performed to identify variation. A qualitative assessment of differential expression was also conducted. This involved the identification of proteins that were completely lacking from a specific treatment. Proteins that were completely missing from all replicates of a particular group but present in other groups were determined manually from the data matrix. These proteins are not considered statistically significant as the values for absences are given as NaN (not a number) which is not a valid value for an ANOVA analysis. However the complete absence of a protein from a group may be biologically significant and these proteins were reported as qualitatively differentially expressed.

2.4 Statistical analysis

Statistical analysis was carried out using the unpaired Student's t test. P-values of less than or equal to 0.05 were considered to indicate a statistically significant difference where * indicates p<0.05, ** indicates p<0.005 and *** indicates p<0.001.

Chapter 3

The TIR-adaptor TRAM is required for maximal TLR7 mediated RANTES and type-I IFN production

3.1: Introduction

3.1.1 TRAM Structure

In contrast with TRIF, TRAM is both the smallest adaptor protein (235 aa) and the least functionally diverse, mediating TLR4 and IL-18R signalling only (Figure 3.1) [12, 23].

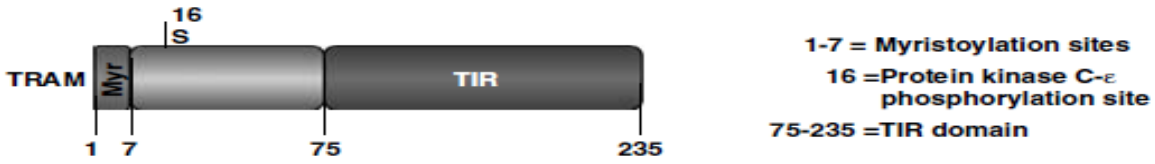

Figure 3.1: Schematic illustrating domain segmentation of TRAM. TRAM can be divide into three separate regions: an N-terminal region containing a myriostoylation site; a central domain containing a phosphorylation site and the C-terminal TIR-domain. Adapted from [26].

Amino acids 1-7 at the N-terminus contain a myristoylation site which is believed to allow TRAM to target to the plasma membrane [82]. Serine 16 can be phosphorylated by protein kinase CΣ (PKCΣ) and this may serve to release TRAM from the plasma membrane upon activation, allowing it to transduce further signals downstream (Figure 3.1). Impairment of this phosphorylation inhibits TRAM signalling [83].

3.1.2 TLR7/8 and TLR9 evolution and structure

The endosomal TLRs, TLR3, TLR7, TLR8 and TLR9 are part of an evolutionary cluster believed to have arisen via an X-linked duplication event approximately 150 million years ago [10, 185]. TLR7/8 and TLR9 are considered a subfamily within the TLRs for a number of reasons. Each contains an extracellular domain greater than 800 aa compared to the TLR1 subfamily for example, which is less than 600 aa [10]. Unlike other TLRs, they each recognise pathogen derived nucleic acids [186] and also share structural similarities that classes them as phylogenetic neighbours [185]. Within the subfamily, crystal structures are currently available for TLR3, bound to its cognate ligand double-stranded RNA (dsRNA) [187] and also for TLR8, bound to its synthetic activators, CL097, CL075 and R848 [188]

(Figure 3.2). Under basal conditions, TLR8 exists as a homodimer [188]. Ligand binding causes a structural rearrangement in which the LRR-LRR interactions, which normally ensure monomer-monomer binding, are rearranged to cause an 'opening-up' of the TLR8 structure by 15Å on its upper face to allow efficient ligand recognition. The resulting rearrangements also cause the two C-termini to come into close proximity from approximately 53 to 30Å (Figure 3.2). Critically, this leads to binding of the cytoplasmic TIR domains which are essential in transducing a downstream signal to the nucleus [188].

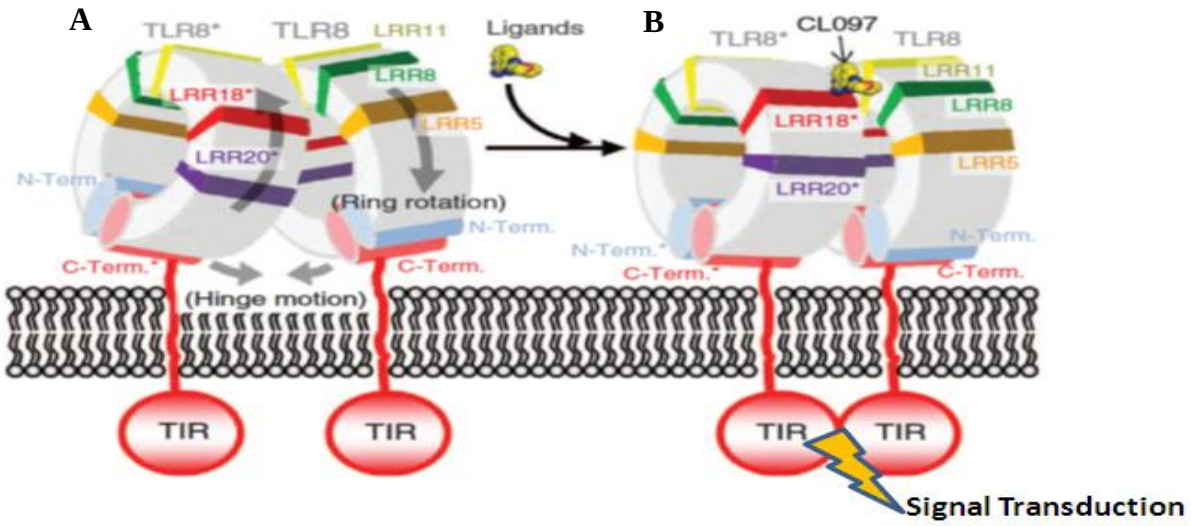

Figure 3.2: Conformational change adopted by TLR8 upon agonist binding. (A) TLR8 exists in dimeric form basally with the C-termini directionally opposed to each other (B) Agonist binding causes a hinge-like conformational change in which the C-termini are brought closer together. This in turn brings the opposing TIR-domains into contact thus transmitting the activation signal. Adapted from [188].

Although the crystal structure for TLR9 has not been determined, its structure has been inferred from various biochemical studies [189, 190] and it would appear that the mechanism of activation is similar to that of TLR8. Like TLR8, TLR9 also exists basally in an inactive dimeric form [190]. In this form, TLR9 is capable of binding both stimulatory and inhibitory DNA but critically, only stimulatory DNA causes conformational changes in the TLR9 homodimers which results in the association of the cytoplasmic TIR-domains [190]. Subtle differences within the nucleotide ligand appear to dictate vastly different responses from

TLR9 possibly indicating an evolutionary strategy to recognise non-host derived nucleotides preferentially.

3.1.3 TLR9 signalling

TLR9 was originally shown to recognise DNA of bacterial origin, specifically unmethylated CpG motifs, a distinction which is much rarer in mammalian DNA than in bacterial or viral DNA [38]. TLR9 can also recognise double stranded DNA containing viruses such as herpes simplex virus 1 and 2 [191, 192]. Synthetically produced CpG containing oligonucelotides are commonly used to specifically activate TLR9 and indeed specific sequence modifications are believed to tailor the cytokine response [193]. However, more recently it has been shown that the endosomal targeting of DNA is the determining factor in TLR9 activation rather than the particular sequence or even the origin of the DNA [194]. This would agree with observations that TLR9 in some cases can recognise self-nucleic acids as well as non-self [195]. TLR9 localises within intracellular compartments particularly the endoplasmic reticulum, endosome and lysosomes [196]. This strategy helps to isolate TLR9 from self-nucleotides which are usually, but not always, excluded from these compartments. For TLR9 to become activated however, it must traffic to the endolysosome where essential acidification occurs [197]. Trafficking is itself a highly regulated process with chaperones including gp96 and UNC93B1 being essential for TLR7/8 and TLR9 to traffic from the ER to the endolysosome. Once in the endolysosome, TLR9's ectodomain is cleaved by cathepsins and this has been shown to increase its affinity for CpG DNA - however it is not essential [186]. Cleavage is however required for TLR9 to bind its downstream adaptor molecule MyD88 and to transmit a signal [198, 199].

Recruitment of MyD88 to TLR9 can lead to both NFκB mediated pro-inflammatory and IRF7 mediated type-I IFN production [200]. N-terminal death domains (DD) on MyD88 interact with and recruit IL-1R associated kinase-4 (IRAK4) via its own DDs [45]. This

causes downstream phosphorylation and activation of kinases IRAK1 (which is dispensible for TLR9 mediated NFκB but not IRF7 activation [201]) and IRAK2 which in turn phosphorylate and activate TNF receptor-associated factor 6 (TRAF6) [202]. TRAF6 utilises its E3 ubiquitin ligase activity to ubquitinate a scaffolding protein, NFκB essential modulator (NEMO) [47]. The combination of TRAF6 mediated ubiquitin chain formation and NEMO functions to recruit TGF-β activated kinase 1 (TAK1) which itself recruits the TAK-1 binding proteins 1 (TAB1) and TAB2. TAK1 phosphorylates IKKβ as well as initiating a MAP kinase cascade leading to activation of the transcription factor CREB. IKKβ phosphorylates the inhibitors of κB (IκB) α and IκBβ leading to NFκB release and nuclear translocation to bind the promoter regions of pro-inflammatory cytokines such as TNFα and IL-12. Other members of the IRF transcription factor family are also believed to be involved such as IRF5 and IRF8 with IRF5 associating with MyD88 and TRAF6 (Figure 3.3) [203, 204].

While the above pathway holds true for many classes of cells including macrophages and conventional dendritic cells, an additional pathway exists in plasmacytoid dendritic cells (pDCs). The exact details of this pathway have not been elucidated to the same extent as the pro-inflammatory pathway above, however it involves initial MyD88, IRAK4, IRAK1 and TRAF6 recruitment, as per the NFκB pathway, followed by engagement of TRAF3, IKKα and IRF7. The kinases IRAK1 and IKKα are believed to phosphorylate IRF7 leading to the production of large quantities of type-I IFN [200, 205]. It has been suggested that engagement of TLR9 in the early endosome leads to preferential activation of the IRF7 signal cascade whereas binding of TLR9 in the late endosome favours the activation of the NFκB pathway (Figure 3.3) [206].

3.1.4 TLR7/8 signalling

Both TLR7 and TLR8 were originally shown to sense synthetic antimicrobial imidazoquinoline derivatives such as imiquimod, an approved treatment for external genital warts, and its more powerful derivative, resiquimod (R848) [40]. Sensitivity to these ligands was abolished in both TLR7 and MyD88 deficient mice indicating that MyD88 was also a critical adaptor molecule in TLR7 signalling. Expression of both human and mouse TLR7 but only human TLR8 in HEK293 cells dose dependently conferred responsiveness to R848. Expression of murine TLR8 did not confer responsiveness and this combined with the observation that TLR7 deficient mice did not respond to R848 despite the presence of TLR8 has led to the suggestion that murine TLR8, unlike its human counterpart, is non-functional [40, 207]. A role for the endosome and lysosome in TLR7 and TLR8 signalling was suspected early on as inhibition of their maturation or acidification inhibited TLR7, TLR8 (and TLR9) mediated signalling and abolished MyD88's endosomal translocation [208, 209]. Further studies confirmed or suggested roles for IRAK1, IRAK4, IRF5, IRF7 and TRAF6 in TLR7/8 signalling and that for the most part, the signalling process involved replicated that of TLR9 (Figure 3.3) [200, 201, 210-212]. Consistent with their endosomal location and signalling similarities with TLR9, the physiological ligand for TLR7/8 was also found to be nucleotide based [213]. Specifically, guanidine (G) and uradine (U) rich ssRNA derived from viruses such as human immunodeficiency virus-1 (HIV-1), VSV, influenza virus as well as non-viral RNA were found to mount a prolific innate response in a TLR7/8 dependent manner [214-216]. TLR7/8 can also sense bacterially derived RNA [217]. TLR8 is expressed in many tissues including the placenta, lung, spleen, lymph node and peripheral blood with TLR7's expression confined to the placenta, lung and spleen [218].

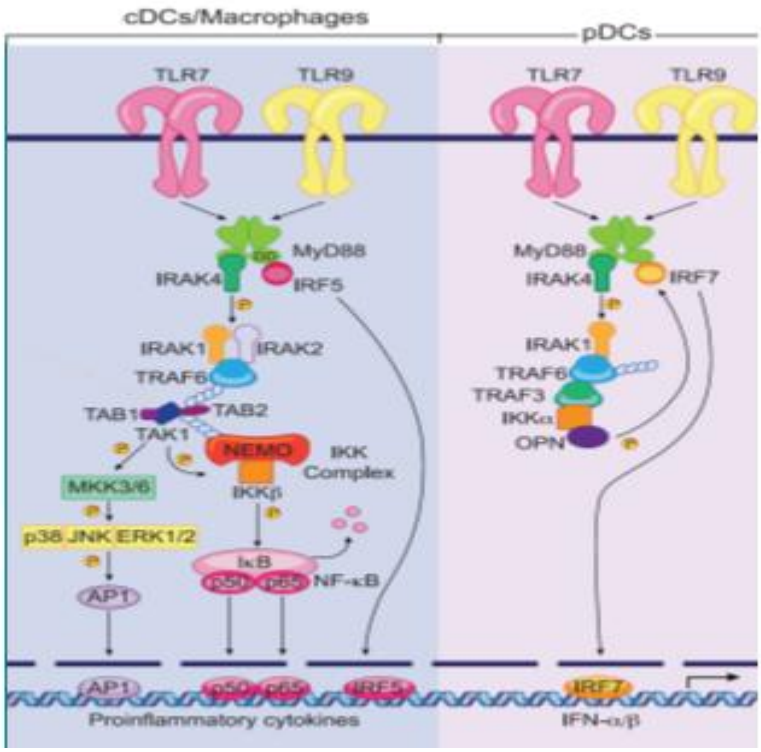

Figure 3.3: Overview of TLR7/8 and TLR9 signalling. Both TLRs from active dimer complexes within the endolysosomal membrane and transmit their downstream signal into the cytosol via MyD88. The inflammatory response from both TLR7/8 and TLR9 is mediated by an MyD88-IRAK1-IRAK2-TRAF6-TAK1 signalosome complex. This can then activate the AP-1 and NFκB transcription factors which bind promoter regions of proinflammatory cytokines in the nucleus. Anti-viral or type-I IFN signalling from both TLRs is mediated by a MyD88-IRAK4-IRAK1-TRAF3/6-IKKα signalosome complex. This serves to recruit and activate IRF7 which binds to the promoter regions of IFNα/β in the nucleus. Adapted from [210].

3.1.5 Chapter aim

The aim of this chapter is to re-evaluate the role of the TIR-domain containing adaptor TRAM in mediating the downstream signalling of multiple TLRs.

3.2: Results

3.2.1 Confirmation of TRAM deficiency in TRAM $^{-/-}$ immortalised bone marrow derived macrophages (iBMDMs).

Prior to initiation of phenotype studies and characterisation of signalling abnormalities as a consequence of TRAM loss in macrophages, qRT-PCR was used to test for the expression of the *tram* gene in TRAM deficient cells compared to WT cells. As expected, expression of *tram* was completely abolished in TRAM $^{-/-}$ cells compared to WT cells (Figure 3.4). Based on this result, it was decided to characterise the phenotype of WT and TRAM deficient cells in response to various TLR ligands.

It should be stated at this point that major difficulties were experienced during initial optimisation studies using WT and TRAM $^{-/-}$ iBMDMs. The different cell lines often grew at notably different rates, with TRAM deficient cells growing faster and more reliably than WT cells. Moreover, the ability to replicate previous findings that would serve to phenotypically confirm TRAM's absence from TRAM $^{-/-}$ cells, such as loss of TLR4 mediated signalling, often proved difficult with many attempts required, often requiring different vials of cells to be brought up from cryogenic storage. This led to a situation where the generation of reliable figures, particularly those relating to cytokine induction, took an extraordinarily long period of time. This was because a higher level of confidence, beyond what would be needed when using normal cells, had to be ensured before moving on to the next experiement.

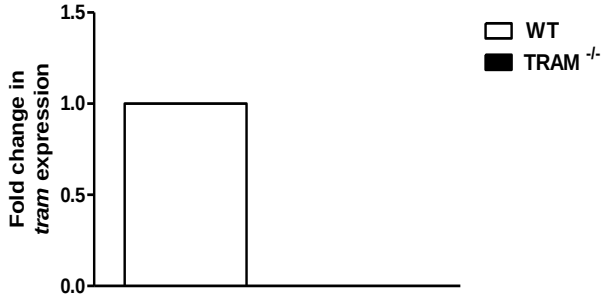

Figure 3.4: Confirmation of the absence of *tram* gene expression in TRAM deficient iBMDMs. WT and TRAM deficient iBMDMs were plated at a density of $1.3x10^6$ cells/ml in a six-well plate and incubated for 24 hr at 37°C. Cells were then harvested, total RNA isolated and from this, cDNA was synthesised. The cDNA was then used as a template for qRT-PCR using forward and reverse primers specific to either murine *tram.* Fold changes were compared to the level of the housekeeping gene *gapdh*. Graph is representative of two independent experiments.

3.2.2 Comparison of TNFα production in WT and TRAM $^{-/-}$ iBMDMs

Studies to date indicate that TRAM and TRIF mediate 'late-stage' NFκB activation and TNFα secretion upon ligand binding to TLR4 [219]. However, the role of TRAM in TNFα secretion following activation of the other TLRs, namely TLR1/2, TLR2/6, TLR3, TLR7 and TLR9, has not been adequately addressed. To this end, WT and TRAM $^{-/-}$ iBMDMs were stimulated with various TLR ligands. After 24 hr, cell free supernatants were removed and analysed for the presence of TNFα. It was found that ligands corresponding to TLR1/2, TLR2/6 and TLR7 (Pam3CSK4, Pam2CSK4/MALP-2 and R848 respectively) strongly induced the expression of TNFα activated in both WT and TRAM deficient iBMDMs. Ligands corresponding to TLR3, TLR4 and TLR9 (poly(I:C), LPS and CpG respectively) drove a weaker response (Figure 3.5A). Comparable levels of TNFα secretion was observed in TRAM $^{-/-}$ cells compared to WT cells upon stimulation with almost all ligands tested (Figure 3.5A). TRAM has been shown to be a critical adaptor in TLR4 signalling [24] and as expected, reduced TNFα secretion was observed following stimulation of TRAM $^{-/-}$ cells with LPS when compared to WT cells (Figure 3.5A). The LPS phenotype would be expected as TRAM has been shown to be a critical adaptor molecule in TLR4 signalling. These data suggest that TRAM is not required for TNFα production following stimulation of cells with TLR1/2, TLR2/6, TLR3, TLR7 and TLR9 ligands. TRAM's role in TNFα prodcution appears to be limited to the TLR4 pathway which is in line with previous studies [24].

3.2.3 Comparison of RANTES and type-I IFN production in WT and TRAM $^{-/-}$ iBMDMs

Next, TLR mediated production of the chemokine RANTES was examined in WT and TRAM deficient cells. Cells were again stimulated with various ligands and it was found that TLR1/2, TLR2/6, TLR4, TLR7 and TLR9 ligands all induced RANTES secretion (Figure 3.5B). As expected, reduced RANTES secretion was observed upon stimulation of TRAM $^{-/-}$ cells with LPS when compared to WT cells. Interestingly, the loss of TRAM caused a

significant reduction in TLR1/2, TLR2/6, TLR7 and TLR9 mediated RANTES secretion (Figure 3.5B). The loss of function was expected in response to TLR4 activation but not for TLR2, TLR7 or TLR9 responses. As a negative control, RANTES secretion upon TLR3 activation was unchanged in TRAM deficient cells compared to WT cells (Figure 3.5B). As TRAM has not been shown to play a role in TLR3 signalling [24], this precludes the possibility that TRAM $^{-/-}$ cells are unable to produce RANTES at a global level when compared to WT cells. These data support a hypothesis that TRAM may have a specific role to play in RANTES production through selected TLRs. While no role for TRAM has previously been shown in the context of TLR7 or TLR9 signalling, a previous study suggested it may play a role in the TLR2 mediated response to the gram negative pathogen *Francisella tularensis* [178]. Indeed, the study demonstrated that TRAM co-immunoprecipitated with TLR2 following TLR2 activation in macrophages [178].

Next, levels of secreted type-I IFN were determined in supernatants from WT and TRAM $^{-/-}$ cells stimulated with various TLR ligands (Figure 3.5C). In all cases, the levels of secreted type-I IFN was minimal such that only Pam_3CSK_4, poly(I:C), R848 and CpG induced the production of type-I IFN when compared to unstimulated control cells (Figure 3.5C). As expected, levels of TLR3 mediated production of type-I IFN were comparable between TRAM deficient cells and WT cells. Interestingly, levels of type-I IFN were significantly impaired in TRAM $^{-/-}$ cells following stimulation with R848 and this correlates with previous date showing suppressed RANTES secretion in TRAM $^{-/-}$ compared to WT cells (Figure 3.5C, 3.5B). Again, this data contrasts with the unchanged levels of TNFα secretion observed between WT and TRAM deficient cells when stimulated with the same TLR ligands (Figure 3.5A).

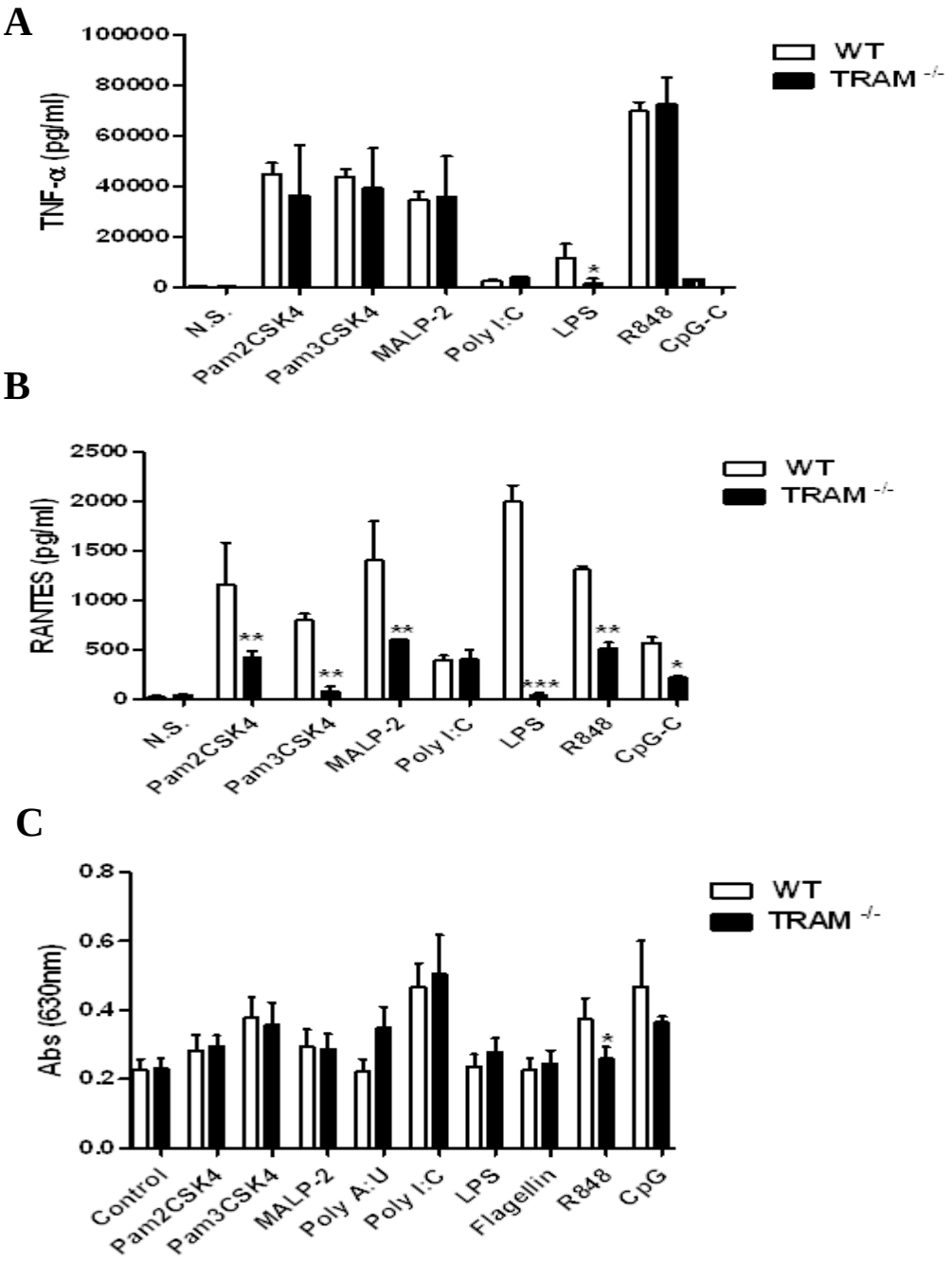

Figure 3.5: TNFα, RANTES and type-I IFN production in WT and TRAM $^{-/-}$ iBMDMs in response to various TLR ligands. WT and TRAM deficient iBMDMs were plated at a density of $1.3x10^6$ cells/ml in a six-well plate and incubated for 24 hr at 37°C. Individual wells were then either left unstimulated or stimulated with ligands specific to various TLRs: Pam_2CSK_4, (TLR2:TLR6 heterodimer) – 1 μg/ml, Pam_3CSK_4 (TLR1:TLR2 heterodimer) – 1 μg/ml, poly(I:C) (TLR3) – 25 μg/ml, LPS (TLR4) – 100 ng/ml, R848 (TLR7) – 1 μg/ml and CpG-C (TLR9) – 5 μg/ml for 4 hr. Cell free supernatants were removed and assayed for levels of murine TNFα (A) and RANTES (B) by ELISA. Type-I IFN levels (C) were detected using B16-Blue™ IFN-α/β cells. * $p<0.05$, ** $p<0.01$ and *** $p<0.001$. Graphs are representative of at least four independent experiments.

3.2.4 Comparison of *rantes*, and *tnfα* and *ifnα* gene expression iBMDMs derived from WT and TRAM $^{-/-}$ mice

Initial studies indicated that TRAM may be required for TLR2, TLR7 and TLR9 mediated RANTES production. TRAM also appears to have a role in TLR7 mediated type-I IFN production (Figure 3.5). However, the potential role of TRAM may be at either the transcriptional or translational level. To examine this further, the genetic expression of *rantes*, *tnfα* and *ifnα* was studied in WT and TRAM deficient cells upon stimulation with various TLR ligands for 4 hr. It was found that all TLR ligands tested caused upregulation of both *tnfα* and *rantes* gene expression (Figure 3.6A-F). As very little type-I IFN was detected in Figure 3.5C, it was decided not to check for *ifn-α* or *ifn-β* gene expression.

Interestingly, Pam_3CSK_4, MALP-2, LPS, R848 and CpG mediated RANTES mRNA expression was significantly reduced in TRAM $^{-/-}$ cells when compared to WT cells (Figure 3.7). In contrast, no significant differences in TNFα mRNA expression were observed in TRAM deficient cells upon TLR ligand stimulation (Figure 3.6). The pattern of TNFα mRNA expression replicated that of TNFα protein expression except in the case of LPS stimulation where no change in the expression of TNFα mRNA was observed between WT and TRAM $^{-/-}$ cells (Figure 3.6D). This finding correlates with a previous study by Wang et al., [220] where they showed that TRAM is required for TNFα translation but not transcription in BMDMs in a process dependent on the regulatory kinase MK_2. However, the same study showed that in peritoneal macrophages, TRAM is required for both transcription and translation [220]. Thus TRAM's exact role in TLR4 signalling therefore appears to be cell-type specific. That TRAM deficient macrophages are significantly attenuated in their response to TLRs 2, 7/8 and 9 at the transcriptional level indicates that TRAM may mediate its effects upstream of gene transcription and therefore agrees with the physiological roles of the other adaptor proteins in TLR signalling.

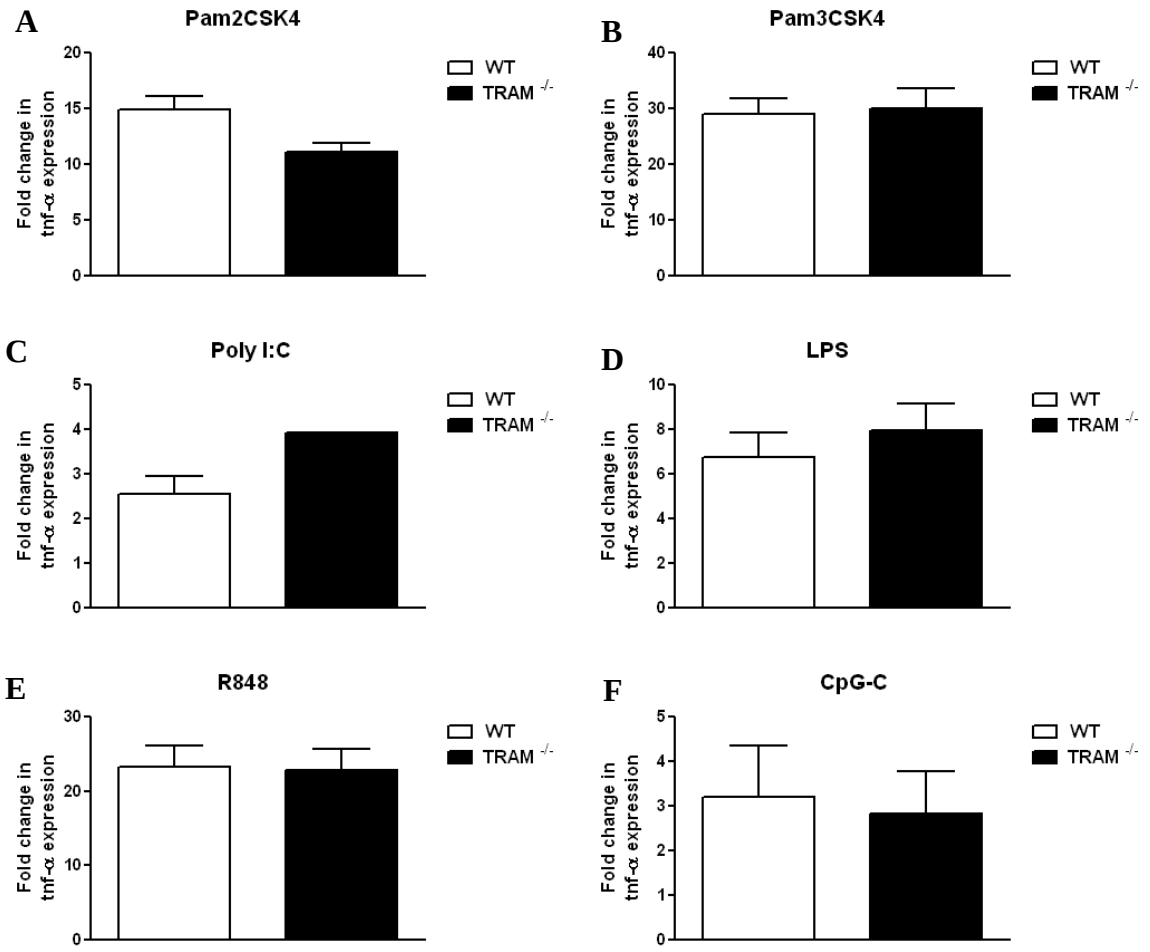

Figure 3.6: TNFα mRNA expression in WT and TRAM $^{-/-}$ iBMDMs in response to various TLR ligands. WT and TRAM deficient iBMDMs were plated at a density of $1.3x10^6$ cells/ml in a six-well plate and incubated for 24 hr at 37°C. Individual wells were then either left unstimulated or stimulated with ligands specific to various TLRs: (A) Pam_2CSK_4, (TLR2:TLR6 heterodimer) – 1 μg/ml, (B) Pam_3CSK_4 (TLR1:TLR2 heterodimer) – 1 μg/ml, (C) poly(I:C) (TLR3) – 25 μg/ml, (D) LPS (TLR4) – 100 ng/ml, (E) R848 (TLR7) – 1 μg/ml and (F) CpG-C (TLR9) – 5 μg/ml for 4 hr. Cells were then harvested and total RNA was isolated and used as a template for first strand cDNA synthesis. The cDNA was then used as a template for qRT-PCR using forward and reverse primers specific to murine *tnf-α* and *gapdh* (housekeeping gene). * $p<0.05$, ** $p<0.01$ and *** $p<0.001$. Graphs are representative of at least four independent experiments.

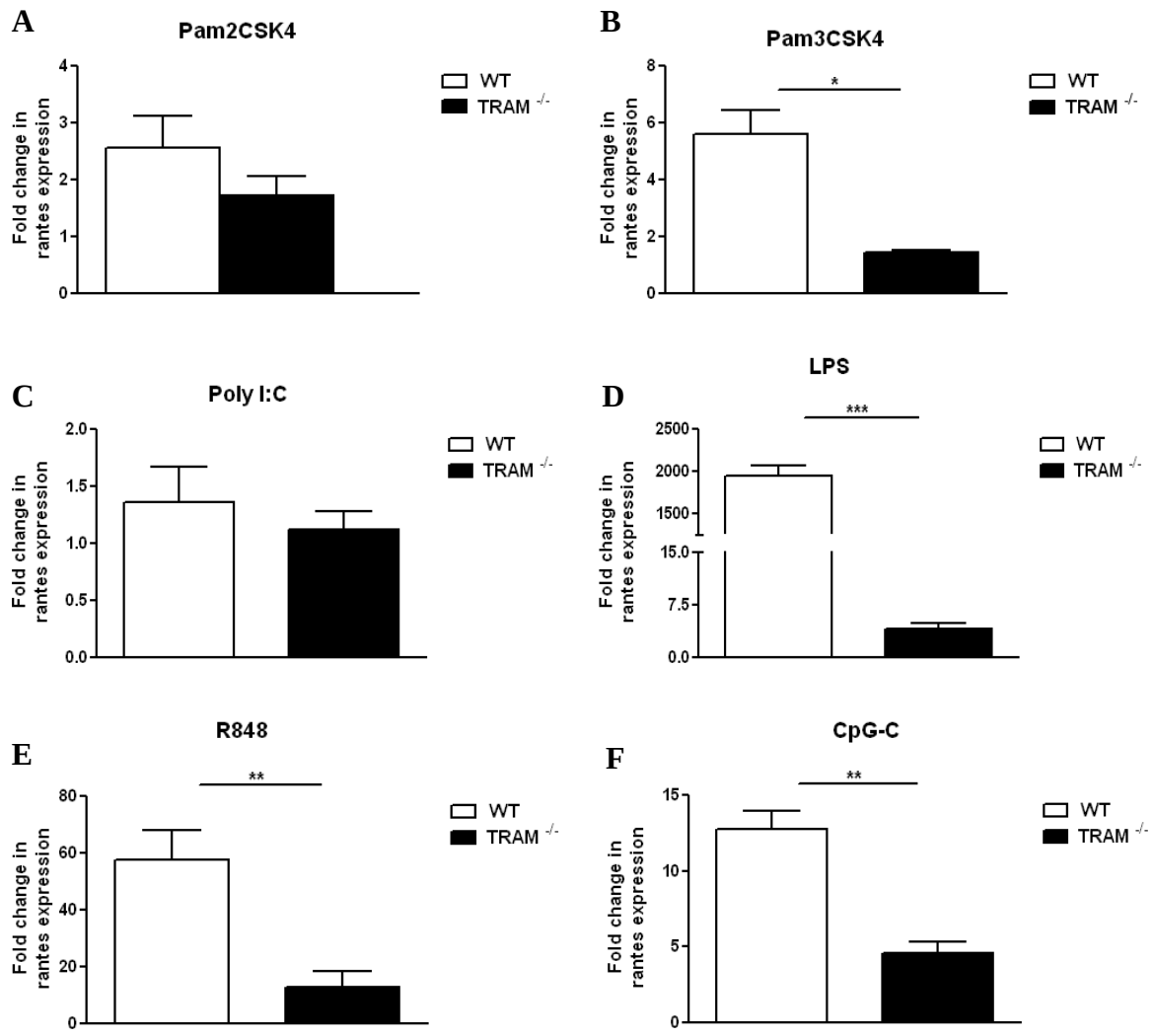

Figure 3.7: RANTES mRNA expression in WT and TRAM $^{-/-}$ iBMDMs in response to various TLR ligands. WT and TRAM deficient iBMDMs were plated at a density of $1.3x10^6$ cells/ml in a six-well plate and incubated for 24 hr at 37°C. Individual wells were then either left unstimulated or stimulated with ligands specific to various TLRs: (A) Pam_2CSK_4, (TLR2:TLR6 heterodimer) – 1 μg/ml, (B) Pam_3CSK_4 (TLR1:TLR2 heterodimer) – 1 μg/ml, (C) poly(I:C) (TLR3) – 25 μg/ml, (D) LPS (TLR4) – 100 ng/ml, (E) R848 (TLR7) – 1 μg/ml and (F) CpG-C (TLR9) – 5 μg/ml for 4 hr. Cells were then harvested and total RNA was isolated and used as a template for first strand cDNA synthesis. The cDNA was then used as a template for qRT-PCR using forward and reverse primers specific to murine *rantes* and *gapdh* (housekeeping gene). * $p<0.05$, ** $p<0.01$ and *** $p<0.001$. Graphs are representative of at least four independent experiments.

3.2.5 Expression levels of *tram* in response to TLR7 and TLR9 activation

Levels of TRAM mRNA expression have previously been examined in response to LPS simulation with the finding that TRAM's mRNA levels remained stable over multiple time points in HEK293-TLR4 cells despite its known role in TLR4 signalling [86]. Currently, it is not possible to measure the levels of endogenous TRAM protein expression despite the testing of over thirteen commercially available and self-raised antibodies towards the detection of endogenous TRAM expression [86]. Therefore, whilst the levels of TRAM gene expression remain unchanged, the possibilities that TRAM protein levels flux upon TLR4 activation cannot be precluded. With this in mind, it was decided to measure TRAM mRNA expression in iBMDMs in response to TLR7, TLR9 and TLR4 activation over multiple time points.

Results showed that levels of TRAM mRNA were decreased within 15 min of stimulation with TLR4 and TLR7 ligands, reaching their lowest levels upon TLR4 activation at 1.5 hr and at 2 hr upon TLR7 activation (Figure 3.8). Levels of TRAM mRNA had decreased approximately 40 % and 20 % respectively at these times. Levels of TRAM mRNA were largely unaffected by TLR9 activation over similar time points (Figure 3.8). The finding that decreased TRAM mRNA expression is evident upon both TLR4 and TLR7 activation is novel. In contrast, a previous study showed that levels of TRAM mRNA remained stable following LPS stimulation of HEK293-TLR4 cells. The disparity may be due to the different cell lines used – iBMDMs in the current study vs. HEK292-TLR4 cells in [86]. Levels of TRAM mRNA were consistently lower in response to both LPS and R848 stimuli and may indicate the presence of a TRAM dependent negative feedback loop in both TLR4 and TLR7 signalling whereby activation of either pathway may cause suppression of TRAM mRNA so as to prevent an overactive immune response. Such intracellular feedback loops are indeed common in cell signalling [221]. The rebounding of TRAM's expression at 4 hr consequently

might indicate to the cell that a PAMP is still present and that the immune response must be sustained (Figure 3.8). However, confirmation of this hypotheis would need to be undertaken by analysing TRAM protein levels.

That TRAM's mRNA undergoes dynamic patterns of expression in response to TLR activation provides further support for the hypothesis that TRAM plays a role within this pathway. The lack of an apparent change in TRAM mRNA in response to stimulation with the TLR9 ligand CpG may be due to CpG being a weaker driver of signalling compared to R848 and LPS as could be observed in Figure 3.5. This may in turn affect activation of downstream pathways including any changes in adaptor expression.

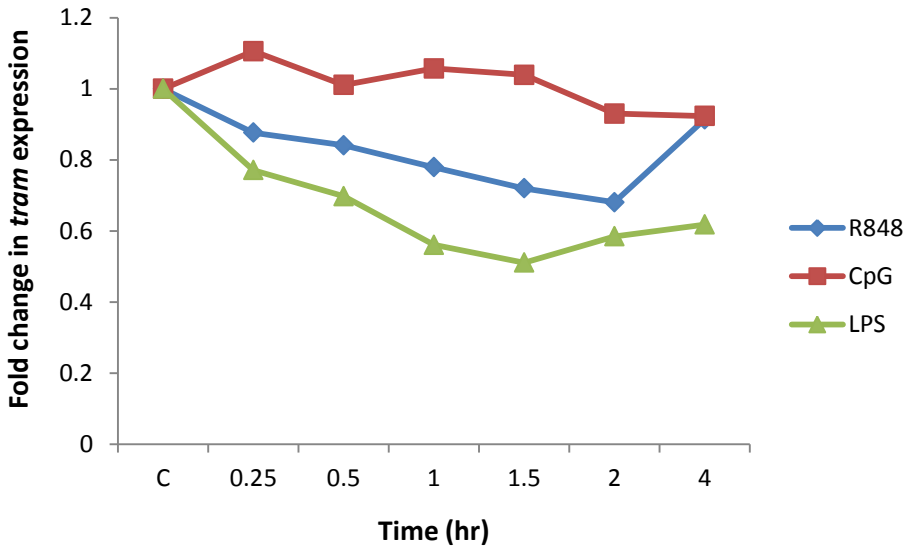

Figure 3.8: Expression of TRAM mRNA in response to TLR7, TLR9 and TLR4 ligand activation. WT iBMDMs were plated at a density of $1.3x10^6$ cells/ml in a six-well plate and incubated for 24 hr at 37°C. Individual wells were then either left unstimulated or stimulated with LPS (100ng/ml), R848 (1 µg/ml) and CpG-C (5 µg/ml) for various time points as indicated. Cells were then harvested and total RNA was isolated and used as a template for first strand cDNA synthesis. The cDNA was then used as a template for qRT-PCR using forward and reverse primers specific to murine *tram* with murine *gapdh* acting as a housekeeping gene for fold-change comparison. Graph is representative of two independent experiments.

3.2.6 R848 and CpG stimulation of iBMDMs causes TRAM dependent activation of IRF3

Previous results indicated that RANTES and type-I IFN secretion were impaired in TRAM $^{-/-}$ cells compared to WT cells when following stimulation with TLR7 and TLR9 ligands (Figure 3.5). Further studies indicated that TRAM exerts its effects at the transcriptional level (Figure 3.7). It was therefore hypothesised that TRAM may be required for transcriptional activation of TLR7 and TLR9 signalling. NFκB and the IRFs are key transcription factors involved in the TLR7 and TLR9 response [15]. In unstimulated cells, NFκB is sequestered in the cytoplasm by a group of inhibitory proteins called inhibitor of κBs (IκBs), the best studied of which is IκBα. IκBα binds to the NFκB subunits and masks its nuclear localisation sequences [222]. Activation of the cell, for example via TLRs, causes activation of the IKK complex which phosphorylates serine residues on IκB proteins causing their ubquitination and subsequent proteosomal degradation. Loss of IκB frees NFκB thus permitting it's translocation into the nucleus where it can bind to the promoter regions of target genes [223]. Monitoring of IκBα degradation is therefore a model of NFκB activation. IRF5 and IRF7 have been shown to be involved in both TLR7 and TLR9 pathways [205, 212] however, commercial phospho-IRF5 antibodies are not available and endogenous levels of IRF7 are generally low in macrophages [224] thus making the detection of activated IRF5 and IRF7 technically difficult. It was therefore decided to measure IRF3 activity by immunoblot analysis using phospho-specific IRF3 antibodies following stimulation of WT and TRAM deficient iBMDMs with R848 and CpG.

WT and TRAM $^{-/-}$ iBMDMs were stimulated with R848, CpG, poly(I:C) and LPS for 30, 60 and 120 min after which whole cell lysates were collected and subjected to immunoblot analysis to detect endogenous levels of phospho-IRF3 (p-IRF3) and IκBα with total IRF3 and β-actin as loading controls respectively.

Stimulation of cells with R848, CpG, poly(I:C) and LPS resulted in activation of IRF3 in WT cells as evidenced by its increased phosphorylation in comparison to unstimulated controls (Figure 3.9). There appeared to be a pattern of slightly increased levels of basal IRF3 phosphorylation in WT cells compared to TRAM deficient cells (Figure 3.9 A,B). R848 appeared to drive maximal activation in WT cells at 30 min and 60 min with activation beginning to decrease at 120 min (Figure 3.9A). LPS strongly activated IRF3 at 30 min and 60 min when compared to the other ligands tested (Figure 3.9A). Both poly(I:C) and CpG stimulation induced maximal IRF3 phosphorylation at 120 min of stimulation with activation steadily increasing at time points prior to that (Figure 3.9B,C). When comparing IRF3 phosphorylation in WT and TRAM deficient cells, poly(I:C) served as a negative control. As expected, poly(I:C) mediated levels of IRF3 activation in TRAM $^{-/-}$ cells were comparable to that detected in WT cells (Figure 3.9C). As a positive control, levels of IRF3 phosphorylation were abolished in TRAM deficient cells compared to WT following treatment of cells with LPS (Figure 3.9A). These results further confirm that TRAM is involved in TLR4 signalling but not TLR3.

Next, IRF3 phosphorylation was determined in TRAM $^{-/-}$ cells following stimulation with TLR7 and TLR9 ligands. It was found the phosphorylation of IRF3 was abolished in TRAM deficient cells following stimulation with R848 when compared to WT cells (Figure 3.9A). Similarly, phosphorylation of IRF3 was abolished in TRAM $^{-/-}$ cells in response to CpG stimulation when compared to WT cells (Figure 3.9B). That reduced levels of activation were apparent across all time points tested indicates that IRF3 activation upon TLR7 and TLR9 activation in completely dependent on TRAM at both early and late time points. Equitable levels of total IRF3 confirmed equal loading of protein across all lanes (Figure 3.9A-C). As a control to confirm that the phenotype observed was adaptor specific, it was examined whether the adaptor MAL also played a role in the TLR7 pathway using WT and MAL $^{-/-}$

iBMDMs. It was found that comparable IRF3 activation were detected in MAL deficient cells and WT cells (Figure 3.9D). Together, these data suggest that TRAM is required for TLR7 and TLR9 mediated IRF3 activation.

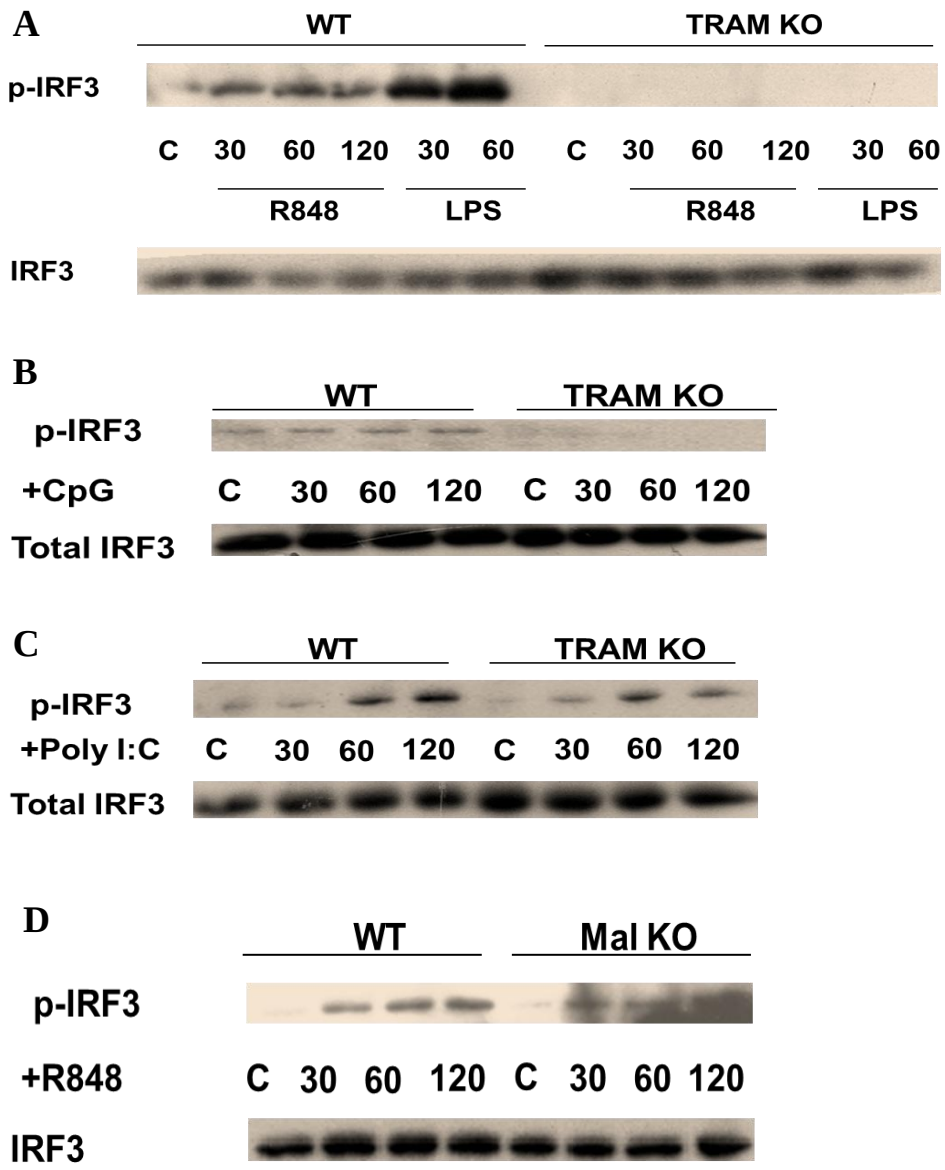

Figure 3.9: R848 and CpG stimulation activates IRF3 in a TRAM dependent manner. WT and TRAM $^{-/-}$ (A-C) and MAL $^{-/-}$ (D) iBMDMs were seeded in a 6-well plate at a density of 1.3x10^{6} cells/ml and incubated for 24 hr at 37°C. Thereafter, cells were stimulated with either R848 (1 µg/ml), CpG-C, (5 µg/ml) or poly(I:C) (25 µg/ml) for 30, 60 and 120 min. Cells were then harvested and each sample lysed in 100 µl H.S. buffer for 20 min on ice. Cell debris was removed by centrifugation with the remaining whole cell lysates mixed with 30 µl 5x Laemmli loading buffer and boiled for 10 min. Proteins were separated by SDS-PAGE and subjected to immunoblot analysis using anti-p-IRF3 and anti-IRF3 antibodies. Results represent a minimum of three (WT vs TRAM $^{-/-}$) and two (WT vs MAL$^{-/-}$) independent experiments.

3.2.7 R848 stimulation of iBMDMs causes TRAM dependent nuclear translocation of IRF3

Like NFκB, unactivated IRF3 exists within the cytosol. However, serine phosphorylation by the upstream kinases TBK-1 and IKKε leads to conformational changes that cause homodimerisation and binding to nuclear trafficking proteins such as CREB-binding protein (CBP) and p300. This leads to nuclear translocation and accumulation of IRF3 and upon which it binds to DNA targets [225-227]. Therefore, an alternative approach to monitor the activation of IRF3 is to examine its accumulation in the nucleus following TLR activation.

To this end, WT and TRAM $^{-/-}$ iBMDMs were stimulated with R848, CpG and poly(I:C) for 30, 60 and 120 min upon which, cells were lysed and the nuclear fraction purified and subjected to immunoblot analysis using an anti-IRF3 antibody. Nuclear translocation of IRF3 was observed following stimulation with R848, CpG and poly(I:C), correlating with the IRF3 phosphorylation (Figure 3.9A, 3.10A). Regarding CpG, the overall response appears to be weak compared to the other TLR ligands tested (Figure 3.10C). Whilst poly(I:C) mediated nuclear accumulation of IRF3 was unchanged between WT and TRAM $^{-/-}$ cells, R848 and CpG mediated accumulation of IRF3 appeared reduced or abolished in TRAM deficient cells compared to WT cells (Figure 3.9A-C). The nuclear pore protein Lamin A/C was used to confirm equal loading of protein across all lanes (Figure 3.9A-C).

The observation that R848 induced the activation and nuclear translocation of IRF3 in iBMDMs may be cell type specific as a previous study conducted using HEK293 cells showed that overexpressed IRF3 did not translocate to the nucleus upon R848 stimulation [212]. In the same study, endogenous phosphorylation of IRF3 in RAW264.7 macrophages was not detected following stimulation with R848 [212]. Indeed, discrepancies in the modulation of the IRFs between macrophage cell lines have been noted previously [224] Herein, it is clearly demonstrated that IRF3 is both phosphorylated and translocated into the nucleus following stimulation of iBMDMs with R848 and CpG. Moreover, it is shown that

this process is dependent upon the presence of the TLR adaptor protein, TRAM. The role for TRAM in TLR7 and TLR9 signalling is strikingly similar to that of TRAM's role in TLR4 signalling post LPS stimulation whereby TRAM is also required for the activation of IRF3 [228].

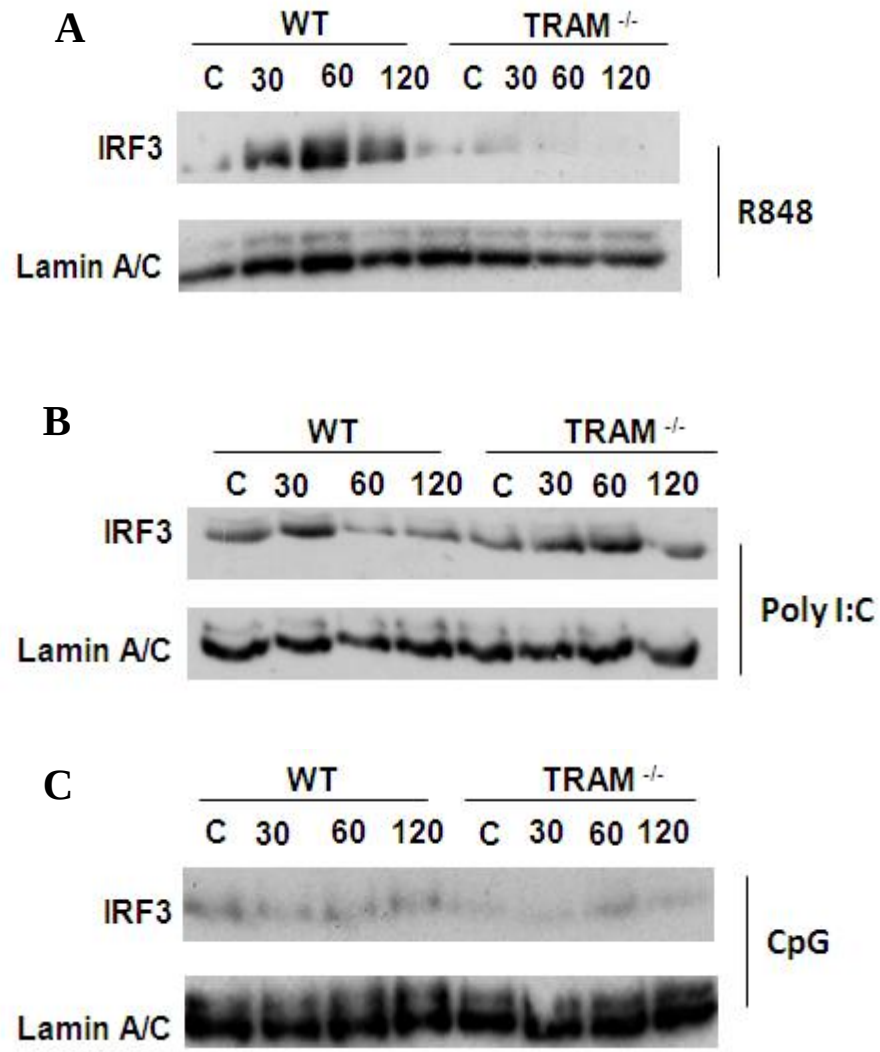

Figure 3.10: R848 and CpG mediated IRF3 nuclear translocation is TRAM dependent. WT and TRAM $^{-/-}$ iBMDMs (A-C) were seeded in a 6-well plate at a density of $1.3x10^6$ cells/ml and incubated for 24 hr at 37°C. Thereafter, cells were stimulated with either (A) R848 (1 µg/ml), (B) poly(I:C) (25 µg/ml) or (C) CpG (5 µg/ml) for 30, 60 and 120 min. Cells were then harvested and each sample subjected to nuclear extraction using a Nuclear Extraction Kit (Cayman Chemical). Nuclear Extracts were mixed with 30 µl 5x Laemmli loading buffer and boiled for 10 min. Proteins were separated by SDS-PAGE and subjected to immunoblot analysis using anti-IRF3 and anti-Lamin A/C antibodies. Results represent a minimum of two independent experiments.

3.2.8 IκBα degradation is unaffected in TRAM $^{-/-}$ cells in response to R848 and CpG

Despite the loss of IRF3 activation following stimulation of TRAM $^{-/-}$ cells with R848 and CpG compared to WT cells, concurrent RANTES and type-I IFN secretion is evident, albeit at reduced levels compared to WT cells (Figure 3.5 C,D). It is plausible to speculate that while TRAM dependent IRF3 activation is required for maximal TLR7 and TLR9 dependent cytokine production, TLR7 and TLR9 dependent activation of alternative transcription factors such as NFκB may be TRAM independent.

With this in mind, the degradation of IκBα in response to R848 and CpG was monitored by Western blot. In WT iBMDMs, IκBα was degraded in response to R848 stimulation at 15 min and was almost completely degraded at 30 min before rebounding fully by 60 min (Figure 3.11A). Interestingly, in contrast to IRF3 phosphorylation, degradation of IκBα was comparable in WT and TRAM deficient cells (Figure 3.11A). It would therefore appear that TRAM'S role in TLR7 signalling is IRF3 dependent and NFκB independent. The kinetics of CpG mediated IκBα degradation difficult to detect as degradation of IκBα was not evident at any of the timepoints selected (Figure 3.11B).

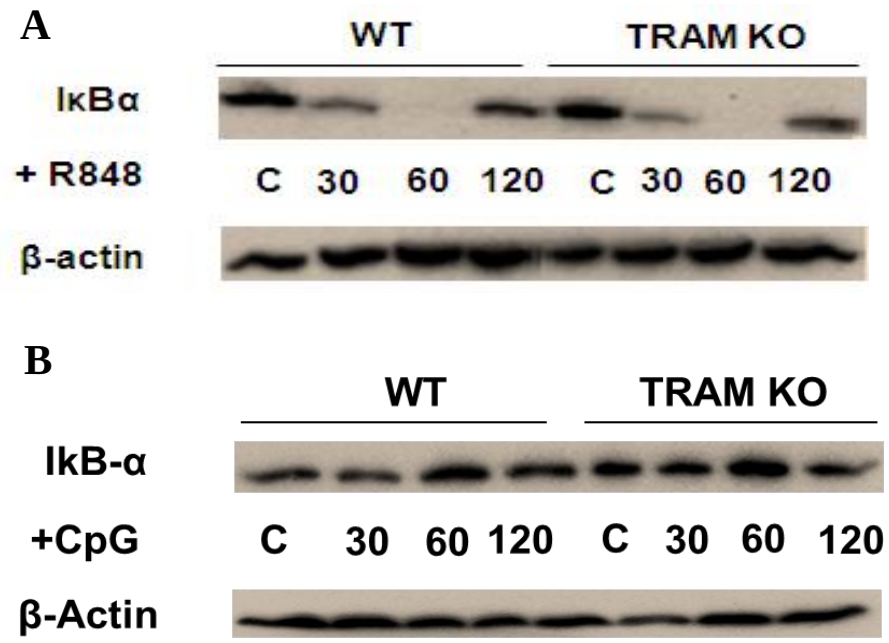

Figure 3.11: R848 and CpG mediated IκBα degradation in WT and TRAM $^{-/-}$ cells. WT and TRAM $^{-/-}$ iBMDMs were seeded in a 6-well plate at a density of $1.3x10^6$ cells/ml and incubated for 24 hr at 37°C. Thereafter, cells were stimulated with either (A) R848 (1 μg/ml) or (B) CpG (5 μg/ml) for 30, 60 and 120 min. Cells were then harvested and each sample lysed in 100 μl H.S. buffer for 20 min on ice. Cell debris was removed by centrifugation with the remaining whole cell lysates mixed with 30 μl 5x Laemmli loading buffer and boiled for 10 min. Proteins were separated by SDS-PAGE and subjected to immunoblot analysis using anti-IκBα and anti-β-Actin antibodies. Results represent a minimum of three independent experiments.

3.2.9 TLR7/8 and TLR9 ligand preparations are incapable of activating TLR4

It is well documented that endotoxin in the form of LPS is known to drive IRF3 phosphorylation in a TLR4 dependent manner [229-231]. Unfortunately, endotoxin contamination of immune cell activator preparations has also been a problem for immune researchers [232, 233]. All TLR ligands used in the current study were commercially sourced from respected suppliers (see Materials and Methods) and preparations were resuspended with supplied endotoxin free water as verified by limulous amoebocyte lysate (LAL) testing. However, it is still conceivable that despite these stringent precautions, endotoxin may still be present in our preparations [233, 234]. Therefore, ligand preparations were additionally tested for endotoxin contamination by examining whether they were capable of specifically activating TLR4. To this end, HEK-293 cells stably transfected with human TLR4, the MD-2/CD14 coreceptors and a secreted embryonic alkaline phosphatase (SEAP) reporter gene were used (HEK-Blue™ TLR4 cells)**.** The SEAP gene is under the control of an IL-12p40 promoter fused to five NFκB and AP-1 transcription factor binding sites. Contaminating LPS in the ligand preparations would bind TLR4 and thus activate NFκB and AP-1 which in turn drive production and secretion of SEAP into the culture medium. The presence of SEAP in medium therefore indicates the original presence of LPS and can itself be detected using a colourimetric alkaline phosphatase detection medium, commercially known as QUANTI-Blue™. Therefore, to account for possible endotoxin contamination of the TLR7/8 ligands (R848 and CLO97) and the TLR9 ligand (CpG) preparations, HEK-Blue™ TLR4 cells were stimulated with increasing concentrations of R848, CLO97, CpG and LPS and TLR4 activation with the presence of SEAP in the culture medium monitored. Addition of 50ng/ml of LPS induced detectable SEAP secretion and this dose-dependently increased with increasing concentration (Figure 3.12). Critically, neither R848, CLO97 or CpG induced detectable SEAP production despite addition of ligand corresponding to ten times the original concentrations used in our previous iBMDM assays (Figure 3.12). It was therefore concluded

that the TLR7/8 and TLR9 ligand preparations were incapable of activating TLR4 and that the results observed in assay's involving these ligands were specifically due to their ability to activate their corresponding TLR and not due to non-specific TLR4 activation.

Post submission script: It has been noted that as iBMDMs can respond to LPS concentrations as low as 0.1 ng/ml, the observed LPS sensitivity of the HEK-TLR4 Blue cells (approximately 50 ng/ml) is not sensitive enough to reliably detect LPS contamination in ligand preparations. A more suitable assay in this case would be a LAL test.

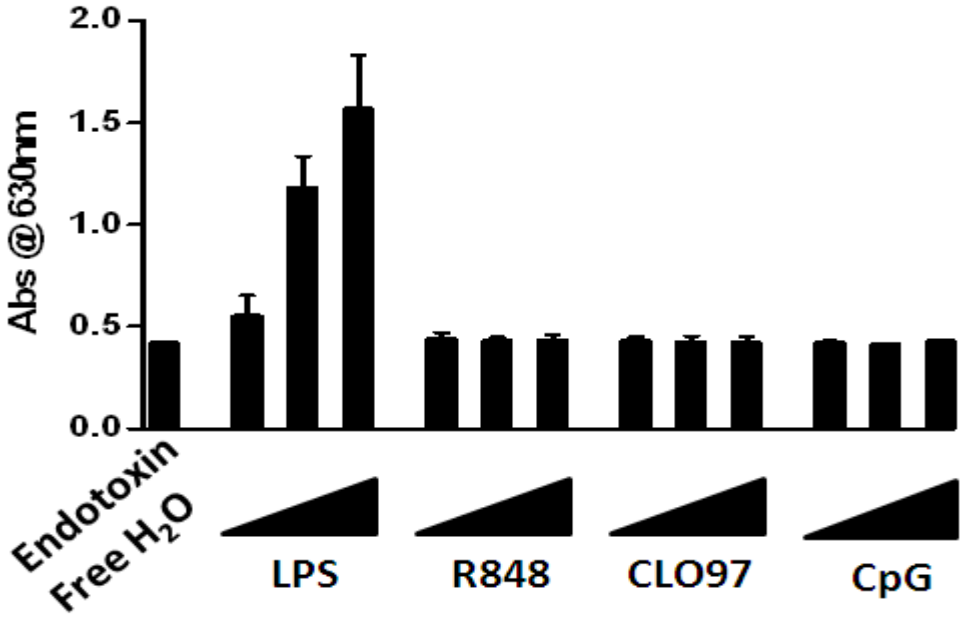

Figure 3.12: R848, CLO97 and CpG ligand preparations are incapable of activating TLR4. HEK-Blue™ hTLR4 cells were plated at a density of $1.4x10^5$ cells/ml in a 96 well plate and incubated for 24 hr at 37 °C. Cells were then stimulated with either endotoxin free H_2O or increasing amounts of LPS (50ng/ml, 100ng/ml and 500ng/ml), R848 (1 μg/ml, 5 μg/ml and 10 μg/ml), CLO97 (1 μg/ml, 5 μg/ml and 10 μg/ml) and CpG-C (5 μg/ml, 10 μg/ml and 50 μg/ml) for a further 24 hr. 20 μl of cell supernatants were then transferred to a separate 96 well plate containing 180 μl/well of pre-warmed QUANTI-Blue™ detection medium and incubated at 37 °C for approximately 2 hr. Induced colour changes in the detection medium were then detected and quantified by spectrophotometry at 630 nm. Results are representative of three independent experiments.

3.2.10 Screening human cell lines for broad TLR responsiveness: PMA differentiated, THP1 macrophages respond to ligand binding to TLR7/8, TLR3, TLR4, TLR9 and to HRV16 infection

Data collected thus far indicate a role for TRAM in the transcriptional control of TLR7 and TLR9 mediated RANTES production in an IRF3 dependent, NFκB independent manner. However, these experiments were conducted exclusively in murine iBMDMs and are therefore relevant only to murine TRAM and the murine TLR7 and TLR9 pathways. Whilst the use of murine models has long been an acceptable method of elucidating signalling pathways and in assigning function to many proteins, murine protein functionality does not always correlate with that of human protein function [235]. It was therefore decided to extend the previous observations on the role of murine TRAM to that of human TRAM. Also, in order to focus more directly on a single signalling pathway and reduce lengthy optimisation procedures, it was decided to concentrate on the role of TRAM in TLR7/8 signalling only in future experiments.

In order to replicate the previous experimental model in a human setting, a human cell line capable of responding efficiently to TLR3, TLR4 and TLR7/8 stimulation was required. The response of multiple available cell lines, namely BEAS-2B lung epithelial cells, HeLa cells, A549s, CD14-U373s, THP1 monocytes and THP1 macrophages was assayed to monitor their ability to drive cytokine gene expression in response to activation of the above TLRs. BEAS-2B cells responded well to poly(I:C) with *rantes*, *cxcl10* and *ifnβ* expression all upregulated (Figure 3.13A). LPS stimulation also drove expression of *rantes* and *cxcl10* but not *ifnβ*. R848 and CpG on the other hand, drove comparatively little *rantes* expression and almost no *cxcl10* and *ifnβ* expression (Figure 3.13A). As weak responders to TLR7/8 and TLR9 simulation, BEAS-2B cells were therefore considered unsuitable. HeLa cells responded relatively well to poly(I:C) stimulation causing an approximately 30-fold increase in *rantes* production but successively less *cxcl10* and *ifnβ* (Figure 3.13B). LPS was a poorer activator

inducing an increase only in *ifnβ* expression. R848 and CpG did not any increase in cytokine production (Figure 3.13B). HeLa cells were therefore also considered unsuitable. A549 cells were extremely poor and responded only weakly to LPS and CpG causing a respective 2 and 1.5 fold increase in *ifnβ* expression. No other ligand was capable of driving a response to any of the cytokines tested (Figure 3.13C). CD14-U373 cells likewise responded only to LPS which drove expression of large amounts of all cytokines tested (Fig 3.13D). CD-14 U373s were therefore also considered unsuitable.

THP1 monocytes can be differentiated into highly sensitive macrophages by the addition to the culture media of nanomolar quantities of PMA. PMA has an analogous structure to diacylglycerol which can activate protein kinase C to drive intracellular calcium release and multiple downstream signalling cascades. These cascades, in THP1 monocytes, ultimately result in various cellular morphological changes including adherence and spreading, as well as physiological changes such as increased CD14 expression and increased cytokine expression [236]. PMA differentiated THP1 macrophages (PMA-THP1s) were therefore also tested with the aforementioned ligand panel. PMA-THP1s responded to all ligands tested (Figure 3.13A). Poly(I:C), LPS and R848 all drove *rantes*, *ifnβ* and *cxcl10* expression. Fold changes compared to unstimulated cells were typically in the 5-fold range although LPS mediated a 150-fold increase in *rantes* expression (Figure 3.13A). As PMA-THP1s appeared to be broadly responsive to a broad panel of ligands, they were subsequently tested for their ability to respond to infection with the ssRNA virus, and physiological TLR7/8 ligand human HRV16.

PMA differentiated THP1 cells were stimulated with HRV16 for 72-80 hr at 37 °C. Again, *rantes, cxcl10,* type-I IFN genes and *tnfα* were all upregulated in response to HRV16 predominantly around 70-96 hr post-infection (Figure 3.13B). HRV16 transcripts were also analysed which showed that intracellular levels of the virus were increasing at similar time

points (Figure 3.13 left panel). Based on these results, it was concluded that PMA-differentiated THP1 cells were suitable for the study of TLR3, TLR4, TLR7/8 and TLR9 activated pathways.

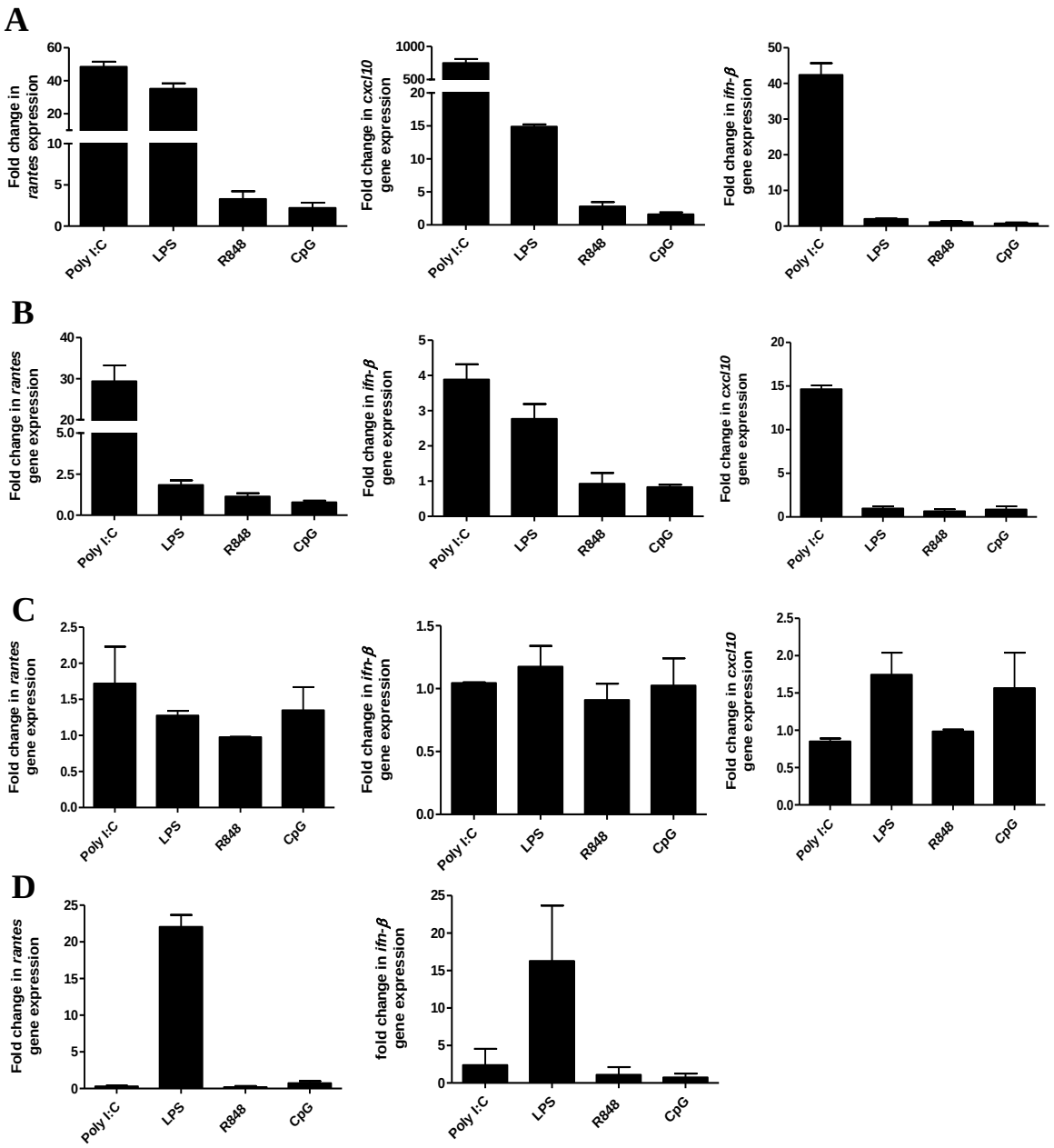

Figure 3.13: BEAS-2B, HeLa, A549 and U373-CD14 cell lines are unsuitable for simultaneous study of TLR3, TLR4, TLR7/8 and TLR9 signalling. (A) BEAS-2B, (B) HeLa, (C) A549 and (D) U373-CD14 cells were plated at densities ranging from $0.7x10^5$-$1x10^6$ cells/ml in six well plates and incubated for 24 hr at 37°C. Each cell line was then either left unstimulated or simulated with poly(I:C) (25 μg/ml), LPS (100 ng/ml), R848 (1 μg/ml) or CpG (5 μg/ml) for 5 hr. Cells were then harvested and total RNA was isolated and used as a template for first strand cDNA synthesis. The cDNA was then used as a template for qRT-PCR using forward and reverse primers specific to murine *rantes*, cxcl10, ifn-*β* and *gapdh* (housekeeping gene). Graphs are representative of two independent experiments.

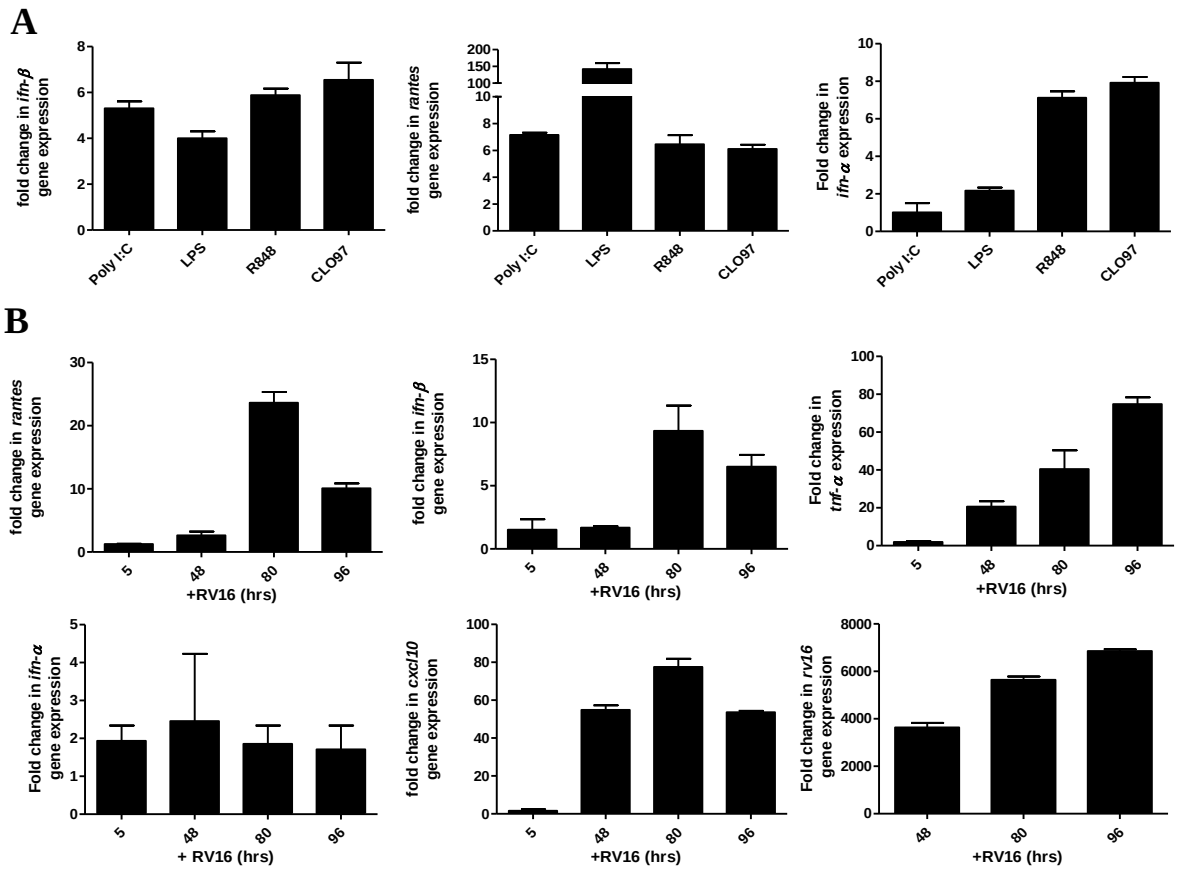

Figure 3.14: PMA differentiated THP1 macrophages are suitable for studying TLR3, TLR4 and TLR7/8 activation. THP1 monocytes were plated in a 12 well plate at a density of $1.4x10^6$ cells/ml and stimulated with 20 nM PMA for 48 hr at 37°C. Cells were then either left unstimulated, stimulated with (A) TLR ligands: poly(I:C) (25 μg/ml), LPS (100 ng/ml), R848 (1 μg/ml and 5 μg/ml), and CLO97 (1 μg/ml and 5 μg/ml) for 6 hr at 37°C or (B) infected with HRV16 for 48, 80 and 96 hr at 33°C. Cells were then harvested and total RNA was isolated and used as a template for first strand cDNA synthesis. The cDNA was then used as a template for qRT-PCR using forward and reverse primers specific to human *rantes*, cxcl10, ifn-*β, ifn-α, tnf-α*, *hrv16* and *gapdh* (housekeeping gene). Graphs are representative of two independent experiments.

3.2.11 Knockdown of endogenous human TRAM using siRNA

To investigate the role played by TRAM in TLR7/8 signalling, knockdown of endogenous TRAM in PMA-differentiated THP1 cells was performed using small interfering RNA (siRNA). SiRNA sequences are RNA nucleotide sequences approximately 21 nucleotides in length with a 2-nucleotide overhang on the 3' end. Introduction of this sequence into the cell results in their integration into the RNA-induced silencing complex (RISC) resulting in complementary base-pairing with its target sequence to initiate its degradation thus impeding translation [237]. This process was harnessed to impede translation of TRAM and thus knockdown its expression. SiRNA corresponding to the unique N-terminal region of TRAM was transfected into PMA differentiated THP1s for 48 hr and knockdown of TRAM's mRNA expression was assessed by qRT-PCR of the tram gene relative to cells transfected with a scrambled control siRNA sequence. It was found that TRAM specific siRNA significantly reduced the expression of TRAM mRNA as assessed by qRT-PCR. Estimated knockdown was 50% when compared to transfection with the scrambled control sequence (Figure 3.15A). It was not possible to observe a decrease of endogenous TRAM at the protein level as reliable anti-TRAM antibodies are not currently available [86].

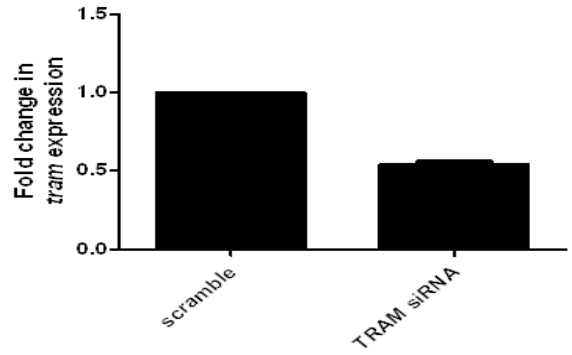

Figure 3.15: Suppression of human TRAM mRNA using RNA interference in PMA differentiated THP1 macrophages. THP1 monocytes were plated in a 12 well plate at a density of $1.4x10^6$ cells/ml and stimulated with 20 nM PMA for 48 hr at 37°C. Cells were then transfected with either 200 nM TRAM specific siRNA or scrambled control siRNA for a further 48 hr. Cells were then harvested and total RNA was isolated and used as a template for first strand cDNA synthesis. The cDNA was then used as a template for qRT-PCR using forward and reverse primers specific to human *tram* and *gapdh* (housekeeping gene). Graph is representative of two independent experiments.

3.2.12 Suppression of TRAM impairs R848 and HRV16 mediated *rantes*, *ifnβ* and *cxcl10* gene expression

To investigate whether the role of human TRAM in TLR7/8 signalling correlated with the role of TRAM in murine cells, levels of *rantes*, *ifnβ*, *cxcl10* and *tnfα* gene expression were monitored in PMA-differentiated THP1 macrophages transfected with either TRAM specific or scrambled siRNA nucleotides. After 48 hr, cells were then stimulated with R848, LPS, poly(I:C) for 6 hr or with HRV16 for 72-80 hr. Suppression of human TRAM significantly decreased R848, LPS and HRV16 mediated *rantes* and *ifnβ* gene expression compared to control cells (Figure 3.16A,B). Levels of *cxcl10* were also significantly reduced in response to R848 and LPS. However, HRV16 infection induced minimal levels of *cxcl10* and this may explain why no difference was observed between the control and TRAM-specific siRNA treatments (Figure 3.16C). R848, LPS and HRV16 all induced the expression of *tnfα* mRNA (Figure 3.16D). In contrast, suppression of TRAM expression failed to inhibit *tnfα* mRNA induction in response to R848 and HRV16. However, TRAM suppression significantly reduced LPS mediated *tnfα* expression compared to control cells (Figure 3.16D). Suppression of TRAM did not affect poly(I:C) mediated induction of *rantes*, *ifnβ, tnfα* and *cxcl10* when compared to the control cells. The poly(I:C) control was particularly important in this experiment as HRV16, despite being a ssRNA virus known to signal through TLR7/8, also produces dsRNA during its replication which has been shown to signal through the dsRNA sensing PRRs, TLR3 and retinoic acid-inducible 1 (RIG-I) [238]. It could therefore be argued that HRV16 is signalling via these PRRs and not TLR7/8 and this would eliminate the specificity of the conclusions that could be drawn. However, as poly(I:C) is itself, synthetic dsRNA that can activate both TLR3 and RIG-I and stimulation using it indicated no difference in cells in which levels of TRAM were reduced, it can logically be suggested that the cytokine phenotype observed upon HRV16 infection of TRAM-suppressed cells is specific to TLR7/8 signalling and not to TLR3/RIG-I.

Attempts were also made to compare cytokine secretion between TRAM supredded and control cells by ELISA. However, it was found that PMA was causing major basal cytokine secretion such that stimulation with LPS, R848, poly(I:C) or HRV16 resulted in little or no increase in cytokine production compared to unstimulated controls. Further time would be required to optimise PMA mediated basal cytokines activity in the THP1 cells.

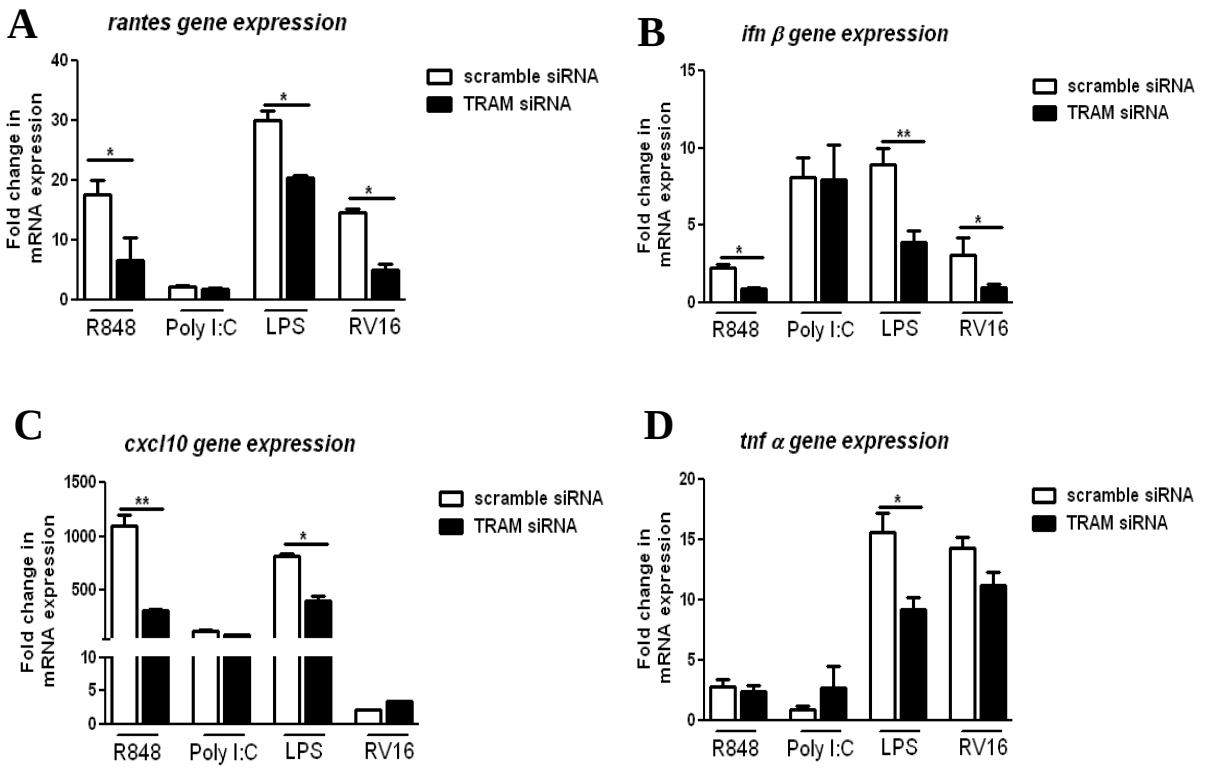

Figure 3.16: Suppression of endogenous levels of human TRAM reduces TLR7/8 and RV16 mediated *rantes, ifn-β, cxcl10* but not *tnf-α* gene expression. THP1 monocytes were plated in a 12 well plate at a density of $1.4x10^6$ cells/ml and stimulated with 20 nM PMA for 48 hr at 37°C. Cells were then transfected with either 200nM TRAM specific siRNA or scrambled control siRNA for a further 48 hr. At this point, cells were either left unstimulated, stimulated with poly(I:C) (25 μg/ml), LPS (100ng/ml) and R848 (1 μg/ml), for 6 hr at 37°C, or infected with HRV16 for 80 hr at 33°C. Cells were then harvested and total RNA was isolated and used as a template for first strand cDNA synthesis. The cDNA was then used as a template for qRT-PCR using forward and reverse primers specific to human (A) *rantes*, (B) ifn-*β,* (C) cxcl10, (D) *tnf-α* and *gapdh* (housekeeping gene). * $p<0.05$, ** $p<0.01$ and *** $p<0.001$. Graphs are representative of three independent experiments.

3.2.13 A TRAM mutant inhibits TLR7 mediated gene reporter activation

TLR7 and TLR8 have been shown to localise to the endoplasmic reticulum (ER), endosome and lysosomes. In resting cells, they reside in the ER lumen but transverse to the endolysosome via the golgi apparatus in order to detect nucleic acids released into the endolysosome by acidification [210, 239]. TRAM has previously been shown to localise to the plasma membrane and golgi apparatus in resting cells but can also traffic independently of TLR4 to endosome membranes via a bipartite sorting motif [84]. Myriostoylation of TRAM has been shown to be required for both plasma and endosomal membrane localisation as mutation of the myriostoylation sequence causes mislocalisation and in fact negates the functionality of TRAM's role in TLR4 signalling leading to reduced cytokine production in response to LPS [82, 84].

With this in mind, it was decided to examine whether overexpression of a dominant-negative TRAM mutant (TRAM G2A) [82], which is unable to undergo myriostoylation, could inhibit TLR7 mediated responses. To this end, HEK293 cells stably expressing TLR7, and therefore responsive to the TLR7 activator CLO97, were transiently transfected with the IFN-α, IFN-β, NF-κB and RANTES reporter gene constructs as well as increasing amounts of the TRAM G2A plasmid. As previously reported [82], overexpression of TRAM G2A did not drive promoter activation in all cases examined (Figure 3.17A-D). In agreement with our data in murine TRAM $^{-/-}$ iBMDMs and siRNA interference of human TRAM in THP1 cells, increasing amounts of dominant negative TRAM inhibited TLR7 mediated RANTES, IFN-β, IFN-α. It was also observed that NFκB promoter activation was similarily reduced upon overexpression of TRAMG2A suggesting that TRAM's role in HEK293 cells may not be restricted to IRF3 mediated signalling (Figure 3.17A-D). To confirm that the phenotype exhibited by TRAM G2A was attributable to a defect in the ability of TRAM to signal and not a non-specific consequence of overexpression, we repeated the same experiment using a

dominant-negative form of the adaptor MAL which has no known role in TLR7 signalling. Indeed, overexpression of dominant-negative MAL had no significant effect on TLR7 mediated RANTES, IFN-β, IFN-α or NFκB promoter activation (Figure 3.18A-D). From these data, it would appear that myriostoylation of TRAM, and therefore the ability of TRAM to membrane localise, is required for its ability to mediate TLR7 induced RANTES, IFN-α and IFN-β promoter activation.

3.2.14 TRAM and MyD88 physically interact upon activation of TLR7

The data obtained thus far definitively indicates a role for TRAM in TLR7/8 signalling. However, whilst perturbations to TRAM resulting in its genetic loss, genetic reduction or protein modification all indicate a specific role for TRAM in TLR7 signalling, evidence for the physical presence of TRAM in the TLR7 pathway is still lacking. A recent study demonstrated that TRAM can act as a linker molecule between MyD88 and the IL-18 receptor (IL-18R), allowing IL-18 signalling to be transduced in a manner resembling the role of TRAM linking TRIF to TLR4 signalling [23, 179]. The study in question used overexpression to demonstrate an interaction between TRAM and MyD88 which surprisingly dissociated upon activation of the IL-18R with exogenous IL-18 [179]. Herein, to extend this study towards establishing a physical association between TRAM and the TLR7 signalling pathway, Flag-tagged TRAM and myc-tagged MyD88 were overexpressed in HEK-TLR7 cells followed by stimulation of cells for 15, 30 and 60 min with the TLR7 ligand CLO97. Flag-TRAM was immunoprecipitated with the resulting complex subjected to SDS-PAGE followed by immunobloting for myc-MyD88. The finding that TRAM and MyD88 interacted in resting cells could not be replicated despite many attempts (Figure 3.19). This could be due to the aforementioned study introducing higher concentrations of Flag-TRAM and myc-MyD88 (4 μg per plasmid vs 3 μg of plasmid in the current study). Interestingly, co-expression of TRAM and MyD88 followed by TLR7 stimulation with CLO97 induced the

physical interaction between the two proteins at 15, 30 and 60 min with distinct myc-MyD88 specific bands appearing directly underneath the heavy chain band (Figure 3.19). It should be noted that myc-MyD88 band (~ 38 kDa) and the anti-flag antibody heavy chain band (~ 50 kDa) appear so close due to the high percentage (18 %) acrylamide gel used in this experiement which combined with the lack of allowed seperation time meant that protein bands within this region did not sepearte well. A previous study indicated that TRAM did not interact with TLR7 or TLR8 in resting cells but did interact with TLR4 [240]. Other studies have shown that TRAM is present at the plasma membrane and cytoplasm in resting cells and traffics to the endosome upon TLR4 activation [84, 86]. This would suggest that TRAM preferentially localises to endosomes upon pathogen challenge. Here it may encounter the 'TLR7 signalosome', binding to MyD88 to direct IRF3 activation. It is known that MyD88, whilst present in the cytoplasm of resting cells, also traffics to endosomal compartments upon TLR7 and TLR9 activation [196, 209]. This could explain the observation that TRAM did not interact with MyD88 in unstimulated cells, but did interact upon TLR7 stimulation, as both TRAM and MyD88 had by now trafficked to the endosome to mediate TLR7's signalling requirements. Endosomal acidification and maturation has also been shown to be critical for TLR7 activation as treatment of cells with the inhibitor of the vacuolar H(+)-ATPase, bafilomycin A1, which inhibits maturation, prevents TLR7 signalling. TRAM has been shown to be present in both early and late (mature) endosomes during TLR4 signalling [86] which again suggests that TRAM is capable of localising to TLR7 containing structures. The downstream implications of the TRAM-MyD88 interaction are unclear at present. TRAM is required for IRF3 activation so further experiments ascertain whether TRAM binds to IRF3 or any of the several proteins involved in the downstream signalling of TLR7. MyD88 has also been shown to interact with TLR7 but it would be interesting to know if this requires an additional 'linker' adaptor, such as TRAM to facilitate this interaction as is the case with

MAL and MyD88 in TLR2 and TLR4 signalling [12] as well as with TRAM and MyD88 in IL-18 signalling [179].

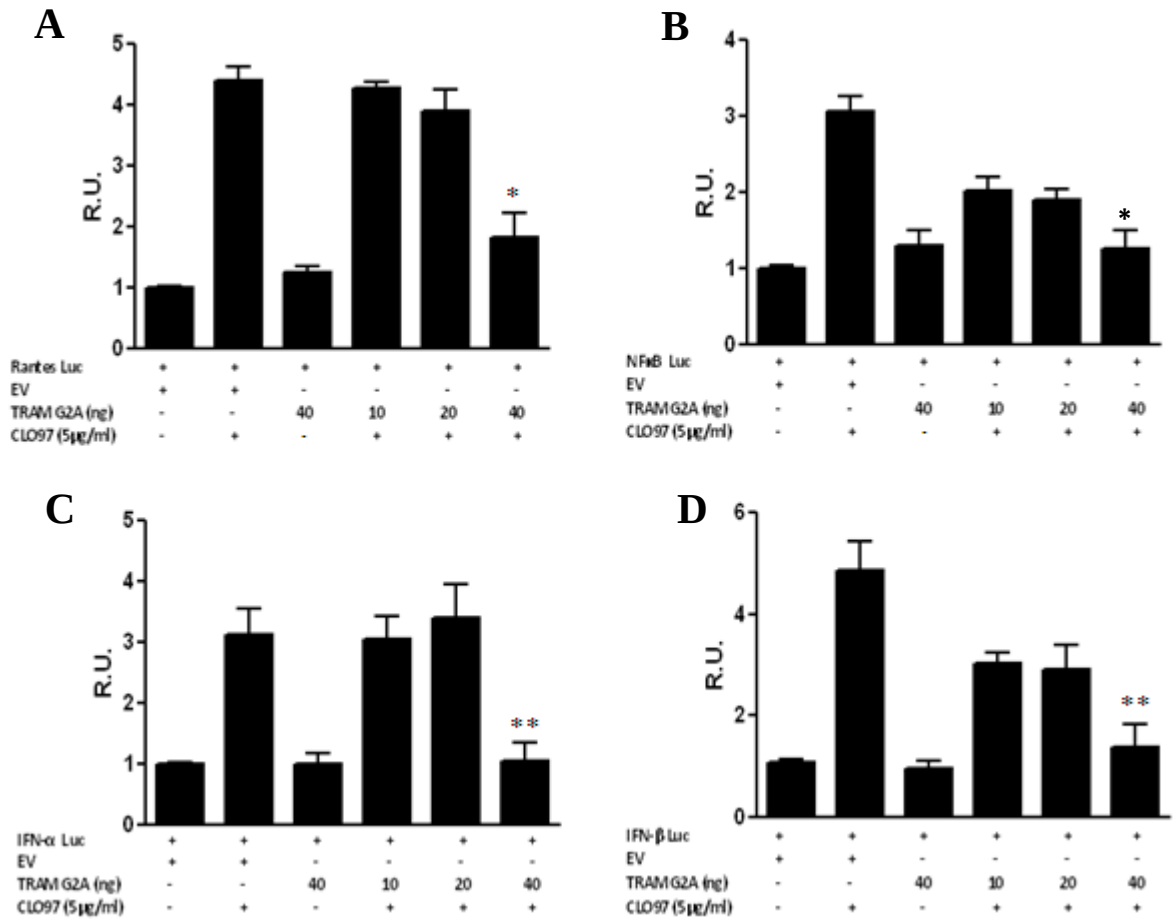

Figure 3.17: A dominant negative mutant of TRAM (TRAM G2A), negatively regulates TLR7 induced RANTES, IFN-β, IFN-α, but not NF-κB reporter gene activity. A–D, HEK293-TLR7 cells were cotransfected with vectors encoding either a reporter gene for the RANTES (A), NF-κB (B) IFN-α (C) or IFN-β (D) promoters and either empty vector (pcDNA3; 40 ng) or increasing amounts of an expression vector encoding TRAM G2A (10, 20, 40 ng) as indicated. After 24 h, cells were stimulated with CLO97 (5 µg/ml) for a further 24 hr followed by harvesting and lysis. Cell lysates were frozen at -80°C overnight prior to assessment of luciferase reporter gene activity. * $p<0.05$, ** $p<0.01$ and *** $p<0.001$. Results are representative of at least three independent experiments.

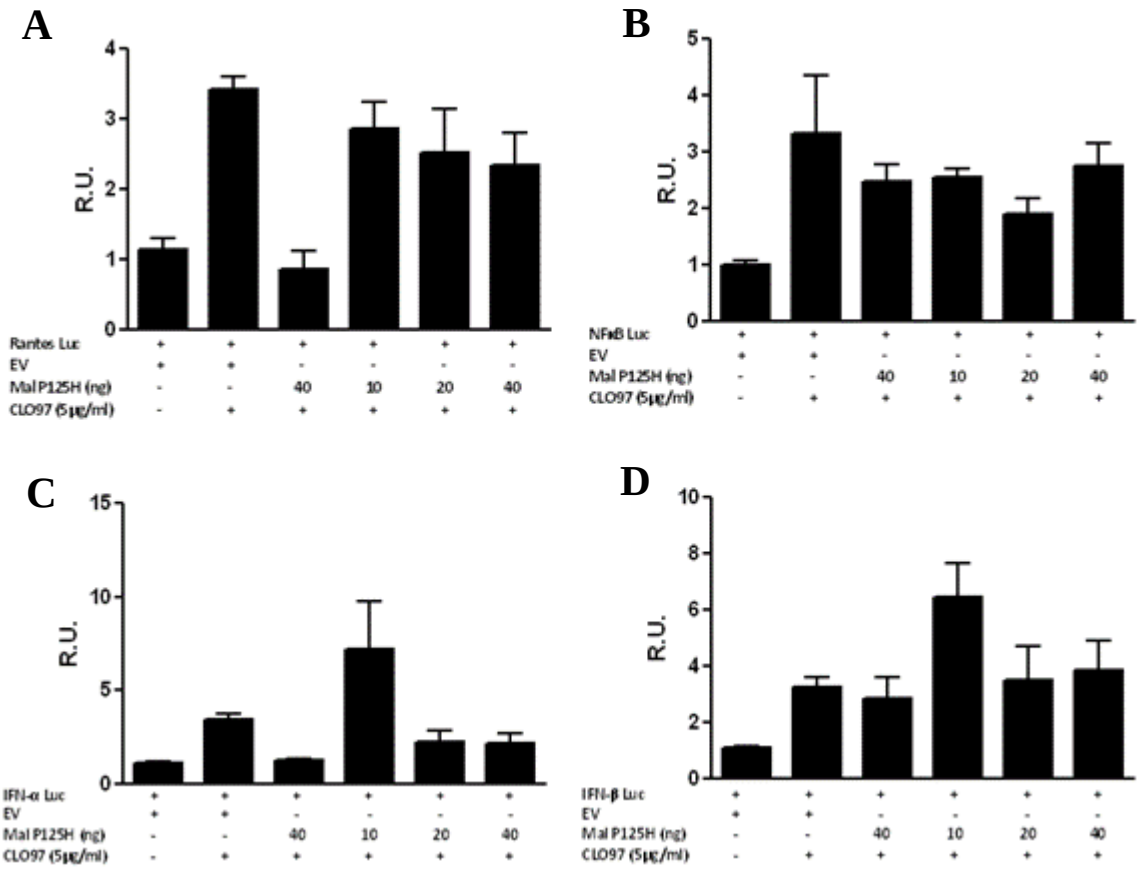

Figure 3.18: A dominant negative mutant of MAL (MAL P126H) has no effect on TLR7 induced RANTES, IFN-β, IFN-α, or NF-κB reporter gene activity. A–D, HEK293-TLR7 cells were cotransfected with vectors encoding either a reporter gene for the RANTES (A), NF-κB (B) IFN-α (C) or IFN-β (D) promoters and either empty vector (pcDNA3; 40 ng) or increasing amounts of an expression vector encoding MAL P126H (10, 20, 40 ng) as indicated. After 24 h, cells were stimulated with CLO97 (5 µg/ml) for a further 24 hr followed by harvesting and lysis. Cell lysates were frozen at -80°C overnight prior to assessment of luciferase reporter gene activity. * $p<0.05$, ** $p<0.01$ and *** $p<0.001$. Results are representative of at least three independent experiments.

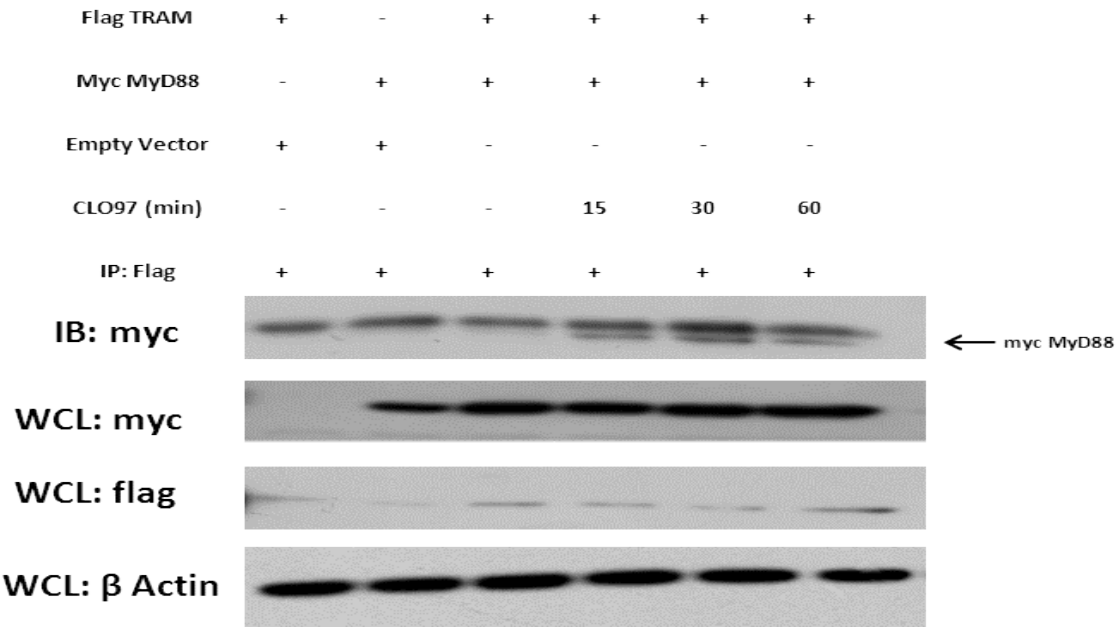

Figure 3.19: TRAM interacts with MyD88 upon TLR7 activation. HEK293-TLR7 cells were seeded into 6-well plates at a density of $1.4x10^6$ and incubated for approximately 24 hr at 37°C. At 70% confluency, cells were co-transfected with 3 µg Flag-TRAM and 3 µg EV or 3 µg Flag-TRAM and 3 µg Myc-MyD88. Approximately 24 hr after transfection, cells were either left unstimulated or stimulated with CLO97 (5 µg/ml) for 15, 30 and 60 min as indicated. Thereafter, cells were lysed in 200 µl low stringency buffer (LSB) (50 mM HEPES, pH 7.5, 150 mM NaCl, 2 mM EDTA pH 7.6, 1 % NP-40, 0.5 % sodium deoxycholate supplemented with 1 mM PMSF, 1 mM DTT, 1 mM $NaVO_3$, 5 mM EGTA and protease inhibitor cocktail). Cellular debris was removed by centrifugation upon which 20 µl of the remaining whole cell lysate (WCL) was removed, mixed with an equal volume of 5x Lamelli loading buffer, boiled for 10 min and frozen for later WCL analysis. Remaining cell lysates were incubated with 1 µg of anti-Flag monoclonal antibody overnight with gentle shaking followed by addition of 25 µl Protein A/G beads for a second night with gentle shaking. Samples were then washed 4 times with unsupplemented LSB and released from the beads by addition of 50 µl of 5x Laemmli loading buffer, followed by boiling for 10 min. Both these immunoprecipitated samples and the WCL samples were separated by SDS-PAGE gel electrophoresis and subjected to immunoblot analysis using anti-Flag and anti-Myc and anti β-Actin antibodies.

3.3 Discussion

The TIR-domain containing adaptor protein TRAM has until recently, been associated with TLR4 signalling only, acting a linker molecule bridging TLR4 and TRIF to facilitate MyD88 independent, predominantly anti-viral signalling [15]. Recent studies however, have suggested additional roles for TRAM. A novel role has been proposed in IL-18 signalling whereby TRAM acts as a linker molecule between MyD88 and IL-18R to enable downstream inflammatory cytokine production [179]. There is also evidence to indicate a role for TRAM in TLR2 signalling in response to the gram negative, TLR2 specific bacteria *Francisella tularensis [178]*. The current data provides evidence for an additional role for TRAM in TLR7 signalling whereby it mediates production of RANTES, IFNβ, CXCL10 but not TNFα. A significant reduction in secretion of the cytokine RANTES but not TNFα was observed in TRAM deficient iBMDMs compared to WT cells when stimulated with the TLR7 ligand R848. The role of TRAM appears to be at the transcriptional level as levels of the *rantes* gene transcript were also significantly reduced. This phenotype was replicated in PMA-differentiated THP1 macrophages using siRNA specific to the unique N-terminal region of TRAM with levels of *rantes*, *ifnβ* and *cxcl10* significantly reduced. It was planned to also monitor modulation of cytokine secretion upon suppression of TRAM. However, due to time constraints, it was not possible to optimise basal levels of secretion from PMA differentiated THP1 cells. Results would be expected to mirror those obtained by monitoring cytokine mRNA induction.

To date, MyD88 is the only TIR-domain containing adaptor known to be involved in TLR7 and TLR8 signalling. Evidence for the lack of involvement of other adaptors in this pathway derives mainly from studies where the adaptors are used as negative controls and have examined only at their role in mediating inflammatory cytokines such as TNFα, IL-6 and IL-

12p40 [23, 24]. Therefore, to our knowledge, this is the first study to examine TRAM's role in anti-viral cytokine induction mediated by the TLR7 pathway.

Co-immunoprecipitation experiments in HEK-293 cells stably expressing TLR7 indicated that TRAM and MyD88 do not interact basally but do co-localise upon stimulation with the TLR7 ligand, CLO97 at 15, 30 and 60 minutes. TRAM and MyD88 have previously been shown to co-immunoprecipitate to mediate IL-18R signalling but in that case, the complex dissociated upon stimulation with IL-18 [179]. Although presenting a different mode of localisation, this study does agree, first with our ability to co-immunoprecipitate TRAM and MyD88 and second, with the observed dynamism exhibited by TRAM upon ligand-receptor binding. TRAM has also been shown to be phosphorylated on serine-16 upon TLR4 activation and this phosphorylation event is required for its ability to transmit the TLR4 signal [83]. In this respect, it would be interesting to examine whether phosphorylation of TRAM is required for its ability to mediate TLR7 signalling or whether there are other important residues involved.

Overexpression of a TRAM myriostoylation mutant, TRAM G2A, which is unable to membrane localise within cells, dose dependently inhibited RANTES, IFNβ, IFN-α but not NFκB promoter activation in HEK-TLR7 cells. In contrast, overexpression of a dominant negative version of MAL had no significant effect on the same pathway. Myriostoylation of TRAM has been shown to be important for its ability to transmit TLR4 dependent signals in that it is required for TRAM's localisation to the plasma membrane and by extension, for it to interact with TLR4. Indeed, overexpression of the TRAM G2A mutant is unable to drive NFκB or RANTES reporter gene activation in human cells and in fact dose-dependently repressed LPS mediated activation of the same reporter genes [82]. Basally, TRAM has been shown to be expressed on the plasma membrane, golgi apparatus and on endosomal structures in resting cells [84, 86, 87]. Its presence on endosomal structures remains even when

dynamin dependent TLR4 endocytosis is inhibited [84] suggesting that TRAM targets independently to the endosomal membrane and that its endosomal presence may be non-exclusive regarding TLR4. Based on the data presented here, it is proposed that the presence of TRAM on endosomal structures is myriostoylation dependent and serves to aid signalling from both TLR4 and TLR7.

An additional finding was that TLR7 mediated, TRAM dependent phosphorylation of the transcription factor IRF3. IRF3 was phosphorylated in WT iBMDMs by the TLR7 ligand R848 in a time dependent manner from 15 minutes to two hours. Confirmation of its activation was the observance of IRF3 nuclear translocation, again mediated by TLR7, in a TRAM dependent manner. It is suspected that the observed activation of IRF3 is cell type, or even cell line specific as a previous study conducted in HEK293 cells indicated that overexpressed IRF3 did not translocate to the nucleus upon R848 stimulation. The same study was unable to detect endogenous phosphorylation of IRF3 in RAW264.7 macrophages in response to R848 [212]. It is well documented that endotoxin in the form of LPS is known to drive IRF3 phosphorylation in a TLR4 dependent manner and so to account for possible endotoxin contamination of the R848 preparation, HEK-TLR4 cells were stimulated with increasing concentrations of R848 with no activation of TLR4 apparent.

The majority of our current knowledge on TLR7's role in anti-viral signalling comes from studies conducted in pDCs owing to their ability to secrete higher levels of type-I IFN than macrophages and conventional dendritic cells [241]. Both type-I IFN and inflammatory cytokines are produced in a MyD88 dependent manner however type-1 IFN secretion utilises IRAK-1 recruited IRF7 whereas inflammatory cytokines are induced via TRAF6, IRAK-4 and the IKK complex to drive NFκB activation [12]. Comparatively little work has been undertaken regarding TLR7 mediated IFN signalling in macrophages however and there is a

dearth of information regarding the role of the adaptors in mediating this pathway. It is notable that loss of TRAM did not abolish TLR7 signalling as has been previously reported with MyD88 [40] and that while it is required for TLR4 mediated anti-viral signalling, TLR4's MyD88 dependent pathway remains intact in TRAM deficient cells [28]. IL-18 signalling can still occur in TRAM deficient cells, albeit to a limited extent [179]. Therapeutic targeting of TRAM could therefore provide a significant but not detrimental suppression of innate derived, predominantly anti-viral cytokines.

As mentioned in section 3.2.1, the iBMDM cell lines were problematic in a number of ways. Growth rates differed between the WT and TRAM $^{-/-}$ iBMDMs and at times they failed to consistently replicate previously published phenotypes such as reduced signalling in TRAM deficient cells compared to WT in response to LPS [24]. Therefore, relatively simple experiments often became extremely drawn-out affairs. It was originally intended to attempt a proteomic comparision of WT versus TRAM $^{-/-}$ iBMDMs for the following two results chapters however in light of the problems experienced during completion of Chapter 3, and due to the implicit time constraints inherent to the current work, it was decided to modify future experiements to avoid investing excess time conducting experiments involving iBMDMs. Therefore, a proteomic study using a single cell line, it was hoped, would generate useful publication quality data without the complications experienced in the current chapter. The following two results chapters therefore attempt to characterise proteomic changes induced in a single respiratory cell line in response to two respiratory pathogens: *B. pertussis* and HRV16.

Chapter 4

Investigations into respiratory cell proteome changes in response to infection with the respiratory pathogen *Bordetella pertussis*

4.1 Chapter Aim

The aim of this chaper was to analyse proteome modulation of a lung epithelial cell line in response to infection with the gram negative bacterium *B. pertussis*. This would be accomplished using 2D-DIGE combined with LC-MS and also using LFQ-MS. Protein hits obtained from both techniques would be compared to see if the techniques are complementary. A selection of hits would then be validated and an analysis of their role in immune signalling undertaken by supresssion their expression priot to infection with *B. pertussis*.

4.2 Results

4.2.1 *B. pertussis* activation of BEAS-2B cells

In order to identify an optimal timepoint for *B. pertussis* to activate the immune response, a timecourse experiment was carried out in which *B. pertussis* was allowed to infect BEAS-2B cells for 6, 12, 24, 32 and 48 hr. Inflammatory cytokine gene expression was then monitored at each timepoint in order to identify the point at which the immune response was maximally activated (Figure 4.1).

Upon infection of BEAS-2B cells with *B. pertussis*, levels of IL-6 mRNA were upregulated at both 6 and 24 hr with maximal activation occurring at 12 hr (Figure 4.1A). A significant, but much smaller upregulation of TNFα gene expression was also observed at 12 hr but not at 6 hr or 24 hr (Figure 4.1B).Based on these observations, it was decided to infect BEAS-2B cells with *B. pertussis* for 12 hr prior to protein solubilisation and preparation for 2D-DIGE and LFQ analysis.

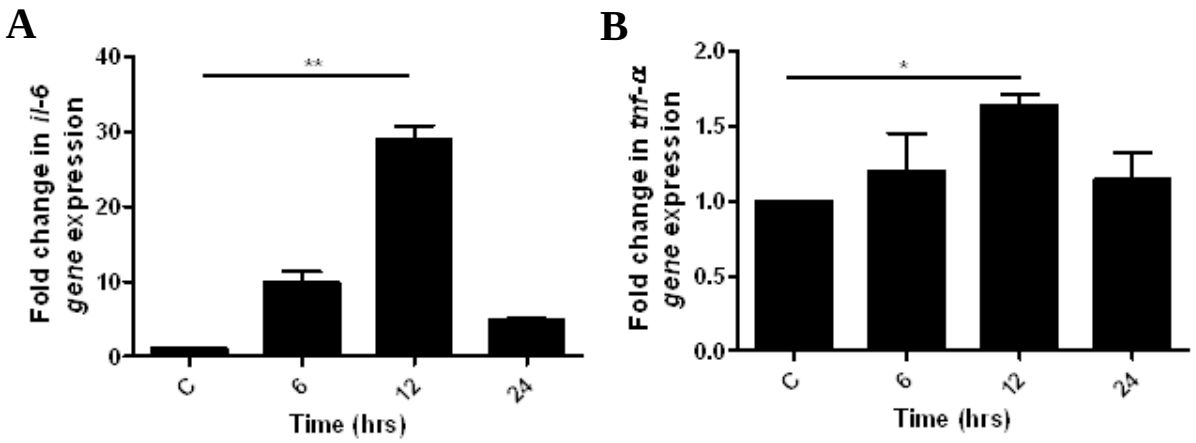

Figure 4.1: *B. pertussis* infection of BEAS-2B cells activates the immune response. BEAS-2B cells were plated at a density of $0.7x10^6$ cells/ml in a six-well plate and incubated for 24 hr at 37°C. Individual wells were then either left unstimulated or stimulated with *B. pertussis* (200 bacteria/cell) for the timepoints indicated. Cells were then harvested, total RNA isolated and from this, cDNA was synthesised. The cDNA was then used as a template for qRT-PCR using forward and reverse primers specific to human *il-6* and *gapdh* (housekeeping gene). * $p<0.05$, ** $p<0.01$ and *** $p<0.001$. Graphs are representative of two independent experiments.

4.2.2 Proteomic response to *B. pertussis* infection – common trends and functional annotation of protein hits obtained by 2D-DIGE / MS

Protein hits that were significantly up or down regulated in response to *B. pertussis* infection of BEAS-2B cells, as identified by 2D-DIGE with MS were categorised first based on a broad generalisation of their biological role (Figure 4.2A). A protein was considered to be a true hit when it fulfilled a number of statistical criteria. First was that the protein in question, derived from whole cell lysates from *B. pertussis* stimulated cells, must have exhibited a fold change equal to or greater than plus or minus 1.3 fold compared to unstimulated cells. This fold change also must have been detected across N=4 independent experiments. From this then the statistical significance was based on a P value below 0.05. At this point the equivalent protein spot on the 2D-DIGE gel was extracted for MS analysis. Using software analysis, recognised peptides were then matched to proteins. A peptide was considered matched upon recognition of extensive homology with a P value below 0.05 which typically equated to a 'Mascot Score' of ≥50 (Appendix Table A1.1) [242].

A total of 47 protein hits were found to be significantly up or down regulated in response to *B. pertussis* infection (Table 4.1). The observed protein fold changes averaged approximately 1.4 fold indicating that although many proteins underwent modulation of expression, the level of modulation was quite small. This could be a limitation of the 2D-DIGE technique however firther experimentation would be required to confirm this. Of the 47 proteins hits identified, 42 proteins, or 87 % of the total, were found to be upregulated and five proteins, or 13% of the total, were downregulated (Figure 4.2B, Table 4.1). The protein hits were found to fall into seven general functional categories namely the redox response, the immune response, transcription and DNA editing, structural proteins, cancer related proteins, protein synthesis and modification and trafficking (Figure 4.2A). Proteins with previously documented roles in the immune response represented 29 % of the total observed hits, the largest category

observed and indicating that lung epithelial cells are equipped with many defence mechanisms to deal with such as pathogen, perhaps unsurprising as they would be one of the first exposed to a respiratory pathogen such as *B. pertussis* [140]. Structural proteins were the next best represented functional subset with accounting for 15 % of total hits identified (Figure 4.2A). Many of these proteins were found to have known functions in regulating tubulin and actin formation within the cell (Table 4.1). *B. pertussis* is known to actively enter ciliated lung epithelial cells and inhibit intracellular immune responses whist simultaneously evading the extracellular immune response [138, 243-245]. Although it is well documented that intracellular bacteria can modify the host actin network for their own means [246-248], recently, some light has been shed on the mechanism of *B. pertussis* entry into cells and the involvement of the host microtubule network. It has been shown that entry is dependent upon microtubule assembly, lipid raft integrity and activation of tyrosine-kinase mediated signalling [249]. Indeed, treatment of cells with a microtubule depolymerisation agent significantly reduced the number of internalised bacteria [249]. Relating to this, 5 % of proteins identified were involved in trafficking (Figure 4.2A) which likely utilise the cell's structural network to enable the bacteria to internalise. Proteins involved in protein synthesis and modification as well as transcription and DNA editing exhibited large changes in expression accounting for 15 % and 10 % respectively of the observed global changes (Figure 4.2A). Given the immediate threat to the cell's integrity, the accommodation of a new, foreign organism and the mobilisation of defence mechanisms against the pathogen, this observation, was unsurprising. An interesting observation was that 12 % of dynamically regulated proteins in response to *B. pertussis* infection harboured known links to cancer either as known biomarkers or as mediators of cancer signalling (Figure 4.2A, Table 4.1). Many parallels have been drawn between cancer progression and the immune response and it is becoming increasingly clear that the two are intertwined [250-252]. An example of this from

the current study is the protein hit stathmin (Table 4.1). Stathmin has long been known as a marker for cancer progression had recently been shown to be an endogenous activator of TLR3 [253-255]. Finally, proteins involved in the redox response accounted for 9 % of observed protein hits (4.2A). Redox signalling has many roles in cell physiology particularly in defence with reactive oxygen and nitrogen species playing key roles in the innate defence. However, as these reactive species are consequently damaging to both the invading pathogen and the host a large number of proteins are involved in tailoring redox signalling to best benefit the host [256].

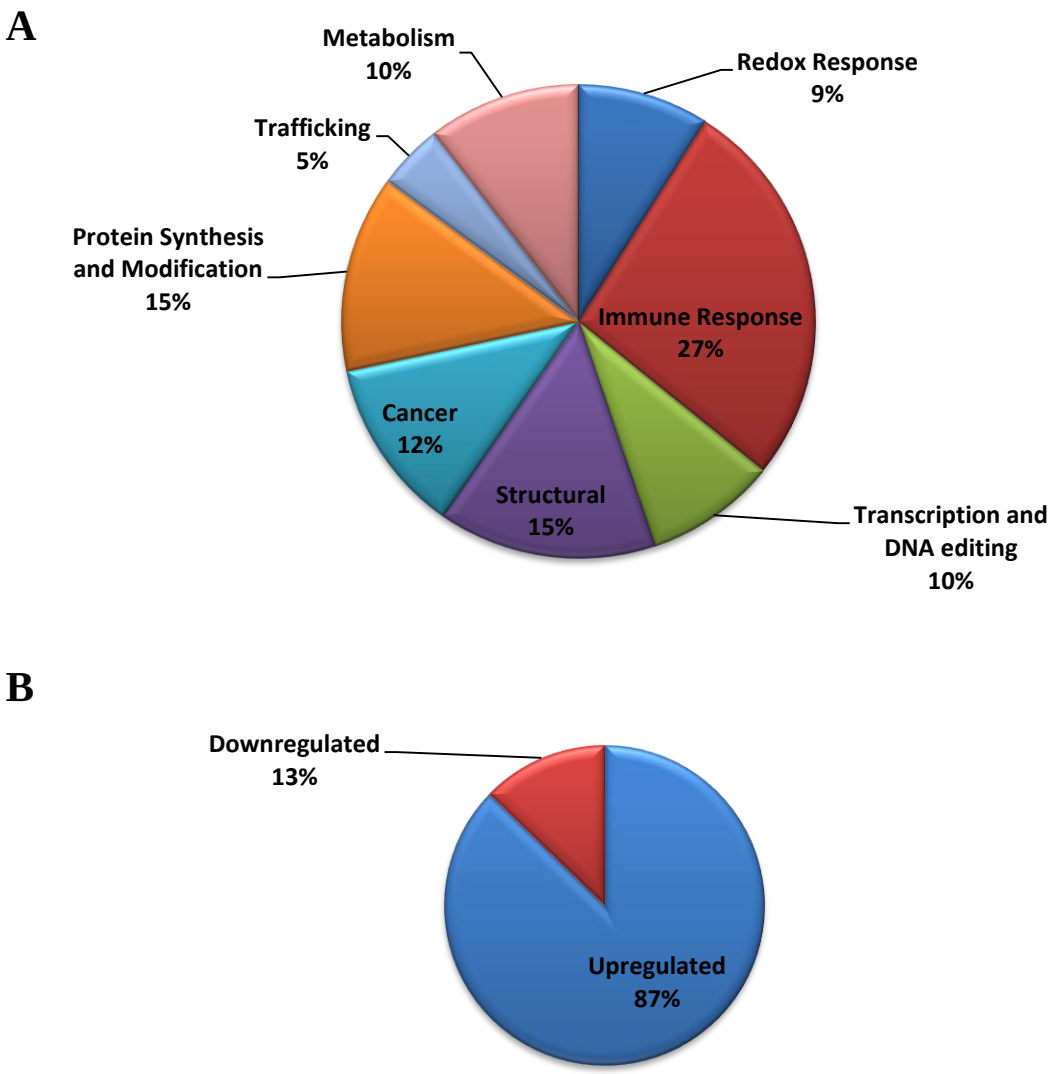

Figure 4.2: Pie chart representations of proteins identified by 2D-DIGE in response to *B. pertussis* infection. (A) Identified proteins were manually researched for functional properties and assigned functions(s) to form the basis of categorisation. Total numbers of proteins assigned to each function were inputted into a pie chart for appropriate visualisation. (B) Protein hits that were adjudged to be up or down regulated via Progenesis software, were inputted into a pie chart in order to visualise the divide.

Overview of protein hits obtained by 2D-DIGE with LC-MS

Fold Ch.	Protein Name	Function
↑1.5	Thioredoxin	Redox Signalling. Regulates NFκB DNA binding [257]
↑1.5	Replication protein A 14 kDa subunit	DNA repair, recombination and replication. Inhibits viral DNA replication [258]
↑4.4	Triose phosphotate Isomerase	Important in glycolytic pathway [259]
↑1.4	Tubulin-specific chaperone A	Tubulin folding [260]
↑1.5	Stathmin	Endogenous TLR3 agonist [255]. Cancer marker. Microtubule regulation [261].
↑1.5	Stathmin-2	Microtubule regulation. Associated with Alzheimer's [262]
↓1.3	Protein disulfide-isomerase	Catalyses protein folding. MHC loading [263]. Required for HIV infection [264].
↓1.5	Transitional endoplasmic reticulum ATPase	Intracellular trafficking [265]
↓1.4	heat shock 70kDa protein 9B	Protein chaperone. Aids protein folding [266]. TLR2/4 activator [267].
↓1.4	Tapasin ERP57	MHC class I peptide loading [268].
↑1.3	Superoxide dismutase [Cu-Zn]	Redox signalling. Indirect NFκB modulator [269].
↑1.3	GSTP1-1	Metabolism. Levels increased in colorectal cancer [270].
↑1.3	Ubiquitin-conjugating enzyme E2 N (Ubc13)	Required for MAP Kinase activation [271]. Role in TRAF6 mediated signalling [272].
↓1.7	Cofilin-1	Actin modulator. Role in cell migration [273].
↑1.3	PRDX3	Redox signalling [274]. Prostate cancer marker [275].
↑1.4	Clic1	Chloride Channel. Aids macrophage phagosome acidification [276].
↑1.3	EB1	Microtubule regulator [277].
↑1.4	Glutathione S-transferase omega-1	Suspected inflammasome modulator. Binds to ASC [278, 279].
↑1.4	NLRP12	Cytosolic PRR. Senses Yersinia pestis. Supresses inflammation [280].

Table 4.1: Proteins identified by 2D-DIGE combined with LC-MS showing changes in expression in response to *B. pertussis* infection. Protein function is also indicated. Full annotation of protein hits can be found in appendix table A1.1.

Overview of protein hits obtained by 2D-DIGE with LC-MS

Fold Ch.	Protein Name	Function
↑1.5	Proteasome subunit beta type-4	Protein degradation [281].
↑1.5	Annexin A2	Vascular homeostasis [282]. Post transcriptional regulation [283]
↑1.5	Thioredoxin domain-containing protein 12	Part of thioredoxin superfamily. Redox signalling [284].
↑1.5	Mitotic spindle-associated MMXD complex	Iron/sulphur incorporation. Involvement in mitosis [285].
↑1.4	Nucleoside diphosphate kinase A (NME1)	Transfers phosphate groups between kinases [286].
↑1.3	Peroxiredoxin-6	Redox signalling. Phospholipase activity [287].
↑1.3	Dj-1	Associated with Parkinson's Disease. Protective against oxidative stress [288].
↑1.3	Acyl-protein thioesterase 1	Fatty acid hydrolysis. Involved in Ras signalling [289].
↑1.4	Phosphoglycerate mutase 1	Phosphate transfer in glycolysis [290].
↑1.3	Transaldolase	Role in pentose phosphate pathway [291].
↑1.4	Serine/threonine-protein phosphatase PPP1Cα	Phosphotase. Required for RIG-I and MDA5 signalling [292].
↓1.3	ER-60 protease	ER resident protein-cysteine protease activity. Degrades misfolded proteins [293]
↑1.3	Human Galectin-1	Inhibits macrophage migration and pathogen killing. Increased in tumours [294]
↑1.4	40S ribosomal protein S12	Ribosome subunit. Site of protein synthesis [295].
↑1.3	IL-25	T_H2 cytokine-induces secretion of IL-4 [296]. Anti-inflammatory [297]
↑1.3	Caspase 3	Protease. Central apoptosis mediator [298].
↑1.4	PSMB10	Proteasome subunit. MHC class I peptide cleavage [299].
↑1.4	Platelet-activating factor acetylhydrolase	Suggested anti-inflammatory. Produced by lymphocytes in atherosclerosis [300].

Table 4.1 (contd): Proteins identified by 2D-DIGE combined with LC-MS showing changes in expression in response to *B. pertussis* Infection. Protein function is also indicated. Full annotation of protein hits can be found in appendix table A1.1.

Overview of protein hits obtained by 2D-DIGE with LC-MS

Fold Ch.	Protein Name	Function
↑1.3	Replication Protein A (Rpa14 And Rpa32)	Binds DNA to ensure efficient replication and repair [301].
↑1.3	Eukaryotic translation initiation factor 4E	Directs ribosomes to mRNA for translation. Viral target to aid replication [302].
↑1.4	Heat shock protein beta-1	Cell stress resistance and actin organization [303].
↑1.3	DNA replication complex GINS protein PSF2	Role in DNA replication. Preferentially binds single stranded DNA [304].
↑1.4	ATP synthase subunit d, mitochondrial	Produces ATP from ADP [305].
↑1.4	Calpain small subunit 1	Calcium dependent cysteine protease. Active in cell migration [306].
↑1.4	14-3-3 protein epsilon	Signal transduction. Inhibits multiple TLR signalling pathways [307].
↑1.4	Complement component 1 Q	Regulator of DC differentiation [308] . Inhibitor of RIG-I and MDA5 [309]
↑1.4	Putative hydrolase RBBP9	Serine hydrolase. Role in TGF-β signalling. Implicated in pancreatic cancer [310]

Table 4.1 (contd): Proteins identified by 2D-DIGE combined with LC-MS showing changes in expression in response to *B. pertussis* Infection. Protein function is also indicated. Full annotation of protein hits can be found in appendix table A1.1.

4.2.3 Verification of protein hits from *B. pertussis* infection.

As can be seen from Table 4.1, over 40 proteins whose expression were significantly up or down regulated in response to *B. pertussis* infection were identified by 2D-DIGE with LC-MS. These proteins have documented functions in diverse cellular processes ranging from structural integrity and metabolism to immune function and redox signalling (Table 4.1 and Figure 4.2A). However, immunoblotting using antibodies specific to selected proteins of interest must also be undertaken in both unstimulated and *B. pertussis* stimulated whole cell lysates in order to confirm the stimulation dependent changes in expression. With this in mind, it was decided to confirm the expression of proteins that were considered interesting with respect to *B. pertussis* infection and which represented a range of the different cellular processes affected by *B. pertussis* infection. Proteins selected for verification include DJ-1 – a protein whose exact function is unknown but is linked to redox prcocesses, Parkinson's disease and pancreatic cancer progression (Table 4.1). The proteins glutathione S-transferase omega 1 (GSTO1) and NLRP12 both have demonstrated roles in immune function but neither have been linked to *B. pertussis* pathogenesis (Table 4.1). Stathmin 1 is known primarily for its role in structural processes within the cell. PPP1Cα is a phosphatase capable of protein modifications and finally, triosephosphate isomerase whose role in is the glycolytic pathway and thus is important in cellular metabolism. Further insight on each protein is provided in the following sections.

4.2.4 2D DIGE Protein Hit Verification: DJ-1

DJ-1, otherwise known as PARK7, is an evolutionarily conserved protein found in all aerobic species including humans, *Drosophila melanogaster, Caenorhabditis elegans* and *Escherichia coli* [288].

Its exact function within the cell is to date, unclear. However it has been shown that a lack of DJ-1 causes increased sensitivity to oxidative stress, leading to cell death. Similarly, overexpression of DJ-1 is protective under the same conditions [311]. This function is dependent upon the modification of cysteine residues on DJ-1 to cysteine-sulfonic residues [312-314]. The observed phenotype was specific to oxidative stress as no correlation was found between DJ-1 and non-oxidative stress [315]. Exactly how DJ-1 mediates these effects is unknown with suggestions ranging from transcriptional coactivaor to molecular chaperone [311]. DJ-1 localises to the cytoplasm and nucleus and is omnipresent throughout human tissue, including the brain [316]. Interestingly, DJ-1 null mice have been shown to release less dopamine which is turn linked to a severe reduction in function of the D2 receptor, a key molecule in the regulation of the dopaminergic system [317]. This study added credence to an earlier publication which showed that a mutation in the DJ-1 gene was associated with early-onset Parkinson's Disease (Figure 4.3) [316].

In recent years, a role for DJ-1 in innate immunity has been suggested. DJ-1 $^{-/-}$ mice have been shown to produce higher levels of nitric oxide in response to stimulation with the TLR4 agnoist LPS compared to WT mice [318]. Furthermore, DJ-1 deficient *Caenorhabditis elegans* (*C. elegans*) showed increased activation of MAP-kinase controlled genes related to the innate immune response compared to WT in response to pathogenic *Pseudomonas aeruginosa* [319].

The current work has shown that when analysed by 2D-DIGE, levels of the DJ-1 protein are elevated 1.3 fold in human lung epithelial cells infected with *B. pertussis* compared to uninfected controls (Figure 4.4A, Table 4.1). This result was verified by western blot (Figure 4.4B). Levels of the DJ-1 gene were also significantly upregulated 2.2 fold compared to unstimulated controls (Figure 4.4C) indicating that upon response to *B. pertussis* infection, DJ-1 levels are regulated at the transcriptional level.

As mentioned previously, DJ-1 has been suggested to be a redox responsive protein in that it undergoes cysteine modifications to mediate a protective effect upon cells [313]. *B. pertussis* PTx has been shown to induce NO production in spleen cells.

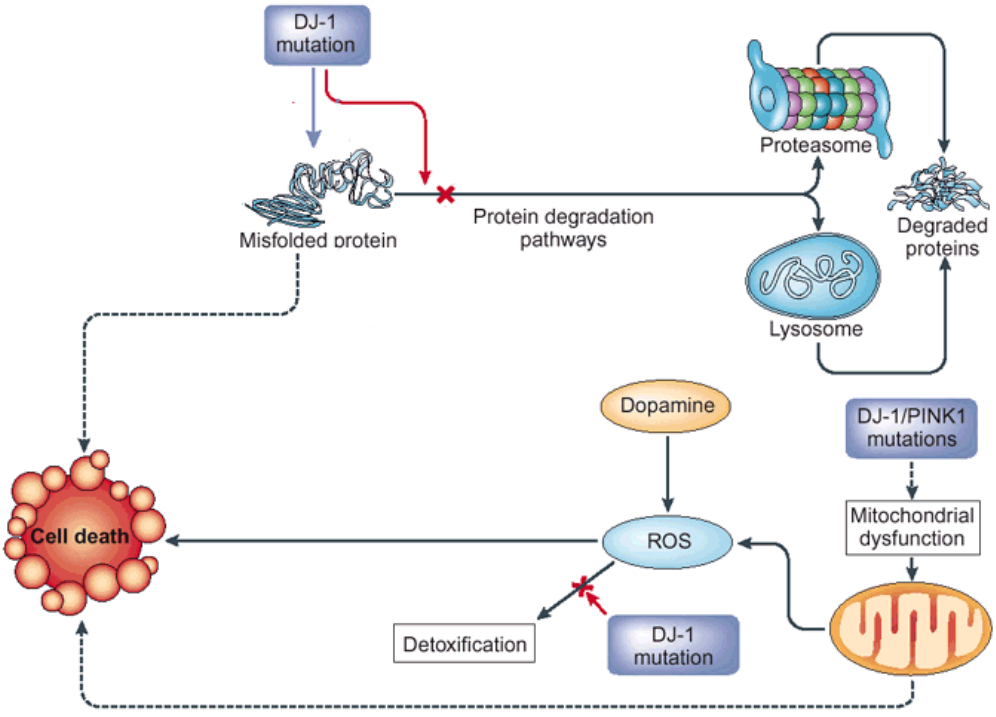

Figure 4.3: Overview of suspected roles for Dj-1. Mutations in DJ-1 can cause misfolding which overloades protein degradation systems causing cytotoxicity that could contribute to PD pathogenesis. Mutations in DJ-1 have also been linked to increased sensitivity to oxidative stress leading to increased cell death. Adapted from [320]

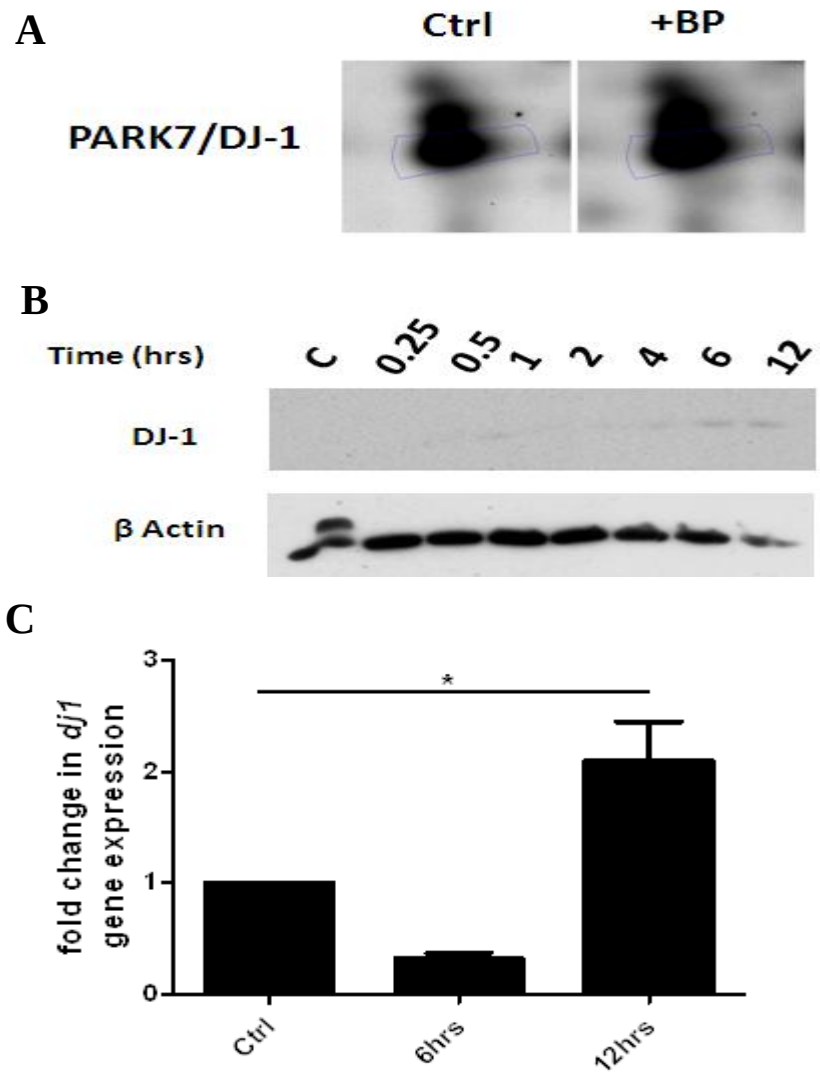

Figure 4.4: Verification of DJ-1 upregulation in response to *B. pertussis*. (A) Screen grab of Progenesis analysis showing DJ-1 presence on 2D-DIGE gel from control (Ctrl) and *B. pertussis* infected (BP) lysates. (B) BEAS-2B cells were seeded in a 6-well plate at a density of $0.7x10^6$ cells/ml and incubated for 24 hr at 37 °C. Thereafter, cells were either left uninfected or infected with *B. pertussis* (MOI of 200) for 15 min, 30 min, 60 min, 2 hr, 4 hr, 6 hr and 12 hr. Cells were then harvested and each sample lysed in 100 µl H.S. buffer for 20 min on ice. Cell debris was removed by centrifugation with the remaining whole cell lysates mixed with 30 µl 5x Laemmli loading buffer and boiled for 10 min. Proteins were separated by SDS-PAGE and subjected to immunoblot analysis using anti-DJ-1 and anti-β-Actin antibodies. Results represent two independent experiments. (C) BEAS-2B cells were plated at a density of $0.7x10^6$ cells/ml in a six-well plate and incubated for 24 hr at 37 °C. Individual wells were then either left unstimulated or stimulated with *B. pertussis* (MOI of 200) for the timepoints indicated. Cells were then harvested, total RNA isolated and from this, cDNA was synthesised. The cDNA was then used as a template for qRT-PCR using forward and reverse primers specific to human *dj-1* and *gapdh* (housekeeping gene). * $p<0.05$, ** $p<0.01$ and *** $p<0.001$. Graph is representative of four independent experiments.

4.2.5 2D-DIGE Protein Hit Verification: GSTO1

Glutathione S-transferases are a family of enzymes that catalyse the conjugation of glutathione, via a sulfhydryl group, to electrophilic centres on a wide range of substrates including carcinogens, oxidative products and synthetic drugs [321]. Based on sequence similarities and immune cross reactivity, there are seven classes of cytosolic GST in humans: Alpha, Mu, Sigma, Pi, Theta, Zeta and a more recently identified class, Omega [322, 323]. They are highly conserved with more classes present across species [324]. A number of features set the omega class apart from the other GST family members. It contains a unique N-terminal, proline rich extension of 19 aa which forms a distinct structural unit in conjunction with the C-terminus. The function of this unit however, is currently unknown [323]. Other GST family members contain a tyrosine or serine residue within hydrogen bonding distance of a sulphur atom of the bound glutathione and mutation of either of these residues results in complete or severe inactivation [325]. The Omega class does not contain equivalent residues but does contain an active site cysteine suggesting the GSTO1 does not have the glutathione conjugation abilities common to other GSTs and instead have another as yet undescribed function [323]. A mouse orthologue of GSTO1, termed p28, also lacks GST activity but changes its subcellular location in response to heat suggesting a role in cellular stress response mechanisms [326].

GSTO1 has been implicated in a number of studies as playing a role in IL-1β processing through its association with cytokine release inhibitory drugs (CRIDs) [278, 279]. Affinity labelling and affinity binding chromatography identified GSTO1 as a target of CRID and this interaction was dependent on the aforementioned active cysteine site, Cys^{32} [278]. The concentration of [^{14}C]CRID required to label cell-associated GSTO1 was also directly proportional to the extent of inhibition of IL-1β posttranslational processing.

A second study examined this finding further by showing the GSTO1 interacts with adapter molecule apoptosis-associated speck-like protein containing a CARD (ASC), a pivotal protein in the assembly of NACHT, LRR and pyrin domain (PYD) domains-containing protein (NLRP) 1, NLRP3 and absent in melanoma 2 (AIM2) inflammasome formation [279]. This study showed that CRID3 inhibited ASC oligomerization in the NLRP3 and AIM2 inflammasome and speculated that glutathionylation of ASC by GSTO1 could be required for ASC function [279].

The current study identified GSTO1 as being upregulated 1.4 fold in BEAS-2B cells in response to infection with *B. pertussis* (Figure 4.5A, Table 4.1). Immunoblotting using an anti-GSTO1 antibody confirmed this result and indeed indicated that GSTO1's expression was upregulated in response to *B. pertussis* after only 30 min of infection with expression being maintained at multiple further timepoints up to and including 12 hr of infection (Figure 4.5B). GSTO1 gene expression was also significantly upregulated at both 6 and 12 hr post infection suggesting its regulation in transcriptionally regulated (Figure 4.5C).

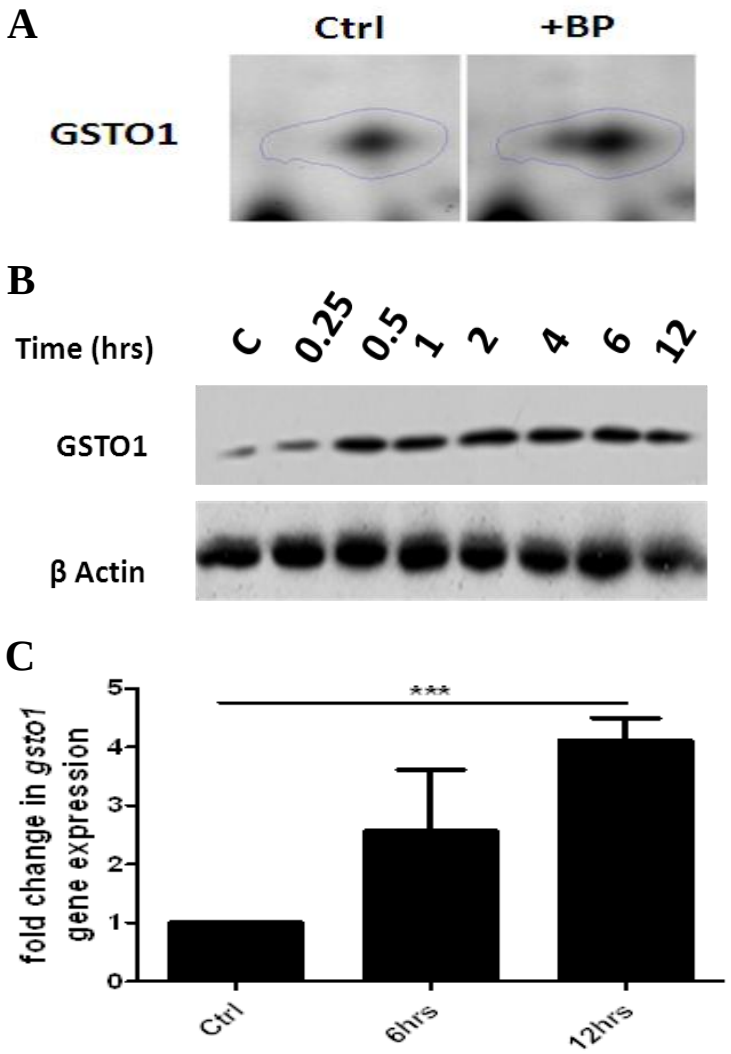

Figure 4.5: Verification of GSTO1 upregulation in response to *B. pertussis*. (A) Screen grab of Progenesis analysis showing GSTO1 presence on 2D-DIGE gel from control (Ctrl) and *B. pertussis* infected (BP) lysates. (B) BEAS-2B cells were seeded in a 6-well plate at a density of $0.7x10^6$ cells/ml and incubated for 24 hr at 37 °C. Thereafter, cells were either left uninfected or infected with *B. pertussis* (MOI of 200) for 15 min, 30 min, 60 min, 2 hr, 4 hr, 6 hr and 12 hr. Cells were then harvested and each sample lysed in 100 µl H.S. buffer for 20 min on ice. Cell debris was removed by centrifugation with the remaining whole cell lysates mixed with 30 µl 5x Laemmli loading buffer and boiled for 10 min. Proteins were separated by SDS-PAGE and subjected to immunoblot analysis using anti-GSTO1 and anti-β-Actin antibodies. Results represent two independent experiments. (C) BEAS-2B cells were plated at a density of $0.7x10^6$ cells/ml in a six-well plate and incubated for 24 hr at 37 °C. Individual wells were then either left unstimulated or stimulated with *B. pertussis* (MOI of 200) for the timepoints indicated. Cells were then harvested, total RNA isolated and from this, cDNA was synthesised. The cDNA was then used as a template for qRT-PCR using forward and reverse primers specific to human *gsto1* and *gapdh* (housekeeping gene). * $p<0.05$, ** $p<0.01$ and *** $p<0.001$. Graph is representative of four independent experiments.

4.2.6 2D-DIGE Protein Hit Verification: Stathmin 1

Stathmin is a ubiquitous phosphorprotein, highly conserved among vertebrates, which was originally discovered from analysis of lysates derived from cells perturbed with hormones such as thyrotropin-releasing hormone and corticotropin-releasing hormone [327, 328]. It was also recognised as a protein that was highly expressed in acute leukaemias [329].

Indeed, stathmin has been shown to be highly expressed in multiple human malignancies and interestingly, a high level of stathmin expression correlates with poor prognosis [253, 254]. Stathmin's main role is in the regulation of microtubule dynamics by promoting depolymerisation of microtubules or preventing polymerisation of tubulin heterodimers [261]. Because of this, stathmin plays a particularly important role in mitotic spindle formation during the cell cycle in both early and late stages of mitosis. Because microtubule formation effects diverse cellular functions, stathmin has also been found to play a role in activated T cell polarization. Polarisation of the microtubule organising center of activated T cells was defective in stathmin null mice causing reduced secretion of cytolysic granules and target cell lysis [330].

In keeping with immune related functions of stathmin, a startling observation was that stathmin acts as an endogenous protein agonist for TLR3 [255]. TLR3 and stathmin were shown to colocalise under neuroinflammatory conditions replicating multiple sclerosis in astrocytes, neurons and microglia. Monocyte derived dendritic cells were also activated by stimulation with stathmin. Cytokine expression profiles of stathmin and poly(I:C) stimulated WT and TLR3 deficient cells were almost identical. The authors hypothesised that as both TLR3 and stathmin can inhibit axon and dendrite formation, the interaction between the two may underlie, or even be required for, their functional similarities [255].

Stathmin was observed by 2D-DIGE with LC-MS to be upregulated 1.5 fold in *B. pertussis* infected cells compared to controls (Figure 4.6A, Table 4.1). This finding was verified by western blot over multiple timepoints up to and including 12 hr (Figure 4.6B). Analysis of stathmin mRNA levels did not indicate any significant increase in transcription of stathmin mRNA indicating that its dynamic regulation is determined by post-transcriptional events (Figure 4.6C).

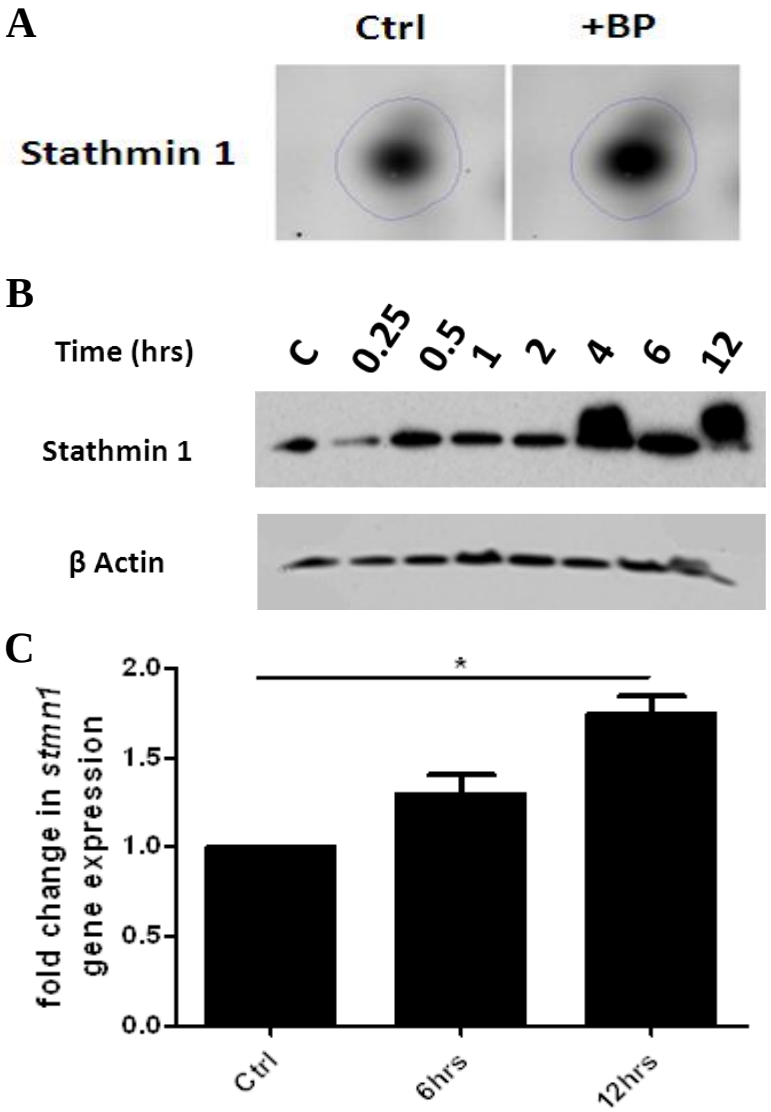

Figure 4.6: Verification of STMN1 upregulation in response to *B. pertussis*. (A) Screen grab of Progenesis analysis showing STMN1 presence on 2D-DIGE gel from control (Ctrl) and *B. pertussis* infected (BP) lysates. (B) BEAS-2B cells were seeded in a 6-well plate at a density of $0.7x10^6$ cells/ml and incubated for 24 hr at 37 °C. Thereafter, cells were either left uninfected or infected with *B. pertussis* (200 bacteria/cell) for 15 min, 30 min, 60 min, 2 hr, 4 hr, 6 hr and 12 hr. Cells were then harvested and each sample lysed in 100 µl H.S. buffer for 20 min on ice. Cell debris was removed by centrifugation with the remaining whole cell lysates mixed with 30 µl 5x Laemmli loading buffer and boiled for 10 min. Proteins were separated by SDS-PAGE and subjected to immunoblot analysis using anti-STMN1 and anti-β-Actin antibodies. Results represent two independent experiments. (C) BEAS-2B cells were plated at a density of $0.7x10^6$ cells/ml in a six-well plate and incubated for 24 hr at 37 °C. Individual wells were then either left unstimulated or stimulated with *B. pertussis* (200 bacteria/cell) for the timepoints indicated. Cells were then harvested, total RNA isolated and from this, cDNA was synthesised. The cDNA was then used as a template for qRT-PCR using forward and reverse primers specific to human *stmn1* and *gapdh* (housekeeping gene). * $p<0.05$, ** $p<0.01$ and *** $p<0.001$. Graph is representative of four independent experiments.

4.2.7 2D-DIGE Protein Hit Verification: PPP1Cα

Protein phosphatase PP1 alpha catalytic subunit (PPP1Cα), also known as PP1α, is one of three catalytic subunits of protein phosphatase 1, the other two subunits being PPP1β and γ. They form a small but vitally important part of the phosphoprotein phosphatase (PPP) superfamily which comprises serine/threonine phosphatases 1-7 [331]. Together, PPP1-7 catalyse over 90% of dephosphorylating reactions in eukaryotic cells [332]. The most important of these seven, in terms of substrate diversity, is PPP1 as it is predicted to hydrolyse the majority of serine and threonine-linked phosphate ester bonds in eukaryotic cells [333]. Further evidence of PPP1's importance is the fact that it is extremely highly conserved between yeast and humans with greater than 80% sequence similarity between the two. Indeed, human PPP1 can rescue the lethal loss of PPP1 in yeast [334]. PPP1 affects such a large proportion of dephosphorylation events by its ability to interact with over 200 known targeting proteins that serve to localise PPP1 to distinct cellular regions whilst also modifying its substrate specificity. The use of these targeting proteins is therefore believed to allow PPP1 to be converted into 100s of highly specific holoenzymes [335]. The phosphatase activity of PPP1 is regulated by endogenous inhibitory proteins such as the aptly named inhibitor-1 and inhibitor-2, as well as CPI-17 and DARPP-32 [336]. As PPP1 interactors are the main determinant of PPP1 function, they too are studied in detail. Their role is predominantly in signalling processes with known involvements in metabolism, the cell cycle and stress responses [337]. The importance of PPP1α in the immune response can be demonstrated by the encoding by herpes simplex virus of a PPP1α interactor termed ICP34.5. This protein interacts with PPP1α directing it to dephosphorylate and thus activate eIF2α which in turn inhibits PKR, a key mediator of the antiviral immune response [338, 339]. A further interactor, nuclear inhibitor of protein phosphatase 1, in combination with PP1 can act as a molecular compass to direct cancer cell migration by affecting guanosine

triphosphate (GTP)ase signalling, with an implied role in cancer cell metastasis [340]. While the current work on PPP1α was proceeding, a striking observation was made regarding its role in innate immune signalling. It has been shown that dephosphorylation of the viral RNA sensors retinoic acid-inducible gene 1 (RIG-I) and melanoma differentiation-associated protein 5 (MDA5) by PPP1α and its isoform PPP1γ is essential for their ability to drive type-I IFN production [292]. Both PPP1α and PPP1γ were shown to interact with RIG-I and MDA5 upon viral infection to inhibit phosphorylation of specific serine residues on CARD domains pertaining to both receptors. Furthermore, mutation of the PPP1 binding motif on both RIG-I and MDA5, led to an almost complete abolishment of their ability to signal [292].

The current study identified PPP1α as being upregulated 1.4 fold in a 2D-DIGE comparison between uninfected and *B. pertussis* infected lung epithelial cells (Figure 4.8A, Table 4.1). This result was verified by western blot at multiple timepoints from 15 min up to 12 hr. Gene expression of PPP1α was also shown to be significantly upregulated 15-fold upon stimulation with *B. pertussis* for 12 hr (Figure 4.8B). PPP1α mRNA was also upregulated approximately 3 fold after 6 hr of infection with *B. pertussis* (Figure 4.8C). This would suggest that PPP1α is somehow induced by *B. pertussis* at the transcriptional level. This result also hints at an increasing role for PPP1α as the infection increase in severity over time.

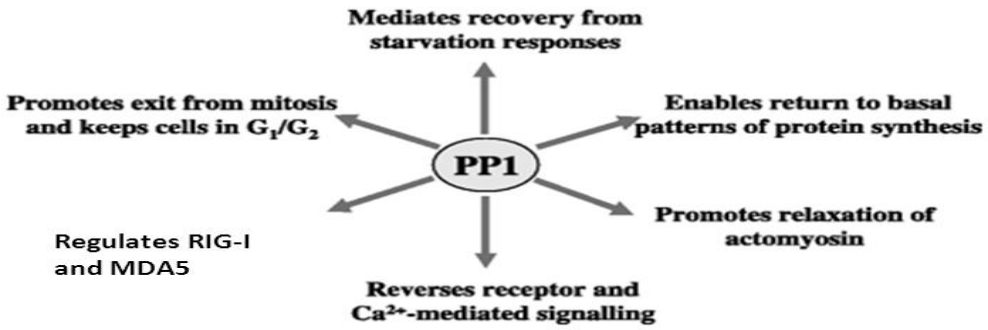

Figure 4.7: General functions of PP1/PPP1. Roles for PPP1 include recovery from starvation, protein synthesis regulation, calcium signalling, immune function and mitosis. Adapted from [341].

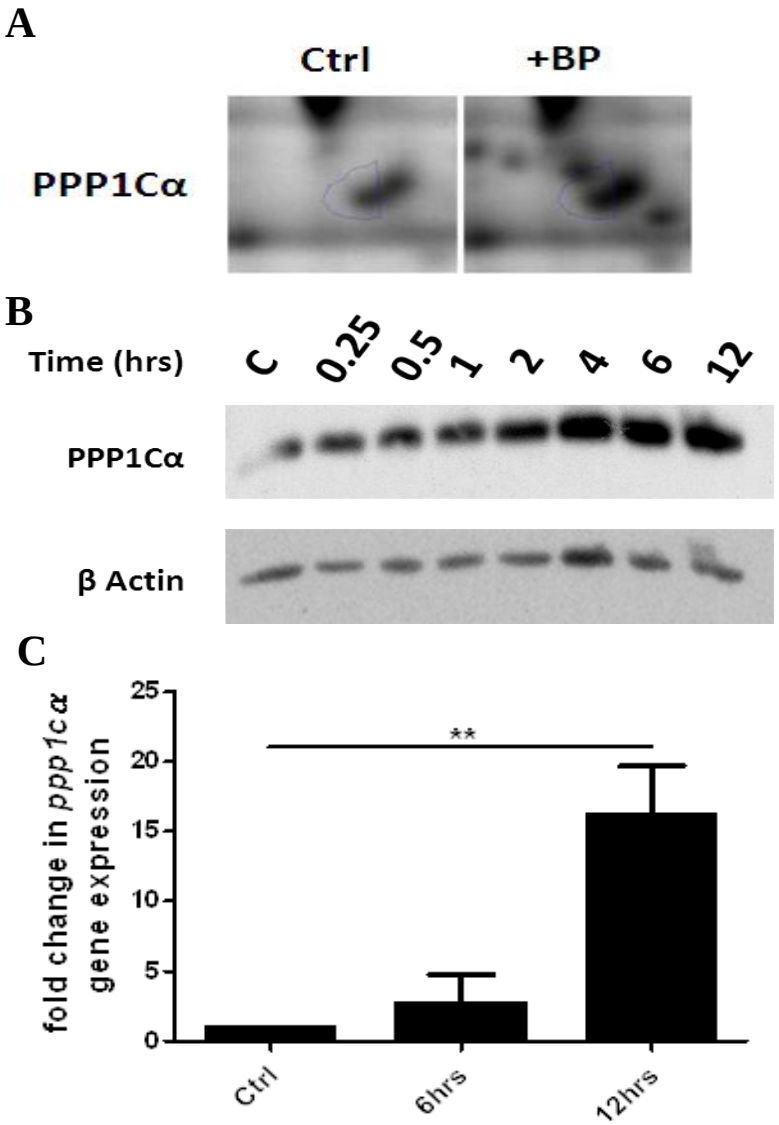

Figure 4.8: Verification of PPP1Cα upregulation in response to *B. pertussis*. (A) Screen grab of Progenesis analysis showing PPP1Cα presence on 2D-DIGE gel from control (Ctrl) and *B. pertussis* infected (BP) lysates. (B) BEAS-2B cells were seeded in a 6-well plate at a density of $0.7x10^6$ cells/ml and incubated for 24 hr at 37 °C. Thereafter, cells were either left uninfected or infected with *B. pertussis* (MOI of 200) and each sample lysed in 100 µl H.S. buffer for 20 min on ice. Cell debris was removed by centrifugation with the remaining whole cell lysates mixed with 30 µl 5x Laemmli loading buffer and boiled for 10 min. Proteins were separated by SDS-PAGE and subjected to immunoblot analysis using anti-PPP1Cα and anti-β-Actin antibodies. Results represent two independent experiments. (C) BEAS-2B cells were plated at a density of $0.7x10^6$ cells/ml in a six-well plate and incubated for 24 hr at 37 °C. Individual wells were then either left unstimulated or stimulated with *B. pertussis* (MOI of 200) for the timepoints indicated. Cells were then harvested, total RNA isolated and from this, cDNA was synthesised. The cDNA was then used as a template for qRT-PCR using forward and reverse primers specific to human *ppp1cα* and *gapdh* (housekeeping gene). * $p<0.05$, ** $p<0.01$ and *** $p<0.001$. Graph is representative of four independent experiments.

4.2.8 2D-DIGE Protein Hit Verification: Triosephosphate Isomerase

Triose phosphate isomerase (TPI) is a dimeric enzyme consisting of two identical subunits of critical importance to the glycolytic pathway. Its specific role is in the interconversion of two triose phosphate isomers, dihydroxyacetone phosphate and D-glyceraldehyde-3-phosphate, which are intermediates in both the glycolytic and pentose phosphate pathways [259]. Humans born with mutations in TPI suffer from multiple pathologies including anaemia, cardiomyopathy, neuromuscular impairment, increased susceptibility to infection and is in most cases fatal by early childhood [342]. With its role exclusively related to metabolism, TPI has no direct documented role in the immune response however absence of evidence is not evidence of absence. Indeed the role of metabolism and metabolites in the inflammatory conditions is fast becoming vogue [343]. The initiation and maintenance of an inflammatory response requires intensive energy usage by the cells involved and similarities have been observed between the increased metabolism exhibited by tumour cells to that of activated T cells [344]. Moreover, it has recently been shown that succinate, an intermediate in the citric acid cycle (which itself requires pyruvate derived from glycolysis) has been shown to be an inflammatory signal which drives LPS mediates IL-1β production in macrophages [345].

TPI was found to by 2D-DIGE to be upregulated 4.4 fold in response to *B. pertussis* infection (Figure 4.9A, Table 4.1). This result was verified by western blot using an anti-triosephosphate isomerase antibody. TPI levels were increased at 15 min post infection, peaking at 2 hr before decreasing slightly by 12 hr (Figure 4.9B). Comparison of TPI mRNA in uninfected and infected cells indicated no significant increase between the two states (Figure 4.9C). This suggests that TPI's levels are being modified post-transcriptionally. The exceptionally high fold change in TPI upon *B. pertussis* infection indicates that metabolism within the cell is increases upon infection.

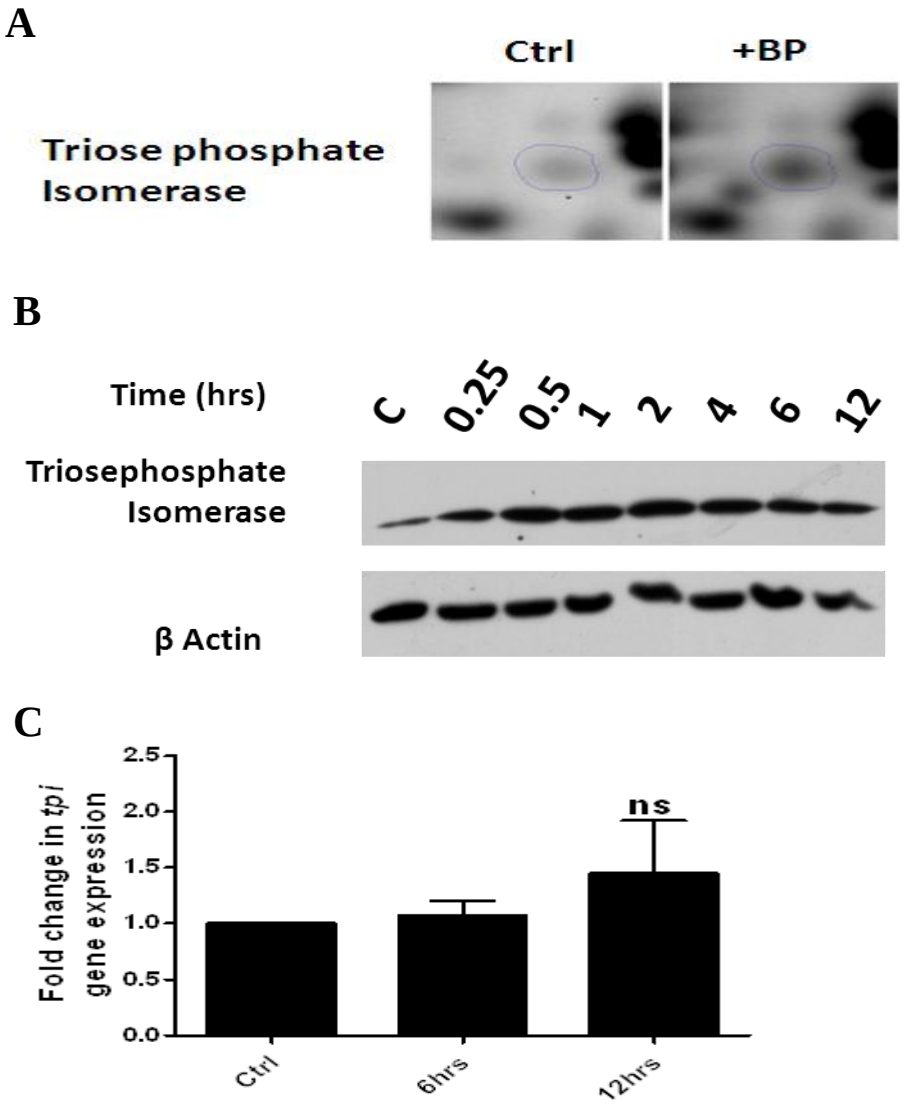

Figure 4.9: Verification of TPI upregulation in response to *B. pertussis*. (A) Screen grab of Progenesis analysis showing TPI presence on 2D-DIGE gel from control (Ctrl) and *B. pertussis* infected (BP) lysates. (B) BEAS-2B cells were seeded in a 6-well plate at a density of $0.7x10^6$ cells/ml and incubated for 24 hr at 37 °C. Thereafter, cells were either left uninfected or infected with *B. pertussis* (MOI of 200) for 15 min, 30 min, 60 min, 2 hr, 4 hr, 6 hr and 12 hr. Cells were then harvested and each sample lysed in 100 µl H.S. buffer for 20 min on ice. Cell debris was removed by centrifugation with the remaining whole cell lysates mixed with 30 µl 5x Laemmli loading buffer and boiled for 10 min. Proteins were separated by SDS-PAGE and subjected to immunoblot analysis using anti-TPI and anti-β-Actin antibodies. Results represent two independent experiments. (C) BEAS-2B cells were plated at a density of $0.7x10^6$ cells/ml in a six-well plate and incubated for 24 hr at 37 °C. Individual wells were then either left unstimulated or stimulated with *B. pertussis* (MOI of 200) for the timepoints indicated. Cells were then harvested, total RNA isolated and from this, cDNA was synthesised. The cDNA was then used as a template for qRT-PCR using forward and reverse primers specific to human *tpi* and *gapdh* (housekeeping gene). * $p<0.05$, ** $p<0.01$ and *** $p<0.001$. NS, not significant. Graph is representative of four independent experiments.

4.2.9 2D-DIGE Protein Hit Verification: NLRP12

NACHT, LRR and PYD domains-containing protein 12 (NLRP12), is a member of the nucleotide oligomerisation and binding domain (NOD)-like receptor (NLR) family of proteins. This family contains more than 20 members and are a relatively recent addition to the cadre of innate PRRs, playing critical roles in the recognition of many infectious pathogens including fungi, bacteria, viruses, protists and helminthes [346-351]. During an infection, NLRs oligomerise into multiprotein complexes termed inflammasomes that cleave pro-caspase-1 into its active form. Active caspase-1 in turn cleaves pro-IL1-β, pro-IL-18 and pro-IL-33 to generate mature proteins which are then secreted to mediate their downstream inflammatory effects (Figure 4.12) [352].

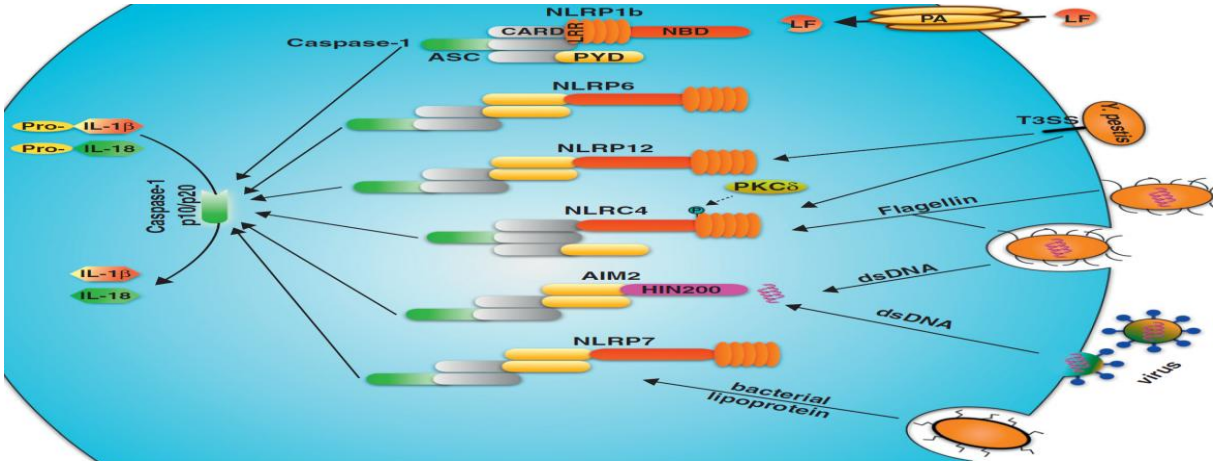

Figure 4.10: Overview of non-NLRP3 inflammasome signalling. NLRP4, 6, 7 and 12 share a C-terminal leucine rich repeat (LRR) region an internal nucleotide-binding-domain (NBD) and an N-terminal PYD. AIM2 has a HIN200 DNA binding domain and a PYD but no NBD. The NLR recruits the adaptor ASC, a PYD domain containing protein and a caspase recruitment and activation domain (CARD) which bridges the NLR with caspase-1. Caspase-1 cleaves pro-IL-1β and pro-IL-18 into their mature, secretory forms. Adapted from [352].

In general, inflammosome forming NLRs exhibit the same structural features. NLRP12, along with NLRP3, NLRP6 and NLRP7 all share a C-terminal LRR region, an internal nucleotide-binding-domain (NBD) and an N-terminal Pyrin domain (PYD). The NLR recruits the adaptor ASC, a PYD domain containing protein and a caspase recruitment and activation domain (CARD) which links the NLR to caspase-1 (Figure 4.10) [352].

NLRP12 was originally shown to play a pro-inflammatory role by driving NFκB induction as well as caspase-1 mediated cleavage and secretion of IL-1β in vitro [353]. A later in vivo study largely agreed with this showing that NLRP12 was required to drive IL-1β and IL-18 production following murine infection with the gram negative bacterium *Yersina pestis*, the causative agent of plague. However, the authors detected minimal NLRP12 mediated NFκB activity [280]. On the other hand, two recent studies presented in-vivo evidence that NLRP12 negatively regulates inflammatory processes relating to colon inflammation and tumorigenesis by specifically inhibiting activation of NFκB [354, 355]. It is worth noting that similar conflicting reports have emerged regarding NLRP6 [356, 357] such that it has been proposed that individual NLRs can play different roles in different infections, the phenotype perhaps depending upon their levels of expression and functionality in the tissues and cells that undergo pathology relating to a particular disease [352].

NLRP12 was identified as being upregulated 1.3 fold in BEAS-2B cells in response to *B. pertussis* infection (Figure 4.11A) (Table 4.1). This result was verified by immunobloting for endogenous NLRP12 where its levels were again found to be increased at multiple timepoints in repose to *B. pertussis* infection (Figure 4.11B). A slight increase was found in levels of NLRP12 mRNA at 12 hr post infection however this increase was not found to be significant (Figure 4.11C).

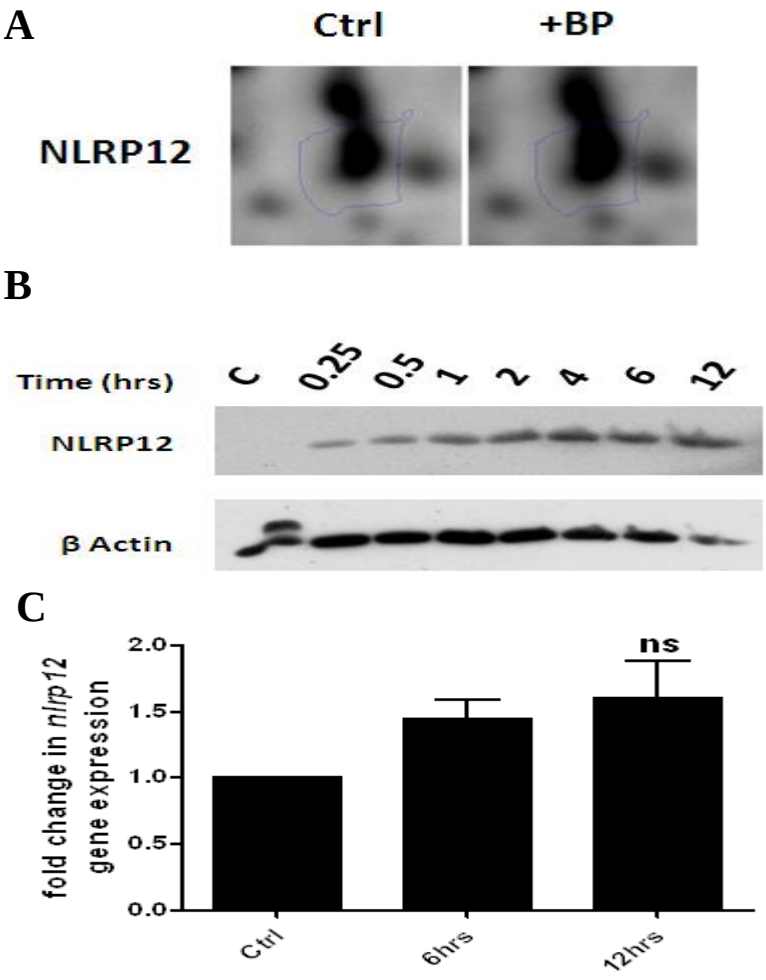

Figure 4.11: Verification of NLRP12 upregulation in response to *B. pertussis*. (A) Screen grab of Progenesis analysis showing NLRP12 presence on 2D-DIGE gel from control (Ctrl) and *B. pertussis* infected (BP) lysates. (B) BEAS-2B cells were seeded in a 6-well plate at a density of $0.7x10^6$ cells/ml and incubated for 24 hr at 37 °C. Thereafter, cells were either left uninfected or infected with *B. pertussis* (MOI of 200) for 15 min, 30 min, 60 min, 2 hr, 4 hr, 6 hr and 12 hr. Cells were then harvested and each sample lysed in 100 µl H.S. buffer for 20 min on ice. Cell debris was removed by centrifugation with the remaining whole cell lysates mixed with 30 µl 5x Laemmli loading buffer and boiled for 10 min. Proteins were separated by SDS-PAGE and subjected to immunoblot analysis using anti-NLRP12 and anti-β-Actin antibodies. Results represent two independent experiments. (C) BEAS-2B cells were plated at a density of $0.7x10^6$ cells/ml in a six-well plate and incubated for 24 hr at 37 °C. Individual wells were then either left unstimulated or stimulated with *B. pertussis* (MOI of 200) for the timepoints indicated. Cells were then harvested, total RNA isolated and from this, cDNA was synthesised. The cDNA was then used as a template for qRT-PCR using forward and reverse primers specific to human *nlrp12* and *gapdh* (housekeeping gene). * $p<0.05$, ** $p<0.01$ and *** $p<0.001$. NS, not significant. Graph is representative of four independent experiments.

4.2.10 Proteomic response to *B. pertussis* infection – common trends and functional annotation of protein hits obtained by LFQ MS

2D-DIGE is based upon the quantitative labelling of proteins within a gel matrix, followed by protein excision, digestion and MS identification. As previously discussed however, this method has drawbacks such as the masking of low abundance proteins by high abundant ones and a low throughput. LFQ MS, as previously discussed, does not suffer from either of these drawbacks and may therefore be capable of identifying expression changes in low abundant proteins that were missed by 2D-DIGE analysis. Thus the same whole cell lysates from uninfected and *B. pertussis* infected BEAS-2B cells that were used for 2D-DIGE analysis were also used for LFQ MS.

As with the 2D-DIGE study, protein hits that were significantly up or down regulated in response to *B. pertussis* infection, as identified LFQ MS were categorised first based on a broad generalisation of their biological role (Figure 4.12). Again, a protein was considered to be a true hit when it fulfilled certain statistical criteria. Protein intensities were normalized across all runs (N=4 for control and infected) and the resulting 'LFQ intensities' were grouped based on treatment and an ANOVA test performed to identify statistically significant variation in protein intensity between all control and infected samples. Proteins that were completely lacking from one treatment but present in the other were determined manually. Statistics could not be performed on these proteins as one treatment set had no intensity values. Therefore, LFQ intensities and ANOVA values for these proteins are presented as NaN (Section 2.4.6 and Appendix Table A1.2).

Proteome analysis by LFQ MS found a total of 60 protein hits that were significantly up or down regulated in response to *B. pertussis* infection. Of these, 29 proteins, or 48 % of the total were found to be upregulated and 31 proteins, or 52 % of the total were downregulated (Figure 4.13A,B), Table 4.2). The protein hits were grouped into the same seven general functional categories as the proteins identified by 2D-DIGE (Figure 4.12A,B). There were

some protein functionalities differentially represented with LFQ MS than with 2D DIGE. LFQ MS identified more proteins involved in transcription/DNA synthesis and trafficking than 2D DIGE. LFQ MS also identified fewer proteins involved in maintaining structural integrity and those involved in protein synthesis and redox reactions compared to 2D-DIGE (Figure 4.12A,B). Furthermore, there was a notable difference in the number of proteins identified as being significantly up or down regulated with an almost even split in the LFQ analysis compared to 2D-DIGE where the vast majority were upregulated (Figure 4.13A,B). Differences between the two methods were expected to a certain extent and indeed have been demonstrated previously in a similar study which compared 2D gel electrophoresis with an LFQ analysis [358]. Surprisingly, there was very little overlap between the two techniques in terms of actual proteins identified with only two proteins identified using both techniques despite samples for both coming from the same whole cell lysates (4.13A,B) (Table 4.2).

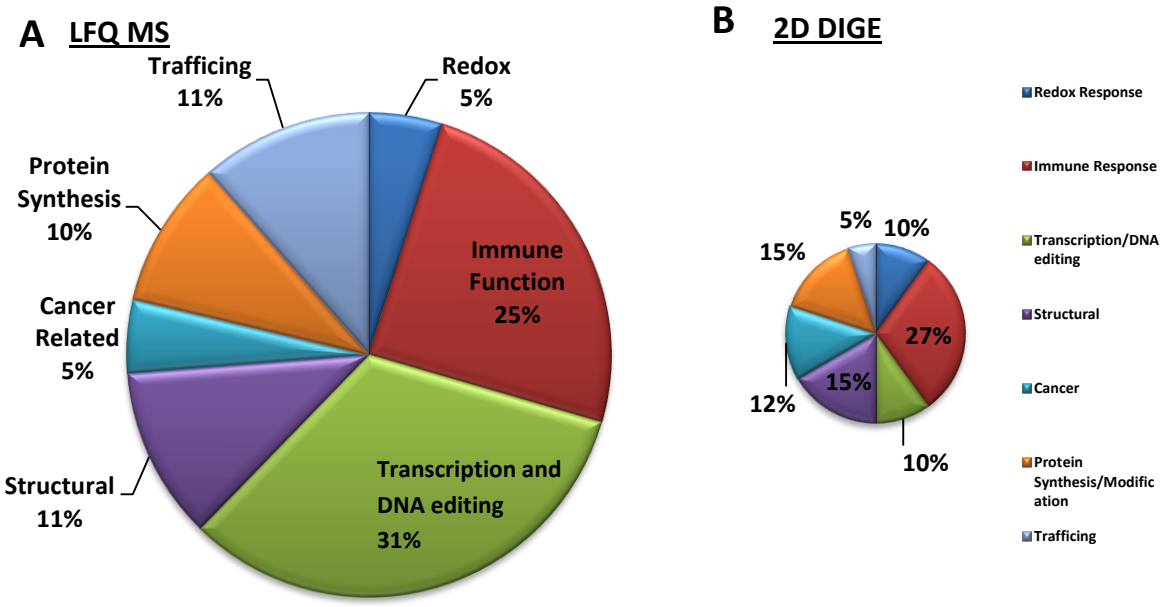

Figure 4.12: Pie chart representation and comparison of proteins identified by LFQ and 2D-DIGE in response to *B. pertussis* infection. (A) LFQ identified proteins were manually researched for functional properties and assigned functions(s) to form the basis of categorisation. Total numbers of proteins assigned to each function were inputted into a pie chart for appropriate visualisation. (B) 2D-DIGE identified proteins from Figure 2 for comparative purposes

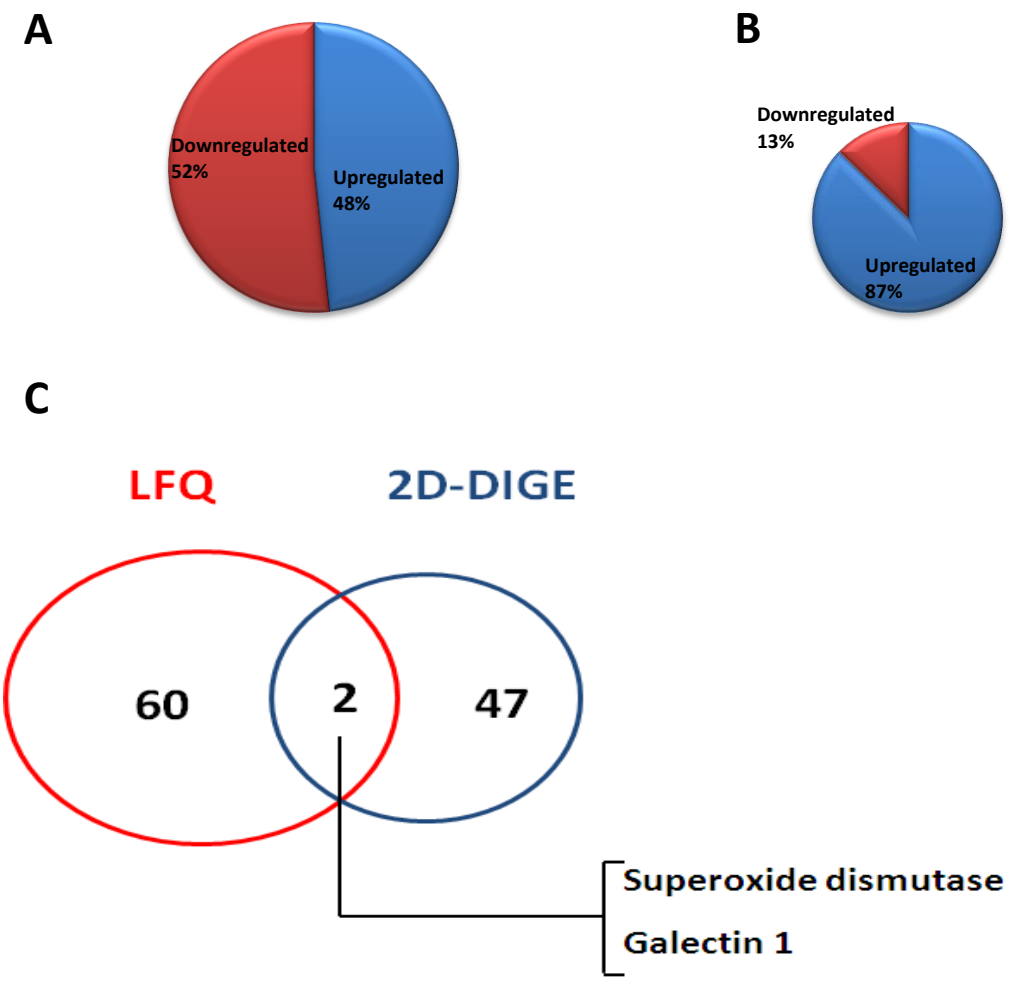

Figure 4.13: Pie chart representation and comparison of proteins identified by LFQ in response to *B. pertussis* infection. (A) Total number of LFQ derived protein hits that were adjudged to be up or down regulated via MaxQuant was inputted into a pie chart in order to visualise the divide. (B) Total number of 2D-DIGE derived up and downregulated proteins adapted from Figure 2 for comparative purposes. (C) Venn diagram illustrating the total number of protein hits identified by LFQ (red circle) and 2D-DIGE (blue circle) with the number of identical hits detected by both methods in the centre. Identical hits are annotated.

Protein hits obtained by LFQ MS

Fold Ch.	Protein Name	Function
BP+	Elongation Factor gamma	Delivers tRNA's to ribosome. Aids replication of VSV [359].
BP+	Sodium/potassium-transporting ATPase	Ion transporter across plasma membrane [360].
BP+	Adenylyl cyclase-associated protein 1	Regulation of actin cytoskeleton, cell adhesion and motility [361].
BP+	Exportin-2	Transports proteins out of nucleus into cytoplasm [362].
BP+	Pre mRNA slicing factor SYF2	Involved in DNA damage response and cell cycle [363].
BP+	60S ribosomal protein L9	Ribosomal subunit. Involved in protein synthesis [364].
BP+	Pre-rRNA-processing protein TSR2	Inhibits transcriptional activity of NFκB [365].
BP+	Glucose-6-phosphate 1-dehydrogenase	Metabolism. Involved in pentose phosphate pathway. Maintains levels of NADPH [366].
BP+	Caspase-7	Critical role in apoptosis [298].
BP+	B-cell receptor-associated protein 31	Possible role in caspase 8 mediated apoptosis [367]. Protein transporter [368].
BP+	Small kinetochore-associated protein	Mitosis. Essential component of mitotic spindle [369].
BP+	DNA-dependent protein kinase	Serine/Threonine protein kinases. Important in DNA recombination [370].
BP+	Laminin subunit gamma-1	Major functional component of basement membranes [371].
BP+	60S ribosomal protein L7a	Ribosomal subunit. Involved in protein synthesis [295]
BP+	60S ribosomal protein L17	Ribosomal subunit. Involved in protein synthesis [295]
BP+	Ribosome-binding protein p34 (p34)	Contains leucine rich repeat domain. Localises to endosome [372].
BP+	RACK1	Protein transporter and anchor. Interacts with 14-3-3ζ a known TLR mediator [373].
BP-	RNA-binding protein 4	Mediates RNA functions such as alternative splicing and translation regulation [374].
BP-	Protein S100-A13	Exports certain proteins with no signal peptide for example IL-1α [375].

Table 4.2: Proteins identified by LFQ MS showing changes in expression in response to *B. pertussis* Infection. Protein function is also indicated. BP+ indicates proteins detected in *B. pertussis* infected samples but not in uninfected samples. BP- indicated proteins detected in uninfected samples but not in *B. pertussis* infected samples. Full annotation of protein hits can be found in appendix table A1.2.

Protein hits obtained by LFQ MS

Fold Ch.	Protein Name	Function
BP-	NUDT15	Helps to prevent mutations in DNA, possibly by degrading oxygen radicals [376].
BP-	Upstream stimulatory factor 2	Transcription factor. Binding site on HLA locus [377, 378].
BP-	Nck-1	Adaptor protein. Regulates activation of downstream mediators [379].
BP-	BRO1 domain-containing protein BROX	Aid formation of intraluminal vesicle formation. Also required for virus budding [380].
BP-	E3 ubiquitin-protein ligase RNF181	Targets proteins for proteosomal degradation. Inhibits ERK/MAPK pathway [381].
BP-	Caspase activity and apoptosis inhibitor 1	Anti-apoptotic via caspase 3, 9 and 10 [382].
BP-	RNA polymerase-associated protein RTF1	Involved in transcription [383].
BP-	Kanadaptin	Function unknown. Human form localized predominantly to nucleus [384].
BP-	Cx9C motif-containing protein 4	Localises to mitochondria [385].
↓0.64	RNA-binding protein 8A	Component of exon splicing junction complex [386].
↓0.75	Serine/arginine-rich splicing factor 2	Pre mRNA splicing [387].
↑0.85	Putative RNA-binding protein Luc7-like 2	Function unknown. May bind to RNA (Uniprot).
↓1.23	UV excision repair protein RAD23	Negatively regulates RIG-I and MDA5 by ubquitination [388].
↑3.87	Intercellular adhesion molecule 1	Induced by *B. pertussis* [136]. Receptor for leukocytes to migrate into tissue [389].
↓0.88	Serine/arginine-rich splicing factor 6	Involved in pre-mRNA splicing and RNA metabolism [390].
↓0.59	Calponin-2	Inactivated by Wnt signalling [391]. Regulates macrophage phagocytosis [392].
↑1.53	Uncharacterized protein C14orf119	Function unknown
↓0.64	SNX15	Links clathrin vesicles to early endosomes [393]
↓1.21	U4/U6.U5 Nuclear ribonucleoprotein	Pre mRNA splicing [394].

Table 4.2 (contd): Proteins identified by LFQ MS showing changes in expression in response to *B. pertussis* Infection. Protein function is also indicated. BP+ indicates proteins detected in *B. pertussis* infected samples but not in uninfected samples. BP- indicated proteins detected in uninfected samples but not in *B. pertussis* infected samples. Full annotation of protein hits can be found in appendix table A1.2.

Protein hits obtained by LFQ MS

Fold Ch.	Protein Name	Function
↓2.38	SH3-containing Grb-2-like 1 protein	Function unknown. May be similar to GRB2 [395].
↓1.19	Calreticulin / ER resident protein 60	Pro-phagocytic signal on cancer cell surface [396]. Found in NK & T cell granules [397]
↑4.13	Superoxide dismutase	Redox Signalling. Indirect NFκB modulator [398].
↓0.77	Zinc finger Ran-binding domain protein 2	Role in alternative splicing [399].
↑1.73	Tenascin	Associated with tissue injury and inflammation. Endogenous TLR4 activator [400].
↑1.23	U6 snRNA-associated Sm-like protein	Pre mRNA splicing [401].
↓1.73	RNA-binding protein - serine rich domain	Pre mRNA splicing [402].
↓0.84	Coiled-coil domain-containing protein 97	Function unknown
↑0.87	40S ribosomal protein S29	Component of 40S ribosome subunit. Involved in protein synthesis [295].
↑0.67	Galectin-1	Inhibits macrophage migration and pathogen killing. Overexpressed in tumours [294].
↓0.97	N-alpha-acetyltransferase 38	Spliceosome component (Uniprot).
↓1.14	Cdc42 effector protein 3	Involved in maintenance of actin cytoskeleton [403].
↑1.00	TSC22 domain family protein 1	Transcriptional repressor activity [404]. Implicated in tumourgenesis [405].
↓0.64	Protein TSSC4	Function unknown.
↓2.11	Serine/arginine repetitive matrix protein 1	Involved in pre-mRNA processing [406].
↑3.02	Ferritin	Critical in iron storage. Upregulated during inflammatory processes [407].
↑1.06	Periphilin-1	Suspected role in Parkinson's Disease [408]. Involved in cell cycle progression [409].
↓0.89	Transcription elongation factor A	May be involved in transcription (Uniprot).
↑3.64	Ferritin heavy chain	Component of ferritin. Upregulated during inflammatory processes [407].

Table 4.2 (contd): Proteins identified by LFQ MS showing changes in expression in response to *B. pertussis* Infection. Protein function is also indicated. BP+ indicates proteins detected in *B. pertussis* infected samples but not in uninfected samples. BP- indicated proteins detected in uninfected samples but not in *B. pertussis* infected samples. Full annotation of protein hits can be found in appendix table A1.2.

Protein hits obtained by LFQ MS

Fold Ch.	Protein Name	Function
↓0.91	Transcription elongation factor A	Necessary for efficient RNA polymerase II transcription [410].
↓2.01	Serine/arginine repetitive matrix protein 2	Involved in pre-mRNA splicing [411].
↓0.68	Suppressor of G2 allele of SKP1 homolog	May have role in ubquitination [412]. Nuclear translocation upon heat shock [413].

Table 4.2 (contd): Proteins identified by LFQ MS showing changes in expression in response to *B. pertussis* Infection. Protein function is also indicated. BP+ indicates proteins detected in *B. pertussis* infected samples but not in uninfected samples. BP- indicated proteins detected in uninfected samples but not in *B. pertussis* infected samples. Full annotation of protein hits can be found in appendix table A1.2.

4.2.11 Verification of LFQ MS derived protein hits from *B. pertussis* infection.

Two hits were selected for verification by immunoblotting. These were superoxide dismutase (SOD) and ferritin. SOD was selected because it was one of two proteins that appeared in both the 2D-DIGE with MS and the LFQ MS studies and also because SODs play important roles in innate immunity (Table 4.2). Ferritin was selected due to its critical role in iron storage which is important for host metabolism. It is also known to be upregulated during inflammatory processes (Table 4.2).

4.2.12 Verification of LFQ MS protein hit: Superoxide Dismutase

SODs play a key role in metabolising O_2 radicals thus pre-empting the formation of damaging reactive oxygen reactive species (ROS) such as hypochlorite, peroxynitrate and hydrogen peroxide [398]. High levels of these ROS lead to oxidative stress which is implicated in may cardiovascular diseases. However, low levels are important in innate immune defences as well as general cell signalling [414]. Although the term superoxide dismutase denotes three independent enzymes (SOD1, SOD2 and SOD3), at the core of each is the ability to convert two molecules of superoxide into dioxegen (O_2) and hydrogen peroxide. The difference between the three SODs resides both in their fold and in the different metal ion(s) in their active site. SOD1 can bind copper and zinc ions, SOD2 contains an manganese ion while SOD3 also binds copper and zinc ions [269]. SOD1 is the major intracellular SOD. It exists as a 32kDa homodimer mainly in the cytosol, with smaller fractions residing within the nucleus, lysosomes, peroxisomes and intermembrane space of mitochondria [398].

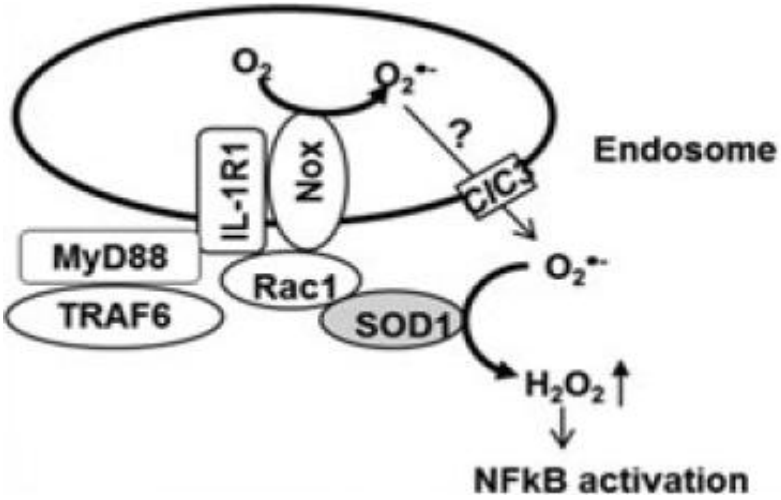

Fig 4.14: Role of SOD1 in NFκB activation. During redox signalling, SOD1 is recruited to the endosomal surface where it indirectly regulates Nox2 mediated O_2 radical formation. O_2 radicals exit via chloride channels (CIC3) whereupon they are dismutated by SOD1to produce hydrogen peroxide and promoting redox activation of NFκB. Adapted from [398].

SOD1's role in redox signalling is well documented with the dismutation of O_2 radicals produced following IL-1 signalling, producing hydrogen peroxide which goes on to activate and modulate the NFκB pathway [398, 415]. SOD2 is an exclusively mitochondrial enzyme utilising a manganese ion. Its function is identical to that of SOD1 (and SOD3) in that it too facilitates the dismutation of O_2 radicals to oxygen and hydrogen peroxide [398].

SOD1 was found to be upregulated in response to *B. pertussis* infection, as detected by LFQ MS (Figure 4.15A). This was verified by immunoblotting for SOD1 in whole cell lysates infected with *B. pertussis* for various timepoints. SOD1's expression was increased at one hour post infection and remained so up to 12 hr (Figure 4.15B). Expression of SOD1 mRNA was not found to be significantly upregulated at 6 or 12 hr post infection (Figure 4.15C) indicating that its expression in response to *B. pertussis* is governed by post-transcriptional processes.

A

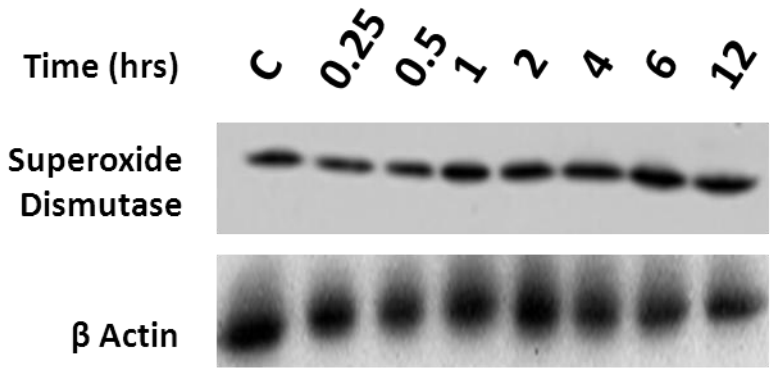

B

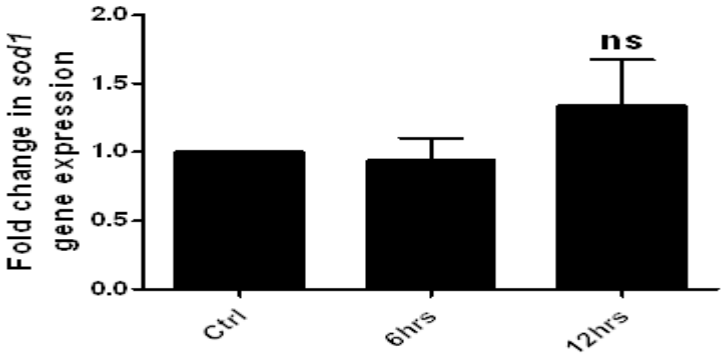

Figure 4.15: Verification of SOD1 upregulation in response to *B. pertussis*. (A) BEAS-2B cells were seeded in a 6-well plate at a density of $0.7x10^6$ cells/ml and incubated for 24 hr at 37 °C. Thereafter, cells were either left uninfected or infected with *B. pertussis* (MOI of 200) for 15 min, 30 min, 60 min, 2 hr, 4 hr, 6 hr and 12 hr. Cells were then harvested and each sample lysed in 100 µl H.S. buffer for 20 min on ice. Cell debris was removed by centrifugation with the remaining whole cell lysates mixed with 30 µl 5x Laemmli loading buffer and boiled for 10 min. Proteins were separated by SDS-PAGE and subjected to immunoblot analysis using anti-SOD1 and anti-β-Actin antibodies. Results represent two independent experiments. (B) BEAS-2B cells were plated at a density of $0.7x10^6$ cells/ml in a six-well plate and incubated for 24 hr at 37 °C. Individual wells were then either left unstimulated or stimulated with *B. pertussis* (MOI of 200) for the timepoints indicated. Cells were then harvested, total RNA isolated and from this, cDNA was synthesised. The cDNA was then used as a template for qRT-PCR using forward and reverse primers specific to human *nlrp12* and *gapdh* (housekeeping gene). * $p<0.05$, ** $p<0.01$ and *** $p<0.001$. NS, not significant. Graph is representative of four independent experiments.

4.2.13 Verification of LFQ MS protein hit: Ferritin

Ferritin is a hollow, spherical and mainly cytosolic protein consisting of 24 subunits whose main function is the periodic sequesterisation and release of intracellular iron (Fe). Ferritin can store up to 4,500 iron atoms within its core with multiple mechanisms regulating its storage and release – mainly determined by the current status of the iron labile pool (free iron available within the cell) at any given time [416]. In addition to iron storage and release, ferritin has enzymatic properties converting Fe(II) to Fe(III) [417]. Iron in the cell has many critical roles. For example, iron in heme is essential for oxygen transport around – essential for survival. It is also an essential component of many enzymes involved in the cell cycle and electron transport. Fe (III) is involved in the generation of the potentially toxic superoxide radical which can damage DNA, lipids and proteins [407]. For these reasons, iron levels are highly regulated with ferritin playing a key role in the buffering of intracellular concentrations. Evidence of its innate importance is that the knocking out of the ferritin gene is embryonic lethal in mice [418]. Ferritin is known to be upregulated during inflammatory processes with the cytokines IL-1α and TNFα playing noted roles in this regard, by transcriptionally upregulating the H-chain of ferritin via NFκB binding sites on the ferritin h-chain gene (Figure 4.16) [407].

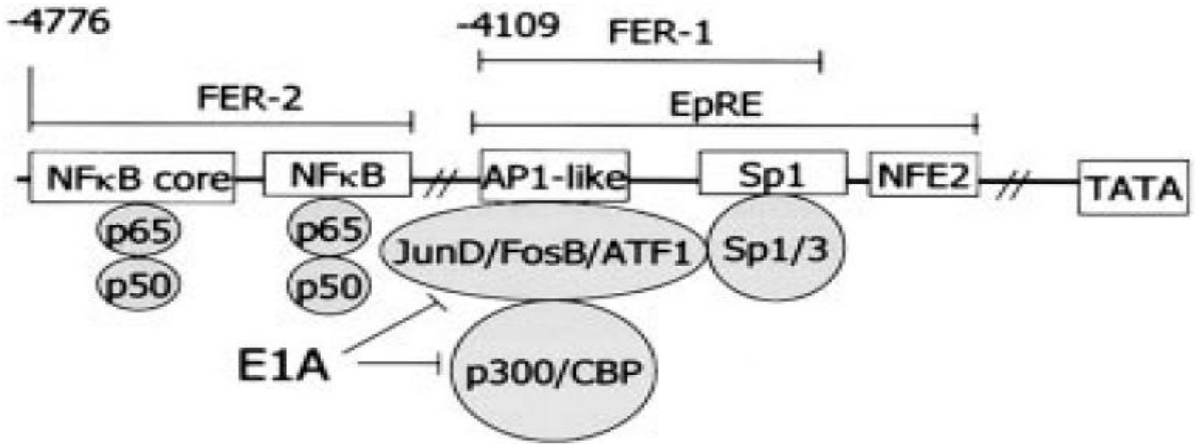

Figure 4.16: Ferritin gene promoter region. Binding sites for NFκB, AP-1 and creb binding protein (CBP) are indicated thus indicating its regulation by inflammatory processes. Adapted from [407].

The current study identified ferritin as being upregulated by LFQ MS in response to *B. pertussis* at 12 hr post infection (Table 4.2). This result was verified by western blot using antibodies specific to both the ferritin heavy chain and the ferritin light chain which indicated that the heavy chain was strongly induced at 6 hr post infection with the light chain upregulated much later at approximately 12 hr (Figure 4.17A,B). Analysis of both Ferritin LC and HC mRNA showed no such increases at either 6 or 12 hr (Figure 4.17C,D). Ferritin HC mRNA showed a slight increase at 12 hr but this approximated to 1.4 fold and was not significant (Figure 4.17C). As Ferritin HC has been shown to be upregulated transcriptionally by both TNF and IL-1 signalling, this would suggest that there are other factors at play in upregulating its expression. LPS for example, when administered endotracheally to rats, had been shown to induce ferritin protein but not mRNA [419]. With *B. pertussis* being a gram negative, LPS containing bacterium, this is one possible mechanism by which ferritin is being induced.

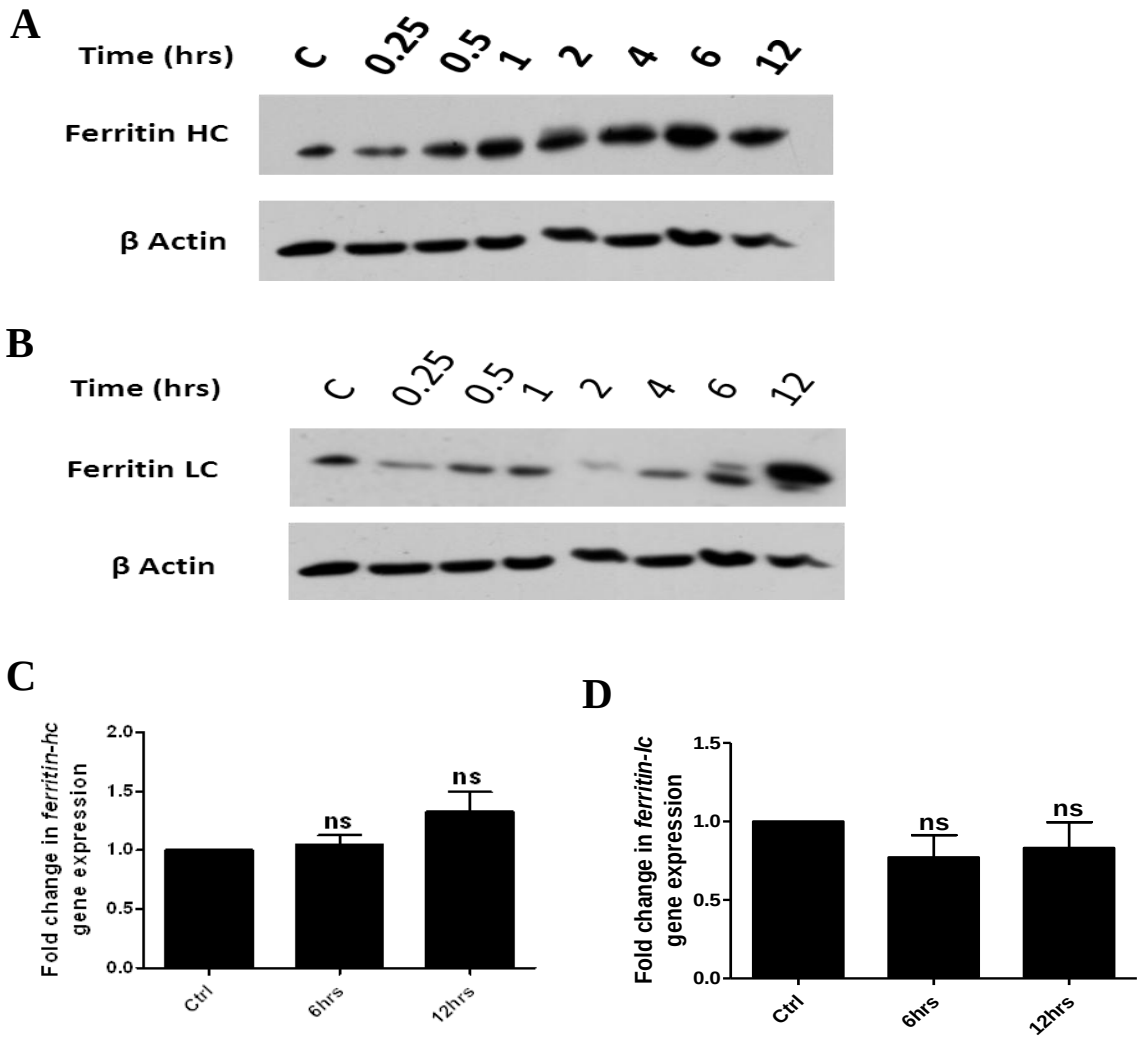

Figure 4.17: Verification of Ferritin upregulation in response to *B. pertussis*. (A and B) BEAS-2B cells were seeded in a 6-well plate at a density of $0.7x10^6$ cells/ml and incubated for 24 hr at 37 °C. Thereafter, cells were either left uninfected or infected with *B. pertussis* (MOI of 200) for 15 min, 30 min, 60 min, 2 hr, 4 hr, 6 hr and 12 hr. Cells were then harvested and each sample lysed in 100 µl H.S. buffer for 20 min on ice. Cell debris was removed by centrifugation with the remaining whole cell lysates mixed with 30 µl 5x Laemmli loading buffer and boiled for 10 min. Proteins were separated by SDS-PAGE and subjected to immunoblot analysis using anti-Ferritin HC, Ferritin LC and anti-β-Actin antibodies. Results represent two independent experiments. (C and D) BEAS-2B cells were plated at a density of $0.7x10^6$ cells/ml in a six-well plate and incubated for 24 hr at 37 °C. Individual wells were then either left unstimulated or stimulated with *B. pertussis* (MOI of 200) for the timepoints indicated. Cells were then harvested, total RNA isolated and from this, cDNA was synthesised. The cDNA was then used as a template for qRT-PCR using forward and reverse primers specific to human *ferritin-lc*, *ferritin-hc* and *gapdh* (housekeeping gene). * $p<0.05$, ** $p<0.01$ and *** $p<0.001$. NS, not significant. Graph is representative of four independent experiments.

4.2.14 Selection and expression knockdown of selected protein hits

Although the identification of proteins whose expression is significantly changed due to system perturbation is often cited as implying function , a deeper analysis of these protein's physiological role is required in order to assign function with better understanding and confidence [112, 420]. With this in mind, it was decided to select a number of verified protein hits for further analysis by utilising RNA interference to knockdown their endogenous expression levels and from this, to examine if, or how, their reduced expression affected the immune response to *B. pertussis* infection. Proteins were selected for further analysis by thoroughly researching their known functionality and from here, inferring potentially unknown roles in the immune response. The proteins selected for further analysis were stathmin 1, PPP1Cα, NLRP12, GSTO1 and DJ-1. All of these proteins shared in common, functions that indicate their capability of playing roles in the innate immune response to *B. pertussis* infection.

To investigate the role played by these proteins in the response to *B. pertussis*, knockdown of their expression was performed in BEAS-2B cells using endoribonuclease-prepared siRNA (esiRNA). EsiRNA's were purchased commercially and are prepared by amplifying cDNA specific to the gene of interest followed by generation of dsRNA from the cDNA, using RNA polymerase. This dsRNA is then chopped by RNase III into a heterogeneous mixture of short, overlapping siRNA fragments all specific to the target gene that triggers highly specific and effective gene silencing [421]. To confirm knockdown of target genes, BEAS-2B cells were transfected with either an esiRNA control sequence against green fluorescent protein (eGFP) or esiRNA specific to one each of the above proteins for 24 hr after which gene expression specific to each protein was monitored by real time PCR (Figure 4.20). Sufficient knockdown of gene expression was found to occur in each of the proteins targeted by esiRNA with approximately 50 % reduction in PPP1Cα mRNA, a 40 % reduction in NLRP12 mRNA, 95 %

reduction in levels of stathmin 1 mRNA levels and a 60 % reduction DJ-1 gene expression (Figure 4.18A-D).

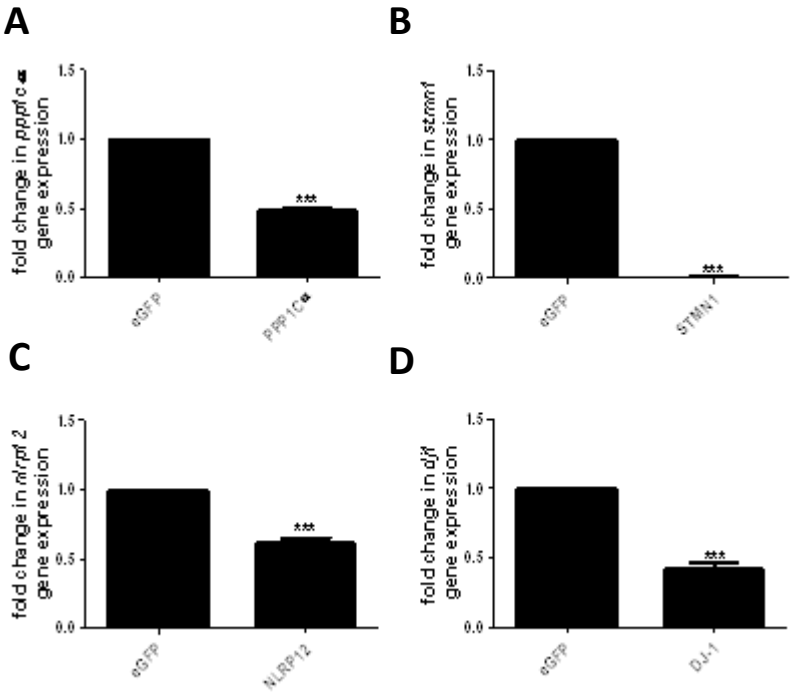

Figure 4.18: Suppression of human PPP1Cα, stathmin 1, NLRP12 and Dj-1 mRNA using RNA interference. BEAS-2B cells were seeded in a 6-well plate at a density of $0.4x10^6$ cells/ml and incubated for 24 hr at 37 °C. Cells were then transfected with either 200 ng target gene specific esiRNA or a control esiRNA (eGFP) for a further 24 hr. Cells were then harvested, total RNA isolated and from this, cDNA was synthesised. The cDNA was then used as a template for qRT-PCR using forward and reverse primers specific to human *ppp1cα* (A), *stmn1* (B), *nlrp12* (C), *dj-1*(D) and *gapdh* (housekeeping gene). * $p<0.05$, ** $p<0.01$ and *** $p<0.001$. Graphs are representative of two independent experiments.

4.2.15 Cytokine production after gene knockdown in response to *B. pertussis* and TLR4 activation

In order to ascertain if the selected protein hits could somehow affect the innate immune response of BEAS-2B cells during *B. pertussis* infection, their expression was individually supressed using esiRNA and the cells immediately infected with the bacteria as normal for 12 hr. Cell supernatants derived from infected cells were then analysed for inflammatory cytokine expression by ELISA in order to evaluate whether or not suppression of each particular protein could affect the inflammatory response. In unstimulated cells, transfection of the various esiRNAs did not drive any major production of IL-6 (Figure 4.19) thus ensuring that any effects observed upon *B. pertussis* stimulation were specific to esiRNA mediated protein supression and not to the presence of the esiRNA nucleotides themselves. Cells transfected with the negative control esiRNA, eGFP, and stimulated with *B. pertussis* for 12 hr produced large quantities of IL-6 with approximately 5000 pg/ml secreted (Figure 4.19A). However, knockdown of expression of NLRP12, PPP1Cα, DJ-1 or stathmin 1 did not significantly modulate IL-6 protein production (Figure 4.19A). *B. pertussis*, like any pathogenic organism, likely activates multiple signalling pathways during an infection process. As well as this, *B. pertussis* is known to encode multiple virulence factors some of which can modulate various immune response signalling pathways in order to preserve its presence within the host. For example, one virulence factor, adenylate cyclase toxin, can supress superoxide production and inflammatory cytokine production [422]. Another virulence factor, FHA , can inhibit IL-12 production while inducing IL-6 and IL-10 [423]. Moreover, LPS can induce IL-6, TNFα, IL-1β, IL-12 and IL-8 secretion whilst inhibiting NO production [424]. *B. pertussis* therefore employs multiple strategies to modulate the immune response and thus the lack of an observed phenotype upon suppression of multiple protein hits may be due to a lack of specificity on the part of *B. pertussis* and how it interacts with the host immune system and not necessarily due to a lack of involvement of the protein hits.

As *B. pertussis* in known to activate TLR4 amongst other PRRs [143, 425], it was next examined whether knowndown of the selected proteins could affect the immune response specific to TLR4. To this end, BEAS-2B cells were again transfected with either control esiRNA or esiRNA specific to each protein 24 hr prior to stimulation with LPS. After 24 hr stimulation, supernatants were removed and examined for secreted levels of proinflammatory cytokines IL-6 and TNFα (Figure 4.19B,C).

Transfection of cells with the various esiRNAs again had little effect on basal levels of IL-6 and TNFα (Figure 4.19B,C). Transfection with the negative control esiRNA, eGFP, and stimulation with LPS caused detectable secretion of IL-6 but not TNFα from BEAS-2B cells (Figure 4.21B,C). LPS induced IL-6 production was significantly increased upon suppression of NLRP12 thus agreeing with previous studies showing that it could exert a negative influence on inflammatory cytokine production (Figure 4.19B) [354, 355]. Suppression of DJ-1 gave rise to a slight increase in IL-6 production but this was determined to be non-significant (Figure 4.19B). Interestingly, knockdown of statmin-1 and PPP1Cα both led to a significant reduction in TLR4 mediated IL-6 production (Figure 4.19B).

Apart from the previously discussed role for stathmin 1 as an endogenous activator of TLR3 signalling [255], no other role for stathmin in mediating the innate immune response has previously been identified. Stathmin has been shown to colocalise with TLR3 in MS lesions on both the surface of astrocytes and neurons and also in intracellular vesicular structures of astrocytes and microglia [255]. This observation would suggest that stathmin is capable of localising to areas of the cell where TLRs are expressed and with TLR4 known to localise to the cell surface as well as vesicular structures within the cell, this leaves open the possibility that stathmin 1 can localise to the TLR4 signalling pathway. Stathmin 1 is also a key regulator of microtubule dynamics within the cell during lymphocyte activation [330] and as the ‘TLR4 signalosome’ is known to traffic between the plasma membrane and endosomal

compartments in a process dependent upon microtubule transport, it is conceivable that suppression of stathmin 1 is inhibiting the ability of TLR4 and/or its adaptors and interactors to localise to the signalling complex thereby reducing downstream cytokine production [84, 86].

PPP1Cα has a known role in innate signalling in that it dephosphorylates RIG-I and MDA5 to allow them to signal recognition of RNA viruses such as influenza virus, paramyxovirus, dengue virus, and picornavirus [292]. As a negative control, the authors of this study examined the role of PPP1Cα in TLR3 signalling (where it had no effect) but did not examine its role in other TLRs including TLR4. Many proteins within the TLR4 pathway are phosphorylated on either serine or threonine residues including MAL, TRAM, IRAK4, STAT1, IRF3, IRF7 and IκB kinase β (IKKβ) [15, 57, 83, 426-428]. However, as PPP1Cα is a phosphatase, it would be expected that suppression on PPP1Cα would lead to increased phosphorylation. Knockdown of PPP1Cα led to a decrease in inflammatory cytokine production (Figure 4.19B) and so it would also be expected that PPP1Cα is acting on a protein which requires dephosphorylation for its activity, similar to RIG-I and MDA5. Proteins that are dephosphorylated to aid relay of TLR4 signal include eukaryotic initiation factor 2B and heat shock protein 27 (Hsp27) [429, 430]. It is possible that PPP1Cα acts on these molecules in order to drive TLR4 signalling.

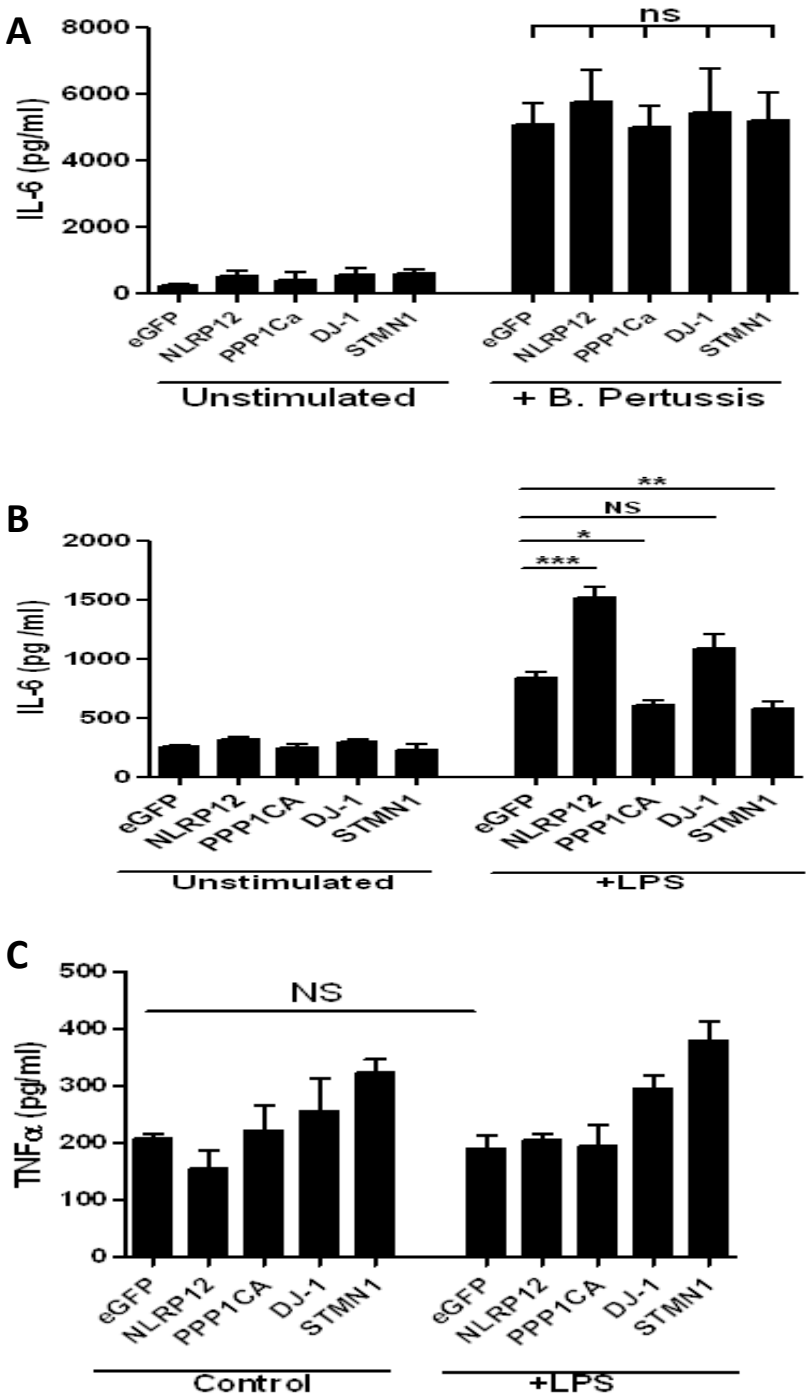

Figure 4.19: *B. pertussis* and LPS meditated inflammatory response upon suppression of human PPP1Cα, stathmin 1, NLRP12 and Dj-1. BEAS-2B cells were seeded in a 6-well plate at a density of $0.4x10^6$cells/ml and incubated for 24 hr at 37 °C. Cells were then transfected with either 200ng target gene specific esiRNA or a control esiRNA (eGFP) for 24 hr. At this point, medium was removed and fresh medium added. After 2 hr, cells were either left unstimulated or stimulated with either *B. pertussis* (400 bacteria/cell) or LPS (500ng/ml) for a further 12 and 24 hr respectively. Cell free supernatants were then harvested and analysed for the presence of (A) *B. pertussis* mediated IL-6 (N=5) and (B, C) LPS mediated IL-6 and TNFα by ELISA (N=3). * $p<0.05$, ** $p<0.01$ and *** $p<0.001$. NS, not significant.

4.2.16 Examination of stathmin 1's and PPP1Cα's ability to drive NFκB/AP-1 activation

Due to the observed reduction of TLR4 mediated IL-6 production upon suppression of stathmin 1 and PPP1Cα, it was hypothesised that their signalling could in some way drive activation of the transcription factors NFκB and AP-1, both of which have binding sites on the IL-6 promoter sequence [431]. To investigate whether either of these proteins are capable of driving activation of these transcription factors in a TLR4 dependent manner, increasing amounts of plasmid DNA corresponding to either stathmin or PPP1Cα were expressed in HEK-Blue™-hTLR4 cells. After 24 hr, cells were stimulated with LPS for a further 24 hr after which signal activation was assayed.

Although stimulation of the cells with LPS drove activation, expression of increasing amounts of plasmid DNA corresponding to 10-80 ng of either stathmin 1 or PPP1Cα failed to increase the intensity of the LPS generated signal (Figure 4.20A,B). This could mean that additional cofactors are required for both proteins to activated TLR4 signalling that are not present in the parental HEK cell line used. Recently, stathmin was shown to be an endogenous ligand for TLR3 and this was proven using a number of methods including the use of TLR3 deficient mice and RNA interference [255]. Interestingly, TLR3 transfected HEK293 cells were unable to respond to stathmin despite responding normally to poly(I:C) leading the authors to conclude that HEK 293 cells are missing cofactors that are required for the stathmin mediated activation of TLR3 [255]. Therefore, the observed results obtained in the current study are not without precedent.

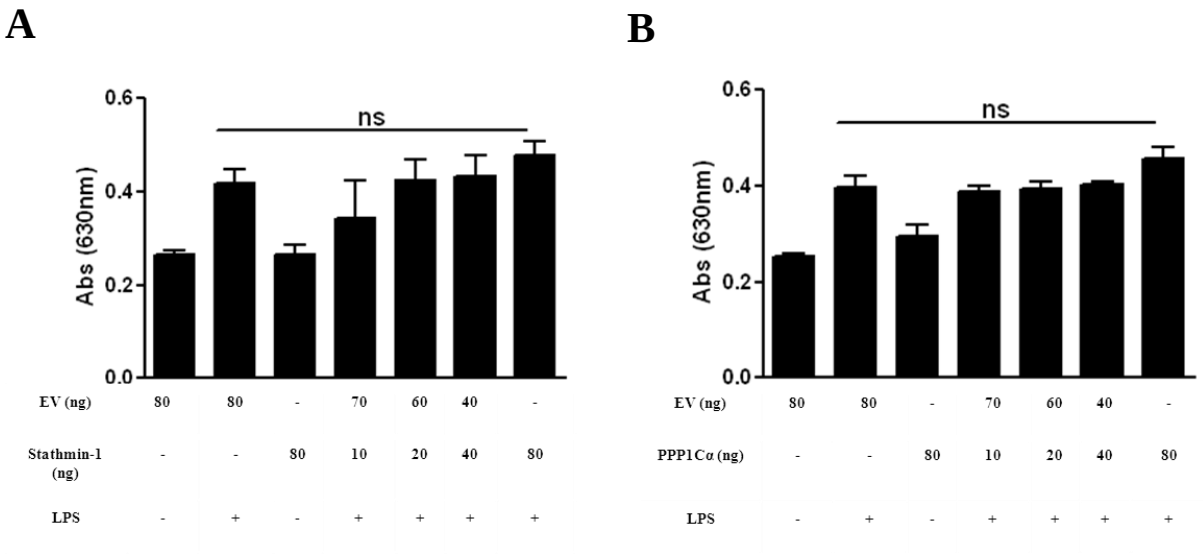

Figure 4.20: Investigation of ability of stathmin 1 and PPP1Cα to independently drive NFκB and AP-1 signalling. A, HEK-Blue™-hTLR4 cells were plated at a density of 25,000 cells/well in a 96-well plates and incubated at 37 °C for 24 hr. Cells were then transfected with either empty vector (EV) or increasing amounts of either stathmin 1 or PPP1Cα plasmid DNA as indicated and incubated for 24 hr. Cells were then stimulated with LPS (100 ng/ml) for a further 24 hr followed addition of 20 µl of supernatant from each well to 180 µl/well of prewarmed Quanti-Blue detection medium. Colour changes were measured by spectrometry reading at a wavelength of 630 nm. Results are representative of two independent experiments. NS, not significant.

4.3 Discussion

The current study was conceived around the need to better characterise the physiological response to *B. pertussis* - a human pathogen that despite a widely available vaccine with high uptake has seen the recent doubling of reported cases in western countries. Taking Ireland as an example, in 2012, 444 cases were reported. This was double the number of cases reported in 2011 which itself was double the number of cases reported in 2010 [432]. Of the reported 2012 cases, 30 % required hospitilisation and two were fatal [432]. Similar figures have been noted in the UK also [433]. The ability to improve the *B. pertussis* vaccine in order to increase the longevity and strength of its protection from the earliest point in life is the ultimate aim but to do this, a better understanding of both vaccine development and also *B. pertussis* infection is required [139].

To this end, it was decided to characterise changes induced in the proteome of a human lung epithelial cell line upon infection with *B. pertussis* with the aim of cataloguing the proteins induced or repressed during infection which may ultimately play a role in its pathogenesis. Two separate proteomic techniques were used in this regard namely 2D-DIGE with LC-MS and LFQ MS. One of the most striking initial observations from the two studies was the lack of overlap in identified propteins between 2D-DIGE and LFQ MS. Proteins identified by LFQ MS but 2D-DIGE could be due to the higher sensitivity of LFQ MS compared to the more restrictive 2D-DIGE. However, the inability of LFQ MS to identify almost any proteins identified by 2D-DIGE is puzzling. One factor could be that during the preparation of protein lysates for LFQ MS, difficulties were experienced when trying to resuspend required quantities of protein in the resuspension buffer (Section 2.3). It could be possible that only proteins exhibiting particular characteristics regarding solubility were reuspended which could have led to exclusion of others that happened not be as solubule.

Another observation was that approximately one quarter of all proteins identified by both techniques as being significantly up or down regulated in response to infection were proteins with previously known roles in the immune response but of which, critically few have been shown to play a role in the response to *B. pertussis* (Figure 4.12 and Tables 4.1, 4.2). This result in itself would suggest that there is still a large amount of work still to be done in the characterisation of the immune response to *B. pertussis* and similarily to any bacterium. Other functional areas that were well represented were transcription and DNA editing, structural proteins and those involved in protein synthesis. The involvement of transcription and translation processes would be expected as the cell gears up to respond to infection. However it is interesting to correlate this observation the real time-PCR and immunoassay vertifications of various protein hits. Of the eight hits selected for verification, four did not correlate increased protein expression with increased gene expression (Figures 4.9, 4.11, 4.15 and 4.17). This would suggest that approximately half of all protein regulation in response to *B. pertussis* is occurring at the post-transcriptional level. Post transcriptional control plays an important role in the regulation of immune effector proteins. Transcript specific regulation requires individual factors that bind to particular mRNA targets. The functional fate of a particular transcript is often defined by a myriad of RNA-binding proteins (RBPs) can stabilise mRNA transcripts and stimulate their translation or vice-versa [434]. Indeed, four separate RBPs were identified from the LFQ MS study and these, along with many other RNA modifying proteins, comprised 31 % of all proteins identified as being dynamically regulated in response to *B. pertussis* infection (Figure 4.12, Table 4.2). This would suggest that targeting the post-transcriptional regulation of immune signalling is a field with therapeutic potential. Indeed, a relatively recently characterised subset of post-transcriptional regulators, the micro-RNAs, which typically supress translation by targeting mRNA

transcripts of degradation have been identified as one such contributor to immune modulatory therapy in the future [435, 436].

Unfortunately, upon suppression of a number of selected protein hits, no striking inflammatory based phenotype was observed during *B. pertussis* infection (Figure 4.19A). As previously stated, this could be due to the myriad of documented immune modulatory mechanisms possessed by *B. pertussis* and the many concurrent detection and signalling pathways employed by humans to respond to *B. pertussis* [139]. Therefore, the suppression of one individual protein with a function in one pahtway may have no overall effect. Interestingly however, significant modulation of the inflammatory response was noted upon suppression of the selected protein's expression prior to stimulation with a purified version of a known *B. pertussis* PAMP, LPS (Figure 4.19B). Specifically, suppression of NLRP12 led to significantly increased IL-6 secretion while suppression of both the protein phosphotase PPP1Cα and the microtubule regulator stathmin 1 led to significantly decreased IL-6 production (Figure 4.19B). As LPS, through its membrane receptor TLR4, is a key sensor of gram negative bacteria and consequently a major driver of the symptoms of septic shock, a role for these two proteins in mediating this response is a tantalising possibility. They do not appear to be intrinsic activators of the transcription factors NFκB and AP-1 upon overexpression of their wild-type forms in a TLR4 dependent system however perhaps overexpression of mutant forms of the proteins could inhibit activation. Alternatively, their role in TLR4 signalling may be more abstract and require the presence of other cellular proteins not present in the HEK293 cells used.

Chapter 5

Investigations into respiratpry cell proteome changes in response to infection with the respiratory pathogen human rhinovirus 16.

5.1 Chapter Aim

The aim of this chaper was to analyse proteome modulation of a lung epithelial cell line in response to infection with the respiratory virus HRV16. This would be accomplished by 2D-DIGE combined with LC-MS. Protein hits obtained would be compared to those obtained upon infection with the same cell line with *B. pertussis*. A selection of hits would then be validated and an analysis of their role in immune signalling undertaken by supresssion their expression priot to infection with HRV16.

5.2 Results

5.2.1 Optimisation of HRV16 infection protocol

As with *B. pertussis* in Chapter 4, an infection protocol had to be designed that would drive a sufficient immune response to HRV16 infection in BEAS-2B cells. It has been shown that HRV infects cells more efficiently at temperatures below 37 °C and this has been suggested as a reason why the human nasal cavity, which is exposed and therefore cooler, serves as the primary site of natural inoculation for HRVs [162, 437]. It has also been shown that infecting cells *in vitro* with HRV is more efficient when the cell monolayer is subconfluent [437]. For these reasons, BEAS-2B cells were infected with HRV16 (MOI of 3) at an estimated 50-60% confluency at 33 °C covering timpoints between 24 and 72 hr.

Infection of BEAS-2B cells with HRV16 drove significant increases in RANTES, IL-6 and IFN-β mRNA expression however this only became apparent at 72 hr post infection (Figure 5.1B,C). There was little or no change in gene expression at 6 or 24 hr with increases beginning at 48 hr. A possible explanation for the requirement of such a long timescale for an immune response to become apparent is simply the level of viral replication occurring. This was measured by quantitative PCR with primers specific to HRV16 (Figure 5.1D). This indicated that although there was an approximate 10-fold increase in HRV16 presence at 24 hr post infection compared to 6 hr, it then took until 72 hr for this level be doubled (Figure 5.1D). This would suggest that the HRV16's replication was being impeded by the host's immune response, activation of which was being detected at approximately 48 hr and at significant levels by 72 hr (Figure 5.1 A-C). In any case, HRV16 infection of BEAS-2B cells was confirmed along with the activation of an immune response. It was therefore decided to analyse the whole cell proteomic response to HRV16 at 72 hr post infection.

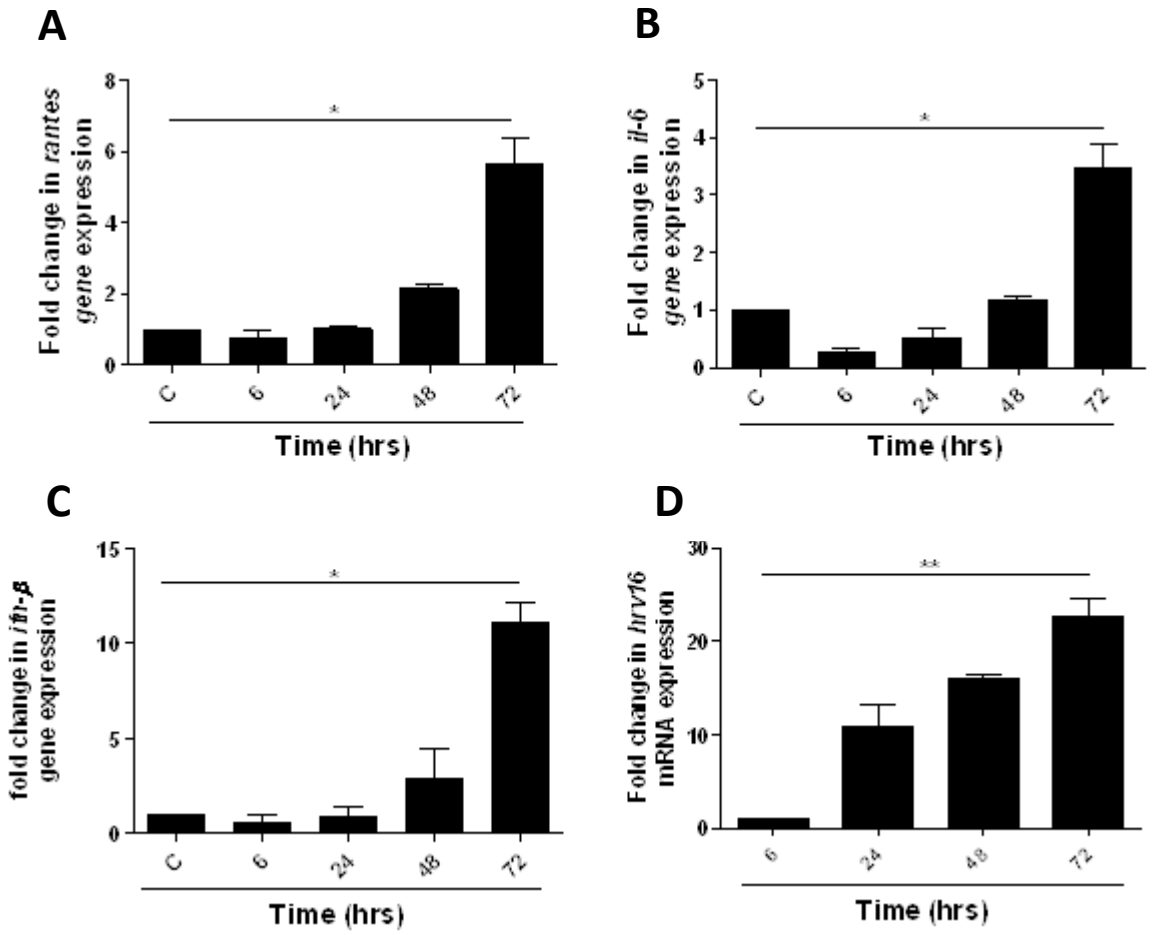

Figure 5.1: HRV16 infection of BEAS-2B cells activates the immune response. BEAS-2B cells were plated at a density of $0.4x10^6$ cells/ml in a six-well plate and incubated for 24 hr at 37 °C. Individual wells were then either left unstimulated or stimulated with HRV16 (MOI of 3) for the timepoints indicated. Cells were then harvested, total RNA isolated and from this, cDNA was synthesised. The cDNA was then used as a template for qRT-PCR using forward and reverse primers specific to human *il-6*, *ifn-β*, *rantes* and *gapdh* (housekeeping gene). * $p<0.05$, ** $p<0.01$ and *** $p<0.001$. Graphs are representative of three independent experiments.

5.2.2 Proteomic response to HRV16 infection – common trends and functional annotation of protein hits obtained by 2D-DIGE with MS

Protein hits that were significantly up or down regulated in response to HRV16 infection of BEAS-2B cells, as identified by 2D-DIGE and MS were categorised as per Figure 4.2. Categorisation of each protein into the same broad functional roles applied to the *B. pertussis* study revealed broadly similar levels of contributions to processes such as immune function (24 % of proteins with HRV16 vs. 27 % with *B. pertussis*), cancer related (14 % of proteins with HRV16 vs. 12 % with *B. pertussis*), structural (15 % vs. 12 %) and redox (7 % vs. 9 %) (Figure 5.2A,B). However, notable differences were evidenced with a reduction of those involved in metabolism (7 % with HRV16 vs. 10 % with *B. pertussis*) and trafficng (12 % vs. 5 %) (Figure 5.2A,B).

It is possible that these differences in overall cellular function mobilisation represent at the broadest level, the contrasting cellular response to infection with a virus versus the response to a bacterium. Increased expression of proteins involved in protein synthesis for example, would align with dogma regarding viral hijacking of host transcription and translation machinery in order to replicate itself [162]. The 30 % reduction in proteins involved in metabolism is interesting but can be explained by the fact that unlike *B. pertussis*, HRV infection does not tend to drive pathology in lung epithelial cells [162, 437, 438]. As HRV infection is less lethal to the cell, it could be hypothesised that the cell in turn expends less energy in fighting it. Also, although both pathogens can reside within the cell [163, 249], the fact that *B. pertussis* is a much more complex organism compared to HRV (viruses are not considered a form of life according to modern taxonomy [439]) could mean that the levels of host metabolism subverted by an intracellular bacterial infection versus an intracellular viral infection are much higher.

The total number of upregulated proteins vs downregulated proteins was broadly similar between HRV16 and *B. pertussis* infection with an approximate 4:1 ratio of upregulated proteins against down regulated proteins observed in both studies (Figure 5.2C,D).

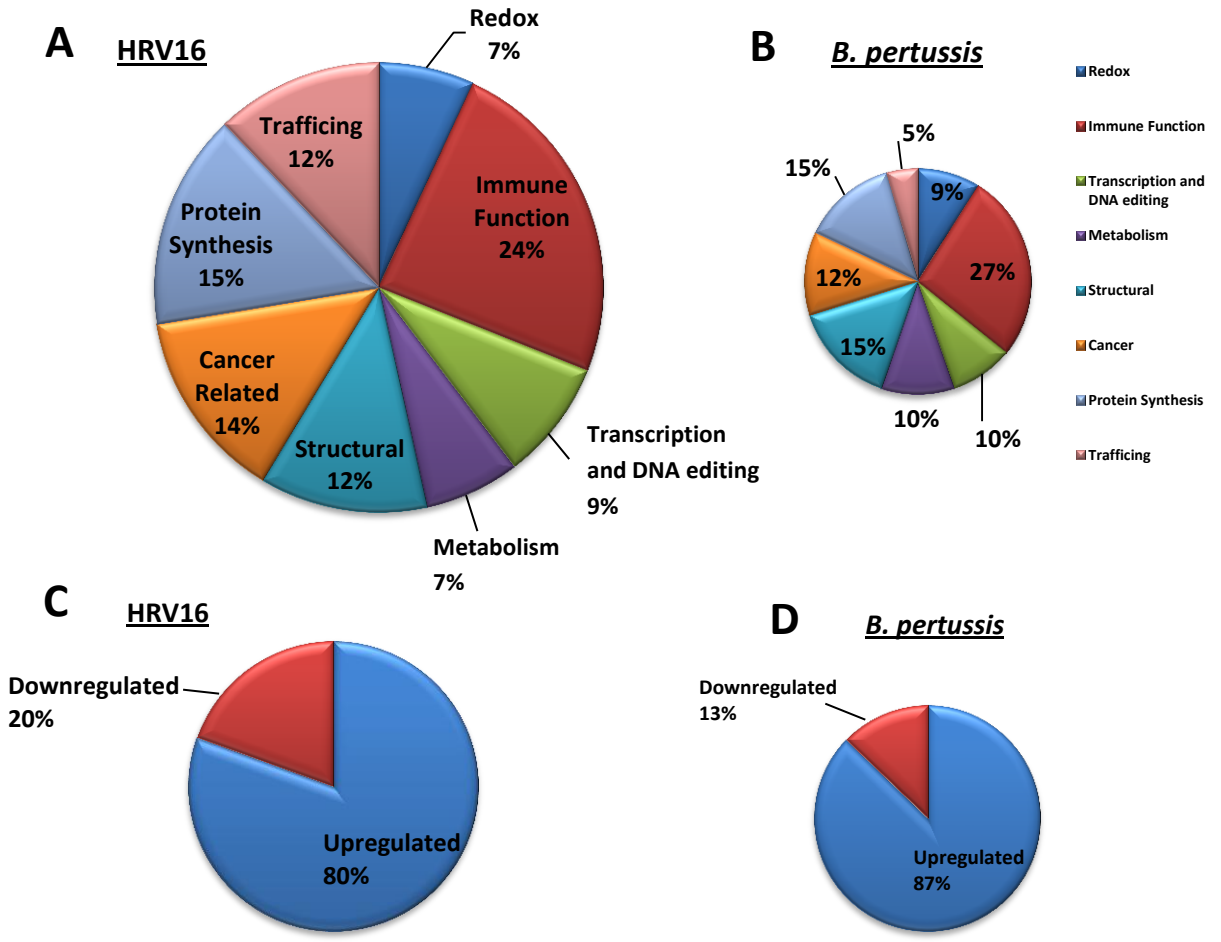

Figure 5.2: Pie chart representation and comparison of protein function from hits identified by 2D-DIGE in response to HRV16 and *B. pertussis* infection. (A) 2D-DIGE identified proteins from HRV16 infected cells were researched for functional properties and grouped according to function(s) in one or more of eight general categories: protein synthesis, trafficking, redox, immune function, transcription/DNA editing, metabolism, structural and cancer. Total numbers of proteins assigned to each function were then displayed in pie chart format for visualisation. (B) 2D-DIGE identified protein hits from *B. pertussis* infected cells underwent a similar process and are displayed for comparative purposes. **(**C) Total numbers of 2D-DIGE MS – HRV16 derived protein hits that were up or down regulated according to Progenesis software were visualised in pie chart format (D) Total numbers of up and downregulated protein hits derived from the 2D-DIGE MS - *B. pertussis* study are shown for comparative purposes.

5.2.3 2D-DIGE protein hits common to both HRV16 and *B. pertussis* infection

An average of 44 protein hits were identified as being significantly up or downregulated in response to either HRV16 or *B. pertussis* infection (Figure 5.3A). Of these, 11, or approximately 25 % of proteins were identified in both infection settings indicating that these play a role in the host response to both viral and bacterial challenge to cells of the respiratory system. These proteins were TPI, SOD1, DJ-1, stathmin 1, ubiquitin conjugating enzyme 13 (Ubc13), peroxiredoxin 3 (PRDX3), nucleoside diphosphate kinase (NDK), gankryin (p28), IL-25, caspase 3 and partner of Sld five 2 (PSF2) (Figure 5.3A). Annotation and categorisation of these proteins according to their function revealed the processes that appear to be most important in the host response immune response to both bacterial and viral infections (Figure 5.3B, Table 5.1).

Proteins with documented roles in immune function represent the majority (one-third) of those whose expression changed significantly in response to both viral and bacterial challenge. Proteins with roles in cancer processes represented slightly less than one quarter of the total with 22 %. Those involved in redox signalling and transcription/DNA editing accounted for 17 % and 11 % respectively. Metabolism, structural and trafficking proteins were each responsible for approximately 6 % (Figure 5.3B). It is interesting to note that when examining the proteome in response to bacterial or viral infection, by either 2D-DIGE MS or LFQ MS, between one quarter and one third of dynamically regulated proteins are known to have some function within the immune response. However, this in turn means that between three quarters and two thirds of identified proteins respectively, have no documented role in the immune response – a large proportion considering that they were identified upon pathogenic infection. While some of these undoubtedly have to date unknown links or roles in the immune response, it is unlikely that all do. Therefore, another avenue of research in terms of defining therapeutic targets could be in targeting proteins involved not in the

immune response, but involved in disregulated cancer signalling pathways for example or redox signalling pathways in response to infection.

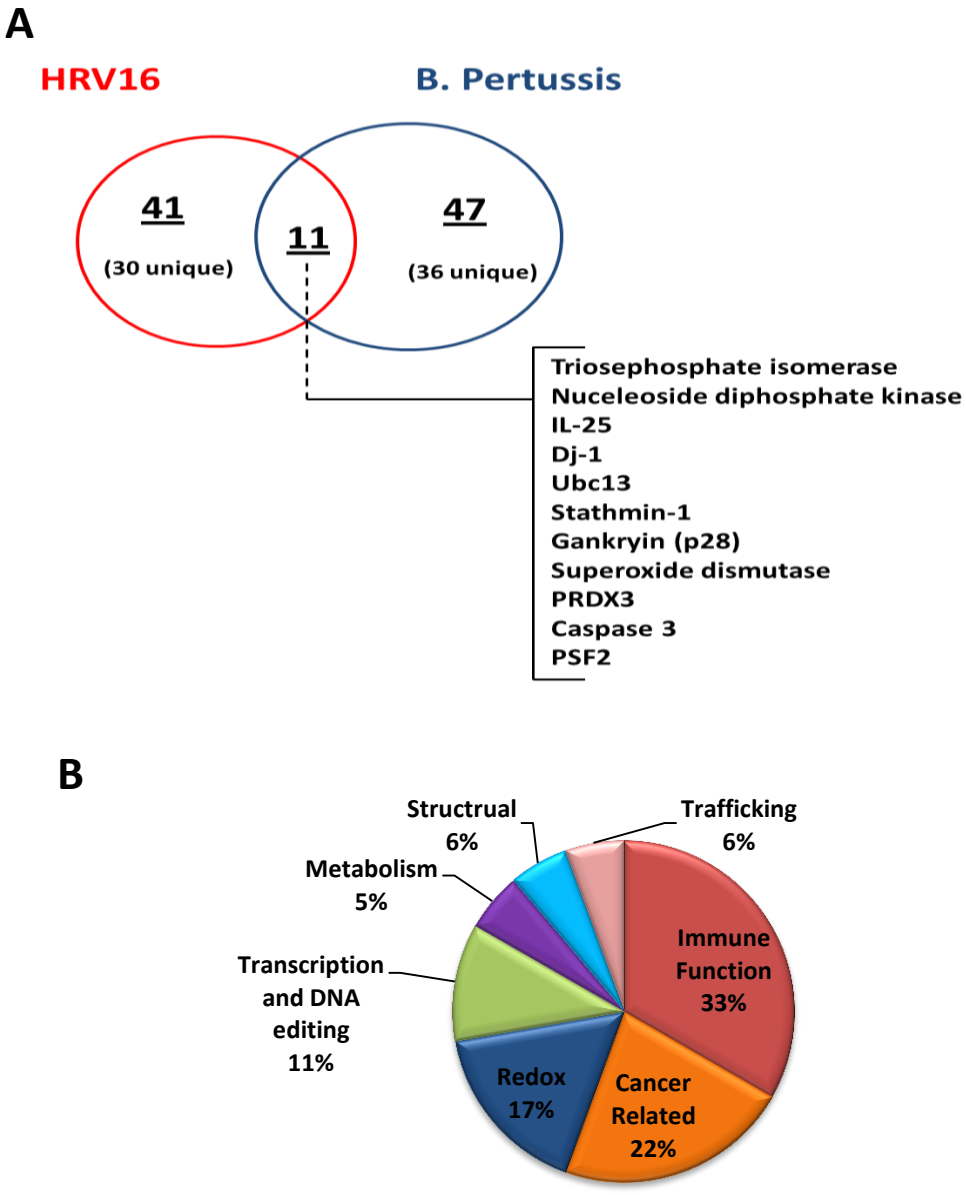

Figure 5.3: Quantification of unique and identical protein hits identified in response to HRV16 and *B. pertussis* infection by 2D-DIGE with LC/MS. (A) Venn diagram illustrating the total number (underlined) of protein hits identified by HRV16 (red circle) and *B. pertussis* (blue circle) infection of BEAS-2B cells. The number of identical protein hits detected in both infections is in the centre and the names of these proteins are annotated below. These identical protein hits were then researched for function and assigned to groups in the pie chart in (B). Functions were found to fall into seven general categories: trafficking, redox, immune function, transcription and DNA editing, metabolism, structural and cancer related.

Protein hits obtained by 2D-DIGE with MS

Fold Ch.	Protein Name	Function
↑1.6	Stathmin	Endogenous TLR3 agonist [255]. Cancer marker. Microtubule regulation [261].
↑1.6	Actin-related protein 2/3 complex subunit 5	Regulates general actin cytoskeleton [440].
↑1.5	Prefoldin subunit 5	Promotes folding of nascent polypeptide chain [441].
↑1.7	Superoxide dismutase [Cu-Zn]	Redox signalling. Indirect NFκB modulator [269].
↑1.6	Deoxyuridine 5'-triphosphate nucleotidohydrolase,	Nucleotide metabolism [442].
↑1.5	Nucleoside diphosphate kinase A (NME1)	Transfers phosphate groups.Cancer metastasis marker & link to endocytosis [443].
↑1.5	Putative hydrolase RBBP9	Serine hydrolase.Increased in pancreatic cancer.Suppression of TGFβ signalling[444]
↑1.5	α/β hydrolase domain-containing protein 14B	Unknown
↑1.6	Dj-1	Associated with Parkinson's Disease. Protective against oxidative stress [288].
↑1.5	PRDX3	Redox signalling [274]. Prostate cancer marker [275].
↑1.6	Lysozyme C	Glycoside hydrolase. Damages peptidoglycan layer in bacterial cell walls [274].
↓1.7	Myosin regulatory light chain 12A	Critical in maintain cell structure and cellular integrity [445].
↑1.5	60S acidic ribosomal protein P2	Component of ribosome 60S subunit. Protein synthesis elongation step [446].
↑1.6	Eukaryotic Translation Initiation Factor Eif5a	Translation factor [447]. Regulates iNOS levels [448].
↑1.5	Glia maturation factor beta	Overexpression drives NFκB activation in astrocytes. Neuronal survival [449].
↓1.3	Heme-binding protein 1 (p22HBP)	Binds heme [450].
↑1.4	Glutathione S-Transferase P1	Polymorphisms associated with multiple cancers[451]Inhibits JNK signalling[452]
↑1.5	Gankryin or p28 or GANK	Inhibits NFκB by retaining in cytoplasm [453]. Noted oncoprotein [454].
↑1.3	Caspase 3	Protease. Central apoptosis mediator [454].

Table 5.1: Proteins identified by 2D-DIGE combined with LC-MS showing changes in expression in response to HRV16 Infection. Protein function is also indicated. Full annotation of protein hits can be found in appendix table A1.3.

Protein hits obtained by 2D-DIGE with MS

Fold Ch.	Protein Name	Function
↑1.5	DNA-directed RNA polymerases subunit RPABC1	Transcribes DNA into RNA [455].
↑1.5	Phosphoglycerate mutase 1	Phosphate transfer in glycolysis [290].
↓1.3	unnamed protein product	Unknown
↑1.5	40S ribosomal protein S12	Ribosome subunit. Site of protein synthesis [295].
↑1.5	HINT1	Tumour suppressor. Can inhibit NFκB activity [456]. Can trigger apoptosis [457].
↑1.5	S-phase kinase-associated protein 1	Component of SCF ubiquitin ligase. Targets proteins for degradation [458].
↑1.5	DNA replication complex GINS protein PSF2	Essential in initiation of DNA replication. Preferentially binds to ssDNA [304].
↓1.5	Lamin-B1	Nuclear membrane protein. Structural integrity [459].
↓1.6	Mitogen-activated protein kinase kinase kinase 5	Serine/threonine kinase-mediates inflammatory and stress signals via AP-1[460].
↑1.5	Splicing factor 3A subunit 1	Complex required for mRNA splicing [461].
↓1.7	Menin	Primarily nuclear. Inhibits AP-1 transcription factor jun-D [462].
↓1.7	Glycogen debranching enzyme	Metabolism. Glycogen breakdown [463].
↓1.6	Tetratricopeptide repeat protein 21B	Component of IFT complex which maintains cilia (Uniprot).
↑1.4	IL-25	T_H2 cytokine-induces secretion of IL-4 and others[296].Anti-inflammatory[297]
↑1.4	Histidine triad nucleotide-binding protein 2	Mitochondrial apoptotic sensitiser[464]. Regulates intracellular calcium levels [465]
↑1.4	Cofilin-1	Actin modulator. Role in cell migration [273].
↑1.4	Ubiquitin-conjugating enzyme E2 N (Ubc13)	Required for MAP Kinase activation [271]. Role in TRAF6 mediated signalling [271]
↑1.4	Triosephosphate isomerase	Important in glycolytic pathway [259].
↑1.3	coiled-coil domain containing 69	Mitosis. Regulates spindle formation [466].

Table 5.1 (contd): Proteins identified by 2D-DIGE combined with LC-MS showing changes in expression in response to HRV16 Infection. Protein function is also indicated. Full annotation of protein hits can be found in appendix table A1.3.

Protein hits obtained by 2D-DIGE with MS

Fold Ch.	Protein Name	Function
↑1.4	Prefoldin subunit 3	Prefoldin promotes folding of nascent polypeptide chain [441].
↑1.4	Acyl-protein thioesterase 1	T-cell activation . Depalmitoylation . Affects Ras signalling [467].
↑1.4	NME1-NME2 protein (Nucleoside diphosphate kinase A and B)	NME1 is a tumour suppressor. NME2 involved in activation of G proteins [468].

Table 5.1 (contd): Proteins identified by 2D-DIGE combined with LC-MS showing changes in expression in response to HRV16 Infection. Protein function is also indicated. Full annotation of protein hits can be found in appendix table A1.3.

5.2.4 Verification of protein hits from HRV16 infection.

As mentioned previously, approximately 25 % of proteins whose expression was significantly modulated in response to HRV16 infection were similarly modulated in response to *B. pertussis* infection (Figure 5.3A). Because expression of these proteins appeared modulated in response to two distinct pathogenic challenges, particular importance was assigned to them as they may play central roles host defence. With this in mind, it was decided to verify a selection of proteins which appeared in response to HRV16 that were also identified in *B. pertussis* infection. These proteins were further selected based on their contribution to each of the broad functional categories alluded to in Figure 5.3B. These were NDK (or NME) which has roles in cancer and trafficking, TPI which is involved in metabolism, SOD1 which has redox and immune functions, DJ-1 which is also involved in redox signalling and finally stathmin 1 which has demonstrated roles in immune function, cell structure and cancer (Table 5.1). These proteins therefore play diverse roles within the cell and may play equally diverse roles in the response to pathogen challenge.

5.2.5 Verification of HRV16 protein hit: Nucleoside diphosphate kinase (NME1-NME2)

NDK A, also known as NME1 or nm23-H1 and NDK B, also known as NME2 or nm23-H2, are highly conserved and expressed enzymes with roles in many cellular processes. First, as its name suggests, it is a kinase that transfers phosphate groups between nucleoside tri- and diphosphates, for example, between adenosine triphosphate (ATP) and guanosine diphosphate (GDP) [443]. It can also bind to DNA to modulate transcription [469, 470]. Moreover, NDK has a granzyme-A dependent DNase activity during caspase independent apoptosis [471]. Somewhat controversially, NDK levels have been inversely associated with cancer metastasis in xenografts of human breast cancer and oral squamous cancer with reduced expression correlating with increased metastasis [472, 473]. However, other studies have doubted this [443, 474]. More recently, NDK has been shown to interact with the

Epstein-Barr virus (EBV) virulence factor nuclease antigen 1 which inhibits NDK's ability to supress cell migration in lymphoblastoid cell lines [475]. Finally, NDK has also been shown to play a role in dynamin dependent processes such as cytokinesis and endocytosis by way of its role in GTP production, which is required for dynamin activity [476, 477]. The exact mechanism for this role has not been ascertained.

The current 2D-DIGE with MS study identified both NDK A and its isoform NDK B as being upregulated 1.5 fold in BEAS-2B cells infected with HRV16 for 72 hr compared to uninfected control cells (Figure 5.4A, Table 5.1). This result was verified by western blot using an anti-NME2 antibody. This showed that levels of both isoforms undergo major upregulation upon infection with HRV16 at 24 hr with this upregulation being maintained at 112 hr (Figure 5.4B). Levels of NME2 mRNA were also analysed by real time PCR which did not indicate any significant upregulation at the gene level suggesting that NDK undergoes post-transcriptional or translational modifications to increase its expression (Figure 5.4C).

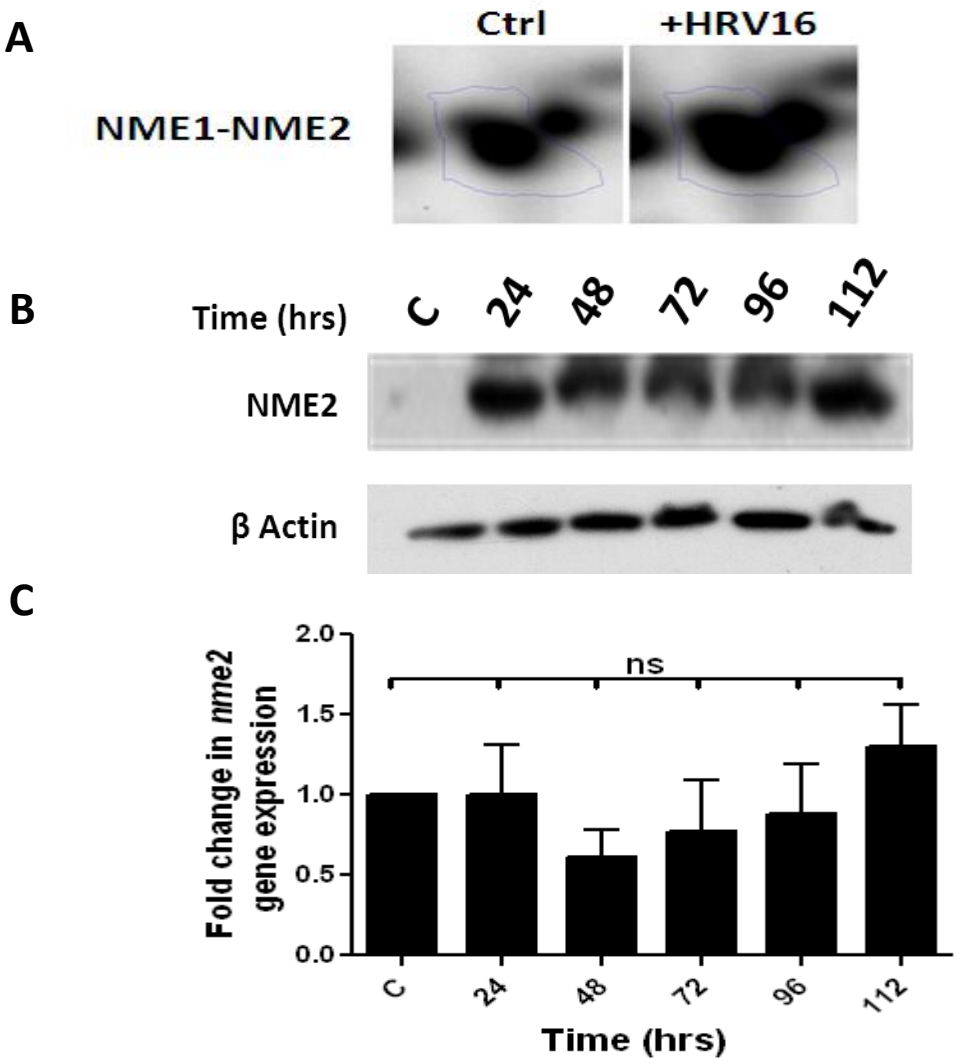

Figure 5.4: Verification of NME2 upregulation in response to HRV16. (A) Screen grab of Progenesis analysis showing NME2 presence on a reference 2D-DIGE gel image from control (Ctrl) and HRV16 infected (72 hr) lysates. Image represents four independent experiments (B) BEAS-2B cells were seeded in a 6-well plate at a density of $0.4x10^6$ cells/ml and incubated for 24 hr at 37 °C. Thereafter, cells were transferred to a 33 °C incubator and either left uninfected or infected with HRV16 (MOI of 3) for the timepoints indicated. Cells were then harvested and each sample lysed in 100 µl H.S. buffer for 20 min on ice. Cell debris was removed by centrifugation with the remaining whole cell lysates mixed with 30ul 5x Laemmli loading buffer and boiled for 10 min. Proteins were separated by SDS-PAGE and subjected to immunoblot analysis using anti-NME2 and anti-β-Actin antibodies. Results represent two independent experiments. Image is representative of three independent experiments (C) BEAS-2B cells were plated, incubated and stimulated according to (B). Cells were then harvested, total RNA isolated and from this, cDNA was synthesised. The cDNA was then used as a template for qRT-PCR using forward and reverse primers specific to human *nme2* and *gapdh* (housekeeping gene). * $p<0.05$, ** $p<0.01$ and *** $p<0.001$. NS, not significant. Graph is representative of two independent experiments.

5.2.6 Verification of HRV16 protein hits: DJ-1 and stathmin 1

DJ-1 and stathmin 1 were both found to be upregulated 1.6 fold in HRV16 infected BEAS-2B cells compared to uninfected controls (Figure 5.5A, 5.6A). These results were verified by western blot which in the case of DJ-1, showed increased expression at 72 and 96 hr of HRV16 infection (Figure 5.5B). Stathmin 1 expression was found to be increased at 24 hr post infection and this was maintained until 96 hr (Figure 5.6B). DJ-1 mRNA was not found to be significantly changed across multiple timepoints indicating that its levels are being regulated post-transcriptionally (Figure 5.5C). This contrasts with its expression upon *B. pertussis* infection which indicated a small but significant increase in gene DJ-1 gene expression upon *B. pertussis* infection (Figure 4.4C). Expression of stathmin 1 mRNA was significantly upregulated upon HRV16 by approximately 4 fold compared to uninfected cells. This result correlates with stathmin 1's gene expression upon *B. pertussis* infection which was also upregulated (Figure 5.6C and 4.6C). Further discussion of both DJ-1 and stathmin 1 can be found in Section 4.2.1 and 4.2.6 respectively.

5.2.7 Verification of HRV16 protein hits: TPI and SOD

TPI and SOD were both found by 2D-DIGE MS to be upregulated 1.4 and 1.7 fold respectively upon HRV16 infection at 72 hr (Figures 5.7A, 5.8A) (Table 5.1). Again, both results were verified by western blot with TPI undergoing upregulation between 48 hr and 96 hr (Figure 5.7B). Levels of SOD were also increased at 48 hr and remained so at 112 hr of infection (Figure 5.8B). Analysis of mRNA corresponding to both proteins revealed no significant changes in expression across all timepoints analysed (Figure 5.7C and 5.8C). These results agreed with observations of the levels of the same mRNAs in response to *B. pertussis* infection which were also unchanged (Figure 4.16C and 4.15C). Further discussion of both TPI and SOD can be found in Section 4.2.8 and 4.2.12 respectively.

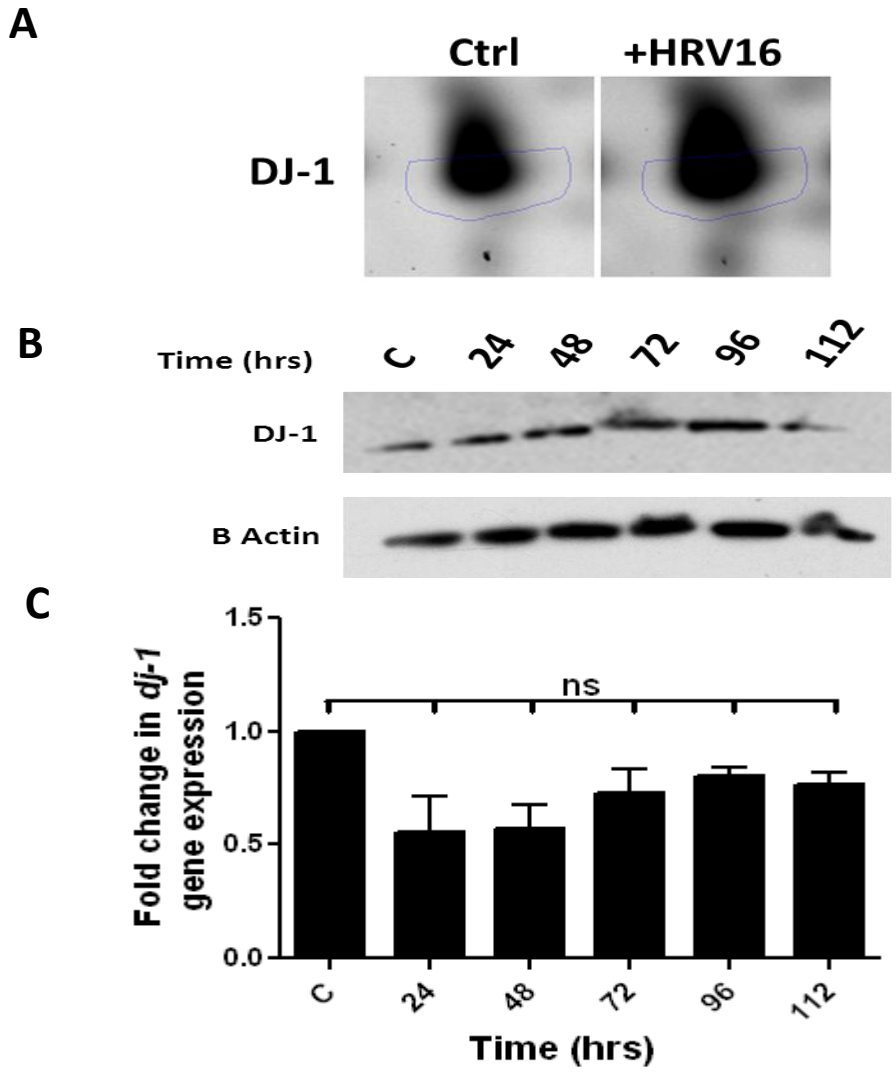

Figure 5.5: Verification of DJ-1 upregulation in response to HRV16. (A) Screen grab of Progenesis analysis showing DJ-1 presence on a reference 2D-DIGE gel image from control (Ctrl) and HRV16 infected (72 hr) lysates. Image represents four independent experiments (B) BEAS-2B cells were seeded in a 6-well plate at a density of $0.4x10^6$ cells/ml and incubated for 24 hr at 37 °C. Thereafter, cells were transferred to a 33 °C incubator and either left uninfected or infected with HRV16 (MOI of 3) for the timepoints indicated. Cells were then harvested and each sample lysed in 100 µl H.S. buffer for 20 min on ice. Cell debris was removed by centrifugation with the remaining whole cell lysates mixed with 30ul 5x Laemmli loading buffer and boiled for 10 min. Proteins were separated by SDS-PAGE and subjected to immunoblot analysis using anti-DJ-1 and anti-β-Actin antibodies. Results represent two independent experiments. Image is representative of three independent experiments (C) BEAS-2B cells were plated, incubated and stimulated according to (B). Cells were then harvested, total RNA isolated and from this, cDNA was synthesised. The cDNA was then used as a template for qRT-PCR using forward and reverse primers specific to human *dj-1* and *gapdh* (housekeeping gene). * $p<0.05$, ** $p<0.01$ and *** $p<0.001$. NS, not significant. Graph is representative of two independent experiments.

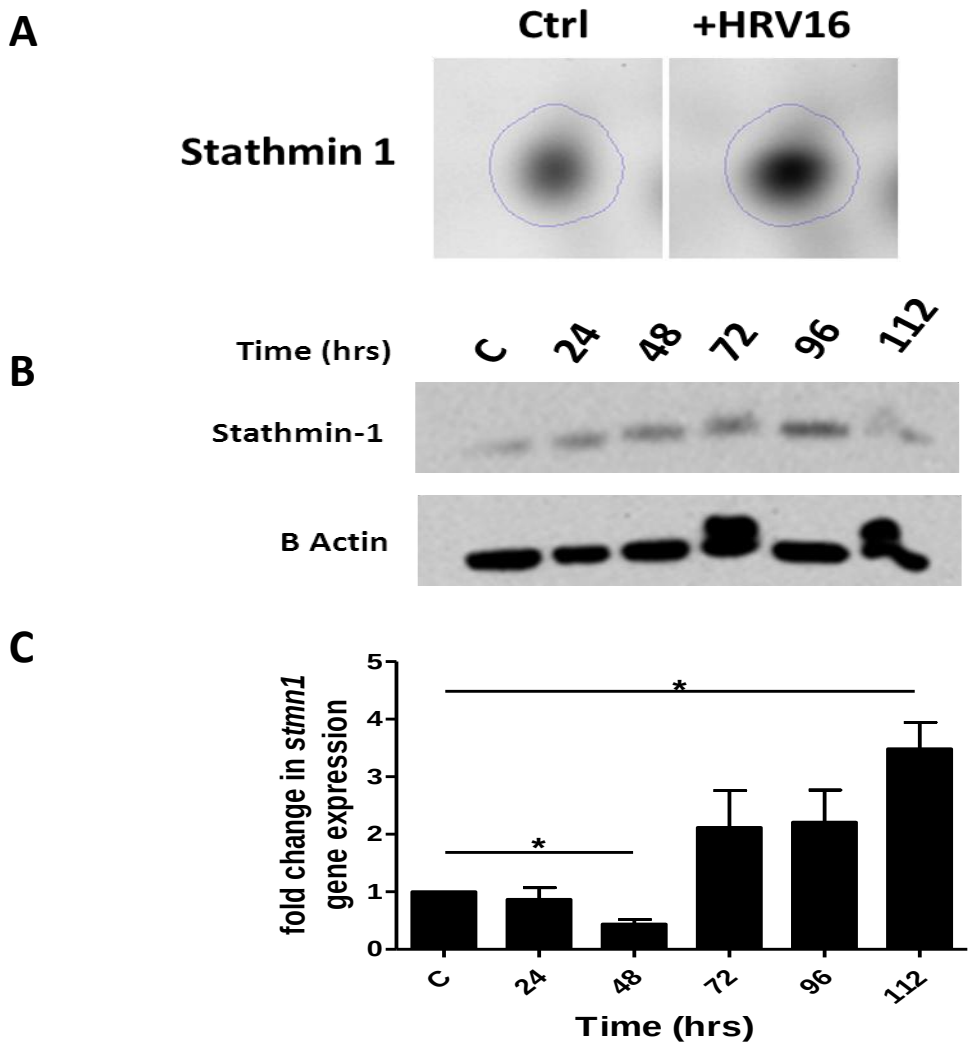

Figure 5.6: Verification of stathmin 1 upregulation in response to HRV16. (A) Screen grab of Progenesis analysis showing stathmin 1 presence on a reference 2D-DIGE gel image from control (Ctrl) and HRV16 infected (72 hr) lysates. Image represents four independent experiments (B) BEAS-2B cells were seeded in a 6-well plate at a density of $0.4x10^6$ cells/ml and incubated for 24 hr at 37 °C. Thereafter, cells were transferred to a 33 °C incubator and either left uninfected or infected with HRV16 (MOI of 3) for the timepoints indicated. Cells were then harvested and each sample lysed in 100 µl H.S. buffer for 20 min on ice. Cell debris was removed by centrifugation with the remaining whole cell lysates mixed with 30ul 5x Laemmli loading buffer and boiled for 10 min. Proteins were separated by SDS-PAGE and subjected to immunoblot analysis using anti-stathmin 1 and anti-β-Actin antibodies. Results represent two independent experiments. Image is representative of three independent experiments (C) BEAS-2B cells were plated, incubated and stimulated according to (B). Cells were then harvested, total RNA isolated and from this, cDNA was synthesised. The cDNA was then used as a template for qRT-PCR using forward and reverse primers specific to human *stmn1* and *gapdh* (housekeeping gene). * $p<0.05$, ** $p<0.01$ and *** $p<0.001$. NS, not significant. Graph is representative of two independent experiments.

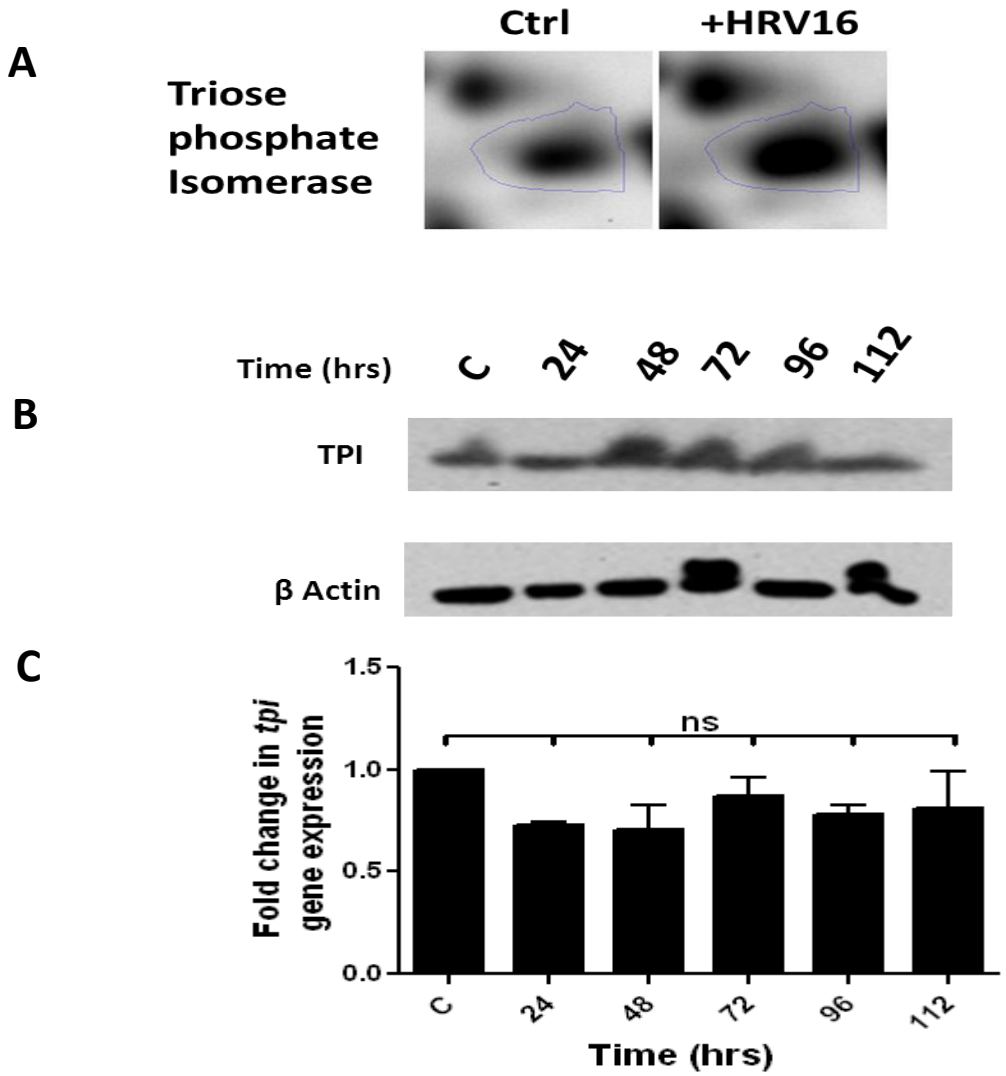

Figure 5.7: Verification of triose phosphate isomerase upregulation in response to HRV16. (A) Screen grab of Progenesis analysis showing triose phosphate isomerase (TPI) presence on a reference 2D-DIGE gel image from control (Ctrl) and HRV16 infected (72 hr) lysates. Image represents four independent experiments (B) BEAS-2B cells were seeded in a 6-well plate at a density of $0.4x10^6$ cells/ml and incubated for 24 hr at 37 °C. Thereafter, cells were transferred to a 33 °C incubator and either left uninfected or infected with HRV (MOI of 3) for the timepoints indicated. Cells were then harvested and each sample lysed in 100 µl H.S. buffer for 20 min on ice. Cell debris was removed by centrifugation with the remaining whole cell lysates mixed with 30ul 5x Laemmli loading buffer and boiled for 10 min. Proteins were separated by SDS-PAGE and subjected to immunoblot analysis using anti-TPI and anti-β-Actin antibodies. Results represent two independent experiments. Image is representative of three independent experiments (C) BEAS-2B cells were plated, incubated and stimulated according to (B). Cells were then harvested, total RNA isolated and from this, cDNA was synthesised. The cDNA was then used as a template for qRT-PCR using forward and reverse primers specific to human *tpi* and *gapdh* (housekeeping gene). * $p<0.05$, ** $p<0.01$ and *** $p<0.001$. NS, not significant. Graph is representative of two independent experiments.

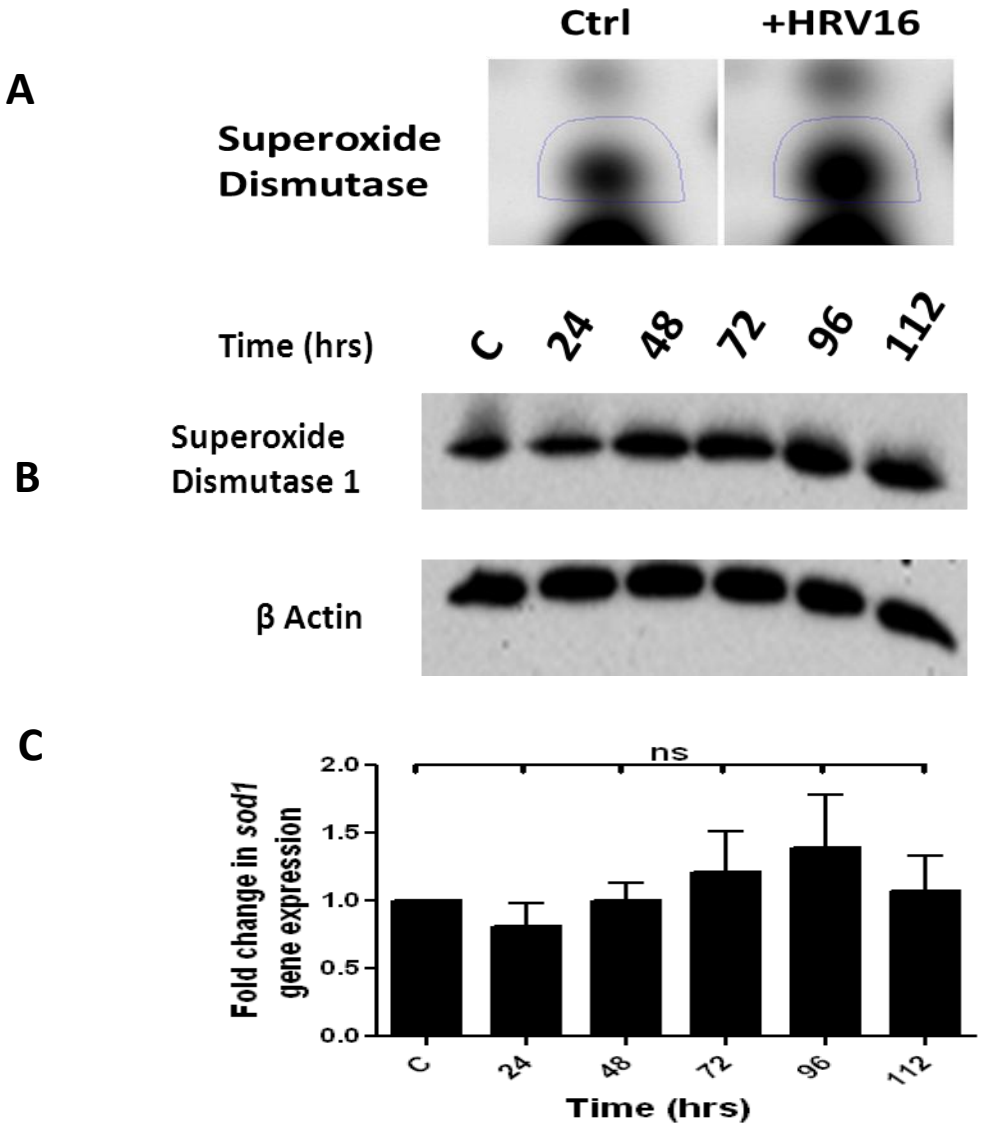

Figure 5.8: Verification of superoxide dismutase upregulation in response to HRV16. (A) Screen grab of Progenesis analysis showing superoxide dismutase (SOD) presence on a reference 2D-DIGE gel image from control (Ctrl) and HRV16 infected (72 hr) lysates. Image represents four independent experiments (B) BEAS-2B cells were seeded in a 6-well plate at a density of $0.4x10^6$ cells/ml and incubated for 24 hr at 37 °C. Thereafter, cells were transferred to a 33 °C incubator and either left uninfected or infected with HRV (MOI of 3) for the timepoints indicated. Cells were then harvested and each sample lysed in 100 µl H.S. buffer for 20 min on ice. Cell debris was removed by centrifugation with the remaining whole cell lysates mixed with 30ul 5x Laemmli loading buffer and boiled for 10 min. Proteins were separated by SDS-PAGE and subjected to immunoblot analysis using anti-SOD and anti-β-Actin antibodies. Results represent two independent experiments. Image is representative of three independent experiments (C) BEAS-2B cells were plated, incubated and stimulated according to (B). Cells were then harvested, total RNA isolated and from this, cDNA was synthesised. The cDNA was then used as a template for qRT-PCR using forward and reverse primers specific to human *sod* and *gapdh* (housekeeping gene). * $p<0.05$, ** $p<0.01$ and *** $p<0.001$. NS, not significant. Graph is representative of two independent experiments.

5.2.8 HRV16 and poly(I:C) mediated cytokine production post knockdown of stathmin 1 and DJ-1 expression in BEAS-2B cells

As previously discussed, stathmin 1's primary function in microtubule organisation implies possible roles in diverse cellular functions [253, 261, 330]. Indeed, previous data has indicated a role for stathmin 1 in TLR4 mediated IL-6 production (Figure 4.19). Moreover, stathmin 1 has been described as a candidate TLR3 agonist and TLR3 is also known to sense dsRNA produced by HRV16 in BEAS-2B cells [478]. DJ-1 is a known biological marker for Parkinson's disease susceptibility and may play a role in its pathogenesis [313]. Furthermore, DJ-1 has been shown to play a conserved role in the regulation of NO production in response to gram-negative bacteria [318, 319]. However a role for either proteins in mediating the immune response to viral infection has not been shown.

In order to attain a greater understanding of the role that stathmin 1 and DJ-1 play in the host innate immune response to HRV16 infection, their levels were endogenously supressed in BEAS-2B cells immediately prior in HRV16 infection. Resulting cytokine expression in infected cells with suppressed levels of either protein were therefore compared to control infected cells.

Validation of esiRNA mediated suppression of mRNA expression corresponding to both stathmin 1 and DJ-1 was previously carried out (Figure 4.18). Estimated knockdown efficiency was 95 % and 60 % respectively compared to controls (Figure 4.18B,D). Transfection of esiRNA specific to either stathmin 1 or DJ-1 did not significantly alter basal IL-6, RANTES or type-I IFN cytokine production (Figure 5.9A-E). Infection with HRV16 induced production of IL-6 with approximately 400 pg/ml secreted compared to uninfected controls (Figure 5.9A). However, minimal RANTES or type-I IFN was detected (Figure 5.9B,E). In contrast, poly(I:C) stimulation mediated strong production of all three cytokines compared to unstimulated controls (Figure 5.9C-E). Knockdown of stathmin 1 expression did not significantly modulate secretion of IL-6, RANTES or type-I IFN in response to HRV16

infection or poly(I:C) stimulation compared to uninfected or unstimulated controls (Figure 5.9A-E). The same result was obtained upon suppression of DJ-1 (Figure 5.9A-E). Levels of IL-6 increased slightly upon stathmin 1 and DJ-1 suppression during HRV16 infection but this was not significant (Figure 5.9A). It would therefore appear that stathmin 1 and DJ-1 do not play a role in both pro-inflammatory cytokine and type-I IFN production in response to TLR3 activation and infection with HRV16.

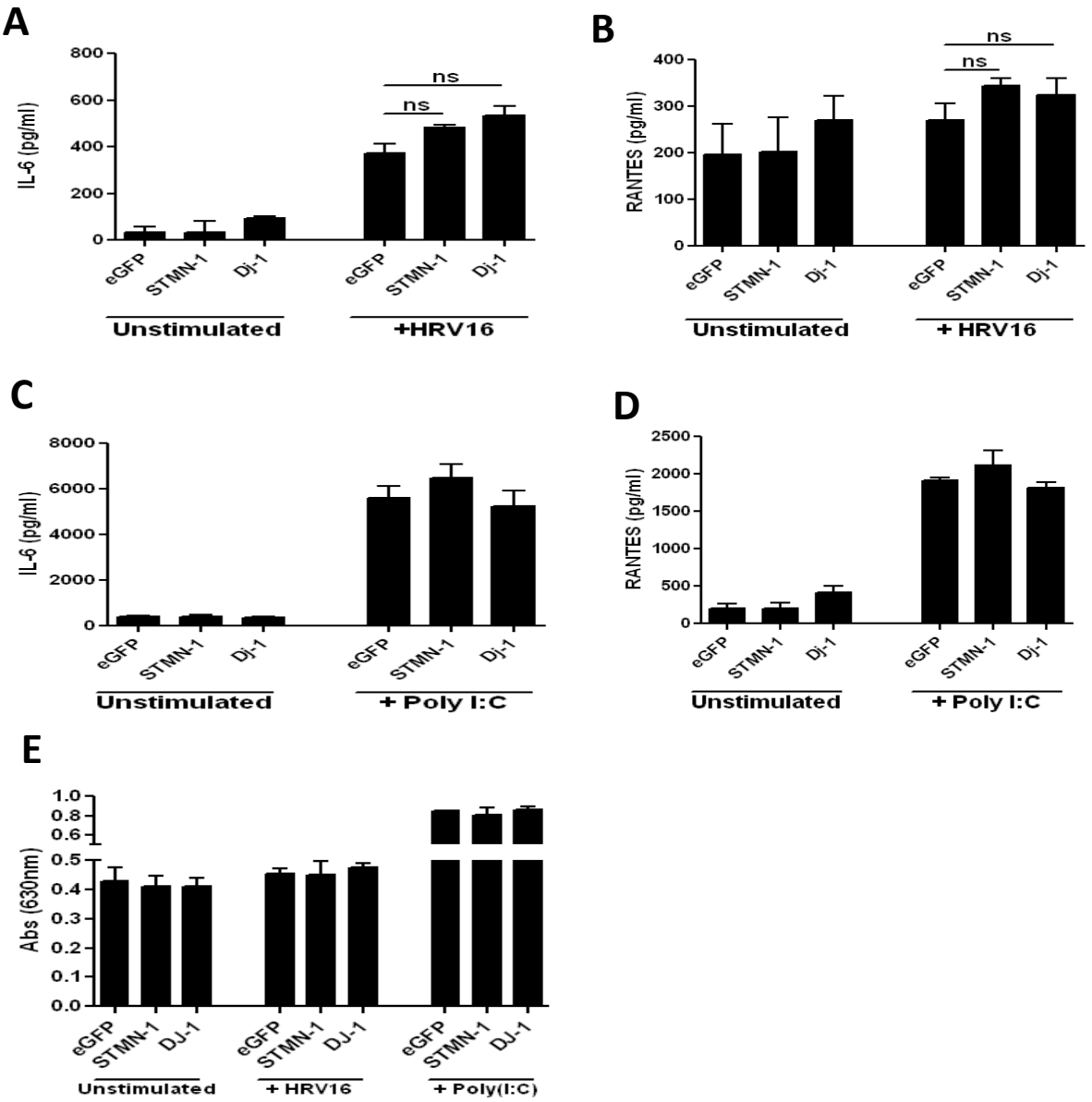

Figure 5.9: HRV16 and poly(I:C) mediated cytokine production upon suppression of stathmin 1 and Dj-1. For HRV16 mediated responses, BEAS-2B cells were seeded in a 6-well plate at a density of $0.4x10^6$cells/ml and either left uninfected or infected with HRV16 (MOI of 3) in an incubator at 33 °C for 24 hr. Cells were then transfected with either 200 ng of target gene specific esiRNA or a control esiRNA (eGFP) for a further 24 hr. At this point, medium was removed and fresh medium containing HRV16 (MOI of 3) was added for a further 24 hr. Cell free supernatants were then harvested and analysed for the presence of human IL-6 (A), RANTES (B) and type-I IFN (E). For poly(I:C) mediated responses, BEAS-2B cells were seeded in a 6-well plate at a density of $0.4x10^6$cells/ml for 24 hr at 37 °C. Cells were then transfected with either 200 ng of target gene specific esiRNA or a control esiRNA (eGFP) for a further 24 hr. At this point, medium was removed and fresh medium was added for 2 hr upon which cells were either left unstimulated or stimulated with poly(I:C) (25 μg/ml) for 24 hr. Cell free supernatants were then harvested and analysed for the presence of human IL-6 (C), RANTES (D) and type-I IFN (E). Results are representative of 3 independent experiments. NS, not significant.

5.3 Discussion

Viral respiratory tract infections (VRTIs) are among the most common illnesses in humans [479]. Non-influenza related VRTIs, particularly the picnoraviruses place a significant economic burden on society in terms of missing direct medical costs and indirect losses in productivity including absences from work and school [480]. Annual losses to the US economy for example, have been estimated to total $40 billion annually, with a close to 50:50 split between direct and indirect expenditures [479]. Unlike influenza, for which there is a limited vaccine available that requires annual doses, there is no such prophylaxis currently available for protection against HRVs, despite the aforementioned economic toll. Antiviral therapies are therefore seen as a feasible method of control which serves to limit the virus's ability hijack the host's machinery and thus prevent replication, dissemination and the associated inflammatory symptoms. As previously mentioned, no analysis of the HRV induced changes to the host cell's proteome have been conducted and a greater understanding of this area could aid the design of more effective antiviral drugs that target host response mechanisms, which the virus requires to survive, instead of targeting the virus itself.

To this end, the whole cell proteome of a lung epithelial cell line, BEAS-2B, was assessed following infection with HRV16 using uninfected cells as a control. A total of 41 proteins were found to be significantly differentially regulated upon HRV16 viral infection (Figure 5.3A, Table 5.1). Of these, 80% were upregulated and 20% were downregulated (Figure 5.2C). Major cellular processes involved in the response to HRV16 appear to be immune function, protein synthesis, cancer related and structural processes (Figure 5.2A). Interestingly, approximately 25% of proteins identified as undergoing significant expression changes in response to HRV16 infection also underwent similar changes in response to *B. pertussis* infection (Figure 5.3A,B). As previously mentioned, these proteins in particular

may be of significant interest to future attempts at curbing the growth and pathogenesis of these two infections. It was interesting that the cytokine IL-25 was found to be significantly upregulated in response to both bacterial and viral challenge. IL-25 has only recently been discovered and is known to promote T helper cell 2 (T_H2) associated pathology by augmenting production of T_H2 cytokines such as IL-4, IL-5, IL-13 but not IL-17 (a T_H1 associated cytokine) despite IL-25 being a member of the IL-17 family [296]. A recent study has implicated IL-25 in enhancing herpes simplex virus 1 and VACV replication by inhibiting expression of an epithelial barrier protein, filaggrin as well as by synergistically acting with other T_H2 cytokines to aid replication [481]. Moreover, HRV is known to induce higher clinical illness severity in asthmatic patients and this has been associated with significantly higher levels of T_H2 cytokines and impaired T_H1 immunity [482, 483]. As IL-25 is a key driver of T_H2 response it stands to reason that inhibiting its activity could lead to reduced viral replication and symptom severity. *B. pertussis* infection in infants and mice tends to drive a T_H1 cytokine profile and it is difficult to speculate upon the effects of supressing IL-25 in this respect [484]. The number of proteins known to be cancer markers was surprising. Several of these have only transient if any known role in the host response to pathogens (Figure 5.2A and Table 5.1). NDK, RBBP9, PRDX3 and GSTP1 are examples of this trend and thus their identification as markers of host homeostatic disregulation, whether in a cancer or infection setting, signals their importance to host homeostasis. Either way, their dynamic regulation during the host response to HRV16 signifies a possible role in host defence against the virus or in viral subversion of the host response. Further experiments will need to be undertaken in order to identify the exact nature of their roles.

Two proteins that were significantly upregulated in response to HRV16 infection, stathmin 1 and Dj-1 were further assessed using RNA interference to examine if they were involved in mediating cytokine production in response to infection. Suppression of each protein

individually led to slight increases in IL-6 production during HRV16 however this was not significant. No change was similarly detected in the production of HRV16 or poly(I:C) mediated RANTES or type-I IFN upon suppression of either protein. As no significant phenotype was observed, their exact role in the host innate immune response viral infection can only be speculated upon. Stathmin 1's role in microtubule formation would suggest that it is involved in modulating intracellular structures or trafficking in response to viral entry within the cell. DJ-1's role in host protection against oxidative stress could serve to limit collateral damage to the host upon activation of ROS, a known human defence mechanism against viruses [485].

In conclusion, multiple proteins have been identified as being dynamically regulated in response to HRV16 infection. These proteins have documented roles in a wide variety of cellular processes and shed light on the host response to viral infection. Whilst no specific HRV16 infection related function could be found upon the suppression of expression of two of these proteins, more rigorous approaches are likely to yield dividends. These approaches would include the use of broad scale RNAi panels to supress many protein hits, both individually and simultaneously as well as a wider range of functional assays such as the monitoring of viral replication and ROS production in response to these protein knockdowns.

Chapter 6

General Discussion

6.1 Discussion

The overarching aim of the current work was to add new dimension(s) to our current knowledge regarding the host response to pathogen challenge. To this end, the aim of chapter 3 was to examine the effects of the loss of a single, relatively understudied TLR adaptor molecule, TRAM, upon activation of multiple TLR signalling pathways. The central aim here was not to confirm previous findings regarding TRAM's function but rather to re-evaluate its role in TLR signalling. Although it is generally accepted that TRAM functions solely as a linker molecule, bridging TLR4 with TRIF to primarily drive anti-viral cytokine production [15, 24], a careful reading of the primary papers that originally defined TRAM's isolated role show that this hypothesis had not been stringently tested, particularly with regard to its possible role(s) in TLR4 independent IRF mediated cytokine production [23, 24]. Control experiments aiming to demonstrate that TRAM does not participate in TLR signalling pathways that are distinct from TLR4 have, to date, only examined NF-κB driven inflammatory cytokines such as TNFα and IL-6 upon perturbation of TRAM [23, 24]. This is surprising as the role of TRAM in TLR4 signalling has always been linked to the production of cytokines and chemokines associated with strong IRF3 and IRF7 regulation, such as type-I IFN [15]. Thus re-evaluating the role of TRAM in TLR signalling, whilst factoring in IRF3 and IRF7 modulated cytokines, revealed a number of unanticipated roles for TRAM in TLR2, TLR7 and TLR9 signalling. Notably, these roles were not related to the production of the pro-inflammatory, primarily NF-κB controlled cytokine TNFα, but rather the IRF3 controlled chemokine RANTES and the type-I IFN (Figure 3.5). The observed phenotypes were unexpected for a number of reasons. Firstly, TLR2, TLR7 and TLR9 are primarily known as MyD88-dependent TLRs, which, upon recognition of their cognate PAMP, transduce their intracellular signal using only MyD88 (TLR2 also utilises the adaptor MAL at low PAMP concentrations) [15, 21]. TRAM, on the other hand is primarily known to mediate the MyD88 independent signalling axis via TLR4 and thus it was surprising that it was found to play a

role in mediating MyD88-dependent TLR2, TLR7 and TLR9 signalling. However, the recent demonstration that TRAM physically interacts with MyD88 to mediate IL-18R signalling provides a precedent for a role for TRAM in mediating signalling via MyD88 dependent receptors. This result was verified in the current study, wherein an interaction between TRAM and MyD88 was demonstrated upon TLR7 stimulation and as elaborated upon earlier, suggests that TRAM is capable of localising to endosomal compartments upon TLR7 signalling, just as it does during TLR4 signalling [84].

Another reason for the unexpected phenotype was the observation that TRAM, at least in the case of TLR7 and TLR9 signalling, appears to mediate their signalling through a mechanism that involves IRF3 (Figure 3.9). The finding that IRF3 is activated in response to TLR7 or TLR9 signalling is novel and perhaps controversial, as it has previously been asserted that IRF3 is not involved in TLR7 signalling in Raw264.7 macrophages [212]. In contrast to the previous study that utilised the TLR7 ligand R848 at a concentration of 10 μM to activate the Raw264.7 macrophages, the current study demonstrated that 2.8 μM R848 (1 μg/ml) resulted in the activation of iBMDMs. This suggests that iBMDMs may be more sensitive than Raw264.7 macrophages to TLR7 stimulation and that this may be due in part to their ability to utilise IRF3 to supplement their signalling. Thus, the observed TRAM-dependent IRF3 activation may be cell type specific whereby iBMDMs display a lower TLR7 activation threshold due to their ability to activate IRF3 in a TRAM dependent manner. From a (patho)physiological perspective, the reliance sole reliance on a MyD88-IRF5 or MyD88-IRF7 for type-I IFN production by the endosomal TLRs seems a risky strategy for the cell. Although other cytosolic PRRs can also sense foreign nucleotides leading to the activation of Type-I IFN in an IRF3 and IRF7 dependent manner [486], the endosomsal TLRs nevertheless play an important role in pathogen response and the potential to utilise IRF3, via a TLR7-MyD88-TRAM-IRF3 axis, would at least expand their ability to successfully transmit a

danger signal to the nucleus if IRF7 and in the case of TLR7, IRF5 also, were to become antagonised by a viral subversion mechanism [487].

It should be noted that the involvement of TRAM in TLR7 signalling does not negate its reliance on MyD88. The TLR7 dependent co-immunoprecipitation of TRAM and MyD88 suggests that TLR7-TRAM signalling is dependent upon MyD88 (Figure 3.19). Thus, a remaining question is whether TRAM is required for the interaction of MyD88 with TLR7, as it is for the interaction of TRIF with TLR4, or is it the case that TRAM binds downstream of MyD88 to act as a linker to the IRF3 pathway. Contrasting with MyD88 deficient cells [40], suppression of TRAM does not completely abolish TLR7 signalling (Figure 3.5, 3.16) suggesting that there are still transcription factor(s), likely IRF5 and IRF7 via MyD88, mediating type-I IFN in the absence of the TRAM-IRF3 pathway. This would therefore suggest that TRAM functions downstream of MyD88. If it were upstream of MyD88, TRAM deficient cells would be completely unresponsive to TLR7 or TLR9 stimulation, which is not the case (Figure 3.5). Thus, it may be proposed that TLR7 signalling in BMDMs may be mediated by three MyD88 dependent signalling pathways. These are a TLR7-MyD88-NF-κB axis, a TLR7-MyD88-IRF5/IRF7 axis and a novel TLR7-MyD88-TRAM-IRF3 axis which complements the IRF5/IRF7 pathway. Future work would include elucidation of the factors that modulate TLR7 signalling downstream of TRAM but upstream of IRF3 in this pathway. IRF3 is known to be phosphorylated by the combined action of the kinases TBK1 and IKKε and would therefore be expected to be involved in any activation of IRF3 [488]. Furthermore, confocal imaging of TRAM, TLR7, TLR9 and IRF3 upon stimulation with the corresponding TLR ligands would be hugely useful in both visualising the trafficking patterns of these proteins during active signalling and also in conforming the roles of TRAM and IRF3 in these pathways.

If such novel insights can still be made regarding the function of the adaptor TRAM, one of the basic tenants of TLR signalling, then one must wonder as to the scale of the 'novelties' still to be discovered with roles in the host defence against pathogen invasion. One could argue that almost all proteins in a cell can potentially play some role in this regard as any change to cell homeostasis, be it from a pathogenic, cancerous, aging or autoimmune source, can signal to host systems to mobilise in order to revert the cell back to its homeostatic equilibrium. The host response to a pathogen for example, could therefore be considered not just in terms of the immune response, but should also consider the multitude of ways in which cellular process are disrupted and thus respond to threats [489]. Paying attention to these processes and how they dictate the balance of survival between say pathogen and host could provide many new targets for therapeutic interventions or at the very least bring a greater understand of what exactly occurs to a cell during pathogenic insult.

With the above concept in mind, the aim of chapters four and five were to delineate the host response to pathogenic insult – not at the level of a single protein, namely TRAM, but on a global scale, utilising a whole cell proteomic approach. Proteins whose expression is significantly modified in response to infection are considered mediators of host homeostatic change and are therefore potential targets for therapies that seeks to restore homeostasis. Two respiratory pathogens, one bacterial (*B. pertussis*) and one viral (HRV16), were chosen as the model pathogens owning to their contrasting taxonomy and comparable target in humans, the respiratory tract. Humans are also the primary reservoir for *B. pertussis* and HRV16 and both have thus evolved remarkable abilities to stubbornly resist eradication despite advances in medical science. The host proteomic response upon infection with each pathogen was thus characterised with comparisons between the two also made in order to more succinctly illustrate protein responses that are exclusive to either pathogen or that are inclusive of both.

Chapter four sought to examine the host whole cell proteomic response to *B. pertussis* infection and is the first time such a study has been attempted. Previously, a transcriptomic study using high density DNA microarrays examined the in-vitro host response to *B. pertussis* infection in the same cell-line (BEAS-2B) that was used the current study [181]. The researchers investigated the transcriptome of BEAS-2B cells following exposure to *B. pertussis* at a single time point and MOI in order to create an easily controlled and reproducible model of the interaction between the pathogen and its target cell type. The transcriptomic study found that upon *B. pertussis* infection for three hours, a dominant pro-inflammatory response was generated with numerous inflammatory genes upregulated including those encoding IL-8, IL-6 and IL-1β [181]. It was interesting that both IL-6 and IL-1β mRNAs were upregulated as the current work documented copious IL-6 production in response to *B. pertussis* (Figure 4.19), however no detectable IL-1β was detected. It may be possible that while IL-β mRNA is upregulated in response to *B. pertussis*, its secretion at the protein level may be somehow inhibited by a *B. pertussis* virulence factor. A further possibility is that BEAS-2B cells either lack, or express low levels of the inflammasome machinery required to sense *B. pertussis* and thus process pro-IL-1β into its mature, secretory form. The expression of NLRP12 was shown to be upregulated in response to *B. pertussis* however as no detectable IL-1β was secreted, this suggests that NLRP12 is not a major sensor of *B. pertussis* in BEAS-2B cells, at least with regard to mature IL-1β production. The disconnect between gene and protein expression was a recurring theme in the analysis of hits obtained through both 2D-DIGE MS and LFQ MS. Many proteins which were upregulated in response to *B. pertussis* infection such as SOD, TPI, NLRP12 and ferritin were not due to increased gene expression (Figures 4.15, 4.9 and 4.11). Similarly, the disconnect between IL-1β mRNA upregulation in [181] and the lack of secreted mature IL-1β in the current study illustrates a key drawback of transcriptomic studies. Dynamic gene expression in response to

cell perturbation does not necessarily correlate with protein expression [490]. Inferring that this is the case, without verification of corresponding protein levels, leads to false conclusions being drawn. Thus, a key benefit of the proteomic approach is simultaneously illustrated. Taking the trancriptomic study at face-value, one could be forgiven for expecting both IL-6 and IL-1β to be key effector molecules produced by BEAS-2B cells in response to *B. pertussis* when in fact only IL-6 is secreted in detectable quantities.

Both the transcriptomic [181] and current proteomic studies revealed the upregulation of several apoptosis factors with anti-apoptotic genes such as *tnfaip3* and *api2* dominating in the transcriptomic study and more pro-apoptotic proteins such as caspase 3 and caspase 7 in the proteomic study (Table 4.1, 4.2). This apparent shift to a pro-apoptotic fate can be explained by the different time points used in both studies with the transcriptional study infecting for 3 hr and the proteomic study for 12 hr. As *B. pertussis* is known to drive apoptosis in infected cells [438, 491], the shift from anti-apoptotic to pro-apoptotic proteins likely reflects the detrimental effect the replicating bacteria are having on the host cell viability at the later time point of 12 hr. Thus *B. pertussis* mediated apoptosis of infected cells in likely to proceed in a caspase 3 and caspase 7-dependent manner.

Another interesting pattern was the relatively large contribution that proteins associated with cancer and transcriptional/DNA editing processes appear to make to the changes in host homeostasis upon *B. pertussis* infection (Figure 4.12). It is estimated that approximately 15% of malignant cancers are attributed to infections with bacteria and viruses [492]. Examples include *Hylobacteria pyori* and gastric cancer and *Streptococcus bovis* with colon cancer [493, 494]. There is no known link between *B. pertussis* and cancer, however the large number of detected proteins with roles in DNA damage repair, DNA and RNA modifications and the cell cycle agree with the consensus that bacterial agents are capable of causing or at

least inducing similar pathways involved in tumorigenesis [492]. Pathogens such as *B. pertussis* that are capable of residing within the cell, like tumours, require metabolic resources which must be derived from the host. Thus like tumours [495], these requirements could potentially be targeted for disruption to supress bacterial replication – particularly during chronic infections. *B. pertussis*, if undetected regularly causes chronic infections [496] and this paradigm could potentially be used to target *B. pertussis*. However, a more useful intervention would be against antibiotic resistant bacteria such as methicillin-resistant *Staphylococcus aerus* (MRSA), which is also capable of surviving intracellularly [497]. Preventing these bacteria from increasing host intracellular metabolism and subverting it for their own needs could inhibit intracellular survival and thus reduce lethality.

Suppression of a number of protein hits failed to elicit any change in secretion of IL-6 (Figure 4.19A). However, this does not in any way mean that these proteins have no role to play in the host response to *B. pertussis*. Cytokine secretion is but one effector mechanism used by the cell and does not paint a complete picture regarding host response. Other defence mechanisms such as NO production could also be monitored as well as levels of bacterial replication and host cell death. Even better would be the use of in-vivo studies using mice deficient in each protein of interest. Alteration of survival upon loss of one of the protein hits would be the ideal illustration of a role for a particular protein in *B. pertussis* pathogenesis. Despite the lack of a cytokine related phenotype upon *B. pertussis* infection, suppression of PPP1Cα and stathmin 1 caused a significant reduction in TLR4 mediated IL-6 secretion (Figure 4.19B). The TLR4 ligand, LPS, is a noted virulence factor of *B. pertussis* however whilst *B. pertussis* is known to be recognised by TLR4, it is a relatively weak activator of this PRR compared to other members of the Bordetella family [498]. Thus *B. pertussis* may purposely seek to avoid or suppress the TLR4 response as host proteins stathmin and PPP1Cα, both upregulated by *B. pertussis*, appear to mediate TLR4's inflammatory response which ma

in turn negatively impact upon *B. pertussis* survival. Addition of TLR4 agonists as adjuvants to *B. pertussis* vaccine preparations may therefore aid the protective response generated. Indeed both acellular and whole cell pertussis vaccines show defective protection against disease in TLR4 deficient mice [143].

Chapter five sought to examine the proteome of BEAS-2B cells in response to infection with another respiratory pathogen, HRV16. The aims of the study were to ascertain the proteins that may potentially be involved in the host response to viral infection, whether these had any effect on the immune response to HRV16 and also to probe similarities observed between the proteome alterations upon HRV16 and *B. pertussis* infection.

The reduction in the number of HRV16 mediated protein hits with functions in metabolism compared to *B. pertussis* has already been discussed (Section 5.2.2), and serves to illustrate the difference in the host response to both pathogens. Another interesting observation was that approximately 25 % of protein hits altered upon HRV16 infection were also altered upon *B. pertussis* infection (Figure 5.3). Focusing on these proteins that were identified in both studies, 33 %, had previously demonstrated immune function, one quarter had documented links to cancer progression and one sixth have known involvements in redox pathways (Figure 5.3). Viral and bacterial co-infections in humans have been extensively reported upon with one of the best known examples being the synergism between *Streptococcus pneumoniae* and influenza which caused the 'Spanish flu' pandemic in 1918 [499]. This ability to coexist may be the result of shared patterns of host intracellular modification by certain bacteria and viruses thus rendering the cell weakened and amenable to coinfection [499]. Additionally, immune subversion mechanisms initiated by bacterial infections could increase susceptibility to viral coinfection and vice-versa. Indeed, the propensity for coinfection between *B. pertussis* and HRV was illustrated in a recent Dutch study on a cohort

of children who experienced prolonged coughing episodes found that the two most frequent pathogens encountered from swabs taken from the children were HRV (32 %) and *B. pertussis* (17 %) [500]. Moreover, the most frequent mixed infection was also HRV and *B. pertussis* which occurred in 10% of cases [500]. Thus it is proposed that the similarities in host proteome remodelling observed in response to both *B. pertussis* and HRV16 infection suggests that there are similar pathways utilised by both pathogens to supplement their individual replication. Future work will involve perturbing these pathways with the intention of curbing either individual pathogens or both. Again, the use of knockout mice combined with both individual and co-infection models with a focus on alterations in bacterial or viral load and mouse survival in knockout mice compared to WT strains would be the preferred model.

Knockdown of two protein hits that were upregulated upon HRV16 infection, stathmin 1 and DJ-1 did not have any effect on IL-6 production in response to HRV16 (Figure 5.9). This result mimics that observed upon *B. pertussis* infection as these two proteins, which were also found to be upregulated in response to *B. pertussis*, did not play a role in *B. pertussis* mediated IL-6 production (Figure 4.19A). Suppression of stathmin 1 and DJ-1 followed by stimulation of BEAS-2B cells with a HRV16 PAMP, dsRNA, in the form of poly(I:C) also had no effect on either IL-6, RANTES or type-I IFN secretion (Figure 5.9). It therefore remains to be seen what roles these proteins play in the host response to HRV16 infection. Further studies looking other cellular processes such as iNOS production and metabolism could be investigated. As mentioned earlier, alterations to viral replication could also be studied upon knockdown of these proteins. One interesting caveat that emerged from the poly(I:C) stimulations was that stathmin 1 suppression had no effect on poly(I:C) - TLR3 mediated IL-6 production (Figure 5.9A). This contrasts with LPS (TLR4) mediated IL-production which was significantly reduced upon stathmin 1 knockdown (Figure 4.19B).

Thus, it would appear that stathmin 1's role in TLR signalling is partially exclusive, at least to the TLR4 pathway. Stathmin's role in microtubule formation has already been aluded to (Table 4.1, 5.1). It has also been shown that both TLR4 and TLR2 colocalise with alpha-tubulin and align with microtubules in both dendritic cells and monocytes [501]. Moreover, microtubule disruption disturbed TLR2 and TLR4 expression and led to inhibition of IL-12 production [501]. Thus potential roles in the signalling pathways of other TLRs, particularly those capable of trafficking between the plasma membrane and endosomes, such as TLR2 [502] will have to be investigated in the future in order to further elucidate stathmin 1's role in TLR signalling.

6.2 Future work

Regarding Chapter 3, there are a number of further experiments that could supplement the current data. It was previously attempted to obtain primary WT and TRAM $^{-/-}$ BMDMs in order to confirm the observed phenotypes, however the once shipped, the cells failed to grow. This experiement should be attempted again. TRAM's role in TLR4 signalling has been shown to be dependent upon the adaptor TRIF which is immediately downstram of TRAM. Therefore, obtaining primary TRIF $^{-/-}$ BMDMs in order to define TRIF's role in TLR7 signalling would also be helpful.

RNA interference of TRAM in human cells indicated a similar role for human TRAM in the TLR7 pathway. However, these experiements looked only at cytokine mRNA induction. Measurement of protein secretion by ELISA could not be optimised in time and should be examined in future experiments.

It would be beneficial to provide further confirmation of TRAM's physical presence within the TLR7 pathway and thus TRAM's trafficking, localisation and protein-protein interactions

could be monitored at multiple timepoints using confocal microscopy to probe the position of fluorescently-tagged TRAM and other fluorescently-tagged proteins of interest such as TLR7, MyD88, TRIF, IRF3, IRF5, IRF7, TRAF6 and TRAF3.

Finally, it would be interesting to see if the survival of TRAM deficient mice is in any way altered compared to WT mice upon infection with a TLR7 activating ssRNA virus. One would have to be certain however, that only the TLR7 pathway is being activated. Thus perhaps an intra-peritoneal injection of the TLR7 ligand R848 could be attempted and survival motiored from here.

Focusing on Chapters's 4 and 5, again there are numerous experiments that could append the present data. Regarding the LFQ MS study of *B. pertussis* modulated proteins, it was disappointing that more proteins known to be involved in innate immune signalling were not identified as well as the fact that only two proteins identified by LFQ MS were also found using 2D-DIGE MS. Thus it would be useful to further optimise the LFQ MS protocol particularly the protein lysis, peptide preparation and the specific protocol used for the Q-Exactive MS/MS run. Once optimised, this technique could be applied to studying the whole-cell lysate of HRV16 infected cells also.

The experiements whereby esiRNA was used to reduce the endogenoud expression of selected hit proteins during infection with *B. pertussis* or HRV16 did produce some interesting results however they were limited by the small number of cytokine readouts. It is possible to purchase commercially produced cytokine arrays tailored to specific cell types (such as the epithelial cells used in the current work) which could simultaneously profile the secretion of many cytokines between control and knockdown states upon infection with *B.*

pertussis or HRV16. This could therefore provide a much broader characterisation of the role of the selected proteins in cytokine secretion during an infection scerario.

Cytokines are not the only possible downstream effector function that could be modulated by the selected proteins however. Other processes such as ROS production could also be monitored. Additionally, both bacterial and viral load could be tracked in order to see if the survival of *B. pertussis* or HRV16 is being impeded or indeed facilitated by the suppression of the selected proteins.

Chapter 7

Bibliography

1. Turvey, S.E. and D.H. Broide, *Innate immunity.* J Allergy Clin Immunol, 2010. **125**(2 Suppl 2): p. S24-32.
2. O'Neill, L.A., D. Golenbock, and A.G. Bowie, *The history of Toll-like receptors - redefining innate immunity.* Nat Rev Immunol, 2013. **13**(6): p. 453-60.
3. Aderem, A. and R.J. Ulevitch, *Toll-like receptors in the induction of the innate immune response.* Nature, 2000. **406**(6797): p. 782-7.
4. Anderson, K.V., G. Jurgens, and C. Nusslein-Volhard, *Establishment of dorsal-ventral polarity in the Drosophila embryo: genetic studies on the role of the Toll gene product.* Cell, 1985. **42**(3): p. 779-89.
5. Lemaitre, B., et al., *The dorsoventral regulatory gene cassette spatzle/Toll/cactus controls the potent antifungal response in Drosophila adults.* Cell, 1996. **86**(6): p. 973-83.
6. Williams, M.J., et al., *The 18-wheeler mutation reveals complex antibacterial gene regulation in Drosophila host defense.* EMBO J, 1997. **16**(20): p. 6120-30.
7. Poltorak A, H.X., Smirnova I, Liu MY, Van Huffel C, Du X, Birdwell D, Alejos E, Silva M, Galanos C, Freudenberg M, Ricciardi-Castagnoli P, Layton B, Beutler B., *Defective LPS signaling in C3H/HeJ and C57BL/10ScCr mice: mutations in Tlr4 gene.* Science, 1998. **282**(5396): p. 2085-8.
8. Rock, F.L., et al., *A family of human receptors structurally related to Drosophila Toll.* Proc Natl Acad Sci U S A, 1998. **95**(2): p. 588-93.
9. Boyd, A., V.J. Philbin, and A.L. Smith, *Conserved and distinct aspects of the avian Toll-like receptor (TLR) system: implications for transmission and control of bird-borne zoonoses.* Biochem Soc Trans, 2007. **35**(Pt 6): p. 1504-7.
10. Roach, J.C., et al., *The evolution of vertebrate Toll-like receptors.* Proc Natl Acad Sci U S A, 2005. **102**(27): p. 9577-82.
11. Jordan, T., S. Schornack, and T. Lahaye, *Alternative splicing of transcripts encoding Toll-like plant resistance proteins - what's the functional relevance to innate immunity?* Trends Plant Sci, 2002. **7**(9): p. 392-8.
12. O'Neill, L.A. and A.G. Bowie, *The family of five: TIR-domain-containing adaptors in Toll-like receptor signalling.* Nat Rev Immunol, 2007. **7**(5): p. 353-64.
13. Miggin, S.M. and L.A. O'Neill, *New insights into the regulation of TLR signaling.* J Leukoc Biol, 2006. **80**(2): p. 220-6.
14. Lu, J. and P.D. Sun, *The structure of the TLR5-flagellin complex: a new mode of pathogen detection, conserved receptor dimerization for signaling.* Sci Signal, 2012. **5**(223): p. pe11.
15. Kawai, T. and S. Akira, *The role of pattern-recognition receptors in innate immunity: update on Toll-like receptors.* Nat Immunol, 2010. **11**(5): p. 373-84.
16. Hasan, U., et al., *Human TLR10 is a functional receptor, expressed by B cells and plasmacytoid dendritic cells, which activates gene transcription through MyD88.* J Immunol, 2005. **174**(5): p. 2942-50.
17. Chen, G.Y. and G. Nunez, *Sterile inflammation: sensing and reacting to damage.* Nat Rev Immunol, 2010. **10**(12): p. 826-37.
18. Gay, N.J., M. Gangloff, and A.N. Weber, *Toll-like receptors as molecular switches.* Nat Rev Immunol, 2006. **6**(9): p. 693-8.
19. Akira, S. and K. Takeda, *Toll-like receptor signalling.* Nat Rev Immunol, 2004. **4**(7): p. 499-511.
20. Kawai, T. and S. Akira, *TLR signaling.* Cell Death Differ, 2006. **13**(5): p. 816-25.
21. Kenny, E.F., et al., *MyD88 adaptor-like is not essential for TLR2 signaling and inhibits signaling by TLR3.* J Immunol, 2009. **183**(6): p. 3642-51.
22. Fitzgerald, K.A., et al., *Mal (MyD88-adapter-like) is required for Toll-like receptor-4 signal transduction.* Nature, 2001. **413**(6851): p. 78-83.
23. Fitzgerald, K.A., et al., *LPS-TLR4 signaling to IRF-3/7 and NF-kappaB involves the toll adapters TRAM and TRIF.* J Exp Med, 2003. **198**(7): p. 1043-55.

24. Yamamoto, M., et al., *TRAM is specifically involved in the Toll-like receptor 4-mediated MyD88-independent signaling pathway.* Nat Immunol, 2003. **4**(11): p. 1144-50.
25. Carty, M., et al., *The human adaptor SARM negatively regulates adaptor protein TRIF-dependent Toll-like receptor signaling.* Nat Immunol, 2006. **7**(10): p. 1074-81.
26. Watters, T.M., E.F. Kenny, and L.A. O'Neill, *Structure, function and regulation of the Toll/IL-1 receptor adaptor proteins.* Immunol Cell Biol, 2007. **85**(6): p. 411-9.
27. Lord, K.A., B. Hoffman-Liebermann, and D.A. Liebermann, *Nucleotide sequence and expression of a cDNA encoding MyD88, a novel myeloid differentiation primary response gene induced by IL6.* Oncogene, 1990. **5**(7): p. 1095-7.
28. Jenkins, K.A. and A. Mansell, *TIR-containing adaptors in Toll-like receptor signalling.* Cytokine, 2010. **49**(3): p. 237-44.
29. Wesche, H., et al., *MyD88: an adapter that recruits IRAK to the IL-1 receptor complex.* Immunity, 1997. **7**(6): p. 837-47.
30. Muzio, M., et al., *IRAK (Pelle) family member IRAK-2 and MyD88 as proximal mediators of IL-1 signaling.* Science, 1997. **278**(5343): p. 1612-5.
31. Harroch, S., et al., *5' upstream sequences of MyD88, an IL-6 primary response gene in M1 cells: detection of functional IRF-1 and Stat factors binding sites.* Nucleic Acids Res, 1995. **23**(17): p. 3539-46.
32. Adachi, O., et al., *Targeted disruption of the MyD88 gene results in loss of IL-1- and IL-18-mediated function.* Immunity, 1998. **9**(1): p. 143-50.
33. Kawai, T., et al., *Unresponsiveness of MyD88-deficient mice to endotoxin.* Immunity, 1999. **11**(1): p. 115-22.
34. Takeuchi, O., et al., *Cellular responses to bacterial cell wall components are mediated through MyD88-dependent signaling cascades.* Int Immunol, 2000. **12**(1): p. 113-7.
35. Takeuchi, O., et al., *Cutting edge: preferentially the R-stereoisomer of the mycoplasmal lipopeptide macrophage-activating lipopeptide-2 activates immune cells through a toll-like receptor 2- and MyD88-dependent signaling pathway.* J Immunol, 2000. **164**(2): p. 554-7.
36. Schnare, M., et al., *Recognition of CpG DNA is mediated by signaling pathways dependent on the adaptor protein MyD88.* Curr Biol, 2000. **10**(18): p. 1139-42.
37. Takeuchi, O., K. Hoshino, and S. Akira, *Cutting edge: TLR2-deficient and MyD88-deficient mice are highly susceptible to Staphylococcus aureus infection.* J Immunol, 2000. **165**(10): p. 5392-6.
38. Hemmi, H., et al., *A Toll-like receptor recognizes bacterial DNA.* Nature, 2000. **408**(6813): p. 740-5.
39. Hayashi, F., et al., *The innate immune response to bacterial flagellin is mediated by Toll-like receptor 5.* Nature, 2001. **410**(6832): p. 1099-103.
40. Hemmi, H., et al., *Small anti-viral compounds activate immune cells via the TLR7 MyD88-dependent signaling pathway.* Nat Immunol, 2002. **3**(2): p. 196-200.
41. Oshiumi, H., et al., *TICAM-1, an adaptor molecule that participates in Toll-like receptor 3-mediated interferon-beta induction.* Nat Immunol, 2003. **4**(2): p. 161-7.
42. Hidmark, A., A. von Saint Paul, and A.H. Dalpke, *Cutting edge: TLR13 is a receptor for bacterial RNA.* J Immunol, 2012. **189**(6): p. 2717-21.
43. Lin, S.C., Y.C. Lo, and H. Wu, *Helical assembly in the MyD88-IRAK4-IRAK2 complex in TLR/IL-1R signalling.* Nature, 2010. **465**(7300): p. 885-90.
44. Motshwene, P.G., et al., *An oligomeric signaling platform formed by the Toll-like receptor signal transducers MyD88 and IRAK-4.* J Biol Chem, 2009. **284**(37): p. 25404-11.
45. Suzuki, N., et al., *Severe impairment of interleukin-1 and Toll-like receptor signalling in mice lacking IRAK-4.* Nature, 2002. **416**(6882): p. 750-6.
46. Qian, Y., et al., *IRAK-mediated translocation of TRAF6 and TAB2 in the interleukin-1-induced activation of NFkappa B.* J Biol Chem, 2001. **276**(45): p. 41661-7.

47. Skaug, B., X. Jiang, and Z.J. Chen, *The role of ubiquitin in NF-kappaB regulatory pathways.* Annu Rev Biochem, 2009. **78**: p. 769-96.
48. Takeda, K. and S. Akira, *TLR signaling pathways.* Semin Immunol, 2004. **16**(1): p. 3-9.
49. Horng, T., G.M. Barton, and R. Medzhitov, *TIRAP: an adapter molecule in the Toll signaling pathway.* Nat Immunol, 2001. **2**(9): p. 835-41.
50. Kagan, J.C. and R. Medzhitov, *Phosphoinositide-mediated adaptor recruitment controls Toll-like receptor signaling.* Cell, 2006. **125**(5): p. 943-55.
51. Dunne, A., et al., *Structural complementarity of Toll/interleukin-1 receptor domains in Toll-like receptors and the adaptors Mal and MyD88.* J Biol Chem, 2003. **278**(42): p. 41443-51.
52. Nunez Miguel, R., et al., *A dimer of the Toll-like receptor 4 cytoplasmic domain provides a specific scaffold for the recruitment of signalling adaptor proteins.* PLoS One, 2007. **2**(8): p. e788.
53. Moynagh, P.N., *The Pellino family: IRAK E3 ligases with emerging roles in innate immune signalling.* Trends Immunol, 2009. **30**(1): p. 33-42.
54. Sheedy, F.J. and L.A. O'Neill, *The Troll in Toll: Mal and Tram as bridges for TLR2 and TLR4 signaling.* J Leukoc Biol, 2007. **82**(2): p. 196-203.
55. Mansell, A., et al., *Suppressor of cytokine signaling 1 negatively regulates Toll-like receptor signaling by mediating Mal degradation.* Nat Immunol, 2006. **7**(2): p. 148-55.
56. Gray, P., et al., *MyD88 adapter-like (Mal) is phosphorylated by Bruton's tyrosine kinase during TLR2 and TLR4 signal transduction.* J Biol Chem, 2006. **281**(15): p. 10489-95.
57. Dunne, A., et al., *IRAK1 and IRAK4 promote phosphorylation, ubiquitination, and degradation of MyD88 adaptor-like (Mal).* J Biol Chem, 2010. **285**(24): p. 18276-82.
58. Miggin, S.M., et al., *NF-kappaB activation by the Toll-IL-1 receptor domain protein MyD88 adapter-like is regulated by caspase-1.* Proc Natl Acad Sci U S A, 2007. **104**(9): p. 3372-7.
59. Khor, C.C., et al., *A Mal functional variant is associated with protection against invasive pneumococcal disease, bacteremia, malaria and tuberculosis.* Nat Genet, 2007. **39**(4): p. 523-8.
60. Ferwerda, B., et al., *Functional and genetic evidence that the Mal/TIRAP allele variant 180L has been selected by providing protection against septic shock.* Proc Natl Acad Sci U S A, 2009. **106**(25): p. 10272-7.
61. Hawn, T.R., et al., *A polymorphism in Toll-interleukin 1 receptor domain containing adaptor protein is associated with susceptibility to meningeal tuberculosis.* J Infect Dis, 2006. **194**(8): p. 1127-34.
62. Yamamoto, M., et al., *Cutting edge: a novel Toll/IL-1 receptor domain-containing adapter that preferentially activates the IFN-beta promoter in the Toll-like receptor signaling.* J Immunol, 2002. **169**(12): p. 6668-72.
63. Yamamoto, M., et al., *Role of adaptor TRIF in the MyD88-independent toll-like receptor signaling pathway.* Science, 2003. **301**(5633): p. 640-3.
64. Hoebe, K., et al., *Identification of Lps2 as a key transducer of MyD88-independent TIR signalling.* Nature, 2003. **424**(6950): p. 743-8.
65. Tatematsu, M., et al., *A molecular mechanism for Toll-IL-1 receptor domain-containing adaptor molecule-1-mediated IRF-3 activation.* J Biol Chem, 2010. **285**(26): p. 20128-36.
66. Sasai, M., et al., *Cutting Edge: NF-kappaB-activating kinase-associated protein 1 participates in TLR3/Toll-IL-1 homology domain-containing adapter molecule-1-mediated IFN regulatory factor 3 activation.* J Immunol, 2005. **174**(1): p. 27-30.
67. Tamura, T., et al., *The IRF family transcription factors in immunity and oncogenesis.* Annu Rev Immunol, 2008. **26**: p. 535-84.
68. Oganesyan, G., et al., *Critical role of TRAF3 in the Toll-like receptor-dependent and -independent antiviral response.* Nature, 2006. **439**(7073): p. 208-11.
69. Hacker, H., et al., *Specificity in Toll-like receptor signalling through distinct effector functions of TRAF3 and TRAF6.* Nature, 2006. **439**(7073): p. 204-7.

70. Sasai, M., et al., *Direct binding of TRAF2 and TRAF6 to TICAM-1/TRIF adaptor participates in activation of the Toll-like receptor 3/4 pathway.* Mol Immunol, 2010. **47**(6): p. 1283-91.
71. Gauzzi, M.C., M. Del Corno, and S. Gessani, *Dissecting TLR3 signalling in dendritic cells.* Immunobiology, 2010. **215**(9-10): p. 713-23.
72. Meylan, E., et al., *RIP1 is an essential mediator of Toll-like receptor 3-induced NF-kappa B activation.* Nat Immunol, 2004. **5**(5): p. 503-7.
73. Cusson-Hermance, N., et al., *Rip1 mediates the Trif-dependent toll-like receptor 3- and 4-induced NF-{kappa}B activation but does not contribute to interferon regulatory factor 3 activation.* J Biol Chem, 2005. **280**(44): p. 36560-6.
74. Han, K.J., et al., *Mechanisms of the TRIF-induced interferon-stimulated response element and NF-kappaB activation and apoptosis pathways.* J Biol Chem, 2004. **279**(15): p. 15652-61.
75. Choi, Y.J., et al., *TRIF mediates Toll-like receptor 5-induced signaling in intestinal epithelial cells.* J Biol Chem, 2010. **285**(48): p. 37570-8.
76. Choi, Y.J., et al., *TRIF modulates TLR5-dependent responses by inducing proteolytic degradation of TLR5.* J Biol Chem, 2010. **285**(28): p. 21382-90.
77. Zhang, Z., et al., *DDX1, DDX21, and DHX36 helicases form a complex with the adaptor molecule TRIF to sense dsRNA in dendritic cells.* Immunity, 2011. **34**(6): p. 866-78.
78. Stack, J., et al., *Vaccinia virus protein A46R targets multiple Toll-like-interleukin-1 receptor adaptors and contributes to virulence.* J Exp Med, 2005. **201**(6): p. 1007-18.
79. Harte, M.T., et al., *The poxvirus protein A52R targets Toll-like receptor signaling complexes to suppress host defense.* J Exp Med, 2003. **197**(3): p. 343-51.
80. Li, K., et al., *Immune evasion by hepatitis C virus NS3/4A protease-mediated cleavage of the Toll-like receptor 3 adaptor protein TRIF.* Proc Natl Acad Sci U S A, 2005. **102**(8): p. 2992-7.
81. Bin, L.H., L.G. Xu, and H.B. Shu, *TIRP, a novel Toll/interleukin-1 receptor (TIR) domain-containing adapter protein involved in TIR signaling.* J Biol Chem, 2003. **278**(27): p. 24526-32.
82. Rowe, D.C., et al., *The myristoylation of TRIF-related adaptor molecule is essential for Toll-like receptor 4 signal transduction.* Proc Natl Acad Sci U S A, 2006. **103**(16): p. 6299-304.
83. McGettrick, A.F., et al., *Trif-related adapter molecule is phosphorylated by PKC{epsilon} during Toll-like receptor 4 signaling.* Proc Natl Acad Sci U S A, 2006. **103**(24): p. 9196-201.
84. Kagan, J.C., et al., *TRAM couples endocytosis of Toll-like receptor 4 to the induction of interferon-beta.* Nat Immunol, 2008. **9**(4): p. 361-8.
85. Lysakova-Devine, T., et al., *Viral inhibitory peptide of TLR4, a peptide derived from vaccinia protein A46, specifically inhibits TLR4 by directly targeting MyD88 adaptor-like and TRIF-related adaptor molecule.* J Immunol, 2010. **185**(7): p. 4261-71.
86. Palsson-McDermott, E.M., et al., *TAG, a splice variant of the adaptor TRAM, negatively regulates the adaptor MyD88-independent TLR4 pathway.* Nat Immunol, 2009. **10**(6): p. 579-86.
87. Doyle, S.L., et al., *The GOLD domain-containing protein TMED7 inhibits TLR4 signalling from the endosome upon LPS stimulation.* Nat Commun, 2012. **3**: p. 707.
88. Mink, M., et al., *A novel human gene (SARM) at chromosome 17q11 encodes a protein with a SAM motif and structural similarity to Armadillo/beta-catenin that is conserved in mouse, Drosophila, and Caenorhabditis elegans.* Genomics, 2001. **74**(2): p. 234-44.
89. Couillault, C., et al., *TLR-independent control of innate immunity in Caenorhabditis elegans by the TIR domain adaptor protein TIR-1, an ortholog of human SARM.* Nat Immunol, 2004. **5**(5): p. 488-94.
90. Hou, Y.J., et al., *SARM is required for neuronal injury and cytokine production in response to central nervous system viral infection.* J Immunol, 2013. **191**(2): p. 875-83.
91. Szretter, K.J., et al., *The immune adaptor molecule SARM modulates tumor necrosis factor alpha production and microglia activation in the brainstem and restricts West Nile Virus pathogenesis.* J Virol, 2009. **83**(18): p. 9329-38.

92. Johnson, A.C., X. Li, and E. Pearlman, *MyD88 functions as a negative regulator of TLR3/TRIF-induced corneal inflammation by inhibiting activation of c-Jun N-terminal kinase.* J Biol Chem, 2008. **283**(7): p. 3988-96.
93. Siednienko, J., et al., *Absence of MyD88 results in enhanced TLR3-dependent phosphorylation of IRF3 and increased IFN-beta and RANTES production.* J Immunol, 2011. **186**(4): p. 2514-22.
94. Siednienko, J., et al., *TLR3-mediated IFN-beta gene induction is negatively regulated by the TLR adaptor MyD88 adaptor-like.* Eur J Immunol, 2010. **40**(11): p. 3150-60.
95. Wilkinson, K.D., *The discovery of ubiquitin-dependent proteolysis.* Proc Natl Acad Sci U S A, 2005. **102**(43): p. 15280-2.
96. McCarthy, J.J., H.L. McLeod, and G.S. Ginsburg, *Genomic medicine: a decade of successes, challenges, and opportunities.* Sci Transl Med, 2013. **5**(189): p. 189sr4.
97. Cox, J. and M. Mann, *Is proteomics the new genomics?* Cell, 2007. **130**(3): p. 395-8.
98. Latz, E., T.S. Xiao, and A. Stutz, *Activation and regulation of the inflammasomes.* Nat Rev Immunol, 2013. **13**(6): p. 397-411.
99. Tyers, M. and M. Mann, *From genomics to proteomics.* Nature, 2003. **422**(6928): p. 193-7.
100. Paul, D., et al., *Mass spectrometry-based proteomics in molecular diagnostics: discovery of cancer biomarkers using tissue culture.* Biomed Res Int, 2013. **2013**: p. 783131.
101. Ong, S.E., et al., *Stable isotope labeling by amino acids in cell culture, SILAC, as a simple and accurate approach to expression proteomics.* Mol Cell Proteomics, 2002. **1**(5): p. 376-86.
102. Zhu, W., J.W. Smith, and C.M. Huang, *Mass spectrometry-based label-free quantitative proteomics.* J Biomed Biotechnol, 2010. **2010**: p. 840518.
103. Hanash, S.M., J. Madoz-Gurpide, and D.E. Misek, *Identification of novel targets for cancer therapy using expression proteomics.* Leukemia, 2002. **16**(4): p. 478-85.
104. Hanash, S., *Disease proteomics.* Nature, 2003. **422**(6928): p. 226-32.
105. Evans, G., et al., *Construction of HSC-2DPAGE: a two-dimensional gel electrophoresis database of heart proteins.* Electrophoresis, 1997. **18**(3-4): p. 471-9.
106. Heinke, M.Y., et al., *Protein changes observed in pacing-induced heart failure using two-dimensional electrophoresis.* Electrophoresis, 1998. **19**(11): p. 2021-30.
107. Zhou, G., et al., *2D differential in-gel electrophoresis for the identification of esophageal scans cell cancer-specific protein markers.* Mol Cell Proteomics, 2002. **1**(2): p. 117-24.
108. McKenna, M., *Antibiotic resistance: the last resort.* Nature, 2013. **499**(7459): p. 394-6.
109. Lasonder, E., et al., *Analysis of the Plasmodium falciparum proteome by high-accuracy mass spectrometry.* Nature, 2002. **419**(6906): p. 537-42.
110. Florens, L., et al., *A proteomic view of the Plasmodium falciparum life cycle.* Nature, 2002. **419**(6906): p. 520-6.
111. Gardner, M.J., et al., *Genome sequence of the human malaria parasite Plasmodium falciparum.* Nature, 2002. **419**(6906): p. 498-511.
112. Huber, L.A., *Is proteomics heading in the wrong direction?* Nat Rev Mol Cell Biol, 2003. **4**(1): p. 74-80.
113. Hill, A.A., et al., *Genomic analysis of gene expression in C. elegans.* Science, 2000. **290**(5492): p. 809-12.
114. Caron, H., et al., *The human transcriptome map: clustering of highly expressed genes in chromosomal domains.* Science, 2001. **291**(5507): p. 1289-92.
115. Huang, Q., et al., *The plasticity of dendritic cell responses to pathogens and their components.* Science, 2001. **294**(5543): p. 870-5.
116. Luber, C.A., et al., *Quantitative proteomics reveals subset-specific viral recognition in dendritic cells.* Immunity, 2010. **32**(2): p. 279-89.
117. Meissner, F., et al., *Direct proteomic quantification of the secretome of activated immune cells.* Science, 2013. **340**(6131): p. 475-8.
118. Gerlach, G., et al., *Evolutionary trends in the genus Bordetella.* Microbes Infect, 2001. **3**(1): p. 61-72.

119. Mallory, F.B. and A.A. Hornor, *Pertussis: The histological Lesion in the Respiratory Tract.* J Med Res, 1912. **27**(2): p. 115-124 3.
120. Groisman, E.A., *Principles of bacterial pathogenesis*. 2000, San Diego, Calif. ; London: Academic.
121. Guiso, N., *Bordetella pertussis and pertussis vaccines.* Clin Infect Dis, 2009. **49**(10): p. 1565-9.
122. Bordet J., G.O., *Le microbe de la coqueluche.* Ann. Inst. Pasteur (Paris) 1906. **20**: p. 731–741
123. Bergey, D.H. and J.G. Holt, *Bergey's manual of systematic bacteriology*. 1984, Baltimore, Md.: Williams & Wilkins.
124. Leslie, P.H. and A.D. Gardner, *The Phases of Haemophilus pertussis.* J Hyg (Lond), 1931. **31**(3): p. 423-34.
125. Goldman, W.E., D.G. Klapper, and J.B. Baseman, *Detection, isolation, and analysis of a released Bordetella pertussis product toxic to cultured tracheal cells.* Infect Immun, 1982. **36**(2): p. 782-94.
126. Furman, B.L., A.C. Wardlaw, and L.Q. Stevenson, *Bordetella pertussis-induced hyperinsulinaemia without marked hypoglycaemia: a paradox explained.* Br J Exp Pathol, 1981. **62**(5): p. 504-11.
127. Crawford, J.G. and C.W. Fishel, *Growth of Bordetella pertussis in tissue culture.* J Bacteriol, 1959. **77**(4): p. 465-74.
128. Gray, D.F. and C. Cheers, *The steady state in cellular immunity. II. Immunological complaisance in murine pertussis.* Aust J Exp Biol Med Sci, 1967. **45**(4): p. 417-26.
129. Hopewell, J.W., L.B. Holt, and T.R. Desombre, *An electron-microscope study of intracerebral infection of mice with low-virulence Bordetella pertussis.* J Med Microbiol, 1972. **5**(1): p. 154-7.
130. Ewanowich, C.A., et al., *Invasion of HeLa 229 cells by virulent Bordetella pertussis.* Infect Immun, 1989. **57**(9): p. 2698-704.
131. Mattoo, S. and J.D. Cherry, *Molecular pathogenesis, epidemiology, and clinical manifestations of respiratory infections due to Bordetella pertussis and other Bordetella subspecies.* Clin Microbiol Rev, 2005. **18**(2): p. 326-82.
132. Kerr, J.R. and R.C. Matthews, *Bordetella pertussis infection: pathogenesis, diagnosis, management, and the role of protective immunity.* Eur J Clin Microbiol Infect Dis, 2000. **19**(2): p. 77-88.
133. Munoz, J.J. and M.G. Peacock, *Action of pertussigen (pertussis toxin) on serum IgE and on Fc epsilon receptors on lymphocytes.* Cell Immunol, 1990. **127**(2): p. 327-36.
134. Tuomanen, E. and A. Weiss, *Characterization of two adhesins of Bordetella pertussis for human ciliated respiratory-epithelial cells.* J Infect Dis, 1985. **152**(1): p. 118-25.
135. Cahill, E.S., et al., *Mice are protected against Bordetella pertussis infection by intra-nasal immunization with filamentous haemagglutinin.* FEMS Microbiol Lett, 1993. **107**(2-3): p. 211-6.
136. Ishibashi, Y. and A. Nishikawa, *Bordetella pertussis infection of human respiratory epithelial cells up-regulates intercellular adhesion molecule-1 expression: role of filamentous hemagglutinin and pertussis toxin.* Microb Pathog, 2002. **33**(3): p. 115-25.
137. Relman, D., et al., *Recognition of a bacterial adhesion by an integrin: macrophage CR3 (alpha M beta 2, CD11b/CD18) binds filamentous hemagglutinin of Bordetella pertussis.* Cell, 1990. **61**(7): p. 1375-82.
138. Lamberti, Y.A., et al., *Intracellular trafficking of Bordetella pertussis in human macrophages.* Infect Immun, 2010. **78**(3): p. 907-13.
139. Higgs, R., et al., *Immunity to the respiratory pathogen Bordetella pertussis.* Mucosal Immunol, 2012. **5**(5): p. 485-500.
140. Khelef, N., et al., *Characterization of murine lung inflammation after infection with parental Bordetella pertussis and mutants deficient in adhesins or toxins.* Infect Immun, 1994. **62**(7): p. 2893-900.

141. McGuirk, P., et al., *Compartmentalization of T cell responses following respiratory infection with Bordetella pertussis: hyporesponsiveness of lung T cells is associated with modulated expression of the co-stimulatory molecule CD28.* Eur J Immunol, 1998. **28**(1): p. 153-63.
142. Mahon, B.P. and K.H. Mills, *Interferon-gamma mediated immune effector mechanisms against Bordetella pertussis.* Immunol Lett, 1999. **68**(2-3): p. 213-7.
143. Higgins, S.C., et al., *TLR4 mediates vaccine-induced protective cellular immunity to Bordetella pertussis: role of IL-17-producing T cells.* J Immunol, 2006. **177**(11): p. 7980-9.
144. Byrne, P., et al., *Depletion of NK cells results in disseminating lethal infection with Bordetella pertussis associated with a reduction of antigen-specific Th1 and enhancement of Th2, but not Tr1 cells.* Eur J Immunol, 2004. **34**(9): p. 2579-88.
145. Wood, N. and P. McIntyre, *Pertussis: review of epidemiology, diagnosis, management and prevention.* Paediatr Respir Rev, 2008. **9**(3): p. 201-11; quiz 211-2.
146. Ntezayabo, B., G. De Serres, and B. Duval, *Pertussis resurgence in Canada largely caused by a cohort effect.* Pediatr Infect Dis J, 2003. **22**(1): p. 22-7.
147. Guris, D., et al., *Changing epidemiology of pertussis in the United States: increasing reported incidence among adolescents and adults, 1990-1996.* Clin Infect Dis, 1999. **28**(6): p. 1230-7.
148. Celentano, L.P., et al., *Resurgence of pertussis in Europe.* Pediatr Infect Dis J, 2005. **24**(9): p. 761-5.
149. He, Q., et al., *Bordetella pertussis protein pertactin induces type-specific antibodies: one possible explanation for the emergence of antigenic variants?* J Infect Dis, 2003. **187**(8): p. 1200-5.
150. Vidakovics, M.L., et al., *Profiling the Bordetella pertussis proteome during iron starvation.* J Proteome Res, 2007. **6**(7): p. 2518-28.
151. Serra, D.O., et al., *Proteome approaches combined with Fourier transform infrared spectroscopy revealed a distinctive biofilm physiology in Bordetella pertussis.* Proteomics, 2008. **8**(23-24): p. 4995-5010.
152. Williamson, Y.M., et al., *A gel-free proteomic-based method for the characterization of Bordetella pertussis clinical isolates.* J Microbiol Methods, 2012. **90**(2): p. 119-33.
153. Price, W.H., *The Isolation of a New Virus Associated with Respiratory Clinical Disease in Humans.* Proc Natl Acad Sci U S A, 1956. **42**(12): p. 892-6.
154. Bochkov, Y.A., et al., *Molecular modeling, organ culture and reverse genetics for a newly identified human rhinovirus C.* Nat Med, 2011. **17**(5): p. 627-32.
155. Peltola, V., et al., *Clinical effects of rhinovirus infections.* J Clin Virol, 2008. **43**(4): p. 411-4.
156. Uncapher, C.R., C.M. DeWitt, and R.J. Colonno, *The major and minor group receptor families contain all but one human rhinovirus serotype.* Virology, 1991. **180**(2): p. 814-7.
157. Hadfield, A.T., et al., *The refined structure of human rhinovirus 16 at 2.15 A resolution: implications for the viral life cycle.* Structure, 1997. **5**(3): p. 427-41.
158. Oliveira, M.A., et al., *The structure of human rhinovirus 16.* Structure, 1993. **1**(1): p. 51-68.
159. Olson, N.H., et al., *Structure of a human rhinovirus complexed with its receptor molecule.* Proc Natl Acad Sci U S A, 1993. **90**(2): p. 507-11.
160. Bella, J. and M.G. Rossmann, *ICAM-1 receptors and cold viruses.* Pharm Acta Helv, 2000. **74**(2-3): p. 291-7.
161. Lonberg-Holm, K. and B.D. Korant, *Early interaction of rhinoviruses with host cells.* J Virol, 1972. **9**(1): p. 29-40.
162. Jacobs, S.E., et al., *Human rhinoviruses.* Clin Microbiol Rev, 2013. **26**(1): p. 135-62.
163. Kennedy, J.L., et al., *Pathogenesis of rhinovirus infection.* Curr Opin Virol, 2012. **2**(3): p. 287-93.
164. Andino, R., et al., *Intracellular determinants of picornavirus replication.* Trends Microbiol, 1999. **7**(2): p. 76-82.
165. Winther, B., et al., *Light and scanning electron microscopy of nasal biopsy material from patients with naturally acquired common colds.* Acta Otolaryngol, 1984. **97**(3-4): p. 309-18.

166. Winther, B., et al., *Sites of rhinovirus recovery after point inoculation of the upper airway.* JAMA, 1986. **256**(13): p. 1763-7.
167. Sajjan, U., et al., *Rhinovirus disrupts the barrier function of polarized airway epithelial cells.* Am J Respir Crit Care Med, 2008. **178**(12): p. 1271-81.
168. Corne, J.M., et al., *Frequency, severity, and duration of rhinovirus infections in asthmatic and non-asthmatic individuals: a longitudinal cohort study.* Lancet, 2002. **359**(9309): p. 831-4.
169. Triantafilou, K., et al., *Human rhinovirus recognition in non-immune cells is mediated by Toll-like receptors and MDA-5, which trigger a synergetic pro-inflammatory immune response.* Virulence, 2011. **2**(1): p. 22-9.
170. Slater, L., et al., *Co-ordinated role of TLR3, RIG-I and MDA5 in the innate response to rhinovirus in bronchial epithelium.* PLoS Pathog, 2010. **6**(11): p. e1001178.
171. Turner, R.B., et al., *Association between interleukin-8 concentration in nasal secretions and severity of symptoms of experimental rhinovirus colds.* Clin Infect Dis, 1998. **26**(4): p. 840-6.
172. Proud, D., et al., *Kinins are generated in nasal secretions during natural rhinovirus colds.* J Infect Dis, 1990. **161**(1): p. 120-3.
173. Kainulainen, L., et al., *Recurrent and persistent respiratory tract viral infections in patients with primary hypogammaglobulinemia.* J Allergy Clin Immunol, 2010. **126**(1): p. 120-6.
174. Barclay, W.S., et al., *The time course of the humoral immune response to rhinovirus infection.* Epidemiol Infect, 1989. **103**(3): p. 659-69.
175. Fraenkel, D.J., et al., *Lower airways inflammation during rhinovirus colds in normal and in asthmatic subjects.* Am J Respir Crit Care Med, 1995. **151**(3 Pt 1): p. 879-86.
176. Tacon, C.E., et al., *Rhinovirus-induced MMP-9 expression is dependent on Fra-1, which is modulated by formoterol and dexamethasone.* J Immunol, 2012. **188**(9): p. 4621-30.
177. Zalman, L.S., et al., *Inhibition of human rhinovirus-induced cytokine production by AG7088, a human rhinovirus 3C protease inhibitor.* Antimicrob Agents Chemother, 2000. **44**(5): p. 1236-41.
178. Ian Morris, L.L., Haiqian Shen, Edward Medina, Molly Bergman, and Michael Berton1. *A novel TRIF-independent role for the TLR adaptor molecule TRAM during infection with Francisella tularensis.* in *The Journal of Immunology*. 2012.
179. Ohnishi, H., et al., *TRAM is involved in IL-18 signaling and functions as a sorting adaptor for MyD88.* PLoS One, 2012. **7**(6): p. e38423.
180. Tanaka, S., et al., *Transcriptome analysis of mouse brain infected with Toxoplasma gondii.* Infect Immun, 2013. **81**(10): p. 3609-19.
181. Belcher, C.E., et al., *The transcriptional responses of respiratory epithelial cells to Bordetella pertussis reveal host defensive and pathogen counter-defensive strategies.* Proc Natl Acad Sci U S A, 2000. **97**(25): p. 13847-52.
182. Laemmli, U.K., *Cleavage of structural proteins during the assembly of the head of bacteriophage T4.* Nature, 1970. **227**(5259): p. 680-5.
183. Bradford, M.M., *A rapid and sensitive method for the quantitation of microgram quantities of protein utilizing the principle of protein-dye binding.* Anal Biochem, 1976. **72**: p. 248-54.
184. Shevchenko, A., et al., *In-gel digestion for mass spectrometric characterization of proteins and proteomes.* Nat Protoc, 2006. **1**(6): p. 2856-60.
185. Du, X., et al., *Three novel mammalian toll-like receptors: gene structure, expression, and evolution.* Eur Cytokine Netw, 2000. **11**(3): p. 362-71.
186. Ewald, S.E., et al., *Nucleic acid recognition by Toll-like receptors is coupled to stepwise processing by cathepsins and asparagine endopeptidase.* J Exp Med, 2011. **208**(4): p. 643-51.
187. Liu, L., et al., *Structural basis of toll-like receptor 3 signaling with double-stranded RNA.* Science, 2008. **320**(5874): p. 379-81.
188. Tanji, H., et al., *Structural reorganization of the Toll-like receptor 8 dimer induced by agonistic ligands.* Science, 2013. **339**(6126): p. 1426-9.

189. Peter, M.E., et al., *Identification of an N-terminal recognition site in TLR9 that contributes to CpG-DNA-mediated receptor activation.* J Immunol, 2009. **182**(12): p. 7690-7.
190. Latz, E., et al., *Ligand-induced conformational changes allosterically activate Toll-like receptor 9.* Nat Immunol, 2007. **8**(7): p. 772-9.
191. Krug, A., et al., *Herpes simplex virus type 1 activates murine natural interferon-producing cells through toll-like receptor 9.* Blood, 2004. **103**(4): p. 1433-7.
192. Lund, J., et al., *Toll-like receptor 9-mediated recognition of Herpes simplex virus-2 by plasmacytoid dendritic cells.* J Exp Med, 2003. **198**(3): p. 513-20.
193. Wagner, H., *The sweetness of the DNA backbone drives Toll-like receptor 9.* Curr Opin Immunol, 2008. **20**(4): p. 396-400.
194. Yasuda, K., et al., *CpG motif-independent activation of TLR9 upon endosomal translocation of "natural" phosphodiester DNA.* Eur J Immunol, 2006. **36**(2): p. 431-6.
195. Lamphier, M.S., et al., *TLR9 and the recognition of self and non-self nucleic acids.* Ann N Y Acad Sci, 2006. **1082**: p. 31-43.
196. Ahmad-Nejad, P., et al., *Bacterial CpG-DNA and lipopolysaccharides activate Toll-like receptors at distinct cellular compartments.* Eur J Immunol, 2002. **32**(7): p. 1958-68.
197. Hacker, H., et al., *CpG-DNA-specific activation of antigen-presenting cells requires stress kinase activity and is preceded by non-specific endocytosis and endosomal maturation.* EMBO J, 1998. **17**(21): p. 6230-40.
198. Ewald, S.E., et al., *The ectodomain of Toll-like receptor 9 is cleaved to generate a functional receptor.* Nature, 2008. **456**(7222): p. 658-62.
199. Park, B., et al., *Proteolytic cleavage in an endolysosomal compartment is required for activation of Toll-like receptor 9.* Nat Immunol, 2008. **9**(12): p. 1407-14.
200. Kawai, T., et al., *Interferon-alpha induction through Toll-like receptors involves a direct interaction of IRF7 with MyD88 and TRAF6.* Nat Immunol, 2004. **5**(10): p. 1061-8.
201. Uematsu, S., et al., *Interleukin-1 receptor-associated kinase-1 plays an essential role for Toll-like receptor (TLR)7- and TLR9-mediated interferon-{alpha} induction.* J Exp Med, 2005. **201**(6): p. 915-23.
202. Kawagoe, T., et al., *Sequential control of Toll-like receptor-dependent responses by IRAK1 and IRAK2.* Nat Immunol, 2008. **9**(6): p. 684-91.
203. Steinhagen, F., et al., *IRF-5 and NF-kappaB p50 co-regulate IFN-beta and IL-6 expression in TLR9-stimulated human plasmacytoid dendritic cells.* Eur J Immunol, 2013. **43**(7): p. 1896-906.
204. Takaoka, A., et al., *Integral role of IRF-5 in the gene induction programme activated by Toll-like receptors.* Nature, 2005. **434**(7030): p. 243-9.
205. Honda, K., et al., *IRF-7 is the master regulator of type-I interferon-dependent immune responses.* Nature, 2005. **434**(7034): p. 772-7.
206. Guiducci, C., et al., *Properties regulating the nature of the plasmacytoid dendritic cell response to Toll-like receptor 9 activation.* J Exp Med, 2006. **203**(8): p. 1999-2008.
207. Jurk, M., et al., *Human TLR7 or TLR8 independently confer responsiveness to the antiviral compound R-848.* Nat Immunol, 2002. **3**(6): p. 499.
208. Lee, J., et al., *Molecular basis for the immunostimulatory activity of guanine nucleoside analogs: activation of Toll-like receptor 7.* Proc Natl Acad Sci U S A, 2003. **100**(11): p. 6646-51.
209. Heil, F., et al., *The Toll-like receptor 7 (TLR7)-specific stimulus loxoribine uncovers a strong relationship within the TLR7, 8 and 9 subfamily.* Eur J Immunol, 2003. **33**(11): p. 2987-97.
210. Blasius, A.L. and B. Beutler, *Intracellular toll-like receptors.* Immunity, 2010. **32**(3): p. 305-15.
211. Honda, K., et al., *Role of a transductional-transcriptional processor complex involving MyD88 and IRF-7 in Toll-like receptor signaling.* Proc Natl Acad Sci U S A, 2004. **101**(43): p. 15416-21.
212. Schoenemeyer, A., et al., *The interferon regulatory factor, IRF5, is a central mediator of toll-like receptor 7 signaling.* J Biol Chem, 2005. **280**(17): p. 17005-12.

213. Crozat, K. and B. Beutler, *TLR7: A new sensor of viral infection.* Proc Natl Acad Sci U S A, 2004. **101**(18): p. 6835-6.
214. Diebold, S.S., et al., *Innate antiviral responses by means of TLR7-mediated recognition of single-stranded RNA.* Science, 2004. **303**(5663): p. 1529-31.
215. Heil, F., et al., *Species-specific recognition of single-stranded RNA via toll-like receptor 7 and 8.* Science, 2004. **303**(5663): p. 1526-9.
216. Lund, J.M., et al., *Recognition of single-stranded RNA viruses by Toll-like receptor 7.* Proc Natl Acad Sci U S A, 2004. **101**(15): p. 5598-603.
217. Mancuso, G., et al., *Bacterial recognition by TLR7 in the lysosomes of conventional dendritic cells.* Nat Immunol, 2009. **10**(6): p. 587-94.
218. Chuang, T.H. and R.J. Ulevitch, *Cloning and characterization of a sub-family of human toll-like receptors: hTLR7, hTLR8 and hTLR9.* Eur Cytokine Netw, 2000. **11**(3): p. 372-8.
219. Covert, M.W., et al., *Achieving stability of lipopolysaccharide-induced NF-kappaB activation.* Science, 2005. **309**(5742): p. 1854-7.
220. Wang, L., et al., *Regulation of lipopolysaccharide-induced translation of tumor necrosis factor-alpha by the toll-like receptor 4 adaptor protein TRAM.* J Innate Immun, 2011. **3**(5): p. 437-46.
221. Mueller, D.L., *Tuning the immune system: competing positive and negative feedback loops.* Nat Immunol, 2003. **4**(3): p. 210-1.
222. Jacobs, M.D. and S.C. Harrison, *Structure of an IkappaBalpha/NF-kappaB complex.* Cell, 1998. **95**(6): p. 749-58.
223. Baltimore, D., *NF-kappaB is 25.* Nat Immunol, 2011. **12**(8): p. 683-5.
224. Beattie, L., et al., *Interferon regulatory factor 7 contributes to the control of Leishmania donovani in the mouse liver.* Infect Immun, 2011. **79**(3): p. 1057-66.
225. Yoneyama, M., et al., *Direct triggering of the type I interferon system by virus infection: activation of a transcription factor complex containing IRF-3 and CBP/p300.* EMBO J, 1998. **17**(4): p. 1087-95.
226. Wathelet, M.G., et al., *Virus infection induces the assembly of coordinately activated transcription factors on the IFN-beta enhancer in vivo.* Mol Cell, 1998. **1**(4): p. 507-18.
227. Sato, M., et al., *Involvement of the IRF family transcription factor IRF-3 in virus-induced activation of the IFN-beta gene.* FEBS Lett, 1998. **425**(1): p. 112-6.
228. Honda, K. and T. Taniguchi, *IRFs: master regulators of signalling by Toll-like receptors and cytosolic pattern-recognition receptors.* Nat Rev Immunol, 2006. **6**(9): p. 644-58.
229. Poltorak, A., et al., *Genetic and physical mapping of the Lps locus: identification of the toll-4 receptor as a candidate gene in the critical region.* Blood Cells Mol Dis, 1998. **24**(3): p. 340-55.
230. Sakaguchi, S., et al., *Essential role of IRF-3 in lipopolysaccharide-induced interferon-beta gene expression and endotoxin shock.* Biochem Biophys Res Commun, 2003. **306**(4): p. 860-6.
231. McCoy, C.E., et al., *Glucocorticoids inhibit IRF3 phosphorylation in response to Toll-like receptor-3 and -4 by targeting TBK1 activation.* J Biol Chem, 2008. **283**(21): p. 14277-85.
232. Tsan, M.F. and B. Gao, *Pathogen-associated molecular pattern contamination as putative endogenous ligands of Toll-like receptors.* J Endotoxin Res, 2007. **13**(1): p. 6-14.
233. Erridge, C., *Endogenous ligands of TLR2 and TLR4: agonists or assistants?* J Leukoc Biol, 2010. **87**(6): p. 989-99.
234. Dentener, M.A., et al., *Antagonistic effects of lipopolysaccharide binding protein and bactericidal/permeability-increasing protein on lipopolysaccharide-induced cytokine release by mononuclear phagocytes. Competition for binding to lipopolysaccharide.* J Immunol, 1993. **151**(8): p. 4258-65.
235. Mestas, J. and C.C. Hughes, *Of mice and not men: differences between mouse and human immunology.* J Immunol, 2004. **172**(5): p. 2731-8.
236. Park, E.K., et al., *Optimized THP-1 differentiation is required for the detection of responses to weak stimuli.* Inflamm Res, 2007. **56**(1): p. 45-50.

237. Whitehead, K.A., R. Langer, and D.G. Anderson, *Knocking down barriers: advances in siRNA delivery.* Nat Rev Drug Discov, 2009. **8**(2): p. 129-38.
238. Calven, J., et al., *Viral stimuli trigger exaggerated thymic stromal lymphopoietin expression by chronic obstructive pulmonary disease epithelium: role of endosomal TLR3 and cytosolic RIG-I-like helicases.* J Innate Immun, 2012. **4**(1): p. 86-99.
239. Bao, M. and Y.J. Liu, *Regulation of TLR7/9 signaling in plasmacytoid dendritic cells.* Protein Cell, 2013. **4**(1): p. 40-52.
240. Oshiumi, H., et al., *TIR-containing adapter molecule (TICAM)-2, a bridging adapter recruiting to toll-like receptor 4 TICAM-1 that induces interferon-beta.* J Biol Chem, 2003. **278**(50): p. 49751-62.
241. Fitzgerald-Bocarsly, P., *Natural interferon-alpha producing cells: the plasmacytoid dendritic cells.* Biotechniques, 2002. **Suppl**: p. 16-20, 22, 24-9.
242. Koenig, T., et al., *Robust prediction of the MASCOT score for an improved quality assessment in mass spectrometric proteomics.* J Proteome Res, 2008. **7**(9): p. 3708-17.
243. Paddock, C.D., et al., *Pathology and pathogenesis of fatal Bordetella pertussis infection in infants.* Clin Infect Dis, 2008. **47**(3): p. 328-38.
244. Friedman, R.L., et al., *Uptake and intracellular survival of Bordetella pertussis in human macrophages.* Infect Immun, 1992. **60**(11): p. 4578-85.
245. Hickey, F.B., C.F. Brereton, and K.H. Mills, *Adenylate cycalse toxin of Bordetella pertussis inhibits TLR-induced IRF-1 and IRF-8 activation and IL-12 production and enhances IL-10 through MAPK activation in dendritic cells.* J Leukoc Biol, 2008. **84**(1): p. 234-43.
246. Gouin, E., et al., *A comparative study of the actin-based motilities of the pathogenic bacteria Listeria monocytogenes, Shigella flexneri and Rickettsia conorii.* J Cell Sci, 1999. **112 (Pt 11)**: p. 1697-708.
247. Aktories, K., et al., *Actin as target for modification by bacterial protein toxins.* FEBS J, 2011. **278**(23): p. 4526-43.
248. Barbieri, J.T., M.J. Riese, and K. Aktories, *Bacterial toxins that modify the actin cytoskeleton.* Annu Rev Cell Dev Biol, 2002. **18**: p. 315-44.
249. Lamberti, Y., et al., *Bordetella pertussis entry into respiratory epithelial cells and intracellular survival.* Pathog Dis, 2013.
250. Tili, E., J.J. Michaille, and C.M. Croce, *MicroRNAs play a central role in molecular dysfunctions linking inflammation with cancer.* Immunol Rev, 2013. **253**(1): p. 167-84.
251. Becker, J.C., et al., *Immune-suppressive properties of the tumor microenvironment.* Cancer Immunol Immunother, 2013. **62**(7): p. 1137-48.
252. Zheng, L., et al., *Role of immune cells and immune-based therapies in pancreatitis and pancreatic ductal adenocarcinoma.* Gastroenterology, 2013. **144**(6): p. 1230-40.
253. Mistry, S.J., A. Bank, and G.F. Atweh, *Targeting stathmin in prostate cancer.* Mol Cancer Ther, 2005. **4**(12): p. 1821-9.
254. Brattsand, G., *Correlation of oncoprotein 18/stathmin expression in human breast cancer with established prognostic factors.* Br J Cancer, 2000. **83**(3): p. 311-8.
255. Bsibsi, M., et al., *The microtubule regulator stathmin is an endogenous protein agonist for TLR3.* J Immunol, 2010. **184**(12): p. 6929-37.
256. Gostner, J.M., et al., *Redox regulation of the immune response.* Redox Rep, 2013. **18**(3): p. 88-94.
257. Matthews, J.R., et al., *Thioredoxin regulates the DNA binding activity of NF-kappa B by reduction of a disulphide bond involving cysteine 62.* Nucleic Acids Res, 1992. **20**(15): p. 3821-30.
258. Mason, A.C., et al., *An alternative form of replication protein a prevents viral replication in vitro.* J Biol Chem, 2009. **284**(8): p. 5324-31.
259. Wierenga, R.K., E.G. Kapetaniou, and R. Venkatesan, *Triosephosphate isomerase: a highly evolved biocatalyst.* Cell Mol Life Sci, 2010. **67**(23): p. 3961-82.

260. Tian, G., et al., *Pathway leading to correctly folded beta-tubulin.* Cell, 1996. **86**(2): p. 287-96.
261. Rubin, C.I. and G.F. Atweh, *The role of stathmin in the regulation of the cell cycle.* J Cell Biochem, 2004. **93**(2): p. 242-50.
262. Okazaki, T., et al., *SCG10, a neuron-specific growth-associated protein in Alzheimer's disease.* Neurobiol Aging, 1995. **16**(6): p. 883-94.
263. Wilkinson, B. and H.F. Gilbert, *Protein disulfide isomerase.* Biochim Biophys Acta, 2004. **1699**(1-2): p. 35-44.
264. Barbouche, R., et al., *Protein-disulfide isomerase-mediated reduction of two disulfide bonds of HIV envelope glycoprotein 120 occurs post-CXCR4 binding and is required for fusion.* J Biol Chem, 2003. **278**(5): p. 3131-6.
265. Gething, M.J. and J. Sambrook, *Transport and assembly processes in the endoplasmic reticulum.* Semin Cell Biol, 1990. **1**(1): p. 65-72.
266. Ryan, M.T. and N. Pfanner, *Hsp70 proteins in protein translocation.* Adv Protein Chem, 2001. **59**: p. 223-42.
267. Vabulas, R.M., et al., *HSP70 as endogenous stimulus of the Toll/interleukin-1 receptor signal pathway.* J Biol Chem, 2002. **277**(17): p. 15107-12.
268. Sadasivan, B., et al., *Roles for calreticulin and a novel glycoprotein, tapasin, in the interaction of MHC class I molecules with TAP.* Immunity, 1996. **5**(2): p. 103-14.
269. Miller, A.F., *Superoxide dismutases: ancient enzymes and new insights.* FEBS Lett, 2012. **586**(5): p. 585-95.
270. Jankova, L., et al., *Glutathione S-transferase Pi expression predicts response to adjuvant chemotherapy for stage C colon cancer: a matched historical control study.* BMC Cancer, 2012. **12**: p. 196.
271. Yamamoto, M., et al., *Key function for the Ubc13 E2 ubiquitin-conjugating enzyme in immune receptor signaling.* Nat Immunol, 2006. **7**(9): p. 962-70.
272. Fukushima, T., et al., *Ubiquitin-conjugating enzyme Ubc13 is a critical component of TNF receptor-associated factor (TRAF)-mediated inflammatory responses.* Proc Natl Acad Sci U S A, 2007. **104**(15): p. 6371-6.
273. Li, J., et al., *Caspase-11 regulates cell migration by promoting Aip1-Cofilin-mediated actin depolymerization.* Nat Cell Biol, 2007. **9**(3): p. 276-86.
274. Brown, K.K., et al., *Mitochondrial peroxiredoxin 3 is rapidly oxidized in cells treated with isothiocyanates.* Free Radic Biol Med, 2008. **45**(4): p. 494-502.
275. Basu, A., et al., *Differential expression of peroxiredoxins in prostate cancer: consistent upregulation of PRDX3 and PRDX4.* Prostate, 2011. **71**(7): p. 755-65.
276. Jiang, L., et al., *Intracellular chloride channel protein CLIC1 regulates macrophage function through modulation of phagosomal acidification.* J Cell Sci, 2012. **125**(Pt 22): p. 5479-88.
277. Nakamura, M., X.Z. Zhou, and K.P. Lu, *Critical role for the EB1 and APC interaction in the regulation of microtubule polymerization.* Curr Biol, 2001. **11**(13): p. 1062-7.
278. Laliberte, R.E., et al., *Glutathione s-transferase omega 1-1 is a target of cytokine release inhibitory drugs and may be responsible for their effect on interleukin-1beta posttranslational processing.* J Biol Chem, 2003. **278**(19): p. 16567-78.
279. Coll, R.C. and L.A. O'Neill, *The cytokine release inhibitory drug CRID3 targets ASC oligomerisation in the NLRP3 and AIM2 inflammasomes.* PLoS One, 2011. **6**(12): p. e29539.
280. Vladimer, G.I., et al., *The NLRP12 inflammasome recognizes Yersinia pestis.* Immunity, 2012. **37**(1): p. 96-107.
281. Kristensen, P., et al., *Human proteasome subunits from 2-dimensional gels identified by partial sequencing.* Biochem Biophys Res Commun, 1995. **207**(3): p. 1059.
282. Flood, E.C. and K.A. Hajjar, *The annexin A2 system and vascular homeostasis.* Vascul Pharmacol, 2011. **54**(3-6): p. 59-67.
283. Vedeler, A., et al., *Multiple roles of annexin A2 in post-transcriptional regulation of gene expression.* Curr Protein Pept Sci, 2012. **13**(4): p. 401-12.

284. Alanen, H.I., et al., *Functional characterization of ERp18, a new endoplasmic reticulum-located thioredoxin superfamily member.* J Biol Chem, 2003. **278**(31): p. 28912-20.
285. Ito, S., et al., *MMXD, a TFIIH-independent XPD-MMS19 protein complex involved in chromosome segregation.* Mol Cell, 2010. **39**(4): p. 632-40.
286. Schneider, B., et al., *Mechanism of phosphoryl transfer by nucleoside diphosphate kinase pH dependence and role of the active site Lys16 and Tyr56 residues.* Eur J Biochem, 2001. **268**(7): p. 1964-71.
287. Fisher, A.B., *Peroxiredoxin 6: a bifunctional enzyme with glutathione peroxidase and phospholipase A(2) activities.* Antioxid Redox Signal, 2011. **15**(3): p. 831-44.
288. Cookson, M.R., *Parkinsonism due to mutations in PINK1, parkin, and DJ-1 and oxidative stress and mitochondrial pathways.* Cold Spring Harb Perspect Med, 2012. **2**(9): p. a009415.
289. Dekker, F.J., et al., *Small-molecule inhibition of APT1 affects Ras localization and signaling.* Nat Chem Biol, 2010. **6**(6): p. 449-56.
290. Jedrzejas, M.J., *Structure, function, and evolution of phosphoglycerate mutases: comparison with fructose-2,6-bisphosphatase, acid phosphatase, and alkaline phosphatase.* Prog Biophys Mol Biol, 2000. **73**(2-4): p. 263-87.
291. Samland, A.K. and G.A. Sprenger, *Transaldolase: from biochemistry to human disease.* Int J Biochem Cell Biol, 2009. **41**(7): p. 1482-94.
292. Wies, E., et al., *Dephosphorylation of the RNA sensors RIG-I and MDA5 by the phosphatase PP1 is essential for innate immune signaling.* Immunity, 2013. **38**(3): p. 437-49.
293. Otsu, M., et al., *A possible role of ER-60 protease in the degradation of misfolded proteins in the endoplasmic reticulum.* J Biol Chem, 1995. **270**(25): p. 14958-61.
294. Camby, I., et al., *Galectin-1: a small protein with major functions.* Glycobiology, 2006. **16**(11): p. 137R-157R.
295. Cech, T.R., *Structural biology. The ribosome is a ribozyme.* Science, 2000. **289**(5481): p. 878-9.
296. Fort, M.M., et al., *IL-25 induces IL-4, IL-5, and IL-13 and Th2-associated pathologies in vivo.* Immunity, 2001. **15**(6): p. 985-95.
297. Kleinschek, M.A., et al., *IL-25 regulates Th17 function in autoimmune inflammation.* J Exp Med, 2007. **204**(1): p. 161-70.
298. Walsh, J.G., et al., *Executioner caspase-3 and caspase-7 are functionally distinct proteases.* Proc Natl Acad Sci U S A, 2008. **105**(35): p. 12815-9.
299. Weimershaus, M., et al., *Peptidases trimming MHC class I ligands.* Curr Opin Immunol, 2013. **25**(1): p. 90-6.
300. Chen, C.H., *Platelet-activating factor acetylhydrolase: is it good or bad for you?* Curr Opin Lipidol, 2004. **15**(3): p. 337-41.
301. Wold, M.S., *Replication protein A: a heterotrimeric, single-stranded DNA-binding protein required for eukaryotic DNA metabolism.* Annu Rev Biochem, 1997. **66**: p. 61-92.
302. Walsh, D., M.B. Mathews, and I. Mohr, *Tinkering with translation: protein synthesis in virus-infected cells.* Cold Spring Harb Perspect Biol, 2013. **5**(1): p. a012351.
303. Gusev, N.B., N.V. Bogatcheva, and S.B. Marston, *Structure and properties of small heat shock proteins (sHsp) and their interaction with cytoskeleton proteins.* Biochemistry (Mosc), 2002. **67**(5): p. 511-9.
304. Kamada, K., et al., *Structure of the human GINS complex and its assembly and functional interface in replication initiation.* Nat Struct Mol Biol, 2007. **14**(5): p. 388-96.
305. Habersetzer, J., et al., *ATP synthase oligomerization: from the enzyme models to the mitochondrial morphology.* Int J Biochem Cell Biol, 2013. **45**(1): p. 99-105.
306. Undyala, V.V., et al., *The calpain small subunit regulates cell-substrate mechanical interactions during fibroblast migration.* J Cell Sci, 2008. **121**(Pt 21): p. 3581-8.
307. Butt, A.Q., et al., *14-3-3epsilon and 14-3-3sigma inhibit Toll-like receptor (TLR)-mediated proinflammatory cytokine induction.* J Biol Chem, 2012. **287**(46): p. 38665-79.

308. Hosszu, K.K., et al., *DC-SIGN, C1q, and gC1qR form a trimolecular receptor complex on the surface of monocyte-derived immature dendritic cells.* Blood, 2012. **120**(6): p. 1228-36.
309. Xu, L., et al., *Inhibition of RIG-I and MDA5-dependent antiviral response by gC1qR at mitochondria.* Proc Natl Acad Sci U S A, 2009. **106**(5): p. 1530-5.
310. Vorobiev, S.M., et al., *Human retinoblastoma binding protein 9, a serine hydrolase implicated in pancreatic cancers.* Protein Pept Lett, 2012. **19**(2): p. 194-7.
311. Abeliovich, A. and M. Flint Beal, *Parkinsonism genes: culprits and clues.* J Neurochem, 2006. **99**(4): p. 1062-72.
312. Kinumi, T., et al., *Cysteine-106 of DJ-1 is the most sensitive cysteine residue to hydrogen peroxide-mediated oxidation in vivo in human umbilical vein endothelial cells.* Biochem Biophys Res Commun, 2004. **317**(3): p. 722-8.
313. Canet-Aviles, R.M., et al., *The Parkinson's disease protein DJ-1 is neuroprotective due to cysteine-sulfinic acid-driven mitochondrial localization.* Proc Natl Acad Sci U S A, 2004. **101**(24): p. 9103-8.
314. Meulener, M.C., et al., *Mutational analysis of DJ-1 in Drosophila implicates functional inactivation by oxidative damage and aging.* Proc Natl Acad Sci U S A, 2006. **103**(33): p. 12517-22.
315. Meulener, M., et al., *Drosophila DJ-1 mutants are selectively sensitive to environmental toxins associated with Parkinson's disease.* Curr Biol, 2005. **15**(17): p. 1572-7.
316. Bonifati, V., et al., *Mutations in the DJ-1 gene associated with autosomal recessive early-onset parkinsonism.* Science, 2003. **299**(5604): p. 256-9.
317. Borrelli, E., *Without DJ-1, the D2 receptor doesn't play.* Neuron, 2005. **45**(4): p. 479-81.
318. Waak, J., et al., *Regulation of astrocyte inflammatory responses by the Parkinson's disease-associated gene DJ-1.* FASEB J, 2009. **23**(8): p. 2478-89.
319. Cornejo Castro, E.M., et al., *Parkinson's disease-associated DJ-1 modulates innate immunity signaling in Caenorhabditis elegans.* J Neural Transm, 2010. **117**(5): p. 599-604.
320. Vila, M. and S. Przedborski, *Genetic clues to the pathogenesis of Parkinson's disease.* Nat Med, 2004. **10 Suppl**: p. S58-62.
321. Hayes, J.D. and D.J. Pulford, *The glutathione S-transferase supergene family: regulation of GST and the contribution of the isoenzymes to cancer chemoprotection and drug resistance.* Crit Rev Biochem Mol Biol, 1995. **30**(6): p. 445-600.
322. Salinas, A.E. and M.G. Wong, *Glutathione S-transferases--a review.* Curr Med Chem, 1999. **6**(4): p. 279-309.
323. Board, P.G., et al., *Identification, characterization, and crystal structure of the Omega class glutathione transferases.* J Biol Chem, 2000. **275**(32): p. 24798-806.
324. Board, P.G., et al., *Zeta, a novel class of glutathione transferases in a range of species from plants to humans.* Biochem J, 1997. **328 (Pt 3)**: p. 929-35.
325. Board, P.G., et al., *Evidence for an essential serine residue in the active site of the Theta class glutathione transferases.* Biochem J, 1995. **311 (Pt 1)**: p. 247-50.
326. Kodym, R., P. Calkins, and M. Story, *The cloning and characterization of a new stress response protein. A mammalian member of a family of theta class glutathione s-transferase-like proteins.* J Biol Chem, 1999. **274**(8): p. 5131-7.
327. Pasmantier, R., et al., *P19, a hormonally regulated phosphoprotein of peptide hormone-producing cells: secretagogue-induced phosphorylation in AtT-20 mouse pituitary tumor cells and in rat and hamster insulinoma cells.* Endocrinology, 1986. **119**(3): p. 1229-38.
328. Sobel, A. and A.H. Tashjian, Jr., *Distinct patterns of cytoplasmic protein phosphorylation related to regulation of synthesis and release of prolactin by GH cells.* J Biol Chem, 1983. **258**(17): p. 10312-24.
329. Hanash, S.M., et al., *Identification of a polypeptide associated with the malignant phenotype in acute leukemia.* J Biol Chem, 1988. **263**(26): p. 12813-5.

330. Filbert, E.L., et al., *Stathmin regulates microtubule dynamics and microtubule organizing center polarization in activated T cells.* J Immunol, 2012. **188**(11): p. 5421-7.
331. Moorhead, G.B., L. Trinkle-Mulcahy, and A. Ulke-Lemee, *Emerging roles of nuclear protein phosphatases.* Nat Rev Mol Cell Biol, 2007. **8**(3): p. 234-44.
332. Virshup, D.M. and S. Shenolikar, *From promiscuity to precision: protein phosphatases get a makeover.* Mol Cell, 2009. **33**(5): p. 537-45.
333. Bollen, M., et al., *The extended PP1 toolkit: designed to create specificity.* Trends Biochem Sci, 2010. **35**(8): p. 450-8.
334. Gibbons, J.A., et al., *Expression of human protein phosphatase-1 in Saccharomyces cerevisiae highlights the role of phosphatase isoforms in regulating eukaryotic functions.* J Biol Chem, 2007. **282**(30): p. 21838-47.
335. Peti, W., A.C. Nairn, and R. Page, *Structural basis for protein phosphatase 1 regulation and specificity.* FEBS J, 2013. **280**(2): p. 596-611.
336. Shi, Y., *Serine/threonine phosphatases: mechanism through structure.* Cell, 2009. **139**(3): p. 468-84.
337. Heroes, E., et al., *The PP1 binding code: a molecular-lego strategy that governs specificity.* FEBS J, 2013. **280**(2): p. 584-95.
338. Leib, D.A., et al., *Specific phenotypic restoration of an attenuated virus by knockout of a host resistance gene.* Proc Natl Acad Sci U S A, 2000. **97**(11): p. 6097-101.
339. He, B., M. Gross, and B. Roizman, *The gamma(1)34.5 protein of herpes simplex virus 1 complexes with protein phosphatase 1alpha to dephosphorylate the alpha subunit of the eukaryotic translation initiation factor 2 and preclude the shutoff of protein synthesis by double-stranded RNA-activated protein kinase.* Proc Natl Acad Sci U S A, 1997. **94**(3): p. 843-8.
340. Martin-Granados, C., et al., *A role for PP1/NIPP1 in steering migration of human cancer cells.* PLoS One, 2012. **7**(7): p. e40769.
341. Ceulemans, H. and M. Bollen, *Functional diversity of protein phosphatase-1, a cellular economizer and reset button.* Physiol Rev, 2004. **84**(1): p. 1-39.
342. Orosz, F., J. Olah, and J. Ovadi, *Triosephosphate isomerase deficiency: facts and doubts.* IUBMB Life, 2006. **58**(12): p. 703-15.
343. O'Neill, L.A. and D.G. Hardie, *Metabolism of inflammation limited by AMPK and pseudo-starvation.* Nature, 2013. **493**(7432): p. 346-55.
344. Wang, R., et al., *The transcription factor Myc controls metabolic reprogramming upon T lymphocyte activation.* Immunity, 2011. **35**(6): p. 871-82.
345. Tannahill, G.M., et al., *Succinate is an inflammatory signal that induces IL-1beta through HIF-1alpha.* Nature, 2013. **496**(7444): p. 238-42.
346. Chamaillard, M., et al., *An essential role for NOD1 in host recognition of bacterial peptidoglycan containing diaminopimelic acid.* Nat Immunol, 2003. **4**(7): p. 702-7.
347. Kanneganti, T.D., et al., *Critical role for Cryopyrin/Nalp3 in activation of caspase-1 in response to viral infection and double-stranded RNA.* J Biol Chem, 2006. **281**(48): p. 36560-8.
348. Tomalka, J., et al., *A novel role for the NLRC4 inflammasome in mucosal defenses against the fungal pathogen Candida albicans.* PLoS Pathog, 2011. **7**(12): p. e1002379.
349. Shio, M.T., et al., *Malarial hemozoin activates the NLRP3 inflammasome through Lyn and Syk kinases.* PLoS Pathog, 2009. **5**(8): p. e1000559.
350. Lupfer, C. and T.D. Kanneganti, *Unsolved Mysteries in NLR Biology.* Front Immunol, 2013. **4**: p. 285.
351. Ritter, M., et al., *Schistosoma mansoni triggers Dectin-2, which activates the Nlrp3 inflammasome and alters adaptive immune responses.* Proc Natl Acad Sci U S A, 2010. **107**(47): p. 20459-64.
352. Vladimer, G.I., et al., *Inflammasomes and host defenses against bacterial infections.* Curr Opin Microbiol, 2013. **16**(1): p. 23-31.

353. Wang, L., et al., *PYPAF7, a novel PYRIN-containing Apaf1-like protein that regulates activation of NF-kappa B and caspase-1-dependent cytokine processing.* J Biol Chem, 2002. **277**(33): p. 29874-80.
354. Allen, I.C., et al., *NLRP12 suppresses colon inflammation and tumorigenesis through the negative regulation of noncanonical NF-kappaB signaling.* Immunity, 2012. **36**(5): p. 742-54.
355. Zaki, M.H., et al., *The NOD-like receptor NLRP12 attenuates colon inflammation and tumorigenesis.* Cancer Cell, 2011. **20**(5): p. 649-60.
356. Elinav, E., et al., *NLRP6 inflammasome regulates colonic microbial ecology and risk for colitis.* Cell, 2011. **145**(5): p. 745-57.
357. Anand, P.K., et al., *NLRP6 negatively regulates innate immunity and host defence against bacterial pathogens.* Nature, 2012. **488**(7411): p. 389-93.
358. Finamore, F., et al., *Proteomics investigation of human platelets by shotgun nUPLC-MSE and 2DE experimental strategies: a comparative study.* Blood Transfus, 2010. **8 Suppl 3**: p. s140-8.
359. Das, T., et al., *RNA polymerase of vesicular stomatitis virus specifically associates with translation elongation factor-1 alphabetagamma for its activity.* Proc Natl Acad Sci U S A, 1998. **95**(4): p. 1449-54.
360. Tian, J., et al., *Binding of Src to Na+/K+-ATPase forms a functional signaling complex.* Mol Biol Cell, 2006. **17**(1): p. 317-26.
361. Zhang, H., et al., *Mammalian adenylyl cyclase-associated protein 1 (CAP1) regulates cofilin function, the actin cytoskeleton, and cell adhesion.* J Biol Chem, 2013. **288**(39): p. 28306.
362. Kutay, U., et al., *Export of importin alpha from the nucleus is mediated by a specific nuclear transport factor.* Cell, 1997. **90**(6): p. 1061-71.
363. Chu, P.C., et al., *Involvement of p29 in DNA damage responses and Fanconi anemia pathway.* Carcinogenesis, 2009. **30**(10): p. 1710-6.
364. Mazuruk, K., et al., *Structural organization and chromosomal localization of the human ribosomal protein L9 gene.* Biochim Biophys Acta, 1996. **1305**(3): p. 151-62.
365. He, H., et al., *The novel protein TSR2 inhibits the transcriptional activity of nuclear factor-kappaB and induces apoptosis.* Mol Biol (Mosk), 2011. **45**(3): p. 496-502.
366. Kotaka, M., et al., *Structural studies of glucose-6-phosphate and NADP+ binding to human glucose-6-phosphate dehydrogenase.* Acta Crystallogr D Biol Crystallogr, 2005. **61**(Pt 5): p. 495-504.
367. Nguyen, M., et al., *Caspase-resistant BAP31 inhibits fas-mediated apoptotic membrane fragmentation and release of cytochrome c from mitochondria.* Mol Cell Biol, 2000. **20**(18): p. 6731-40.
368. Annaert, W.G., et al., *Export of cellubrevin from the endoplasmic reticulum is controlled by BAP31.* J Cell Biol, 1997. **139**(6): p. 1397-410.
369. Fang, L., A. Seki, and G. Fang, *SKAP associates with kinetochores and promotes the metaphase-to-anaphase transition.* Cell Cycle, 2009. **8**(17): p. 2819-27.
370. Smith, G.C. and S.P. Jackson, *The DNA-dependent protein kinase.* Genes Dev, 1999. **13**(8): p. 916-34.
371. Yousif, L.F., J. Di Russo, and L. Sorokin, *Laminin isoforms in endothelial and perivascular basement membranes.* Cell Adh Migr, 2013. **7**(1): p. 101-10.
372. Skjerpen, C.S., J. Wesche, and S. Olsnes, *Identification of ribosome-binding protein p34 as an intracellular protein that binds acidic fibroblast growth factor.* J Biol Chem, 2002. **277**(26): p. 23864-71.
373. Ron, D., et al., *RACK1 to the future--a historical perspective.* Cell Commun Signal, 2013. **11**: p. 53.
374. Lunde, B.M., C. Moore, and G. Varani, *RNA-binding proteins: modular design for efficient function.* Nat Rev Mol Cell Biol, 2007. **8**(6): p. 479-90.

375. Mandinova, A., et al., *S100A13 mediates the copper-dependent stress-induced release of IL-1alpha from both human U937 and murine NIH 3T3 cells.* J Cell Sci, 2003. **116**(Pt 13): p. 2687-96.
376. Cai, J.P., et al., *Mouse MTH2 protein which prevents mutations caused by 8-oxoguanine nucleotides.* Biochem Biophys Res Commun, 2003. **305**(4): p. 1073-7.
377. Kobayashi, K.S. and P.J. van den Elsen, *NLRC5: a key regulator of MHC class I-dependent immune responses.* Nat Rev Immunol, 2012. **12**(12): p. 813-20.
378. Matsuda, M., et al., *Upstream stimulatory factors 1 and 2 mediate the transcription of angiotensin II binding and inhibitory protein.* J Biol Chem, 2013. **288**(26): p. 19238-49.
379. Latreille, M. and L. Larose, *Nck in a complex containing the catalytic subunit of protein phosphatase 1 regulates eukaryotic initiation factor 2alpha signaling and cell survival to endoplasmic reticulum stress.* J Biol Chem, 2006. **281**(36): p. 26633-44.
380. Zhai, Q., et al., *Structure of the Bro1 domain protein BROX and functional analyses of the ALIX Bro1 domain in HIV-1 budding.* PLoS One, 2011. **6**(12): p. e27466.
381. Wang, S., et al., *RN181 suppresses hepatocellular carcinoma growth by inhibition of the ERK/MAPK pathway.* Hepatology, 2011. **53**(6): p. 1932-42.
382. Zhang, Y., et al., *Identification of a conserved anti-apoptotic protein that modulates the mitochondrial apoptosis pathway.* PLoS One, 2011. **6**(9): p. e25284.
383. Kim, J., M. Guermah, and R.G. Roeder, *The human PAF1 complex acts in chromatin transcription elongation both independently and cooperatively with SII/TFIIS.* Cell, 2010. **140**(4): p. 491-503.
384. Kittanakom, S., et al., *Human kanadaptin and kidney anion exchanger 1 (kAE1) do not interact in transfected HEK 293 cells.* Mol Membr Biol, 2004. **21**(6): p. 395-402.
385. Madani, A., et al., *The 8 kD product of the putative oncogene MTCP-1 is a mitochondrial protein.* Oncogene, 1995. **10**(11): p. 2259-62.
386. Lee, H.C., et al., *Exon junction complex enhances translation of spliced mRNAs at multiple steps.* Biochem Biophys Res Commun, 2009. **384**(3): p. 334-40.
387. Edmond, V., et al., *Acetylation and phosphorylation of SRSF2 control cell fate decision in response to cisplatin.* EMBO J, 2011. **30**(3): p. 510-23.
388. Fang, D.F., et al., *RAD23A negatively regulates RIG-I/MDA5 signaling through promoting TRAF2 polyubiquitination and degradation.* Biochem Biophys Res Commun, 2013. **431**(4): p. 686-92.
389. Yang, L., et al., *ICAM-1 regulates neutrophil adhesion and transcellular migration of TNF-alpha-activated vascular endothelium under flow.* Blood, 2005. **106**(2): p. 584-92.
390. Haynes, C. and L.M. Iakoucheva, *Serine/arginine-rich splicing factors belong to a class of intrinsically disordered proteins.* Nucleic Acids Res, 2006. **34**(1): p. 305-12.
391. Ulmer, B., et al., *Calponin 2 acts as an effector of noncanonical Wnt-mediated cell polarization during neural crest cell migration.* Cell Rep, 2013. **3**(3): p. 615-21.
392. Huang, Q.Q., et al., *Role of H2-calponin in regulating macrophage motility and phagocytosis.* J Biol Chem, 2008. **283**(38): p. 25887-99.
393. Danson, C., et al., *SNX15 links clathrin endocytosis to the PtdIns(3)P early endosome independent of the APPL1 endosome.* J Cell Sci, 2013.
394. Fabrizio, P., et al., *Isolation of S. cerevisiae snRNPs: comparison of U1 and U4/U6.U5 to their human counterparts.* Science, 1994. **264**(5156): p. 261-5.
395. Giubellino, A., T.R. Burke, Jr., and D.P. Bottaro, *Grb2 signaling in cell motility and cancer.* Expert Opin Ther Targets, 2008. **12**(8): p. 1021-33.
396. Chao, M.P., et al., *Calreticulin is the dominant pro-phagocytic signal on multiple human cancers and is counterbalanced by CD47.* Sci Transl Med, 2010. **2**(63): p. 63ra94.
397. Fraser, S.A., et al., *Perforin lytic activity is controlled by calreticulin.* J Immunol, 2000. **164**(8): p. 4150-5.

398. Fukai, T. and M. Ushio-Fukai, *Superoxide dismutases: role in redox signaling, vascular function, and diseases.* Antioxid Redox Signal, 2011. **15**(6): p. 1583-606.
399. Adams, D.J., et al., *ZNF265--a novel spliceosomal protein able to induce alternative splicing.* J Cell Biol, 2001. **154**(1): p. 25-32.
400. Midwood, K., et al., *Tenascin-C is an endogenous activator of Toll-like receptor 4 that is essential for maintaining inflammation in arthritic joint disease.* Nat Med, 2009. **15**(7): p. 774-80.
401. Achsel, T., et al., *A doughnut-shaped heteromer of human Sm-like proteins binds to the 3'-end of U6 snRNA, thereby facilitating U4/U6 duplex formation in vitro.* EMBO J, 1999. **18**(20): p. 5789-802.
402. Mayeda, A., et al., *Purification and characterization of human RNPS1: a general activator of pre-mRNA splicing.* EMBO J, 1999. **18**(16): p. 4560-70.
403. Hirsch, D.S., D.M. Pirone, and P.D. Burbelo, *A new family of Cdc42 effector proteins, CEPs, function in fibroblast and epithelial cell shape changes.* J Biol Chem, 2001. **276**(2): p. 875-83.
404. Kester, H.A., et al., *Transforming growth factor-beta-stimulated clone-22 is a member of a family of leucine zipper proteins that can homo- and heterodimerize and has transcriptional repressor activity.* J Biol Chem, 1999. **274**(39): p. 27439-47.
405. Nakamura, M., et al., *Transforming growth factor-beta-stimulated clone-22 is a negative-feedback regulator of Ras / Raf signaling: Implications for tumorigenesis.* Cancer Sci, 2012. **103**(1): p. 26-33.
406. Eldridge, A.G., et al., *The SRm160/300 splicing coactivator is required for exon-enhancer function.* Proc Natl Acad Sci U S A, 1999. **96**(11): p. 6125-30.
407. Torti, F.M. and S.V. Torti, *Regulation of ferritin genes and protein.* Blood, 2002. **99**(10): p. 3505-16.
408. Soehn, A.S., et al., *Periphilin is a novel interactor of synphilin-1, a protein implicated in Parkinson's disease.* Neurogenetics, 2010. **11**(2): p. 203-15.
409. Kurita, M., et al., *CR/periphilin is a transcriptional co-repressor involved in cell cycle progression.* Biochem Biophys Res Commun, 2007. **364**(4): p. 930-6.
410. Yoo, O.J., et al., *Cloning, expression and characterization of the human transcription elongation factor, TFIIS.* Nucleic Acids Res, 1991. **19**(5): p. 1073-9.
411. Blencowe, B.J., et al., *The SRm160/300 splicing coactivator subunits.* RNA, 2000. **6**(1): p. 111-20.
412. Nowotny, M., et al., *Calcium-regulated interaction of Sgt1 with S100A6 (calcyclin) and other S100 proteins.* J Biol Chem, 2003. **278**(29): p. 26923-8.
413. Prus, W., et al., *Nuclear translocation of Sgt1 depends on its phosphorylation state.* Int J Biochem Cell Biol, 2011. **43**(12): p. 1747-53.
414. Lassegue, B. and K.K. Griendling, *NADPH oxidases: functions and pathologies in the vasculature.* Arterioscler Thromb Vasc Biol, 2010. **30**(4): p. 653-61.
415. Oliveira-Marques, V., et al., *Role of hydrogen peroxide in NF-kappaB activation: from inducer to modulator.* Antioxid Redox Signal, 2009. **11**(9): p. 2223-43.
416. Watt, R.K., *The many faces of the octahedral ferritin protein.* Biometals, 2011. **24**(3): p. 489-500.
417. Lawson, D.M., et al., *Identification of the ferroxidase centre in ferritin.* FEBS Lett, 1989. **254**(1-2): p. 207-10.
418. Ferreira, C., et al., *Early embryonic lethality of H ferritin gene deletion in mice.* J Biol Chem, 2000. **275**(5): p. 3021-4.
419. Carraway, M.S., et al., *Induction of ferritin and heme oxygenase-1 by endotoxin in the lung.* Am J Physiol, 1998. **275**(3 Pt 1): p. L583-92.
420. Mallick, P. and B. Kuster, *Proteomics: a pragmatic perspective.* Nat Biotechnol, 2010. **28**(7): p. 695-709.

421. Yang, D., et al., *Short RNA duplexes produced by hydrolysis with Escherichia coli RNase III mediate effective RNA interference in mammalian cells.* Proc Natl Acad Sci U S A, 2002. **99**(15): p. 9942-7.
422. Bagley, K.C., et al., *Pertussis toxin and the adenylate cyclase toxin from Bordetella pertussis activate human monocyte-derived dendritic cells and dominantly inhibit cytokine production through a cAMP-dependent pathway.* J Leukoc Biol, 2002. **72**(5): p. 962-9.
423. McGuirk, P. and K.H. Mills, *Direct anti-inflammatory effect of a bacterial virulence factor: IL-10-dependent suppression of IL-12 production by filamentous hemagglutinin from Bordetella pertussis.* Eur J Immunol, 2000. **30**(2): p. 415-22.
424. Mills, K.H., *Immunity to Bordetella pertussis.* Microbes Infect, 2001. **3**(8): p. 655-77.
425. Higgins, S.C., et al., *Toll-like receptor 4-mediated innate IL-10 activates antigen-specific regulatory T cells and confers resistance to Bordetella pertussis by inhibiting inflammatory pathology.* J Immunol, 2003. **171**(6): p. 3119-27.
426. Zhang, P., et al., *Protein tyrosine phosphatase with proline-glutamine-serine-threonine-rich motifs negatively regulates TLR-triggered innate responses by selectively inhibiting IkappaB kinase beta/NF-kappaB activation.* J Immunol, 2013. **190**(4): p. 1685-94.
427. Rhee, S.H., et al., *Toll-like receptors 2 and 4 activate STAT1 serine phosphorylation by distinct mechanisms in macrophages.* J Biol Chem, 2003. **278**(25): p. 22506-12.
428. Li, S., et al., *IRAK-4: a novel member of the IRAK family with the properties of an IRAK-kinase.* Proc Natl Acad Sci U S A, 2002. **99**(8): p. 5567-72.
429. Bhattacharyya, S., P.K. Dudeja, and J.K. Tobacman, *Lipopolysaccharide activates NF-kappaB by TLR4-Bcl10-dependent and independent pathways in colonic epithelial cells.* Am J Physiol Gastrointest Liver Physiol, 2008. **295**(4): p. G784-90.
430. Woo, C.W., et al., *Toll-like receptor activation suppresses ER stress factor CHOP and translation inhibition through activation of eIF2B.* Nat Cell Biol, 2012. **14**(2): p. 192-200.
431. Beetz, A., et al., *NF-kappaB and AP-1 are responsible for inducibility of the IL-6 promoter by ionizing radiation in HeLa cells.* Int J Radiat Biol, 2000. **76**(11): p. 1443-53.
432. Centre, H.P.S. *Pertussis (whooping cough) outbreak - update October 2012*. 2012 21-09-2013]; Available from: http://www.hpsc.ie/hpsc/A-Z/VaccinePreventable/PertussisWhoopingCough/News/MainBody,13750,en.html.
433. Agency, H.P. *Health Protection Report*. 2012 13/09/2013]; Available from: http://www.hpa.org.uk/hpr/archives/2012/news1512.htm.
434. Ivanov, P. and P. Anderson, *Post-transcriptional regulatory networks in immunity.* Immunol Rev, 2013. **253**(1): p. 253-72.
435. Broderick, J.A. and P.D. Zamore, *MicroRNA therapeutics.* Gene Ther, 2011. **18**(12): p. 1104-10.
436. Wang, V. and W. Wu, *MicroRNA-based therapeutics for cancer.* BioDrugs, 2009. **23**(1): p. 15-23.
437. Subauste, M.C., et al., *Infection of a human respiratory epithelial cell line with rhinovirus. Induction of cytokine release and modulation of susceptibility to infection by cytokine exposure.* J Clin Invest, 1995. **96**(1): p. 549-57.
438. Abramson, T., H. Kedem, and D.A. Relman, *Proinflammatory and proapoptotic activities associated with Bordetella pertussis filamentous hemagglutinin.* Infect Immun, 2001. **69**(4): p. 2650-8.
439. Cavalier-Smith, T., *A revised six-kingdom system of life.* Biol Rev Camb Philos Soc, 1998. **73**(3): p. 203-66.
440. Robinson, R.C., et al., *Crystal structure of Arp2/3 complex.* Science, 2001. **294**(5547): p. 1679-84.
441. Vainberg, I.E., et al., *Prefoldin, a chaperone that delivers unfolded proteins to cytosolic chaperonin.* Cell, 1998. **93**(5): p. 863-73.

442. Vertessy, B.G. and J. Toth, *Keeping uracil out of DNA: physiological role, structure and catalytic mechanism of dUTPases.* Acc Chem Res, 2009. **42**(1): p. 97-106.
443. Nallamothu, G., V. Dammai, and T. Hsu, *Developmental function of Nm23/awd: a mediator of endocytosis.* Mol Cell Biochem, 2009. **329**(1-2): p. 35-44.
444. Shields, D.J., et al., *RBBP9: a tumor-associated serine hydrolase activity required for pancreatic neoplasia.* Proc Natl Acad Sci U S A, 2010. **107**(5): p. 2189-94.
445. Park, I., et al., *Myosin regulatory light chains are required to maintain the stability of myosin II and cellular integrity.* Biochem J, 2011. **434**(1): p. 171-80.
446. Rich, B.E. and J.A. Steitz, *Human acidic ribosomal phosphoproteins P0, P1, and P2: analysis of cDNA clones, in vitro synthesis, and assembly.* Mol Cell Biol, 1987. **7**(11): p. 4065-74.
447. Gutierrez, E., et al., *eIF5A promotes translation of polyproline motifs.* Mol Cell, 2013. **51**(1): p. 35-45.
448. Maier, B., et al., *The unique hypusine modification of eIF5A promotes islet beta cell inflammation and dysfunction in mice.* J Clin Invest, 2010. **120**(6): p. 2156-70.
449. R. Lim, A.Z., *Glia Maturation Factor in Brain Function*, in *Handbook of Neurochemistry and Molecular Neurobiology*. 2006, Springer US. p. 203-222.
450. Jacob Blackmon, B., et al., *Characterization of a human and mouse tetrapyrrole-binding protein.* Arch Biochem Biophys, 2002. **407**(2): p. 196-201.
451. Li, J., et al., *Glutathione S-transferase M1, T1, and P1 polymorphisms and thyroid cancer risk: a meta-analysis.* Cancer Epidemiol, 2012. **36**(6): p. e333-40.
452. Adler, V., et al., *Regulation of JNK signaling by GSTp.* EMBO J, 1999. **18**(5): p. 1321-34.
453. Chen, Y., et al., *Oncoprotein p28 GANK binds to RelA and retains NF-kappaB in the cytoplasm through nuclear export.* Cell Res, 2007. **17**(12): p. 1020-9.
454. Dong, L.W., et al., *The oncoprotein p28GANK establishes a positive feedback loop in beta-catenin signaling.* Cell Res, 2011. **21**(8): p. 1248-61.
455. Kershnar, E., S.Y. Wu, and C.M. Chiang, *Immunoaffinity purification and functional characterization of human transcription factor IIH and RNA polymerase II from clonal cell lines that conditionally express epitope-tagged subunits of the multiprotein complexes.* J Biol Chem, 1998. **273**(51): p. 34444-53.
456. Wang, L., et al., *HINT1 inhibits beta-catenin/TCF4, USF2 and NFkappaB activity in human hepatoma cells.* Int J Cancer, 2009. **124**(7): p. 1526-34.
457. Weiske, J. and O. Huber, *The histidine triad protein Hint1 triggers apoptosis independent of its enzymatic activity.* J Biol Chem, 2006. **281**(37): p. 27356-66.
458. Schulman, B.A., et al., *Insights into SCF ubiquitin ligases from the structure of the Skp1-Skp2 complex.* Nature, 2000. **408**(6810): p. 381-6.
459. Ruan, J., et al., *Crystal structures of the coil 2B fragment and the globular tail domain of human lamin B1.* FEBS Lett, 2012. **586**(4): p. 314-8.
460. Ichijo, H., et al., *Induction of apoptosis by ASK1, a mammalian MAPKKK that activates SAPK/JNK and p38 signaling pathways.* Science, 1997. **275**(5296): p. 90-4.
461. Kramer, A., et al., *Mammalian splicing factor SF3a120 represents a new member of the SURP family of proteins and is homologous to the essential splicing factor PRP21p of Saccharomyces cerevisiae.* RNA, 1995. **1**(3): p. 260-72.
462. Agarwal, S.K., et al., *Menin interacts with the AP1 transcription factor JunD and represses JunD-activated transcription.* Cell, 1999. **96**(1): p. 143-52.
463. Bao, Y., T.L. Dawson, Jr., and Y.T. Chen, *Human glycogen debranching enzyme gene (AGL): complete structural organization and characterization of the 5' flanking region.* Genomics, 1996. **38**(2): p. 155-65.
464. Martin, J., et al., *Hint2, a mitochondrial apoptotic sensitizer down-regulated in hepatocellular carcinoma.* Gastroenterology, 2006. **130**(7): p. 2179-88.
465. Ndiaye, D., et al., *Characterization of the Effect of the Mitochondrial Protein Hint2 on Intracellular Ca(2+) dynamics.* Biophys J, 2013. **105**(5): p. 1268-75.

466. Pal, D., et al., *Role of a novel coiled-coil domain-containing protein CCDC69 in regulating central spindle assembly.* Cell Cycle, 2010. **9**(20): p. 4117-29.
467. Kong, E., et al., *Dynamic palmitoylation links cytosol-membrane shuttling of acyl-protein thioesterase-1 and acyl-protein thioesterase-2 with that of proto-oncogene H-ras product and growth-associated protein-43.* J Biol Chem, 2013. **288**(13): p. 9112-25.
468. Boissan, M. and M.L. Lacombe, *Learning about the functions of NME/NM23: lessons from knockout mice to silencing strategies.* Naunyn Schmiedebergs Arch Pharmacol, 2011. **384**(4-5): p. 421-31.
469. Postel, E.H., et al., *Human NM23/nucleoside diphosphate kinase regulates gene expression through DNA binding to nuclease-hypersensitive transcriptional elements.* J Bioenerg Biomembr, 2000. **32**(3): p. 277-84.
470. Ma, D., et al., *NM23-H1 and NM23-H2 repress transcriptional activities of nuclease-hypersensitive elements in the platelet-derived growth factor-A promoter.* J Biol Chem, 2002. **277**(2): p. 1560-7.
471. Fan, Z., et al., *Tumor suppressor NM23-H1 is a granzyme A-activated DNase during CTL-mediated apoptosis, and the nucleosome assembly protein SET is its inhibitor.* Cell, 2003. **112**(5): p. 659-72.
472. Sirotkovic-Skerlev, M., et al., *Expression of c-myc, erbB-2, p53 and nm23-H1 gene product in benign and malignant breast lesions: coexpression and correlation with clinicopathologic parameters.* Exp Mol Pathol, 2005. **79**(1): p. 42-50.
473. Ouatas, T., et al., *Basic and translational advances in cancer metastasis: Nm23.* J Bioenerg Biomembr, 2003. **35**(1): p. 73-9.
474. Galani, E., et al., *Correlation of MDR-1, nm23-H1 and H Sema E gene expression with histopathological findings and clinical outcome in ovarian and breast cancer patients.* Anticancer Res, 2002. **22**(4): p. 2275-80.
475. Murakami, M., et al., *Epstein-Barr virus nuclear antigen 1 interacts with Nm23-H1 in lymphoblastoid cell lines and inhibits its ability to suppress cell migration.* J Virol, 2005. **79**(3): p. 1559-68.
476. Conery, A.R., S. Sever, and E. Harlow, *Nucleoside diphosphate kinase Nm23-H1 regulates chromosomal stability by activating the GTPase dynamin during cytokinesis.* Proc Natl Acad Sci U S A, 2010. **107**(35): p. 15461-6.
477. Krishnan, K.S., et al., *Nucleoside diphosphate kinase, a source of GTP, is required for dynamin-dependent synaptic vesicle recycling.* Neuron, 2001. **30**(1): p. 197-210.
478. Hewson, C.A., et al., *Toll-like receptor 3 is induced by and mediates antiviral activity against rhinovirus infection of human bronchial epithelial cells.* J Virol, 2005. **79**(19): p. 12273-9.
479. Fendrick, A.M., et al., *The economic burden of non-influenza-related viral respiratory tract infection in the United States.* Arch Intern Med, 2003. **163**(4): p. 487-94.
480. Monto, A.S., *Viral respiratory infections in the community: epidemiology, agents, and interventions.* Am J Med, 1995. **99**(6B): p. 24S-27S.
481. Kim, B.E., et al., *IL-25 Enhances HSV-1 Replication by Inhibiting Filaggrin Expression, and Acts Synergistically with Th2 Cytokines to Enhance HSV-1 Replication.* J Invest Dermatol, 2013.
482. Message, S.D., et al., *Rhinovirus-induced lower respiratory illness is increased in asthma and related to virus load and Th1/2 cytokine and IL-10 production.* Proc Natl Acad Sci U S A, 2008. **105**(36): p. 13562-7.
483. Pritchard, A.L., et al., *Innate IFNs and plasmacytoid dendritic cells constrain Th2 cytokine responses to rhinovirus: a regulatory mechanism with relevance to asthma.* J Immunol, 2012. **188**(12): p. 5898-905.
484. Ryan, M., et al., *Bordetella pertussis-specific Th1/Th2 cells generated following respiratory infection or immunization with an acellular vaccine: comparison of the T cell cytokine profiles in infants and mice.* Dev Biol Stand, 1997. **89**: p. 297-305.

485. Schwarz, K.B., *Oxidative stress during viral infection: a review.* Free Radic Biol Med, 1996. **21**(5): p. 641-9.
486. Paz, S., et al., *Induction of IRF-3 and IRF-7 phosphorylation following activation of the RIG-I pathway.* Cell Mol Biol (Noisy-le-grand), 2006. **52**(1): p. 17-28.
487. Joo, C.H., et al., *Inhibition of interferon regulatory factor 7 (IRF7)-mediated interferon signal transduction by the Kaposi's sarcoma-associated herpesvirus viral IRF homolog vIRF3.* J Virol, 2007. **81**(15): p. 8282-92.
488. Fitzgerald, K.A., et al., *IKKepsilon and TBK1 are essential components of the IRF3 signaling pathway.* Nat Immunol, 2003. **4**(5): p. 491-6.
489. Oldstone, M.B.A., *Virus Can Alter Cell Function Without Causing Cell Pathology: Disordered Function Leads to Imbalance of Homeostasis and Disease*, in *Concepts In Viral Pathogenesis*1984, Springer. p. 269-276.
490. Vogel, C. and E.M. Marcotte, *Insights into the regulation of protein abundance from proteomic and transcriptomic analyses.* Nat Rev Genet, 2012. **13**(4): p. 227-32.
491. Khelef, N., A. Zychlinsky, and N. Guiso, *Bordetella pertussis induces apoptosis in macrophages: role of adenylate cyclase-hemolysin.* Infect Immun, 1993. **61**(10): p. 4064-71.
492. Mager, D.L., *Bacteria and cancer: cause, coincidence or cure? A review.* J Transl Med, 2006. **4**: p. 14.
493. Ellmerich, S., et al., *Promotion of intestinal carcinogenesis by Streptococcus bovis.* Carcinogenesis, 2000. **21**(4): p. 753-6.
494. Crowe, S.E., *Helicobacter infection, chronic inflammation, and the development of malignancy.* Curr Opin Gastroenterol, 2005. **21**(1): p. 32-8.
495. Schulze, A. and A.L. Harris, *How cancer metabolism is tuned for proliferation and vulnerable to disruption.* Nature, 2012. **491**(7424): p. 364-73.
496. Birkebaek, N.H., et al., *Bordetella pertussis and chronic cough in adults.* Clin Infect Dis, 1999. **29**(5): p. 1239-42.
497. Bayles, K.W., et al., *Intracellular Staphylococcus aureus escapes the endosome and induces apoptosis in epithelial cells.* Infect Immun, 1998. **66**(1): p. 336-42.
498. Mann, P.B., et al., *Comparative toll-like receptor 4-mediated innate host defense to Bordetella infection.* Infect Immun, 2005. **73**(12): p. 8144-52.
499. Bosch, A.A., et al., *Viral and bacterial interactions in the upper respiratory tract.* PLoS Pathog, 2013. **9**(1): p. e1003057.
500. Versteegh, F.G., et al., *Community-acquired pathogens associated with prolonged coughing in children: a prospective cohort study.* Clin Microbiol Infect, 2005. **11**(10): p. 801-7.
501. Uronen-Hansson, H., et al., *Toll-like receptor 2 (TLR2) and TLR4 are present inside human dendritic cells, associated with microtubules and the Golgi apparatus but are not detectable on the cell surface: integrity of microtubules is required for interleukin-12 production in response to internalized bacteria.* Immunology, 2004. **111**(2): p. 173-8.
502. Nilsen, N.J., et al., *Cellular trafficking of lipoteichoic acid and Toll-like receptor 2 in relation to signaling: role of CD14 and CD36.* J Leukoc Biol, 2008. **84**(1): p. 280-91.

Appendix

Spot No.	Protein Name	Fold Change	Accession Code	Mascot Score	MW (kDa)	p*I*	Peptides Matched	Cov (%)	P Value
1221	Thioredoxin	↑1.5	P10599	194	11.7	4.82	4	34	7.1E-04
1221	Replication protein A 14 kDa subunit	↑1.5	P35244	86	13.5	4.96	2	33	7.1E-04
951	Triosephosphotase Isomerase (TPI)	↑4.4	P60174	297	30.7	5.65	5	29	0.008
1179	Tubulin-specific chaperone A	↑1.4	O75347	172	12.8	5.25	6	38	0.002
1120	Stathmin	↑1.5	P16949	142	17.2	5.76	3	21	0.015
1120	Stathmin-2	↑1.5	Q93045	86	20.8	8.4	2	10	0.015
467	Protein disulfide-isomerase	↓1.3	P07237	916	57.0	4.76	25	50	0.015
103	Transitional endoplasmic reticulum ATPase	↓1.5	P55072	791	89.2	5.14	19	29	8E-04
338	heat shock 70kDa protein 9B	↓1.4	BAD96478	376	73.5	5.87	8	15	0.005
527	Tapasin ERP57	↓1.4	3F8U_A	946	54.1	5.61	18	46	1.8E-05
1312	Superoxide dismutase [Cu-Zn]	↑1.3	Q6NR85	55	15.9	5.7	1	9	9.8E-05
1199	HGSTP1-1	↑1.3	4PGT_A	436	23.3	5.43	11	52	0.043
1434	Ubiquitin-conjugating enzyme E2 N (Ubc13)	↑1.3	P61088	281	17.1	6.13	6	51	5.8E-04
1347	Cofilin-1	↓1.7	P23528	256	18.4	8.22	4	42	0.007
1191	PRDX3	↑1.3	P30048	238	27.6	7.67	4	18	0.02
1032	Clic1	↑1.4	3QR6_A	359	26.9	5.01	9	39	0.001
997	EB1	↑1.3	Q15691	446	29.9	5.02	10	45	0.021
1061	Glutathione S-transferase omega-1	↑1.4	P78417	204	27.5	6.23	7	24	0.017
1019	NLRP12	↑1.3	NP_150639	52	102	8.85	2	13	8E-05

Table A1.1: Proteins identified by DIGE/ LC/MS showing changes in expression in response to *B. pertussis* Infection. All proteins were identified using the NCBI and Swiss Prot protein databases and demonstrated a mascot score >52 indicating reliable protein identification.

Spot No.	Protein Name	Fold Change	Accession Code	Mascot Score	MW (kDa)	p*I*	Peptides Matched	Cov (%)	P Value
1032	Proteasome subunit beta type-4	↑1.5	P28070	372	29.1	5.72	9	36	0.005
826	Annexin A2	↑1.5	3GPD_R	125	38.5	7.57	2	6	3.7E-04
1509	Thioredoxin domain-containing protein 12	↑1.5	O75347	200	19.1	5.27	4	30	0.022
1444	Mitotic spindle-associated MMXD complex	↑1.5	Q9Y3D0	84	17.6	5.07	2	26	0.002
1374	Nucleoside diphosphate kinase A (NME!)	↑1.4	Q96Q81	461	17.1	5.83	18	64	5.8E-06
1539	Peroxiredoxin-6	↑1.3	1SOA_A	256	25.0	6	9	44	0.023
1488	Dj-1	↑1.3	2RK6_A	490	19.8	6.33	16	66	0.011
1093	Acyl-protein thioesterase 1	↑1.3	P18669	89	24.6	6.29	2	8	0.004
997	Phosphoglycerate mutase 1	↑1.4	P37837	110	28.7	6.67	2	15	0.025
806	Transaldolase	↑1.3	P62136	323	37.5	5.26	7	21	0.005
1382	Serine/threonine-protein phosphatase PP1α	↑1.4	BAA11928	379	37.4	5.74	7	22	0.007
1415	ER-60 protease	↓1.3	P38657	609	56.7	5.98	13	27	5.9E-05
1442	Galectin-1	↑1.3	P25398	260	14.5	5.34	7	44	0.001
1342	40S ribosomal protein S12	↑1.4	Q969H8	73	14.5	6.81	3	13	9E-07
1325	IL-25	↑1.3	P09211	235	18.7	6.2	6	27	0.002
1047	Caspase 3	↑1.3	O75832	63	21.4	7.67	3	19	0.004
1087	PSMB10	↑1.4	Q6IBR6	100	24.4	5.71	3	17	0.011
1492	Platelet-activating factor acetylhydrolase	↑1.4	1QUQ_A	80	25.5	5.57	2	12	0.003

Table A1.1: Proteins identified by DIGE/ LC/MS showing changes in expression in response to *B. pertussis* Infection. All proteins were identified using the NCBI and Swiss Prot protein databases and demonstrated a mascot score >52 indicating reliable protein identification.

Spot No.	Protein Name	Fold Change	Accession Code	Mascot Score	MW (kDa)	p*I*	Peptides Matched	Cov (%)	P Value
972	Replication Protein A (Rpa14 And Rpa32)	↑1.3	P06730	260	14.4	5.43	6	44	0.008
1028	Eukaryotic translation initiation factor 4E	↑1.3	Q9UC36	74	25.0	5.79	2	11	0.047
1037	Heat shock protein beta-1	↑1.4	P13693	73	22.7	5.98	1	4	4E-04
1109	DNA replication complex GINS protein PSF2	↑1.3	O75947	58	21.4	5.29	1	13	6E-04
1128	ATP synthase subunit d, mitochondrial	↑1.4	P04632	476	18.4	5.21	12	67	1.4E-04
1019	Calpain small subunit 1	↑1.4	Q96L46	485	28.2	5.05	9	51	1.6E-04
1500	14-3-3 protein epsilon	↑1.4	Q07021	123	29.1	4.63	3	15	0.004
886	Complement component 1 Q	↑1.4	P28066	289	31.3	4.74	8	31	3E-04
1494	Putative hydrolase RBBP9	↑1.4	1SOA_A	131	20.9	5.79	2	18	0.017

Table A1.1: Proteins identified by DIGE/ LC/MS showing changes in expression in response to *B. pertussis* Infection. All proteins were identified using the NCBI and Swiss Prot protein databases and demonstrated a mascot score >52 indicating reliable protein identification.

Protein Name	Accession Code	LFQ Intensity (Control)	LFQ Intensity (Infected)	Matched Peptides	Fold Change	PEP	ANOVA
Elongation Factor gamma	IPI:IPI00000875.7	NaN	26.1588	4	N/A	2.49E-16	N/A
Sodium/potassium-transporting ATPase	IPI:IPI00006482.1	NaN	25.2055	6	N/A	8.69E-14	N/A
Adenylyl cyclase-associated protein 1	IPI:IPI00008274.7	NaN	24.056	3	N/A	3.92E-16	N/A
Exportin-2	IPI:IPI00022744.5	NaN	25.1535	7	N/A	1.03E-20	N/A
Pre mRNA slicing factor SYF2	IPI:IPI00022963.3	NaN	24.6667	3	N/A	3.93E-13	N/A
60S ribosomal protein L9	IPI:IPI00031691.1	NaN	25.0996	2	N/A	8.65E-05	N/A
Pre-rRNA-processing protein TSR2	IPI:IPI00056314.1	NaN	23.5004	2	N/A	0.000226	N/A
Glucose-6-phosphate 1-dehydrogenase	IPI:IPI00216008.4	NaN	26.0543	8	N/A	1.20E-25	N/A
Caspase-7	IPI:IPI00216674.1	NaN	24.9004	2	N/A	0.001409	N/A
B-cell receptor-associated protein 31	IPI:IPI00642984.2	NaN	23.1694	4	N/A	1.96E-06	N/A
Small kinetochore-associated protein	IPI:IPI00294680.5	NaN	25.5811	2	N/A	7.50E-05	N/A
DNA-dependent protein kinase	IPI:IPI00296337.2	NaN	26.1313	19	N/A	1.55E-46	N/A
Laminin subunit gamma-1	IPI:IPI00298281.4	NaN	25.1725	3	N/A	1.25E-18	N/A
60S ribosomal protein L7a	IPI:IPI00299573.12	NaN	24.8042	2	N/A	0.000365	N/A
60S ribosomal protein L17	IPI:IPI00413324.6	NaN	25.5323	2	N/A	1.78E-05	N/A
Ribosome-binding protein p34 (p34)	IPI:IPI00396321.1	NaN	25.7962	3	N/A	5.30E-14	N/A
RACK1	IPI:IPI00848226.1	NaN	25.7188	6	N/A	5.44E-32	N/A
RNA-binding protein 4	IPI:IPI00003704.4	25.0283	NaN	3	N/A	2.12E-07	N/A
Protein S100-A13	IPI:IPI00016179.1	26.4933	NaN	2	N/A	1.86E-26	N/A

Table A1.2: Proteins identified by LFQ MS showing changes in expression in response to *B. pertussis* Infection. All proteins were identified using the NCBI and Swiss Prot protein databases and demonstrated a mascot score >52 indicating reliable protein identification.

Protein Name	Accession Code	LFQ Intensity (Control)	LFQ Intensity (Infected)	Matched Peptides	Fold Change	PEP	ANOVA
NUDT15	IPI:IPI00019487.3	24.8133	NaN	3	N/A	6.96E-08	N/A
Upstream stimulatory factor 2	IPI:IPI00020037.1	25.3726	NaN	3	N/A	7.44E-10	N/A
Nck-1	IPI:IPI00028065.1	24.7187	NaN	4	N/A	9.56E-20	N/A
BRO1 domain-containing protein BROX	IPI:IPI00065500.3	25.2597	NaN	2	N/A	1.28E-08	N/A
E3 ubiquitin-protein ligase RNF181	IPI:IPI00292354.8	25.1869	NaN	2	N/A	5.56E-09	N/A
Caspase activity and apoptosis inhibitor 1	IPI:IPI00303812.7	25.4128	NaN	3	N/A	5.77E-05	N/A
RNA polymerase-associated protein RTF1	IPI:IPI00303832.6	25.3318	NaN	6	N/A	5.49E-17	N/A
Kanadaptin	IPI:IPI00306749.8	24.5912	NaN	3	N/A	1.00E-08	N/A
Cx9C motif-containing protein 4	IPI:IPI00446798.1	25.1599	NaN	2	N/A	4.32E-15	N/A
RNA-binding protein 8A	IPI:IPI00001757.1	31.3137	30.9937	10	-0.64	1.98E-228	+
Serine/arginine-rich splicing factor 2	IPI:IPI00005978.8	32.3223	31.9449	12	-0.75	0	+
Putative RNA-binding protein Luc7-like 2	IPI:IPI00006932.4	28.1672	28.5935	10	0.85	3.52E-123	+
UV excision repair protein RAD23	IPI:IPI00008219.1	26.0555	25.4419	8	-1.23	6.40E-18	+
Intercellular adhesion molecule 1	IPI:IPI00008494.4	24.3462	26.2793	6	3.87	4.29E-26	+
Serine/arginine-rich splicing factor 6	IPI:IPI00012345.2	31.5658	31.1274	14	-0.88	1.71E-99	+
Calponin-2	IPI:IPI00910593.1	32.0846	31.7908	17	-0.59	0	+
Uncharacterized protein C14orf119	IPI:IPI00016726.3	25.4719	26.2364	3	1.53	1.26E-12	+
SNX15	IPI:IPI00016820.1	26.9393	26.6184	7	-0.64	1.15E-20	+
U4/U6.U5 Nuclear ribonucleoprotein	IPI:IPI00017289.3	27.4412	26.8387	5	-1.21	2.13E-36	+

Table A1.2: Proteins identified by LFQ MS showing changes in expression in response to *B. pertussis* Infection. All proteins were identified using the NCBI and Swiss Prot protein databases and demonstrated a mascot score >52 indicating reliable protein identification.

Protein Name	Accession Code	LFQ Intensity (Control)	LFQ Intensity (Infected)	Matched Peptides	Fold Change	PEP	ANOVA
SH3-containing Grb-2-like 1 protein	IPI:IPI00019169.3	25.9905	24.7994	5	-2.38	4.06E-31	+
Calreticulin / ER resident protein 60	IPI:IPI00020599.1	32.4786	31.8841	22	-1.19	0	+
Superoxide dismutase	IPI:IPI00022314.1	26.5621	28.6293	6	4.13	4.54E-57	+
Zinc finger Ran-binding domain protein 2	IPI:IPI00029400.2	30.5409	30.158	12	-0.77	2.64E-70	+
Tenascin	IPI:IPI00031008.1	25.256	26.1233	5	1.73	2.16E-27	+
U6 snRNA-associated Sm-like protein	IPI:IPI00032460.3	27.5791	28.196	3	1.23	7.88E-34	+
RNA-binding protein	IPI:IPI00033561.3	30.6525	29.7869	7	-1.73	1.42E-109	+
Coiled-coil domain-containing protein 97	IPI:IPI00061777.4	27.8229	27.401	6	-0.84	1.13E-38	+
40S ribosomal protein S29	IPI:IPI00182289.6	25.5816	26.0145	2	0.87	6.93E-06	+
Galectin-1	IPI:IPI00219219.3	34.1862	34.5223	16	0.67	0	+
N-alpha-acetyltransferase 38	IPI:IPI00219871.5	28.4039	27.9208	4	-0.97	6.85E-19	+
Cdc42 effector protein 3	IPI:IPI00294391.2	26.3264	25.7559	3	-1.14	5.49E-08	+
TSC22 domain family protein 1	IPI:IPI00301610.9	27.7164	28.2144	8	+1.00	5.10E-69	+
Protein TSSC4	IPI:IPI00305144.1	29.2542	28.9348	5	-0.64	1.07E-30	+
Serine/arginine repetitive matrix protein 1	IPI:IPI00328293.3	28.0004	26.944	6	-2.11	2.74E-40	+
Ferritin	IPI:IPI00375676.5	27.9658	29.4761	6	3.02	4.09E-47	+
Periphilin-1	IPI:IPI00410039.1	26.5231	27.0506	7	1.06	3.41E-31	+
Transcription elongation factor A protein-like 3	IPI:IPI00478127.3	30.6756	30.2284	9	-0.89	3.55E-65	+
Ferritin heavy chain	IPI:IPI00554521.2	31.962	33.7804	16	3.64	1.06E-255	+

Table A1.2: Proteins identified by LFQ MS showing changes in expression in response to *B. pertussis* Infection. All proteins were identified using the NCBI and Swiss Prot protein databases and demonstrated a mascot score >52 indicating reliable protein identification.

Protein Name	Accession Code	LFQ Intensity (Control)	LFQ Intensity (Infected)	Matched Peptides	Fold Change	PEP	ANOVA
Transcription elongation factor A protein-like 4	IPI:IPI00647163.1	29.142	28.6857	11	-0.91	3.46E-58	+
Serine/arginine repetitive matrix protein 2	IPI:IPI00782992.3	30.0636	29.0563	24	-2.01	1.29E-221	+
Suppressor of G2 allele of SKP1 homolog	IPI:IPI00828150.1	27.7404	27.4011	6	-0.68	2.53E-70	+

Table A1.2: Proteins identified by LFQ MS showing changes in expression in response to *B. pertussis* Infection. All proteins were identified using the NCBI and Swiss Prot protein databases and demonstrated a mascot score >52 indicating reliable protein identification.

Spot No.	Protein Name	Fold Change	Accession Code	Mascot Score	MW (kDa)	p*I*	Peptides Matched	Cov (%)	P Value
1361	Stathmin	↑1.6	P16949	154	17.2	5.76	3	21	0.009
1375	Actin-related protein 2/3 complex subunit 5	↑1.6	O15511	193	16.3	5.47	5	41	0.003
1383	Prefoldin subunit 5	↑1.5	O99471	97	17.3	5.93	3	21	0.006
1345	Superoxide Dismutase (Cu-Zn)	↑1.7	Q904262A	56	15.9	8.76	2	16	0.009
1325	DUTP	↑1.6	Q96Q81	254	26.5	9.46	8	30	0.006
1334	Nucleoside diphosphate kinase A (NME1)	↑1.5	P15531	379	17.1	5.83	14	63	0.012
1291	Putative hydrolase RBBP9	↑1.5	O75884	202	20.9	5.79	4	30	0.025
1250	α/β hydrolase domain-containing protein 14B	↑1.5	Q96IU4	206	22.3	5.94	4	28	0.028
1550	DJ-1	↑1.6	ISOA_A	473	19.8	6.33	14	68	0.003
1549	PRDX3	↑1.5	P30048	173	27.6	7.67	4	18	0.01
1326	Lysozyme C	↑1.6	P61626	62	16.5	9.38	1	8	0.045
1581	Myosin regulatory light chain 12A	↓1.7	P19105	151	19.7	5.67	3	17	0.001
1417	60S acidic ribosomal protein P2	↑1.5	P05387	261	11.6	4.42	9	69	0.005
1373	Eukaryotic translation factor Eif5a	↑1.6	3CPF_A	321	15.1	5.8	9	40	4.35E-04
1374	Glia maturation factor beta	↑1.5	P60983	199	16.7	5.19	3	29	0.006
1265	Heme-binding protein 1	↓1.3	Q9NRV9	481	21.0	5.71	12	50	0.011
1492	Glutathione S-Transferase P1	↑1.4	1QUQ_A	80	25.5	5.57	2	12	0.003
1240	26S proteasome non-ATPase reg. subunit 10	↑1.5	4PGT_A	644	23335	5.43	16	55	0.003
1261	Caspase 3	↑1.3	EAX04676	57	21.4	7.67	2	21	0.01

Table A1.3: Proteins identified by DIGE/ LC/MS showing changes in expression in response to HRV16. All proteins were identified using the NCBI and Swiss Prot protein databases and demonstrated a mascot score >52 indicating reliable protein identification.

Spot No.	Protein Name	Fold Change	Accession Code	Mascot Score	MW (kDa)	p*I*	Peptides Matched	Cov (%)	P Value
1190	RPABC1	↑1.5	NP_002686	251	24.5	5.69	6	30	0.002
1154	Phosphoglycerate mutase 1	↑1.5	P18669	150	28.7	6.67	4	16	0.033
1518	Unnamed protein product	↓1.3	BAG63158	76	55.7	6.12	3	5	0.022
1429	40S ribosomal protein S12	↑1.5	P25398	69	14.5	6.81	3	13	0.022
1434	HINT1	↑1.5	P49773	88	13.7	6.43	2	24	0.006
1651	S-phase kinase-associated protein 1	↑1.5	P63208	299	18.6	4.4	5	46	0.009
1254	DNA replication complex GINA protein PSF2	↑1.5	Q9Y248	128	21.4	5.29	3	24	0.004
512	Lamin B1	↓1.5	P20700	758	66.3	5.11	7	32	0.012
526	MAP3K1 or ASK1	↓1.6	Q99683	62	154.4	5.52	2	61	0.012
66	Splicing factor 3A subunit 1	↑1.5	Q15459	252	88.3	5.15	8	13	0.009
15	Menin	↓1.7	O00632	54	67.9	6.14	1	2	0.004
17	Glycogen debranching enzyme	↓1.7	Q9UF08	52	174.6	6.31	2	1	0.005
21	Tetratricopeptide repeat protein 21B	↓1.6	Q9HAK8	62	150.8	6.53	2	1	0.006
1411	IL-25	↑1.4	Q969H8	153	18.7	6.2	4	27	0.02
1413	Histidine triad nucleotide-binding protein 2	↑1.4	Q9BX68	147	17.1	9.2	4	36	0.009
1342	Cofilin-1	↑1.4	P23528	242	18.4	8.22	5	42	0.031
1408	Ubquitin-conjugatin enzyme E2 N	↑1.4	P61088	397	17.1	6.13	9	67	0.02
1192	Triose phosphate isomerase	↑1.4	P60174	339	30.7	5.65	8	27	0.003
963	Coiled-coiled domain containing 69	↑1.3	EAW61682	59	34.6	5.49	2	7	0.006

Table A1.3: Proteins identified by DIGE/ LC/MS showing changes in expression in response to HRV16 Infection. All proteins were identified using the NCBI and Swiss Prot protein databases and demonstrated a mascot score >52 indicating reliable protein identification.

Spot No.	Protein Name	Fold Change	Accession Code	Mascot Score	MW (kDa)	p*I*	Peptides Matched	Cov (%)	P Value
1224	Prefoldin subunit 3	↑1.4	P61758	160	22.6	6.63	4	19	0.033
1236	Acyl-protein thioesterase	↑1.4	O75608	88	24.6	6.29	2	8	0.022
1189	NME1-NME2(Nucleoside diphosphate kinase A and B)	↑1.4	NP001018146	340	30.1	9.06	12	36	0.022

Table A1.3: Proteins identified by DIGE/ LC/MS showing changes in expression in response to HRV16. All proteins were identified using the NCBI and Swiss Prot protein databases and demonstrated a mascot score >52 indicating reliable protein identification.

Table A1.4 List of antibodies used

Antibody	**Company**
Phospho-IRF3	Cell Signalling
Total IRF3	Santa Cruz
IκBα	Cell Signalling
β-Actin	Sigma Aldrich
Lamin A/C	Cell Signalling
NLRP12	Biorbyt
DJ-1	Biorbyt
Stathmin-1	Biorbyt
SOD1	Abcam
NME1/NME2	Abcam
GSTO1	Santa Cruz
Ferritin HC	Abcam
Ferritin LC	Abcam
PPP1Cα	Biorbyt

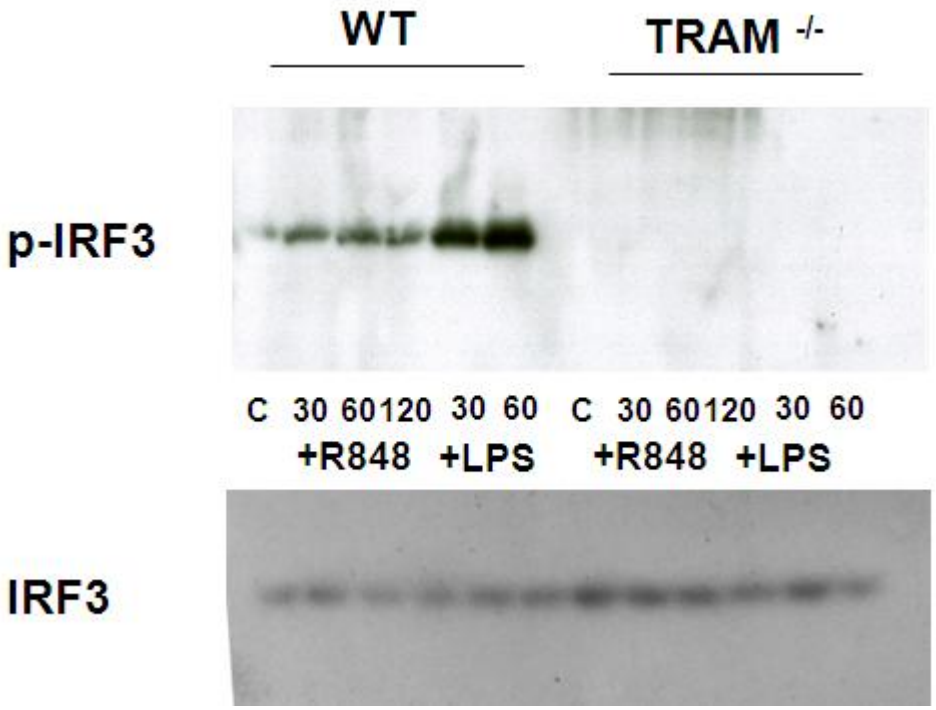

Figure A1.1 IRF3 phosphorylation in WT and TRAM deficient iBMDMs in response to R848 and LPS stimulation

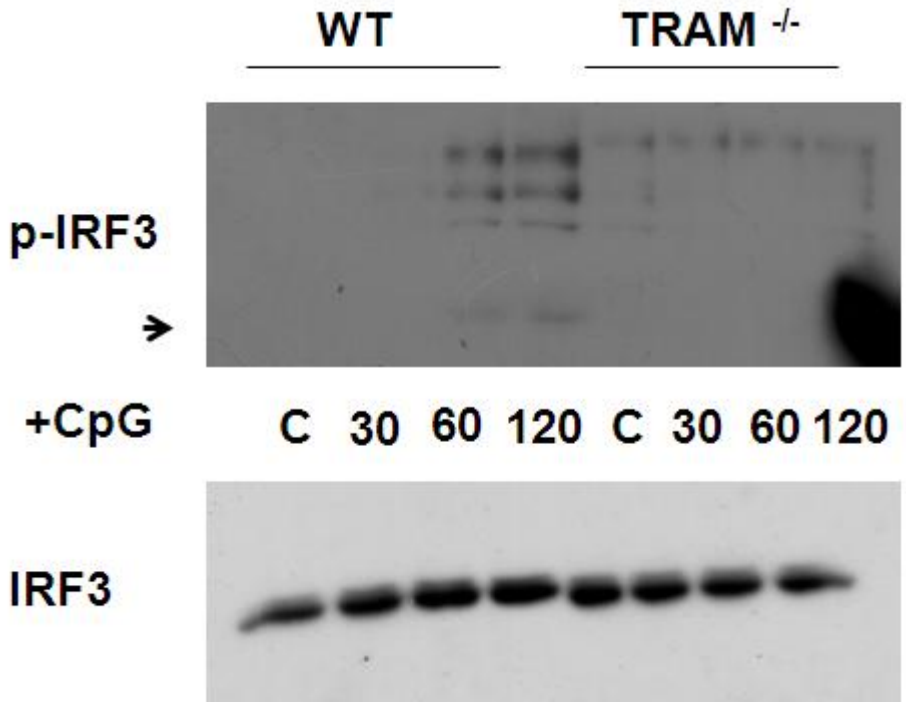

Figure A1.2 IRF3 phosphorylation in WT and TRAM deficient iBMDMs in response to CpG stimulation

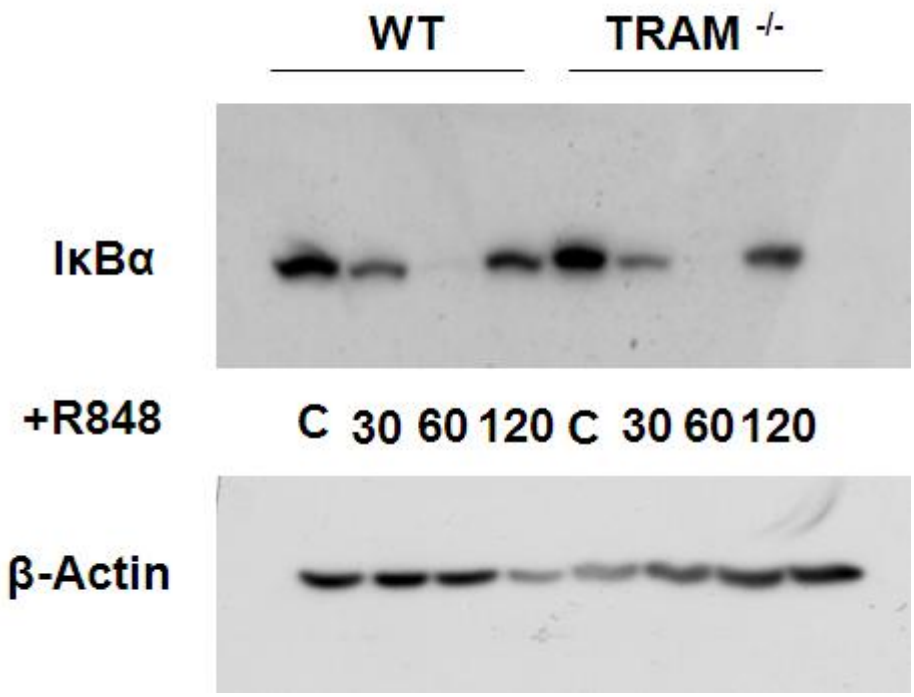

Figure A1.3 IκBα degradation in WT and TRAM deficient iBMDMs in response to R848 stimulation

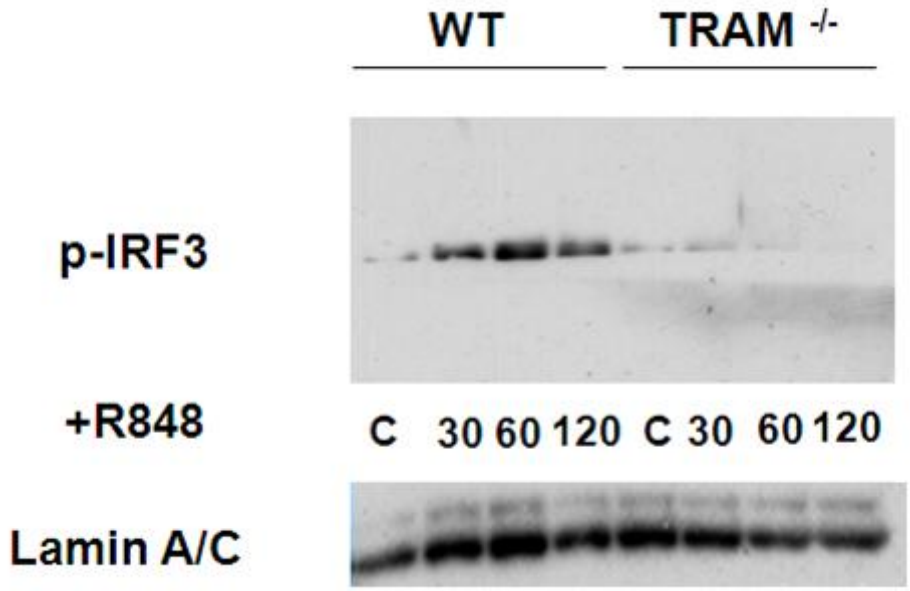

Figure A1.4 IRF3 nuclear translocation in WT and TRAM deficient iBMDMs in response to R848 stimulation